SYNTHESIS, CHARACTERIZATION AND BIOLOGICAL STUDIES OF NICKEL(II) COMPLEXES CONTAINING THIOSEMICARBAZONE AND THIOUREA DERIVATIVES

HANA BASHIR MOHAMMED SHAWISH

FACULTY OF SCIENCE
UNIVERSITY OF MALAYA
KUALA LUMPUR

2014

SYNTHESIS, CHARACTERIZATION AND BIOLOGICAL STUDIES OF NICKEL(II) COMPLEXES CONTAINING THIOSEMICARBAZONE AND THIOUREA DERIVATIVES

HANA BASHIR MOHAMMED SHAWISH

THESIS SUBMITTED IN FULFILMENT OF THE REQUIREMENT FOR THE DEGREE OF DOCTOR OF PHILOSOPHY

DEPARTMENT OF CHEMISTRY
FACULTY OF SCIENCE
UNIVERSITY OF MALAYA
KUALA LUMPUR

2014

ABSTRACT

The aim of this study is the preparation of new nickel(II) complexes with N/S donor ligands and their mixed complexes with co-ligands. A number of nickel(II) complexes of thiosemicarbazone derivatives of 2,3-dihydroxybenzaldehyde and thiourea derivatives of diamines have been synthesized and characterized by a combination of spectroscopic studies, elemental analysis, and X-ray crystallography. Five series of nickel(II) complexes with thiosemicarbazone ligands of the type H_3L (RCH=NNHCSNHR̀; where R = 2,3-dihydroxybenzaldehyde, R̀ = H; H_3L^1, CH_3; H_3L^2, C_6H_5; H_3L^3, C_2H_5; H_3L^4) have been verified by means of IR, NMR and, in some cases, X-ray crystallography. These five series of nickel(II) thiosemicarbazone complexes have been prepared by using different starting nickel(II) compounds, $Ni(ClO_4)_2.6H_2O$, $[NiCl_2(Bpy)]$, $Ni(OAc)_2.4H_2O$, $[NiCl_2(PPh_3)_2]$ and $NiCl_2$ with dppe, giving complexes with the formula $[Ni(H_3L)(H_2L)]ClO_4$, $[Ni(H_2L)_2][Ni(H_3L)_2]Cl_2$, $[Ni_2(HL)_2]$, ($[Ni(H_2L)(PPh_3)]Cl$, $[Ni(HL)(PPh_3)]$) and $[Ni_2(HL)_2(dppe)]$ respectively. Results from spectroscopic data and crystal structure analysis show that in all complexes the thiosemicarbazone ligands coordinate as tridentate ONS donors in different coordination modes. The complexes $[Ni(H_3L)(H_2L)]ClO_4$ and $[Ni(H_2L)][Ni(H_3L)]Cl_2$ are octahedral with two thiosemicarbazone ligands coordinating as neutral H_3L and monodeprotonated H_2L ligand whereas the complexes $[Ni_2(HL)_2]$, ($[Ni(H_2L)(PPh_3)]Cl$, $[Ni(HL)(PPh_3)]$) and $[Ni_2(HL)_2(dppe)]$ are square planar with the thiosemicarbazone ligand coordinating as doubly deprotonated HL in $[Ni_2(HL)_2]$, $[Ni(HL)(PPh_3)]$, $[Ni_2(HL)_2(dppe)]$ and as monodeprotonated H_2L in ($[Ni(H_2L)(PPh_3)]Cl$.

Three series of nickel(II) complexes with thiourea ligands (RNHCSNHRR̀; where R= phenyl, R̀= o-phenylamine, p-phenylamine and o-aminopyridine) have been prepared and characterized. Thiourea diamine ligands have been coordinated to nickel(II) and the differing binding modes of the ligands in the absence and presence of co-ligands have

been investigated. The reaction of the thiourea ligands with nickel(II) salts yields mononuclear diamagnetic complexes with thiourea ligand coordinates as bidentate NS donors, while the reaction of nickel salts with the thiourea ligands in the presence of 1,10-phenanthroline or 2,2'-bipyridine affords binuclear paramagnetic complexes with the thiourea ligands coordinating as tridentate NNS donors. With the aim of evaluating the effect of varying N4 substitution from methyl, ethyl to phenyl in thiosemicarbazone moiety and the coordination environments for nickel complexes with thiosemicarbazones ligands on biological activities, DNA topoisomerase inhibition assay has been carried out. The results from this study showed that the ability of the complex to inhibit the enzyme strengthened as the ligands become more hydrophobic and the coordination environment around the nickel ion is square planar. The gel electrophoresis results of incubating nickel complexes of thiourea as main ligands as well as their mixed complexes with polypyridyl ligands as variable subsidiary ligands showed that all these complexes are able to inhibit the function of topoisomerase enzyme better than the free ligands. In addition, the results suggested that for all complexes the degree of inhibition of the topoisomerase I depended on the concentration of the nickel(II) complexes except for the thiourea series of complexes with *p*-phenylamine and *o*-aminopyridine, which are not concentration dependent.

ABSTRAK

Tujuan kajian ini dijalankan ialah untuk menyediakan kompleks nikel(II) dengan ligan mengandungi N/S sebagai atom penderma dan kompleks campuran mengandungi ligan-bersama. Beberapa kompleks nikel(II) tiosemikarbazon terbitan daripada 2,3-dihidroksibenzaldehid dan terbitan tiourea daripada diamina telah disintesis dan dicirikan oleh gabungan kajian spektroskopi, analisis unsur, dan kajian kristalografi-X. Lima siri kompleks nikel(II) dengan ligan tiosemikarbazon daripada H_3L ($RCH=NNHCSNH\grave{R}$; di mana R = 2,3-dihidroksibenzaldehid, $\grave{R}$ = H; H_3L^1, CH_3; H_3L^2, C_6H_5; H_3L^3, C_2H_5; H_3L^4) telah disahkan melalui IR, NMR, dan dalam beberapa kes, kristalografi sinar-X. Lima siri kompleks nikel(II) tiosemikarbazon ini telah di sediakan dengan menggunakan pelbagai sebatian nikel(II) seperti $NiClO_4.6H_2O$, $[NiCl_2(Bpy)]$, $Ni(OAc)_2.4H_2O$, $[NiCl_2(PPh_3)_2]$ dan $NiCl_2$ dengan dppe, telah menghasilkan kompleks dengan formula $[Ni(H_3L)(H_2L)]ClO_4$, $[Ni(H_2L)_2][Ni(H_3L)_2]Cl_2$, $[Ni_2(HL)_2]$, ($[Ni(H_2L)(PPh_3)]Cl$, $[Ni(HL)(PPh_3)]$) dan $[Ni_2(HL)_2(dppe)]$. Keputusan daripada data spektroskopi dan analisis struktur hablur menunjukkan bahawa dalam semua kompleks ligan tiosemikarbazon berkoordinat sebagai penderma ONS tridentat dalam mod pengikatan yang berbeza. Kompleks $[Ni(H_3L)(H_2L)]ClO_4$ dan $[Ni(H_2L)][Ni(H_3L)]Cl_2$ adalah oktahedral dengan dua ligan tiosemikarbazon berkoordinat sebagai ligan neutral H_3L dan ternyahproton-mono ligan, H_2L manakala kompleks $[Ni_2(HL)_2]$, ($[Ni(H_2L)(PPh_3)]Cl$, $[Ni(HL)(PPh_3)]$) dan $[Ni_2(HL)_2(dppe)]$ bergeometri satah persegi dengan ligan tiosemikarbazon berkoordinat sebagai ternyahproton ganda dua HL dalam $[Ni_2(HL)_2]$, $[Ni(HL)(PPh_3)]$, $[Ni_2(HL)_2(dppe)]$ dan H_2L sebagai ternyahproton-mono dalam $[Ni(H_2L)(PPh_3)]Cl$. Tiga siri kompleks nikel(II) dengan ligan tiourea ($RNHCSNHR\grave{R}$; di mana R= fenil, $\grave{R}$= *o*-fenilamina, *p*-fenilamina and *o*-aminopiridina) telah disediakan dan dicirikan. Tindak balas ligan tiourea diamina dengan nikel(II) telah disempurnakan dan menghasilkan kompleks dengan mod koordinatan yang berbeza

dalam ketiadaan dan kehadiran ligan-bersama. Tindak balas ligan tiourea dengan nikel(II) menghasilkan kompleks mononuclear diamagnetik dengan ligan tiourea berfungsi sebagai penderma N/S duabidentat. Manakala tindak balas garam nikel dengan ligan tiourea dalam kehadiran 1,10-fenanthrolina atau 2,2'-bipiridina menghasilkan kompleks paramagnet dinuklear dengan ligan tiourea berfungsi sebagai penderma NNS tridentat. Dengan tujuan untuk menilai kesan N4 penggantnya berbeza-beza daripada metil, etil dan fenil dalam moieti tiosemikarbazon dan persekitaran koordinatan bagi kompleks nikel dengan tiosemikarbazon ligan aktiviti biologi, asai perenctan DNA topoisomerase telah dijalankan. Hasil daripada kajian ini menunjukkan bahawa keupayaan kompleks untuk menghalang enzim diperkukuhkan sebagai ligan menjadi lebih hidrofobik dan persekitaran koordinatan sekitar ion nikel adalah sesatah segiempat sama. Keputusan gel elektroforesis merangsang kompleks nikel tiourea sebagai ligan utama serta kompleks bercampur dengan ligan polipiridil sebagai anak ligan ubah menunjukkan bahawa semua kompleks membolehkan untuk menghalang fungsi enzim topoisomerase lebih daripada ligan bebas. Sehubungan itu, keputusan mencadangkan bahawa semua kompleks tahap perencatan topoisomerase I bergantung kepada kepekatan nikel(II) kompleks kecuali siri tiourea yang membentuk kompleks dengan *p*-fenilamina and *o*-aminopiridina, yang tidak bergantung kepada kepekatan .

ACKNOWLEDGEMENTS

In the name of Allah, the Most Gracious and Most Merciful

First and foremost, I praise Allah, the almighty for providing me this opportunity and granting me the strength to complete my thesis after all the challenges and difficulties.

TABLE OF CONTENTS

LIST OF TABLES

Table No.		PAGE
2.1	Stoichiometries, color and partial elemental analysis of nickel(II) thiosemicarbazone complexes	43
2.2	Crystal data and structure refinement parameters for complexes **8a** and **9**	48
2.3	Selected bond lengths (Å) and bond angles (º) of complexes **8a** and **9**	49
2.4	Interaction parameters (Å, °) for complex (**8a**)	53
2.5	Hydrogen bonding (Å, °) for complex (**9**)	59
2.6	^{1}H NMR spectral assignments for the thiosemicarbazone ligands and their nickel(II) complexes in DMSO-d_6	62
2.7	^{13}C NMR spectral assignments for the thiosemicarbazone ligands and their nickel(II) complexes in DMSO-d_6	64
2.8	IR spectral assignments for the thiosemicarbazone ligands and their nickel(II) complexes	69

LIST OF FIGURES

LIST OF SYMBOLS AND ABBREVIATIONS

The following abbreviations were used at various parts in the subsequent text:

CODH	Carbon monoxide dehydrogenase
MCR	Methyl-Coenzyme M reductase
Glx I	Glyoxalase I
ARDs	Acireductone dehydrogenases
SODs	Superoxide dismutases
H$_3$L^1	2,3-dihydroxybenzaldehyde thiosemicarbazone
H$_3$L^2	2,3-dihydroxybenzaldehyde 4-methylthiosemicarbazone
H$_3$L^3	2,3-dihydroxybenzaldehyde 4-phenylthiosemicarbazone
H$_3$L^4	2,3-dihydroxybenzaldehyde 4-ethylthiosemicarbazone
PPh$_3$	Triphenylphosphine
dppe	1,2-bis(diphenylphosphino)ethane
PhTUPho-NH$_2$	N-(2-aminophenyl)-N'-phenylthiourea
PhTUPhp-NH$_2$	N-(4-aminophenyl)-N'-phenylthiourea
PhTUPym-NH$_2$	N-(2-aminopyridin-3-yl)-N'-phenylthiourea
Phen	1,10-phenanthroline
Bpy	2,2'-Bipyridine
Topo I	Topoisomerase I
ORTEP	Oak Ridge Thermal-Ellipsoid Plot Program
DMF	N,N-Dimethylformamide

DMSO	Dimethylsulphoxide
B.M	Bohr Magneton
Tris	Tris(hydroxymethyl)aminomethane
TCS	Thiosemicarbazone
TU	Thiourea
CT	Charge transfer
E.coli	*Escherichia coli*

CHAPTER 1

INTRODUCTION

1.1 Biological Importance of Metal Ions

Metal ions are of greatest biological importance because of their involvement in several indispensable biochemical processes for living organisms in both prokaryotes and eukaryotes. Sodium, potassium, magnesium and calcium are the dominant metal ions in the cell which afford the basis for nerve conduction, muscle contraction and stabilizing nucleic acids. A major determinant of the metal ions functional relevance in living systems is that, one in four proteins in the Protein Data Bank (PDB) having a metal ion coordinated to the protein (Sh et al., 2005). Mostly, the prevalent metal ions incorporated into proteins are transition metal ions, which are less abundant than main group elements (Bleackley & MacGillivray, 2011). The main reason for the preference of transition metal ions over the other metal ions is ultimately due to their unique features such as the flexibility to adopt more than one coordination geometry and the ability to exist in multiple oxidation states.

The biochemically functional metal ions include vanadium, manganese, iron, cobalt, nickel, copper, zinc, molybdenum and tungsten, participate in many essential activities. However, the biological systems in which each of them are involved vary significantly. Besides that, the utilization of each metal is dependent on the organism and the corresponding environment. Because of the important roles these trace elements play in cells, considerable progress has been made in defining the pathways by which cells acquire, distribute, store and export metal ions (Zhang & Gladyshev, 2009).

Generally, metal ions are positively charged and act as electrophiles whereas biological molecules such as DNA and protein are electron rich. Hence, the metal ions have a

general tendency to bind and interact with biological molecules. It is essential to determine the identity and the type of donor atoms in the active site as well as the geometry around the metal ion, to correlate the relationship between the structure and the function of the metalloprotein. Knowing the crystal structure of the metalloprotein will reveal all the questions that are ambiguous. For instance, Palmer and co-workers found the identity of different copper centers in fungal laccase by relating the observed properties with that of well known model compounds and protein which were characterized before (Palmer et al., 1999). Even if the crystal structure of the metalloprotein is known, studies on the spectrochemical and physical properties are very necessary. In recent years, considerable progress has been made in the field of bioinorganic chemistry which encompasses many disciplines of chemistry and biology.

1.2 Roles of Nickel in Biochemistry

Nickel is an essential trace element for bacteria, plants, animals and humans. However, its concentration in human tissue is relatively low (1 µg/L) compared with zinc, iron and copper (100 µg/L) (Silva & Williams, 2001). Every organism requires different metal ions depending on their environment and complexity. In human body, there is no specific biochemical function for nickel, however, nickel is critical for several human pathogens, such as *Helicobacter pylori*, which would not be able to colonize and infect the human stomach without nickel (Olson & Maier, 2002).

1.2.1 Nickel–Containing Enzyme Active Sites

Nickel has not been recognized as an important element in nature until the discovery of nickel as the active site metal in the *jack been urease* by Zerner and his co-workers in 1975 (Dixon et al., 1975). Indeed, research on identifying nickel as an essential trace metal in biology exploded dramatically thereafter. Currently, an impressive series of

enzymes is known which depend on nickel include urease, NiFe hydrogenase, CO dehydrogenase, acetyl-CoA synthase, methyl-Coenzyme M reductase, glyoxalase I, aciredcton dioxygenase, and nickel containing superoxide dismutase (Ragsdale, 2009). A diverse range of reactions that utilize nickel's varied coordination numbers, geometries and oxidation states is catalyzed by these nickel-containing enzymes. It is noteworthy that the substrates or the products are dissolved gases: ammonia, hydrogen, carbon monoxide, carbon dioxide, and methane, which are the key component for the carbon cycle (Ragsdale, 2007). In addition to the nickel-metalloenzymes, there are several proteins required for nickel acquisition, transport, storage and assembly of the nickel ion into the active sites of some metalloenzymes (Watt & Ludden, 1999). For instance, the nickel transport system in *Escherichia coli* composed of five proteins, *NiKABCDE*. The characterization of the nickel site in the *NiKA* protein by X-ray spectroscopy has been accomplished showing that nickel is ligated by histidine, aspartic acid and glutamic acid side chains.

Although the most prevalent oxidation state of nickel in biochemistry is apparently Ni(II), the species Ni(0), Ni(I) and Ni(III) species are also observed in some cases (Dey et al., 2007). Like other ions of the first transition series, nickel(II) has the ability to bind to many substances of the biological interest, hence, presenting various coordination modes include square planar, square pyramidal, tetrahedral, octahedral, and trigonal pyramidal. Therefore, the nickel sites in the different classes of nickel-containing enzymes are remarkably diverse. The enzymatic reactions which occur in the nickel metalloenzymes centers can be divided into two categories: redox active enzymes and non-redox active enzymes (known also as hydrolase enzymes). In the hydrolase nickel enzymes, the nickel ion is found to exist only in the Ni(II) state, and the Ni center acts as a Lewis acid. On the other hand, nickel redox active enzymes, which include the

majority of nickel metalloenzymes, access different oxidation states in their catalytic cycles (Maroney et al., 1998).

Metalloenzyme crystal structures have a major impact on the understanding of biological metal centers. They are often the starting point for mechanistic and computational studies. The unveiling of a new metalloenzymes crystal structure to the inorganic chemists typically generates great excitement accompanied by a multitude of questions regarding the active site chemistry. Since the elucidation of urease crystal structure, the structure biology of other nickel enzymes has greatly expanded largely. Due to its content of nickel, urease is a unique example among the hydrolytic enzymes, which typically contain zinc as the active site. Urease catalyzes the hydrolysis of urea to carbamate, which decomposes to ammonia and carbon dioxide. However, X-ray crystallography of the enzyme shows that the active site contains two nickel ions bridged by a carbamylated lysine and hydroxide ion (Jabri et al., 1995). Moreover, each nickel ion coordinates two histidine residues and a water molecule possessing a distorted square pyramidal geometry for one of the nickel ions, Ni(1), while the coordination sphere of the another nickel ion, Ni(2), is completed by an additional terminally bound aspartate resulting in an octahedral ligand environment (Figure 1.1).
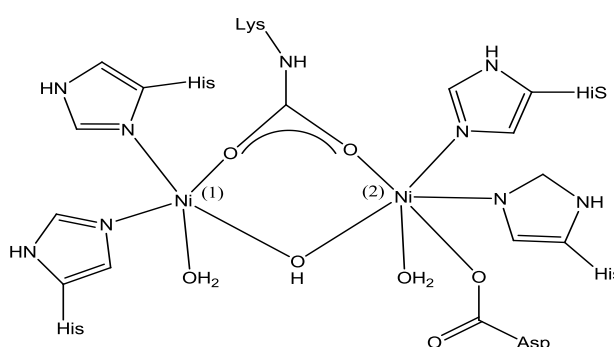
Figure 1.1: Active sites of urease

[NiFe] hydrogenase catalyzes the production or consumption of hydrogen gas in the presence of an electron donor or acceptor. Volbeda and his co-workers revealed the unusual nature of the active site for this enzyme; the active site was shown to contain an unexpected disulfur bridged heterobimetallic Ni-Fe core (Figure 1.2). The nickel ion is further bound to a third bridging OH and two cysteine in a highly distorted square pyramidal geometry, whereas the iron ion is further coordinated by three small non-protein ligands in a distorted octahedral conformation (Volbeda et al., 1996). The non-protein ligands could not be identified by crystallography. Infrared studies combined with isotopic labeling have been used to conclude that there are two cyanide and one carbon monoxide ligand bound to the iron.

Carbon monoxide dehydrogenase CODH catalyzes the reversible reduction of carbon dioxide into carbon monoxide. One form of CODH is known as Acetyl Coenzyme A synthase, which is capable of the synthesis of acetyl Coenzyme A from Co and CH_3.
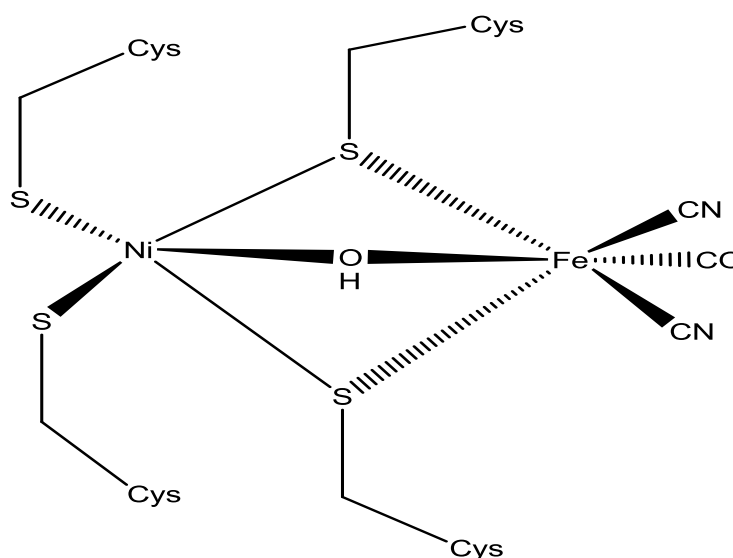
Figure 1.2: Active site of [NiFe] dehydrogenase

Given the catalytic reaction for CO dehydrogenase/CoA synthase, these enzymes are carrying out the important function of fixing CO and CO_2 in the global carbon cycle (Riordan, 2004). Furthermore, CODH/ACS has been implicated in the chemoautotrophic origin in which primitive organisms consumed CO and CO_2 from volcanic or hydrothermal sites for the formation of C-C bonds (Huber & Wachtershauser, 1997). The crystal structure of the system CODH/ACS from the bacteria *Moorella thermoacetica*, (Figure 1.3), elucidate that the active site donated as the A-cluster contains a Ni_d-Ni_p dinuclear site and a $[Fe_4S_4]$ cubane cluster. The Ni_d in the active site is coordinated with two cysteine sulfurs and two carboxyamide nitrogens of the tripeptide Cys-Gly-Cys from the protein backbone, composing a square planar NiN_2S_2 geometry around Ni_d. Meanwhile, Ni_p carries an unidentified ligand X and 3 cysteine sulfurs in a tetrahedral coordination environment (Doukov et al., 2002).

Methyl-Coenzyme M reductase (MCR) catalyzes the final step in methane formation from methyl-Coenzyme M and Coenzyme B as in the reaction:

$$CH_3\text{-S-CoM} + CoB\text{-S-H} \longrightarrow CH_4 + CoM\text{-S-S-CoB}$$
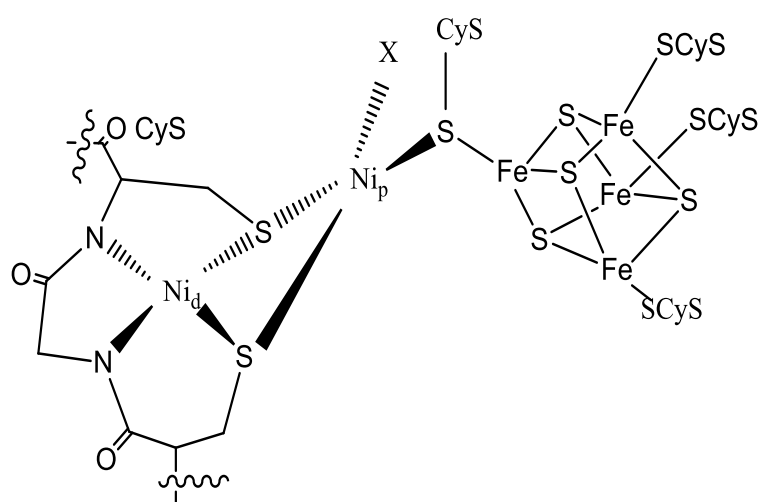
Figure 1.3: Schematic view of CODH/ACS active site

This reaction requires an unusual nickel hydrocorphin cofactor, named F430 for its absorption at 430 nm. The Ni ion is in an octahedral conformation coordinated by four tetrapyrrolic nitrogens in the equatorial plane and by glutamine side chain oxygen in the lower axial position. The upper axial contains either the thiol or the sulfonate groups of CoM depending on the form of the enzyme being isolated.

Glyoxalase I catalyzes the conversion of methylglyoxal, a toxic species that forms covalent adducts with DNA, to lactate. X- ray crystallographic studies have shown that the active site of Ni-containing Glyoxalase I enzyme from *Escherichia Coli* possesses a distorted octahedral geometry, with Ni ion remains in the 2+ state throughout the catalytic reaction. The Ni^{2+} ion is ligated to two histidine residues, two glutamates, and two water molecules, (Figure 1.4). Interestingly, the Glx I enzyme containing Ni^{2+} was found to have catalytic activity while the Glx I containing Zn^{2+}, which have a five coordinated Zn^{2+} in a trigonal bipyramidal geometry with all of the amino acid ligands found in Ni^{2+} Glx I but only one water molecule, is inactive. It has been proposed that there is a correlation between the coordination number at the metal binding and the catalytic activity, therefore, the Ni-containing Glx I is active because of the octahedral geometry (He et al., 2000).
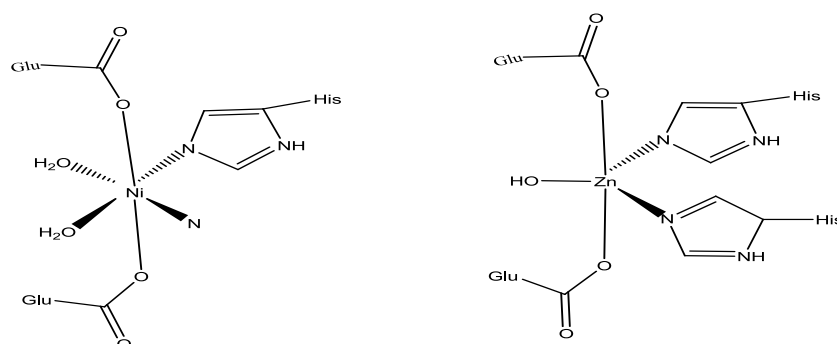
Figure 1.4: Active site of Ni^{2+}-containing Glx I from *E.coli* (left) and active site of Zn^{2+}-dependent Glx I

Acireductone dehydrogenases (ARDs) are enzymes involved in the methionine recycle pathway, which regulates aspects of the cell cycle (Pochapsky et al., 2007). ARDs catalyze oxygen dependent aliphatic C-C bond cleavage in acireductone. This reaction catalyzed by two types of ARD sharing a common polypeptide sequence but differ in the metal active site, which is Fe^{2+} or Ni^{2+}. Each ARD enzyme undergoes acireductone stimulation but composing different compounds. It has been found that Fe^{2+}-containing ARD reacts with acireductone producing formate and 2-keto-4-methylthiobutanoic acid, which is a precursor of methionine. On the other hand, Ni^{2+}-containing ARD does not produce the methionine precursor. Conversely, it produces CO, formate and methylthiopropionic acid, which is cytotoxic (Perreaux et al., 1986). Methylthiopropionic acid, carbon monoxide were found to play a critical role as neurotransmitter in mammals (Barann et al., 1997). Although the precise function of this enzyme is still unclear, it has proposed that the activity of Ni^{2} - ARD might aid in the regulation of methionine levels (Al-Mjeni et al., 2002). The proposed structure of nickel containing acireductone dioxygenase has been only determined based on X-ray absorption spectroscopy (XAS). This study revealed that Ni^{2+} ion is a six coordinated in a pseudo octahedral geometry composed of three histidine imidazole nitrogens, one glutamate, and two water molecules completing the Ni^{2+} coordination sphere.

Superoxide dismutases (SODs) are metalloenzymes that catalyze the disproportionation of superoxide, a harmful oxidative byproduct of aerobic respiration, to peroxide and molecular oxygen. This dismutation reaction requires a metal center that can be reduced and reoxidized by superoxide. There are four classes of SODs exist based on the amino acid sequence homology, which are CuZnSOD, FeSOD, MnSOD and NiSOD (Bannister et al., 1987; Kim et al., 1998).

Ni-containing form of the enzyme was first identified in several strains of streptomyces in 1996 (Youn et al., 1996). However, the crystal structure of Ni-SOD has been reported (Barondeau et al., 2004). The nickel active site in SOD switches between two oxidation states, Ni(II) and Ni(III), during the catalytic reaction illustrated.

$$Ni(II) + O_2^- + 2H^+ \longrightarrow Ni(III) + H_2O_2$$

$$Ni(III) + O_2^- \longrightarrow Ni(II) + O_2$$
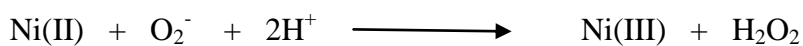
In this reaction, the superoxide binds to the Ni(II) center generates a Ni(II) -peroxo species that undergoes proton and electron transfer resulting in the formation of hydrogen peroxide and Ni(III) oxidized form. Ni(III)-peroxo intermediate, which is generated from another superoxide binding, donates an electron to the Ni(III) center producing dioxygen and reforming the starting Ni(II) state (Szilagyi et al., 2003).

The crystal structure of the active site has been elucidated for both the Ni(II) and Ni(III) states. The central metal ion in the Ni(II) state is square planar, with N_2S_2 coordination environment. The ligands are provided by one amine nitrogen of the terminal histidine, one amide nitrogen of the peptide backbone, and two cysteine thiolates at equatorial positions. While the central metal ion in the Ni(III) state has a square pyramidal geometry, with N_3S_2 coordination environment, composed of one imidazolyl group of the terminal histidine, which moves to an axial position and ligates to the Ni center during the reaction, in addition to the two thiolate sulfurs and the two nitrogens existing in the Ni(II) state (Figure 1.5). Interestingly, the Ni-SOD is a quite distinct from those of other superoxide dismutase enzymes. For example, among the other metals of SODs, nickel is the only metal that does not catalyze the disproportionation of O_2^- in neutral aqueous solutions (Ryan et al., 2010). Another striking feature of Ni-SOD is that the coordinate's active site residues are not found in other superoxide dismutase enzymes.

The MnSOD, CuZnSOD and FeSOD all have only N/O donors binding to the metal center cofactor. Alternatively, NiSOD coordinates two cysteine sulfurs to the Ni center. These sulfur ligands appear to have pose the Ni(II)/Ni(III) redox couple in the appropriate range for catalyzing both the reduction and oxidation of superoxide, and to serve as a proton donor during catalysis (Barondeau et al., 2004).
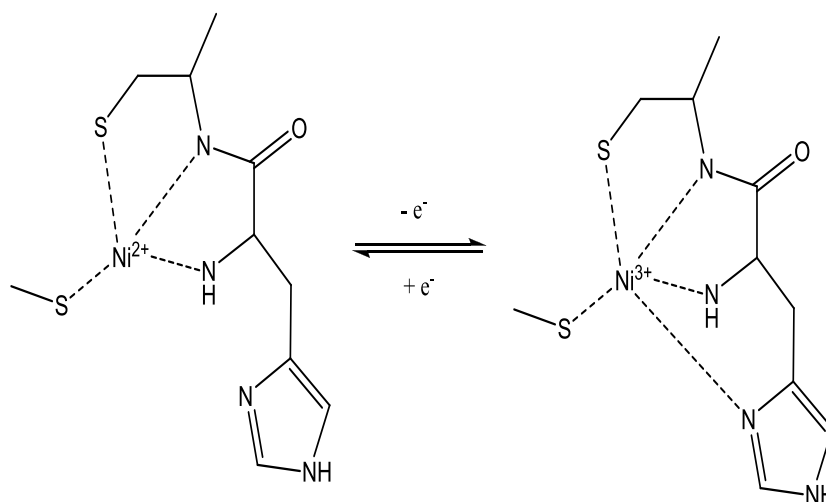
Figure 1.5: Schematic structure of NiSOD active site in the reduced (left) and oxidized (right) states

1.3 Model Complexes of Nickel-Containing Active Site

The primary goal of biomimetic inorganic chemistry is to synthesize molecules that approach or achieve the coordination sphere, oxidation states, and stereochemistry of the native metal-containing sites. Generally, coordination sites of metalloenzymes consist of donation sites within very long protein chains. However, studies of synthetic model complexes of metalloenzymes have provided much insight into the structure-function properties of the active sites as well as for investigating the enzyme mechanisms. Therefore, provide an important tool in designing new artificial catalysts based on biocatalysts especially with the focus of research nowadays on green methodologies. For example, hydrogen as an energy currency has been spurred by recent scientific and technological in order to provide an abundant, clean, and secure

renewable energy sources. Although hydrogen can be used efficiently as fuel, widespread adoption of this technology will be limited by the high cost and limited availability of platinum group metals which are required as catalysts (Gordon et al., 2006). Given the catalytic function of metals-containing hydrogenases in hydrogen production/utilization, provide a promising avenue for research in developing new metal complexes that mimic the active site of hydrogenase as catalyst for hydrogen but do not require platinum group metals. More advantages can be gained from the synthesis of analogues complexes of the active site of metalloenzymes, deeper knowledge about the inherent electronic character of the metal center in the specific metalloenzyme, understanding the ligand environment and comprehension of why nature choose that specific ligand arrangement.

Despite the fact that the crystal structure and coordination environment about the nickel center in some of the nickel-containing enzymes have been elucidated, a number of questions concerning the metalloenzymes remain unanswered. Consequently, there have been substantial efforts toward the synthesis of nickel complexes which can serve as viable mimics for the structure and function of nickel naturally occurring enzymes. The vast majority of research regarding nickel model complexes has focused on sulfur and nitrogen donor ligands although the presence of clusters in some nickel metalloenzymes stimulates the synthesis of model complexes with large number of complexes, which is not related to the donor atom in the active site (Halcrow & Christou, 1994). Furthermore, many synthetic nickel complexes with different oxidation states have been of interest due to the changing in the oxidation states from one to another during the catalytic reaction of many nickel containing enzymes.

1.4 Thiosemicarbazones

Thiosemicarbazones and their metal complexes continue to attract considerable interest since they have shown a broad spectrum of biological activities include, but not limit to cytotoxic, antitumor, antibacterial, antiviral and antifungal properties. Schiff bases of thiosemicarbazones are the products of the condensation reaction of a suitable aldehyde or ketone with a thiosemicarbazide or a substituted thiosemicarbazide at the N(4) position, (Scheme. 1.1). According to the IUPAC nomenclature, thiosemicarbazones are generally named by combining the name of the condensed aldehyde or ketone and the term thiosemicarbazone. Also, it is usual to include in this class derivatives with substituents on the thioamide nitrogen (Casas et al., 2000).
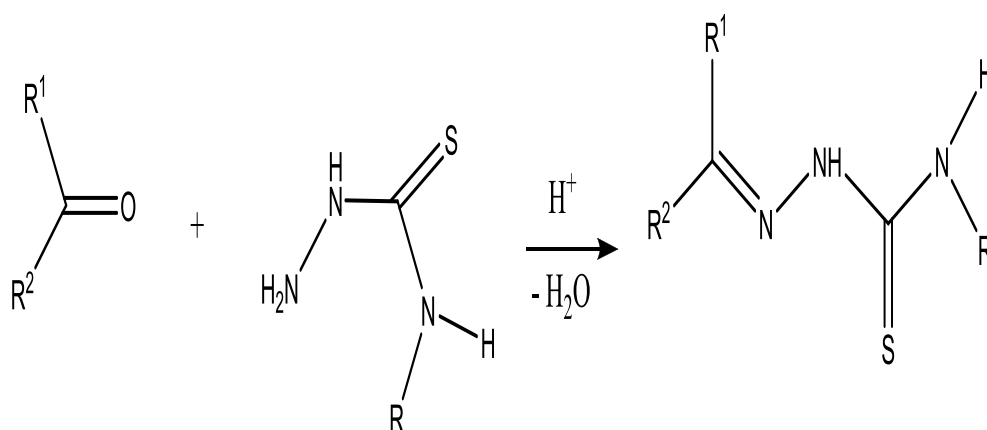
Scheme 1.1: Synthesis of thiosemicarbazones

In general, thiosemicarbazones are represented by the formula 1, where R^1 is an alkyl or aryl group and R^2 is alkyl, aryl or hydrogen atom. Meanwhile, the formula 2, (Figure 1.6), represents the N(4) substituted thiosemicarbazones where R^3 and R^4 can be alkyl, aryl groups or a part of cyclic system (Lobana, Sharma, et al., 2009).

1.4.1 Stereochemistry, bonding and nature of coordination of thiosemicarbazone

Thiosemicarbazones are well known as chelating ligands, and it has been elucidated that their biological activity is related to their ability to coordinate to metal centers in enzymes. When interacting with transition metal ions, thiosemicarbazones adopt different stereochemistries depend essentially on the presence of an additional coordination site on the thiosemicarbazone moiety and the charge on the ligand, which in turn is influenced by the thione – thiol tautomerism.
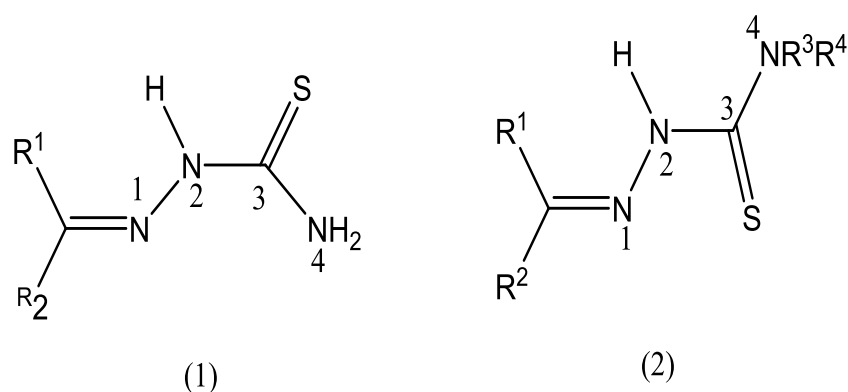
Figure 1.6: Structure of thiosemicarbazone with the numbering scheme

However, thiosemicarbazones found to exist as the thione form in the solid state but as an equilibrium mixture of thione and thiol forms in the solution, (Figure 1.7). The presence of C=N in the thiosemicarbazones moiety makes the possibility for thiosemicarbazones to exist in two configurations E and Z. It has been shown that the E isomer will predominate in the mixture (West et al., 1993). In this case, the thiosemicarbazone will coordinate through sulfur atom only as a monodentate ligand. Significantly, detailed studies have demonstrated that the presence of various substituents in thiosemicarbazone moiety will decide the stereochemistry of the ligand depends on their steric effects (Lobana et al., 2008; Lobana, Sharma, et al., 2009).
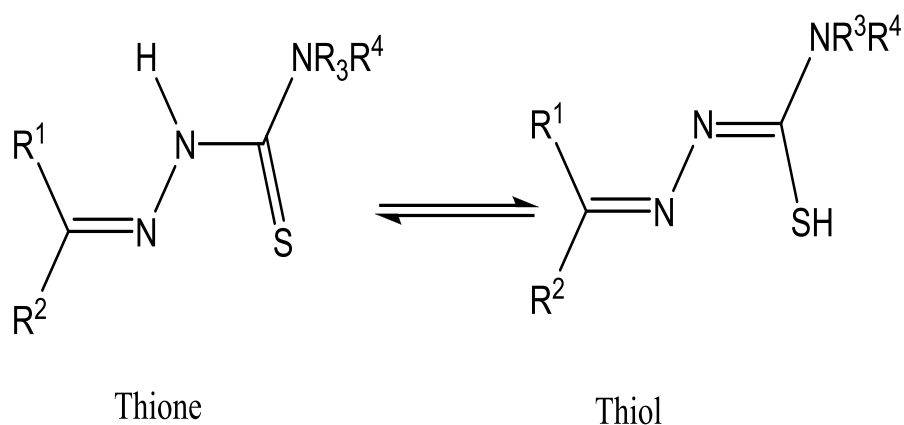
Figure 1.7: Thione – Thiol Equilibrium

Thiosemicarbazones are important and versatile type of ligands due to the number and variety of donor atoms they may possess. They can coordinate to the metal ion in a range of ways either in the neutral thione form or in the negative thiol form. The usual chelating mode is the formation of five membered N,S chelate ring involving N1 hydrazinic nitrogen and thiolate sulfur atoms. It has been reported that the size of the group attached to the azomethine carbon atom of the thiosemicarbazone is an important factor affecting the five membered ring formation. If the attached group is fairly small, then only the formation of NS five membered ring takes place, but if the group is relatively big such a ring cannot be formed and unusual four membered ring utilizing N2 hydrazinic nitrogen and thiolate sulfur resulted (Prabhakaran et al., 2008). However, incorporation of an additional site (X) into the thiosemicarbazone ligand, linked to the carbonylic carbon, normally results in X,N,S tridentate ligands and their coordination behavior depends on the nature of the metal ion concerned (Pedrido et al., 2009).

Among the thiosemicarbazone donor atoms, sulfur is of paramount importance in the metal–ligand linkage. It is well known that the compounds containing C=S moiety have the ability to form linear, binuclear, three-dimensional cluster compounds or high

polymers by coordinating to only one metal or bridging between two metals and more. This fact, together with the presence of different donor atoms, allows thiosemicarbazone to form variety of bridging complexes (Figure 1.8). The most popular donor set involves ONS or NNS atoms displaying versatile coordination behavior like monomers, with one or two ligands attached to the metal ion, or dimers, in which the metal centers can be bridged through either the thiolate sulfur or the non-thiosemicarbazone coligand such as Cl$^-$, N$_3^-$, NCS$^-$, and CH$_3$COO$^-$.
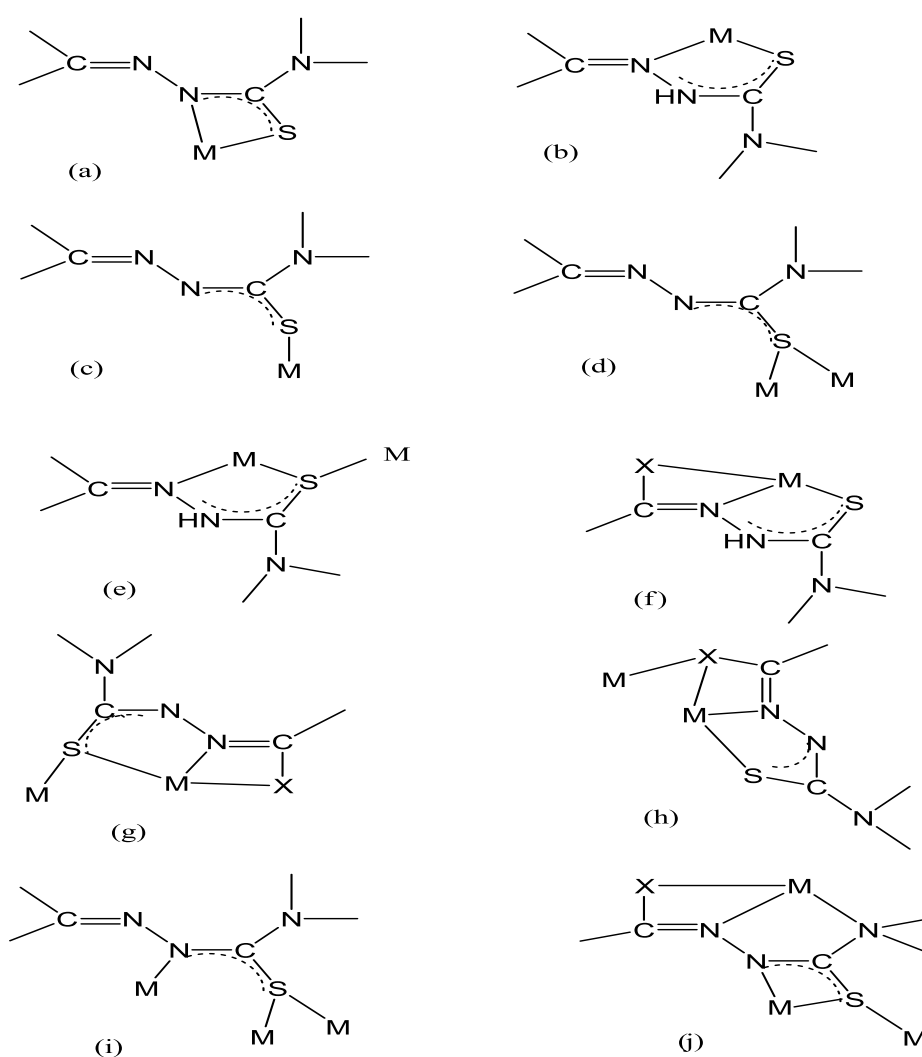
Figure 1.8: Coordination possibilities of thiosemicarbazones

1.4.2 Nickel complexes of thiosemicarbazones

In recent years, a number of researchers have been interested in investigating the biological, medicinal properties and the structure chemistry of nickel thiosemicarbazone complexes as some of them have shown a variety of biological activities like antibacterial, antimalarial, antifungal and anticancer activities. Synthesis and characterization of nickel complexes of thiosemicarbazones and evaluation of their antiproliferative properties in cancer cells and normal cells have been described (Afrasiabi et al., 2005; Ferrari et al., 2002; Pelosi, 2010).

Among the compounds tested, square planar complexes of general formula, $[Ni(NS)_2]$ (NS = anionic forms of S-citronellal thiosemicarbazone) showed a remarkable activity in apoptosis induction. These nickel complexes were able to enter the cell in significant amount, to inhibit cell proliferation and to induce apoptosis in human leukaemia cell lines (Belicchi Ferrari et al., 2010; Buschini et al., 2009).

Chen et al. (2004) and Afrasiabi et al. (2004) have discovered that nickel complexes of 1,2-naphthoquinone thiosemicarbazone are potent anticancer agents that have selective activity against human breast cancer cells. It has been proven that these nickel complexes are the most effective among the complexes studied and based on IC_{50} values, the nickel complexes are more effective than the commercial antitumor drug, etoposide. These studies suggest that nickel complexes of 1,2-naphthoquinone-2-thiosemicarbazone have an antagonizing effect on topoisomerase II activity. This evidence shows that these nickel thiosemicarbazone complexes can coordinate with topoisomerase II and stabilize the topoisomerase II DNA complexes and possibly interact with DNA by forming interhelical crosslinks. These multi inhibition mechanisms would greatly enhance cell cytotoxicity compared to that of the free ligand.

However, the disclosed effects of nickel thiosemicarbazone complexes on topoisomerase II activity are uneven. Hall et al. (1997) have shown that the dinuclear nickel complex of 2-hydroxyacetophenone thiosemicarbazone is a good cytotoxic agent inhibits the ribonucleoside reductase activity but is not an inhibitor for DNA topoisomerase II.

Another interesting approach to design new thiosemicarbazone complexes is to understand the relationship between the structures of thiosemicarbazone, its transition metal complexes and their intercalating mode to DNA. Recently, Pathan et al. (2012) synthesized and characterized new class of compounds, namely ethyl 2-(2-(4-fluorophenylcarbamothioyl) hydrazono) propanoate, and its respective copper, cobalt and nickel complexes. This study showed that the nickel complex has an intercalative mode of interaction with DNA greater than the copper and cobalt complexes.

Besides, nickel(II) complexes of pyridyl thiosemicarbazone have been prepared and screened for their antimicrobial activity by the MIC against four bacteria (*B. subtilis, S. aureus*, *E. coli* and *P. aeruginosa*). The results prove that the compounds exhibit antimicrobial properties and it is important to note that the metal chelates show more inhibitory effects than the parent ligands. The ligand-replacement abilities in these nickel complexes seem to be responsible for their enhanced biological potency (Kasuga et al., 2001).

It has been elucidated that the biological activities may also be related to the redox properties of the complexes. The redox properties include oxidation and reduction of the central metal ion and various oxidations and reduction of the ligands, and the processes involve both the central atom and the ligand (Streeky et al., 1980). Nickel(II)

complexes of acetophenone thiosemicarbazone and salicylaldehyde thiosemicarbazone as well as their N(4)-methyl and N(4)-phenyl analogues have been found to undergo one-electron reduction and oxidation to form the corresponding Ni(I) and Ni(III) compounds, which could be used as one-electron redox reagents since the Ni(I) is a strong reducing agent and the Ni(III) is strong oxidizing agent (El-Shazly et al., 2005).

The most common stereochemistries encountered in nickel thiosemicarbazone complexes are octahedral and square planar although tetrahedral and trigonal bipyramidal are also obtained. Several mononuclear nickel thiosemicarbazone complexes have been studied. Two general classes of [Ni(L)$_2$] are known. Square planar complexes containing monoanionic, bidentate thiosemicarbazone in which the ligand coordinates to nickel(II) through the imine nitrogen and the thiol sulfur. It is noteworthy that the sulfur atom and the imine nitrogen of the two ligands are in *cis* or *trans* configurations (Figure 1.9), and the stereochemistry adopted by these complexes is decided by steric effect of the groups attached at the carbonyl carbon. Lobana et al., (2008) have synthesized a series of Ni(II) complexes of furan and thiophene (N4) substituted thiosemicarbazones. The study revealed that the formation of square planar Ni(II) complexes in the *cis* or *trans* configuration depends on the furan oxygen and the thiophene sulfur bonded to the carbon of aldehyde based thiosemicarbazone. Ferrari and coworkers have determined the crystal structure of a square planar diamagnetic nickel(II) complex [Ni(fbt)$_2$] formed with the thiosemicarbazones of *p*-fluorobenzaldehyde. The complex contains two five-membered chelate rings involving two monodeprotonated *p*-fluorobenzaldehyde thiosemicarbazone ligands and the coordination about the nickel atom involves a square planarity such that the two ligands are in a *trans* configuration (Ferrari et al., 2000).

The structure of four coordinated nickel(II) complex with acetylferrocenyl thiosemicarbazone has been proven to compass NiN_2S_2 coordination environment in a distorted square planar geometry. The bulky ferrocene-containing ligands positioned on the same side forming a complex in *cis* configuration (Chen-jie et al., 2000). It has been elucidated that in the *cis*- NiN_2S_2 complexes with bulky carbonyl moieties attached to N donor atoms, the *cis* square planar geometry is distorted tetrahedrally.
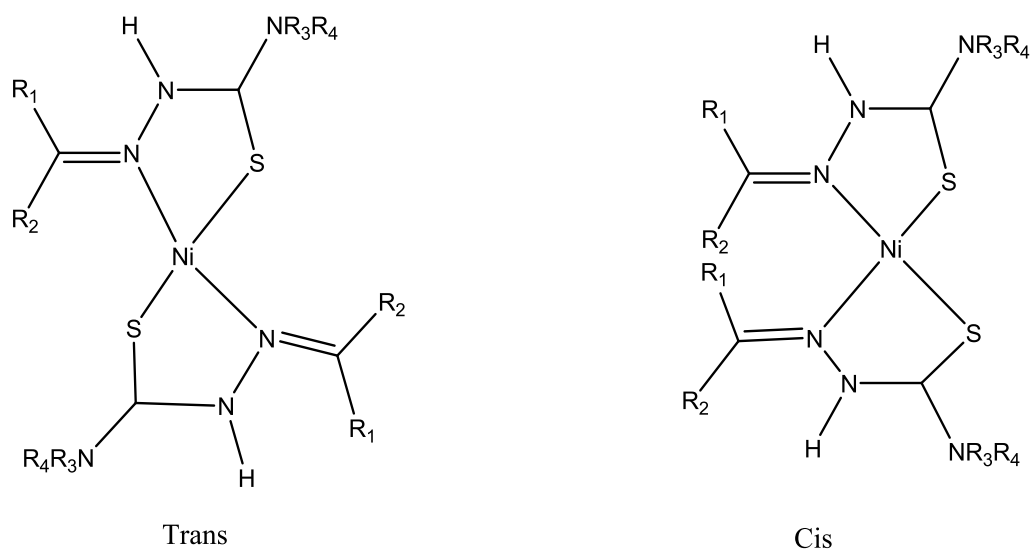
Figure 1.9: Stereochemistries of [NiL$_2$] square planar complexes

Leovac et al. (2007) found that nickel complex with the ligand 1,3-diphenylpyrazole-4-carboxaldehyde thiosemicarbazone is deviated from the regular square planar geometry in which the N-Ni-N angle is ranging from theoretical value 90° to 102.5° .

Bon et al. (2010) reported a new square planar nickel complex of salicylaldehyde 4-phenylthiosemicarbazone with different coordination mode. In this complex, one thiosemicarbazone coordinates as doubly deprotonated tridentate ligand through the thiolate sulfur, azomethine nitrogen and the phenolic oxygen whereas the other

thiosemicarbazone coordinates to nickel ion as neutral monodentate ligand via the thione sulfur.

The second class of [Ni(L)$_2$] complexes is octahedral complexes with monoanionic tridentate thiosemicarbazones. In these complexes, the ligand binds nickel(II) via azomethine nitrogen, thiol/thione sulfur and oxygen or nitrogen atoms of the parent aldehyde or ketone (Lobana et al., 2009). The crystal structures of two six coordinated nickel(II) complexes with isatin-β-thiosemicarbazone have been solved. The coordination around nickel in both complexes is found to be close to that of a distorted octahedron formed by two nitrogen atoms of hydrazine chain, two carbonylic oxygen atoms of the isatin moiety and two sulfur thiolate. In both complexes, the oxygen and sulfur atoms are *cis* to each other while the nitrogen in *trans* position (Rodriguez-Argüelles et al., 1999).

Worthy to note, the reaction of thiosemicarbazones with nickel(II) ions in a constant 1:2 molar ratio led to complexes having different structures depending on the substituent at N4 nitrogen and carbonyl carbon of the thiosemicarbazone moiety. Lobana et al. (2010) have shown that pyridyl based thiosemicarbazones coordinate as uninegative tridentate ligand to nickel(II) forming octahedral complexes while hydroxyl phenyl based thiosemicarbazones act as binegative tridentate and formed square planar complexes however, the influence of N4-methyl and N4-ethyl substituent affect the packing arrangements of the complexes by interaction of the substituent with electronegative atoms of the thiosemicarbazone moiety but did not affect the coordination environments around the nickel ion.

In addition to the [NiL$_2$] type complexes, monomeric square planar of the type [NiLY] or [NiLY]X and octahedral [Ni(HL)$_2$X]X complexes are also obtained. In the square planar complexes, the thiosemicarbazone ligand behaves as tridentate N,N,S or O,N,S donors doubly deprotonated in [NiLY] and monodeprotonated in [NiLY]X where the fourth site occupied by Cl, NCS, NO$_3$, Py or PPh$_3$ whereas the thiosemicarbazone coordinates to nickel(II) as neutral bidentate N,S donor ligand in the [Ni(HL)$_2$X]X complexes. Mathew et al. 1973 have proven that the coordination environment around nickel(II) in the [Ni(ATSC)$_2$X]$^+$ X$^-$ .H$_2$O complexes depends on the ion X. The coordination around nickel is found to be distorted octahedral formed by two nitrogen atoms, two sulfur atoms of the thiosemicarbazone group and two oxygen atoms of the NO$_3$ when acetone thiosemicarbazone was reacted with nickel(II) nitrate while the coordination environment around nickel(II) is found to be close to that of a trigonal bipyramid when nickel(II) chloride was used.

Anionic thiosemicarbazone ligands have been known to form binuclear and multinuclear complexes by bridging two or more metal ions in different ways: (i) thiolate sulfur, (ii) chelation of imine nitrogen and thiolate sulfur to one center and coordination of the hydrazinic nitrogen to the second metal centre (Durãn et al., 1999), (iii) chelation of oxygen atom from the aldehyde or ketone, (iv) chelation of thiolate sulfur and oxygen atom of the aldehyde or ketone. A number of binuclear nickel thiosemicarbazone complexes have been synthesized and characterized in which the two nickel ions are bridged by thiolate sulfur, phenolic oxygen or both of the sulfur and oxygen atoms. However, the geometry around the centre metals is square planar and octahedral.

West and coworkers reported binuclear nickel(II) complexes of a series of N-alkyl substituted derivatives of the tridentate ligand 2-hydroxyacetophenone thiosemicarbazone. In these complexes, the two square planar nickel(II) centers are coordinated to the ligand via the thiolate sulfur, the azomethine nitrogen and the phenoxy oxygen atoms which bridge to occupy the forth coordination site (West et al., 1995).

Kaminsky et al. 2002 have synthesized different nickel complex with N_2SO environment, a dinuclear complex with distorted square planar sphere around the two nickel ions. The bridging in this complex occurs by the oximato N-O resulting in a centrosymmetric arrangement of the two nickel centers.

Datta and co-workers have synthesized several mixed nickel thiosemicarbazone binuclear complexes which adopt different geometries around two nickel ions with three chelating ligands, two thiosemicarbazones and one co-ligand. One nickel center having a distorted octahedral N_3O_2S coordination sphere created by a dianionic O,N,S coordinated thiosemicarbazone, a N,N-coordinated 2,2'-bipyridine and the bridging phenolate oxygen of the other thiosemicarbazone while the other nickel center is nested in a nearly square planar NOS_2 environment created by the second dianionic O,N,S-coordinated thiosemicarbazone and the bridging sulfur of the first thiosemicarbazone. This study demonstrates that the binuclear Ni(II) complexes are good competent complexes for catalyzing the Suzuki coupling reactions (Datta et al., 2011).

Trinuclear complexes of nickel thiosemicarbazone are rare and the only known trimeric nickel thiosemicarbazone complex have been synthesized by (Berkessel et al., 1996). The X-ray structural of this complex revealed that two nickel(II) ions are in distorted

square planar geometry, while the third nickel(II) ion is in octahedral environment. The aggregation to trinuclear species occur by thiolate and phenolic bridges formation.

1.5 Thioureas

The chemistry of thioureas and their derivatives has attracted a great attention because of their interesting physiochemical properties and broad range of applications in several chemical disciplines (Koch, 2001). Thiourea moieties are valuable compounds that have been used as building blocks for the synthesis of a diversity of heterocyclic compounds whose applications in both chemistry and biology fields are numerous (Katritzky et al., 2006). The versatile and synthetically accessible of thiourea has provided the inspiration for the discovery of a number of new antitumor agents with unusual mechanisms of action in recent years. For example, Abdel-Rahman and Morsy, (2007) have synthesized a new series of thiourea derivatives of benzothiazole which displayed high cytotoxic activity against MCF7 breast cancer cells.

In addition, thioureas are well known for their usefulness in medicinal chemistry due to their biological activity as superior pesticidal, fungicidal, and antiviral and plant growth regulating activities (Wang et al., 2005). They have also been found as selective analytical reagents, especially for the separation of metal ions (Arslan et al., 2003). Recently, many researches revealed the potential hydrogen-bond (H-bond) donor capability of the N(H)-C(=S)-N(H)- group, which make the thiourea one of the most crucial events in anion sensing and recognition (Duke & Gunnlaugsson, 2007; Gunnlaugsson et al., 2005).

An attractive feature of the chemistry of thioureas is their ease and straightforward synthesis from inexpensive and readily available starting materials, usually affords high

yields of the pure products. Moreover, the ready modifications of the substituents on the nitrogen atoms of the thioureas enhance their chemical and physical properties as well as their biological activities (Liu & Jiang, 2008).

 In addition to their applications, thioureas have a long history of being used as ligand in coordination chemistry. The thiourea ligands are interesting as such compounds are much more diverse due to their conformational isomerism, steric effects and the presence of various potential donor sites including the sulfur atom of the C=S group and the nitrogen atom of the NH, NH groups (Figure 1.10 a). Beside the sulfur and nitrogen atoms, the acylthiourea derivatives of the type Ar-C(O)NHC(S)NR$_2$ consist of an oxygen atom of the carbonyl group. These hard and soft donor atoms provide a multitude bonding possibilities to a wide range of metal ions in various coordination modes in either a monodentate or bidentate chelating fashion as evidenced from infrared spectroscopy and X-ray crystal structure (Yamaguchri et al., 1958). It is also well known that thiourea ligands are reducing agents for many metal ions. They reduce Cu(II) to Cu(I), Au(III) to Au(I), and Te(IV) to Te(II) and depending on the actual thiourea ligand, they are capable of binding in a range of protonation states as neutral ligands, monoanions or dianions (Lenthall et al., 2007; Livingstone, 1965). They act as neutral, monodentate ligands through the interaction of sulfur atom and its lone pairs forming a six membered ring, and examples comprise complexes of Zn(II), Cd(II), Pd(II), Cu(I), Co(II) and Ni(II) (Saad et al., 2012). However, it has been reported that this coordination fashion is also found in the acylthiourea derivatives with intramolecular hydrogen bonding between the thiourea NH moiety and the amidic O-donor atom form (Figure 1.10b). Cernak et al.,(1991) have explored a series of copper(I) complexes with the derivatives of 2-propenoyl thiourea, Cu(PTU)$_2$Cl, Cu(ETU)$_2$Cl and Cu(BTU)$_2$Cl (PTU: R = phenyl, ETU: R = ethyl, BTU: R = benzyl in

CH$_3$CHCHCONHCSNHR). The X-ray diffraction of the complex Cu(PTU)$_2$Cl revealed two centrosymmetrical dimer molecules in which the thiourea ligand, in its neutral form, is coordinated through the sulfur atom. However, the coordination through the *sp^2* hybridized sulfur in monodentate manner has been also found in the N,N-dialkylthiourea (Asif et al., 2010).

In contrast, the N,N-disubstituted acylthiourea ligands (Figure 1.10 c), which do not form an intramolecular hydrogen bond, tend to coordinate in a bidentate S,O fashion to the transition metal ions through the sulfur and acyl oxygen atoms. It has been noted that the monoanions, S,O bidentate chelation is more common and form stable complexes with the majority of transition metal ions (Koch, 2001).

(a)

(b)   (c)
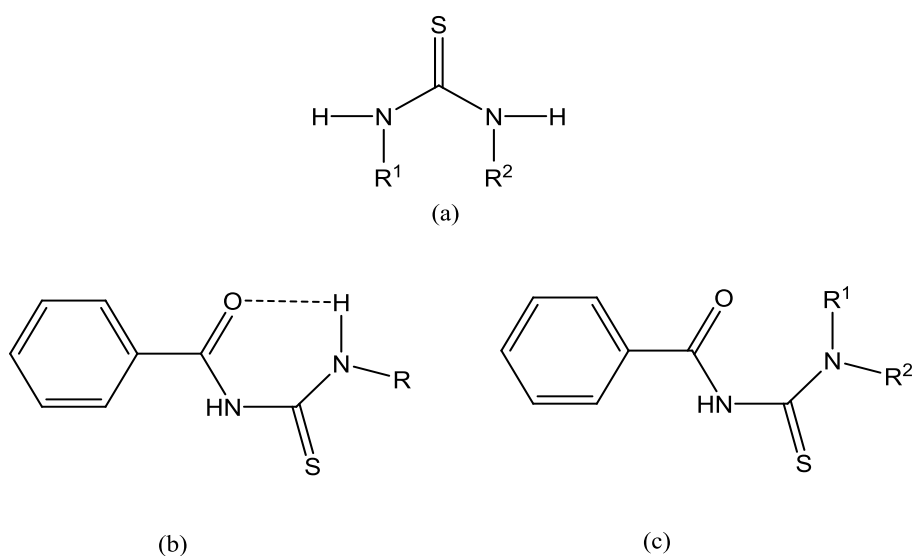
Figure 1.10: Types of thioureas

Besides, another important coordination mode of thiourea derivatives is the binding through the sulfur and nitrogen atoms in a bidentate fashion. An investigation by Kemp et al., (1997) showed that N-acylthiourea displayed another mode of coordination through doubly deprotonated N,O,S to rhodium(I). In this complex, the amidic nitrogen

atom coordinating to one Rh(I) atom, while the N-acylthiourea moiety binds to a second Rh(I) atom in the more usual bidentate S,O mode.

1.5.1 Nickel complexes of thioureas

Since the seminal work by Rosenheim and Meyer, in 1906, thiourea chelate complexes with nickel have continued to play the role of one of the most important stereochemical models in sulfur coordination chemistry due to their diversity, structural variability and remarkable applications in analytical and biological sciences. Octahedral, square planar and tetrahedral geometries are all plausible with nickel(II), and in the case of thiourea complexes, all occur. Meanwhile, the bonding of thioureas to nickel(II) occurs through monodentate sulfur, bidentate sulfur and nitrogen, bidentate sulfur and oxygen and sulfur bridging between metal centers (Figure 1.11). The stability of the nickel complexes with different geometries depends on steric and electronic factors. The presence of bulky ligands, allow the thioureas to coordinate to nickel(II) in a tetrahedral mode more favorable than octahedral form. However, the electronic interactions of the ligand with nickel(II) is a more significant factor affecting the geometry of nickel thiourea complexes (Eaton & Zaw, 1972).

Infrared spectroscopy, visible spectroscopy and magnetic susceptibility techniques, in combination with X-ray crystallography, have greatly improved the understanding of the nature of nickel-thiourea ligands interactions. Several nickel thiourea complexes have been synthesized in which the thiourea coordinated to nickel(II) via monodentate sulfur in octahedral environment. Weininger et al. 1968 have reported the first X-ray crystal structure of nickel thiourea complexes of the series $[M(tu)_6]X_2$. The structure of this complex consists of $Ni[SC(NH_2)_2]^{+2}$ molecular ions and Br^- ions where the nickel

atom is located on a center of symmetry and is coordinated to six sulfur atoms in a distorted octahedral.
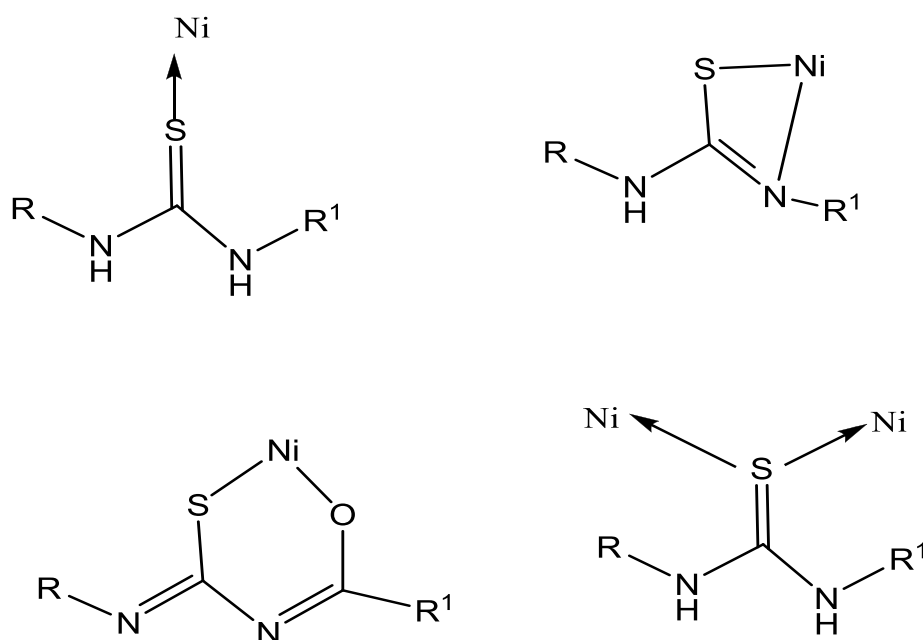
Figure 1.11: Coordination possibilities of thioureas to nickel(II) ion

In addition to the structural diversity, the coordination chemistry of nickel thiourea complexes is of considerable interest due to their biological and catalytic applications. Nickel(II) complexes of the thiourea derivatives of N-butylmethylamine and N-ethylisopropylamine have been reported (del Campo et al., 2004). The complexes have the general formula [NiL$_2$]. Infrared spectra indicate that in both complexes, square planar structures have been assigned for nickel(II) complexes where the ligand acts as a monoanion bidentate ligand coordinating through one of the sulfur atoms and the oxygen atom of the benzoyl moiety. These nickel complexes were shown to have considerable inhibitory activity against fungus *Penicillium digitatum* and against the yeast *Saccharomyces cerevisiae*.

1.6 Objectives and scope of the present work

Transition metal complexes with nitrogen/sulfur donor ligands have gained so much attention in recent years due to their structural chemistry and their wide biological activities against bacteria, fungi and some types of tumors. Generally, nitrogen/sulfur donor ligands are good therapeutic agents and complexation with metal ions enhances their biological activity. The interest in the chemistry of nickel nitrogen/sulfur complexes has increased since the discovery of nickel metalloenzymes in rich nitrogen and sulfur environments; however, the significance of nitrogen/sulfur complexes with nickel is not limited to bioinorganic chemistry. They are also an important class of compounds due to the capability of nickel to bind both soft and hard ligands forming a variety of complexes with different geometries, coordination numbers and oxidation states.

The wide applications and structural diversity of metal complexes of thiosemicarbazones and thioureas, important class of nitrogen and sulfur donor ligands, prompted me to synthesize the nickel complexes of O,N,S and N,N,S donor ligands. I have taken the task with the following objectives:

- Synthesize nickel(II) complexes of O,N,S and N,N,S mixed with triphenylphosphine and polypyridyl ligands.

- Study the coordination chemistry of these ligands with nickel.

- Explore the structures adapted by these compounds through single crystal X-ray diffraction studies.

- Study the effect of the ligands and their complexes on the inhibition of topoisomerase I.

CHAPTER 2

Synthesis and characterization of nickel(II) complexes of 2,3-dihydroxybenzaldehyde-*N*4-substituted thiosemicarbazones

2.1 Introduction

Nickel exhibits a wide variety of oxidation states from -I to IV and occurs widely in biological systems. However, the nickel(II) state ($3d^8\ 4s^0\ 4p^0$), is significantly more common and is extensively involved in most of nickel complexes. Investigations in coordination chemistry of nickel(II) continue to be of interest in developing synthetic models for nickel metalloenzymes and in understanding factors, which give rise to a variety of stereochemistries observed in nickel(II) complexes. The coordination geometry around the nickel center and the physical properties of the complexes are defined through the interactions between the central atom and the ligands and in many of the nickel complexes, the *d* electrons are significantly delocalized over the ligand orbital's. Generally, nickel(II) forms octahedral, tetrahedral and square planar complexes. Occasionally, square pyramidal and trigonal bipyramidal species also form (Macgregor et al., 1994). Besides, bridged complexes in which two or more Ni(II) ions are linked by sulfur, oxygen, nitrogen atoms or anionic ligands are also reported (Datta et al., 2011; Mahendrasinh et al., 2011). Nickel(II) ion is considered to be a borderline metal ion with respect to hardness or softness of transition metal ions. Consequently, nickel(II) has the ability to bind both hard and soft ligands. In the last two decades, there has been a considerable interest in the investigation of nickel complexes with sulfur and nitrogen containing ligands and it has been shown that many of them show biological activities (Afrasiabi et al., 2004; Ferrari et al., 2000).

Thiosemicarbazones are among the most efficacious S,N-donor ligands which have been used as drugs and they are reported to possess a wide variety of biological

activities against bacteria, fungi and certain type of tumors. Biological activities of metal complexes differ from those of ligands and metal ions and are influenced by the nature of the metal ion, its oxidation state, the types and number of bound ligands and isomers of the complex. According to some reports, nickel(II) complexes with tridentate thiosemicarbazone ligands exhibit different antibacterial activities depending on the number of the coordinated ligands around nickel(II) ion (Kasuga et al., 2001). The substituted derivatives of salicylaldehyde thiosemicarbazone and their complexes with different metal ions have been widely studied (Bon et al., 2010; Latheef et al., 2008; Latheef et al., 2009; Seena et al., 2007) and their interaction with enzymes such as ribonucleotide reductase (Dilovic´ et al., 2008; Noblı´a et al., 2005) and DNA polymerase (Kalaivani et al., 2012; Prabhakaran et al., 2008) have been elucidated. In contrast to the salicylaldehyde thiosemicarbazone, less studies have been focused on complexation behavior and biological activities of polyhydroxybenzaldehyde thiosemicarbazone derivatives (Swesi et al., 2007; Tan et al., 2012; Zhu et al., 1997).

Therefore, this chapter describes the synthesis, spectral, and structure characterization of nickel(II) complexes of 2,3-dihydroxybenzaldehyde-N4-substituted thiosemicarbazones.

2.2 Experimental

2.2.1 Materials and solutions

Thiosemicarbazide, 4-methylthiosemicarbazide, 4-phenylthiosemicarbazide, 4-ethylthiosemicarbazide, 2,3-dihydroxybenzaldehyde and nickel(II) perchlorate hexahydrate were purchased from Sigma-Aldrich. Nickel(II) chloride hexahydrate, nickel(II) acetate tetrahydrate and 2,2'-bipyridine were from Merck. The reagents used were of analytical grade and used without further purification.

The complex [NiCl$_2$(Bpy)$_2$] was prepared following the procedure described by (Brewer et al., 2003) as follows: 2,2'-Bipyridine (0.87 g, 5.6 mmol) in 20 ml hot absolute ethanol was added to a hot solution of nickel(II) chloride hexahydrate (2.10 g, 7.7 mmol) in absolute ethanol. The green solution was stirred and refluxed for 2 hours. The green precipitate was filtered and washed with absolute ethanol and dried in a desiccator.

2.2.2 Physical measurements

IR spectra were recorded as KBr pellets by using a Perkin-Elmer Spectrum RX-1 spectrophotometer. ^{1}H NMR and ^{13}C NMR spectra were recorded in DMSO-d$_6$ on a JEOL JNM-LA400 or ECA 400 MHz instrument. Elemental analyses were performed on a Pelkin-Elmer Analyst 400. UV–visible spectroscopic measurements were carried out on Shimadzu UV-3600PC spectrophotometer.

2.2.3 Syntheses

The ligand was synthesized by following the procedure reported by (Swesi et al., 2007).

2.2.3.1 Synthesis of 2,3-dihydroxybenzaldehyde thiosemicarbazone, H$_3$L^1 (1)

Thiosemicarbazide (0.91 g, 10 mmol) and 2,3-dihydroxybenzaldehyde (1.38 g, 10 mmol) were heated in methanol (20 mL) for 4h. Slow evaporation of the solvent yielded off-white crystals. The crystals were filtered, washed with cold methanol and ether, dried in air and kept in a desiccator over silica gel.

(Yield: 1.75 g, 83%). Anal. Calc. for C$_8$H$_9$N$_3$O$_2$S: C, 45.49; H, 4.29; N, 19.89; S, 15.18. Found: C, 45.10; H, 4.09; N, 19.85; S, 14.89%. IR (KBr disc, cm^{-1}): 3368 s, 3288 s, 3259 s , 3177 s, 1611 m, 1584 m, 1559 w, 1508 m, 1474 s, 1340 m, 1279 s, 1249 m,

1200 m, 1160 w, 1104 m, 982 s, 934 w, 825 m, 790 w, 736 m, 574 m 417 w (s, strong; m, medium ; w, weak).

Characteristic ^{1}H NMR signals (DMSO-d$_6$, TMS, p.p.m.): 11.36 (s, 1H, NHCS), 9.22 (s, 2H, OH), 8.38 (s, 1H, CH=N), 8.08 (s, 1H, NH$_2$), 7.86 (s, 1H, NH$_2$), 7.35 (d, 1H, aromatic, J = 7.8 Hz), 6.80 (d, 1H, aromatic, J = 7.8 Hz), 6.63 (t, 1H, aromatic). Characteristic ^{13}C NMR signals (DMSO-d$_6$, TMS, p.p.m.): 178. 06 (C=S), 146.04 (C-O), 145.70 (C-O), 140.81 (C=N), 121.41, 119.61, 117.60, 116.94 (C-aromatic).

2.2.3.2   Synthesis   of   2,3-dihydroxybenzaldehyde-4-methylthiosemicarbazone, H$_3$L^2 (2)

4-Methylthiosemicarbazide (1.10 g, 10 mmol) and 2,3-dihydroxybenzaldehyde (1.38 g, 10 mmol) were heated in methanol (20 mL) for 2h. The white solid was filtered, washed with cold methanol and ether, dried in air and kept in a desiccator over silica gel.

(Yield: 1.79 g, 80%). Anal. Calc. for C$_9$H$_{11}$N$_3$O$_2$S: C, 47.99; H, 4.92; N, 18.65; S, 14.23. Found: C, 48.11; H, 5.08; N, 18.20; S, 14.46%. IR (KBr disc, cm^{-1}): 3453 m, 3421 w, 3150 m, 2999 m, 1573 s, 1475 m, 1389 m, 1326 w, 1290 m, 1268 s, 1228 w, 1214 m, 1166m, 1115 w, 1067 m, 1043 m, 930 w, 853 w, 777 w, 727 m, 603 w, 555 w, 483w (s, strong; m, medium ; w, weak).

Characteristic ^{1}H NMR signals (DMSO-d$_6$, TMS, p.p.m.): 11.41 (s, 1H, NHCS), 9.26 (s, 2H, OH), 8.38(s, 1H, CH=N), 8.39 (s, 1H, *NH*CH$_3$), 7.38 (d, 1H, aromatic, J = 7.8 Hz), 6.81 (dd, 1H, aromatic, J = 7.8 Hz), 6.66 (t, 1H, aromatic), 3.01 (d, 3H, NH*CH$_3$*, J = 4.1 Hz). Characteristic ^{13}C NMR signals (DMSO-d$_6$, TMS, p.p.m.): 178.01 (C=S), 146.09 (C-O), 145.69 (C-O), 140.19 (C=N), 121.56, 119.54, 117.53, 116.83 (C-aromatic), 31.38 (N-CH$_3$).

2.2.3.3 Synthesis of 2,3-dihydroxybenzaldehyde-4-phenyl thiosemicarbazone, H₃L³ (3)

4-Phenylthiosemicarbazide (1.67 g, 10 mmol) and 2,3-dihydroxybenzaldehyde (1.38 g, 10 mmol) were heated in methanol (20 mL) for 4h. The white precipitate which formed was filtered, washed with cold methanol and ether, dried in air and kept in a desiccator over silica gel.

(Yield: 2.49 g, 87%). Anal. Calc. for $C_{14}H_{13}N_3O_2S$: C, 58.52; H, 4.56; N, 14.62; S, 11.16. Found: C, 58.43; H, 4.44; N, 14.30; S, 10.95%. IR (KBr disc, cm^{-1}): 3449 m, 3394m, 3139 m, 2985 m, 1542 s, 1516 s, 1490 w, 1472 m, 1389 w, 1327 m, 1289 w, 1266 s, 1225 m, 1203 s, 1064 w, 931 w,850 w, 779 w, 754 w, 721 m, 692 m, 638 w, 481 w, 443 w (s, strong; m, medium ; w, weak).

Characteristic ^{1}H NMR signals (DMSO-d$_6$, TMS, p.p.m.): 11.78 (s, 1H, NHCS), 10.03 (s, 1H, N*H*C$_6$H$_5$), 9.55 (s, 1H, OH), 9.06 (s, 1H,OH), 8.52 (s, 1H, CH=N), 7.59 (d, 1H, aromatic, J = 7.6 Hz), 7.51 (d, 1H, aromatic, J = 7.1 Hz), 7.37 (t, 2H, aromatic), 7.20 (t, 1H, aromatic), 6.85 (d-d, 1H, aromatic, J = 7.8 Hz), 6.68 (t, 1H, aromatic). Characteristic ^{13}C NMR signals (DMSO-d$_6$, TMS, p.p.m.): 176.20 (C=S), 146.09 (C-O), 145.97 (C-O), 141.26 (C=N), 139.67, 128.58, 126.14, 125.70, 121.30, 119.58, 118.00, 117.15 (C-aromatic).

2.2.3.4 Synthesis of 2,3-dihydroxybenzaldehyde-4-ethylthiosemicarbazone, H₃L⁴ (4)

4-Ethylthiosemicarbazide (1.19 g, 10 mmol) and 2,3-dihydroxybenzaldehyde (1.38 g, 10 mmol) were heated in methanol (20 mL) for 4h. Slow evaporation of the solvent yielded white precipitate. The solid was filtered, washed with cold methanol and ether, dried in air and kept in a desiccator over silica gel.

(Yield: 2.03 g, 85%). Anal. Calc. for $C_{10}H_{13}N_3O_2S$: C, 50.19; H, 5.48; N, 17.56; S, 13.40. Found: C, 50.47; H, 5.28; N, 17.70; S, 13.74%. IR (KBr disc, cm^{-1}): 3455 m, 3136 m, 2981m, 1542 s, 1473 m, 1384 m, 1307 m, 1267 s, 1241 s, 1209 s, 1164 m, 1117 w, 1067 w, 1051 w, 931 w, 807 w, 776 w, 725 m, 616 w, 549 w, 519 w (s, strong; m, medium ; w, weak).

Characteristic ^1H NMR signals (DMSO-d$_6$, TMS, p.p.m.): 11.36 (s, 1H, NHCS), 9.52 (s, 1H, OH), 8.95 (s, 1H, OH), 8.41 (t, 1H, N*H*CH$_2$), 8.38 (s, 1H, CH=N), 7.37 (d, 1H, aromatic, J = 7.8 Hz), 6.81 (d-d, 1H, aromatic, J = 7.7 Hz), 6.66 (t, 1H, aromatic), 3.58 (q, 2H, NHC*H$_2$*-) 1.14 (t, 3H, NCH$_2$C*H$_3$*). Characteristic ^{13}C NMR signals (DMSO-d$_6$, TMS, p.p.m.): 176.64 (C=S), 145.69 (C-O), 145.31 (C-O), 139.90 (C=N), 121.10, 119.09, 117.17, 116.43 (C-aromatic), 38.29 (N-CH$_2$-), 14.62 (NCH$_2$*C*H$_3$).

2.2.3.5 Synthesis of [Ni(H$_3$L^1)(H$_2$L^1)]ClO$_4$.2H$_2$O (5)

To a colorless solution of 2,3-dihydroxybenzaldehyde thiosemicarbazone H$_3$L^1 (0.21 g, 1 mmol) in ethanol (15 mL) was added an ethanolic solution of Ni(ClO$_4$)$_2$.6H$_2$O (0.36 g, 1 mmol). The color of the solution changed to dark green and the contents were stirred for about 4h under reflux. The clear solution after filtration was left for slow evaporation at room temperature.

(Yield: 0.20 g, 68 %). Anal. Calc. for $C_{16}H_{17}N_6O_8S_2ClNi.2H_2O$: C, 31.21; H, 3.44; N, 13.65. Found: C, 31.40; H, 3.12; N, 13.98 %. IR (KBr disc, cm^{-1}): 3366 s, 3287 s, 3185 s, 2969 w, 2892 w, 1616 s, 1577 m, 1459 m, 1420 s, 1335 s, 1270 m, 1227 m, 1213 m, 1173 m, 1143 s, 1112 s, 1087 s, 945 m, 859 w, 779 s, 739 m, 713 w, 671 w, 626 m, 569 m, 553 w, 523 w, 467 m (s, strong; m, medium ; w, weak).

2.2.3.6 Synthesis of [Ni(H$_3$L^2)(H$_2$L^2)]ClO$_4$.2H$_2$O (6)

Complex **6** was similarly prepared as complex **5** by using 2,3-dihydroxybenzaldehyde 4-methylthiosemicarbazone H$_3$L^2 (0.23 g, 1 mmol) as a ligand.

(Yield: 0.23 g, 72%). Anal. Calc. for C$_{18}$H$_{21}$N$_6$O$_8$S$_2$ClNi.H$_2$O: C, 34.55; H, 3.71; N, 13.43. Found: C, 34.37; H, 4.44; N, 13.29 %. IR (KBr disc, cm^{-1}): 3368 s, 2973 s, 2902 m, 1610 m, 1584 s, 1459 m, 1400 w, 1377 w, 1342 m, 1314 m, 1272 m, 1229 m, 1146 m, 1112 m, 1086 s, , 1052 s, 953 w, 879 m, 861 m, 798 m, 732 m, 627 m, 581 w, 474 w (s, strong; m, medium ; w, weak).

2.2.3.7 Synthesis of [Ni(H$_3$L^3)(H$_2$L^3)]ClO$_4$ (7)

A warm ethanolic solution (10 ml) of Ni(ClO$_4$)$_2$.6H$_2$O (0.36g, 1 mmol) was added to a warm solution of 2,3-dihydroxybenzaldehyde-4-phenylthiosemicarbazone, H$_3$L^3 (0.29 g, 1mmol) in an ethanol/CH$_3$CN mixture (20/5 mL). The solution was refluxed for 2h with stirring. On adding 10 mL H$_2$O, a green coloured complex precipitated out. It was filtered, washed with ethanol and dried in air and kept in a desiccator over silica gel.

(Yield: 0.23 g, 64%). Anal. Calc. for C$_{28}$H$_{25}$N$_6$O$_8$S$_2$ClNi: C, 45.95; H, 3.44; N, 11.49. Found: C, 46.01; H, 3.49; N, 11.40 %. IR (KBr disc, cm^{-1}): 3247 m, 2970 m, 1607 m, 1545 s, 1497 m, 1452 m, 1414m, 1324 m, 1264 s, 1203 s, 1170 w, 1061 s, 929 w, 883 m, 850 m, 773 m, 693 m, 622 m, 569 w, 484 w, 455 w (s, strong; m, medium ; w, weak).

2.2.3.8 Synthesis of [Ni(H$_3$L^4)(H$_2$L^4)] ClO$_4$.H$_2$O (8)

Complex **8** was similarly prepared as complex **5** by using 2,3-dihydroxybenzaldehyde 4-ethylthiosemicarbazone, H$_3$L^4(0.24 g, 1 mmol) as a ligand.

(Yield: 0.23 g, 72%). Anal. Calc. for C$_{20}$H$_{25}$N$_6$O$_8$S$_2$NiCl.H$_2$O: C, 36.74; H, 4.16; N, 12.86. Found: C, 36.88; H, 4.05; N, 12.84 %. IR (KBr disc, cm^{-1}): 3322 s, 3136 m,

3276 s, 3056 m, 2980 m, 2933w, 2875 w, 1606 s, 1571 s, 1458 s, 1340 s, 1301 s, 1280 s, 1229 m, 1170 m, 1141 s, 1109 m, 1088 s, 1048 m, 936 m, 857 m, 780 m, 732 m, 698 w, 629 m, 569 m, 464 w (s, strong; m, medium ; w, weak).

Crystals suitable for X-ray analysis were obtained by slow evaporation of a solution of the compound in ethanol. The complex **8** crystallized as $[Ni(H_3L^4)(H_2L^4)]_2$ $(ClO_4)_2.2H_2O$ (**8a**).

2.2.3.9 Synthesis of $[Ni(H_2L^1)_2][Ni(H_3L^1)_2]Cl_2.H_2O$ (9)

This complex was prepared by adding a hot and filtered solution of $[Ni(bpy)Cl_2]$ (0.33g, 1 mmol) in methanol (10) ml to a hot solution of (20 mL) of 2,3-dihydroxybenzaldehyde thiosemicarbazone H_3L^1 (0.21 g, 1 mmol) in methanol with constant stirring. The mixture was heated under reflux for 4 h. The dark green solution was filtered and kept at room temperature. The crystals which separated after several days were washed with little amount of methanol and dried in air and kept in a desiccator over silica gel.

(Yield: 0.27 g, 53%). Anal. Calc. for $C_{32}H_{33}N_{12}O_8S_4Cl_2Ni_2.H_2O$: C, 36.67; H, 3.37; N, 16.03. Found: C, 36.08; H, 3.35; N, 15.84 %. IR (KBr disc, cm^{-1}): 3366 s, 3278 s, 3176 s, 2969 m, 2883 m, 1611 s, 1580 s, 1561 s, 1459 m, 1419 s, 1332 s, 1266 m, 1220 m, 1172 m, 1157 m, 1095 m, 1042 m, 953 m, 855 m, 778 s, 739 m, 670 w, 610 m, 569 m, 548 m, 467 m (s, strong; m, medium ; w, weak).

Green crystals suitable for X-ray analysis were obtained by slow evaporation of a solution of the compound in methanol. The complex **9** crystallized as $[Ni(H_3L^1)(H_2L^1)]_2$ $Cl_2.H_2O$ (**9a**) and the relatively high R-factors of **9a** are due to the bad quality of the crystal. All attempts to get better quality crystals failed.

2.2.3.10 Synthesis of $[Ni(H_2L^2)_2][Ni(H_3L^2)_2]Cl_2.H_2O$ (10)

Complex **10** was similarly prepared as complex **9** by using 2,3-dihydroxybenzaldehyde 4-methylthiosemicarbazone, H_3L^2(0.23 g, 1 mmol) as a ligand.

(Yield: 0.28 g, 51%). Anal. Calc. for $C_{36}H_{41}N_{12}O_8S_4Cl_2Ni_2.H_2O$: C, 39.15; H, 3.92; N, 15.22. Found: C, 38.68; H, 3.91; N, 15.07 %. IR (KBr disc, cm^{-1}): 3246 s, 2973 m, 2873 m, 1609 m, 1581 s, 1460 m, 1399 m, 1341 s, 1309 s, 1267 s, 1220 m, 1121 w, 1079 w, 1037 m, 953 w, 861 m, 784 m, 736 m, 655 w, 618 w, 581 w, 474 w (s, strong; m, medium ; w, weak).

2.2.3.11 Synthesis of $[Ni(H_2L^3)_2][Ni(H_3L^3)_2]Cl_2$ (11)

Complex **11** was similarly prepared as complex **9,** using 2,3-dihydroxybenzaldehyde 4-phenylthiosemicarbazone, H_3L^3(0.29 g, 1 mmol) as a ligand.

(Yield: 0.43 g, 65%). Anal. Calc. for $C_{56}H_{49}N_{12}O_8S_4Cl_2Ni_2$: C, 50.40; H, 3.70; N, 12.59. Found: C, 50.58; H, 3.74; N, 12.65 %. IR (KBr disc, cm^{-1}): 3327 m, 3200 m, 2973 s, 2901 w, 1604 m, 1558 s, 1498 m, 1459 m, 1451 m, 1425 m, 1411 m, 1329 s, 1302 s, 1275 s, 1224 m, 1171 w, 1142 m, 1081 m, 1047 m, 954 w, 880 m, 849 m, 775 m, 727 m, 703 m, 646 w, 578 w, 495 w, 427 w (s, strong; m, medium ; w, weak).

2.2.3.12 Synthesis of $[Ni(H_2L^4)_2][Ni(H_3L^4)_2]Cl_2.H_2O$ (12)

Complex **12** was similarly prepared as complex **9,** using 2,3-dihydroxybenzaldehyde 4-ethylthiosemicarbazone, H_3L^4(0.24 g, 1 mmol) as a ligand.

(Yield: 0.37 g, 66%). Anal. Calc. for $C_{40}H_{49}N_{12}O_8S_4Cl_2Ni_2.H_2O$: C, 40.40; H, 4.43; N, 14.48. Found: C, 40.77; H, 4.38; N, 14.21%. IR (KBr disc, cm^{-1}): 3221 s, 3048 m, 2979 m, 2932 w, 2877 w, 1608 m, 1572 s, 1461 m, 1424 m, 1376 m, 1341 m, 1278 m, 1223 m, 1169 w, 1120 w, 1085 m, 1049 m, 936 w, 859 w, 779 m, 736 m, 690 w, 661 w, 580w, 473 w (s, strong; m, medium ; w, weak).

2.2.3.13 Synthesis of [Ni$_2$(HL^1)$_2$] (13)

2,3-Dihydroxybenzaldehyde thiosemicarbazone, H$_3$L^1 (0.42 g, 2 mmol) was dissolved in 20 mL ethanol. To this, Ni(OAc)$_2$.4H$_2$O (0.248 g, 1 mmol) dissolved in ethanol was added. The mixture was refluxed for 2h. The red solid which precipitated out was filtered and washed thoroughly with water and ethanol and then with ether and dried in air and kept in a desiccator over silica gel.

(Yield: 0.33 g, 62%). Anal. Calc. for C$_{16}$H$_{14}$N$_6$O$_4$S$_2$Ni$_2$: C, 35.86; H, 2.63; N, 15.68. Found: C, 35.54; H, 2.53; N, 15.50%. IR (KBr disc, cm^{-1}): 3434 s, 3330 s, 3190 m, 2972 m, 2900 w, 1601 s, 1525 s, 1457 s, 1404 s, 1331 s, 1320 s, 1265 m, 1226 s, 1049 m, 939 w, 920 w, 876 m, 739 m, 737 m, 590 m, 546 w, 487w, 437 m (s, strong; m, medium ; w, weak).

2.2.3.14 Synthesis of [Ni(H$_2$L^2)$_2$].H$_2$O (14)

Complex **14** was similarly prepared as complex **13,** using 2,3-dihydroxybenzaldehyde 4-methylthiosemicarbazone H$_3$L^2(0.46 g, 2 mmol) as a ligand.

(Yield: 0.40 g, 70%). Anal. Calc. for C$_{18}$H$_{18}$N$_6$O$_4$S$_2$Ni$_2$.H$_2$O: C, 37.15; H, 3.46; N, 14.44 Found: C, 37.12; H, 3.13; N, 14.08%. IR (KBr disc, cm^{-1}): 3346 s, 3232 m, 3056 m, 1591 s, 1559 s, 1458 s, 1401 m, 1333 m, 1260 m, 1229 s, 1118 w, 1090 w, 1037 m, 951 w, 865 m, 788 m, 736 m, 671 w, 447 w (s, strong; m, medium ; w, weak).

2.2.3.15 Synthesis of [Ni(H$_2$L^3)$_2$] (15)

Complex **15** was similarly prepared as complex **13,** using 2,3-dihydroxybenzaldehyde 4-phenyllthiosemicarbazone, H$_3$L^3(0.58 g, 2 mmol) as a ligand.

(Yield: 0.50 g, 73%). Anal. Calc. for C$_{28}$H$_{22}$N$_6$O$_4$S$_2$Ni$_2$: C, 48.88; H, 3.22; N, 12.21. Found: C, 48.76; H, 3.80; N, 12.12%. IR (KBr disc, cm^{-1}): 3221 s, 3384 m, 3291 m, 3056 w, 1597 m, 1559 m, 1467 m, 1363 s, 1263 m, 1225 s, 1178 w, 1095 m, 1027 w,

1004 w, 908 w, 892 w, 844 w, 810 w, 775 m, 737 m, 728 m, 697 m, 661 w, 597w, 554 w, 520 w, 424 w (s, strong; m, medium ; w, weak).

2.2.3.16 Synthesis of [Ni$_2$(HL^4)$_2$] (16)

Complex **16** was similarly prepared as complex **13,** using 2,3-dihydroxybenzaldehyde 4-ethylthiosemicarbazone, H$_3$L^4(0.24 g, 1 mmol) as a ligand.

(Yield: 0.22 g, 76%). Anal. Calc. for C$_{20}$H$_{22}$N$_6$O$_4$S$_2$Ni$_2$: C, 40.58; H, 4.75; N, 14.20. Found: C, 40.74; H, 3.89; N, 14.23%. IR (KBr disc, cm^{-1}): 3221 s, 3292 s, 2971 s, 2932 w, 1595 s, 1554 s, 1458 s, 1393 m, 1316 m, 1206 m, 1230 s, 1155 m, 1098 m, 1066 w, 1046 s, 944 m, 875m, 834 w, 779 m, 734 s, 684 w, 576 w, 521w, 483 w, 445 w (s, strong; m, medium ; w, weak).

2.2.4 X-ray crystallography

X-ray quality crystals were produced for two nickel thiosemicarbazone complexes. Green crystals of dimension and structure suitable for X-ray diffraction analysis for complexes **8** and **9** were grown by slow evaporation of the mother liquors. Single crystal determinations were carried out using a Bruker SMART APEX CCD diffractometer at 100 K using graphite monochromated Mo K$_\alpha$ (λ = 0.71073 Å) radiation. The structures were solved and refined by SHELXL97 (Sheldrick, 2008). The data were corrected using SADABS (Sheldrick, 1996). The APEX2 software was used for data acquisition and the SAINT software for cell refinement and data reduction (Bruker, 2007). Molecular graphics were drawn by using ORTEP (Farrugia, 1997) and PLATON (Spek, 2003). Material for publication was prepared using publCIF (Westrip, 2009). The structures were solved by direct-methods and least squares refinement on F2 was used for all reflections with anisotropic displacement parameters for non-hydrogen atoms. In all cases, hydrogen atoms were located then placed in theoretical positions.

2.3. Results and discussion

2.3.1 Synthesis of nickel complexes

The structure for all thiosemicarbazone ligands used in the formation of nickel thiosemicarbazone complexes and their IUPAC numbering scheme are shown in Figure 2.1. The ligands were prepared by the method described by (Swesi et al., 2007) and purified by recrystallization from methanol and were characterized by elemental analysis ,^{1}H NMR, ^{13}C NMR and IR spectroscopy. The analytical and spectroscopic data are consistent with the proposed structures given in Figure 2.1. The nickel(II) complexes with thiosemicarbazone ligands were obtained in yields ranging from 51-76%. The stoichiometries, partial elemental analysis and colors are shown in Table 2.1. Mononuclear complexes **5**, **6**, **7** and **8** of the general formula [Ni(H$_3$L)(H$_2$L)]ClO$_4$, were prepared by the reaction of thiosemicarbazone ligands with Ni(ClO$_4$)$_2$.6H$_2$O in molar ratio 1:1 (Scheme 2.1). In all mononuclear nickel(II) complexes of 2,3-dihydroxybenzaldehyde N4-substituted thiosemicarbazone of the formula [Ni(H$_3$L)(H$_2$L)]ClO$_4$, it has been noted that the two thiosemicarbazones behaved as tridentate ONS chelating ligands in the thione form as evidenced by the IR spectra and X-ray analysis. Furthermore, one of the ligands is coordinated in its neutral form through the thione sulfur, azomethine nitrogen and the phenol oxygen while the other ligand is coordinated in its monodeprotonated form through the thione sulfur, azomethine nitrogen and phenolic oxygen. However, all these complexes are green in color, air stable and non-hygroscopic in nature but the brightness of the crystals decreases when the crystals were taken out of the solution. They are insoluble in water, soluble in methanol, ethanol, dichloromethane, DMF and DMSO and partially soluble in acetonitrile and chloroform. Some of them contain lattice water as evidenced by single crystal X-ray diffraction study. Magnetic moment measurement indicates the paramagnetic nature of these nickel(II) complexes showing a room temperature

magnetic moment in the range 2.92 - 3.08 B.M indicating that the coordination geometry around nickel(II) complexes to be octahedral. This value agrees well with reported values of several octahedral Schiff bases of Ni(II) complexes (Chandra & Kumar, 2007; Patil et al., 2010; West et al., 1998).

Dimeric complexes **9**, **10**, **11** and **12** were obtained by the reaction of thiosemicarbazone ligands with Ni(II) precursor complex, [Ni(bpy)Cl$_2$]. The thiosemicarbazone ligands in this reaction replaces one 2,2'-bipyridine ligand and two chloride ions from the precursor, forming octahedral complexes of the general formulation [Ni(H$_2$L)$_2$][Ni(H$_3$L)$_2$]Cl$_2$ as shown in Scheme 2.1. The two thiosemicarbazone ligands in these complexes coordinate as ONS tridentate ligand through phenol/phenolic oxygen, azomethine nitrogen and thione/thiol sulfur.

However, binuclear nickel complexes, **13**,**14**,**15** and **16**, of 2,3-dihydroxybenzaldehyde-N4-thiosemicarbazones were prepared by the reaction of the ligands with Ni(OAc)$_2$.4H$_2$O in molar ratio 2:1 (ligand : metal) for **13**, **14** and **15**. The reaction of ethyl substituted thiosemicarbazone with Ni(OAc)$_2$.4H$_2$O in molar ratio 2:1 did not yield any product, thus, complex **16** was prepared using 1:1 molar ratio (Scheme 2.1) These complexes are soluble in DMF and DMSO, but insoluble in other commonly used organic solvents. The room temperature magnetic moment of these complexes were found to be zero, indicating that these complexes are diamagnetic, suggesting a four coordinate square planar geometry for them. Unfortunately, attempts to grow suitable crystals for X- ray crystal structure determination for the series of binuclear complexes were not successful.
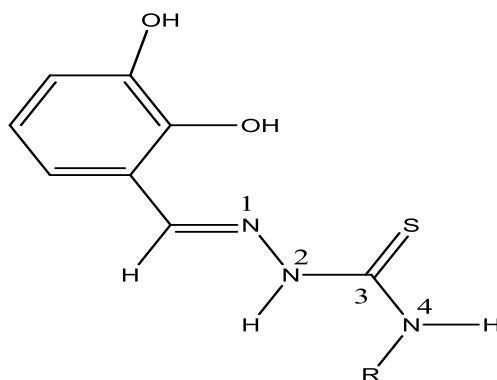
H_3L^1; R= H, H_3L^2; R= CH_3, H_3L^3; R= C_6H_5, H_3L^4; R = C_2H_5

Figure 2.1: Chemical structure of 2,3-dihydroxybenzaldehyde-N4- substituted thiosemicarbazone
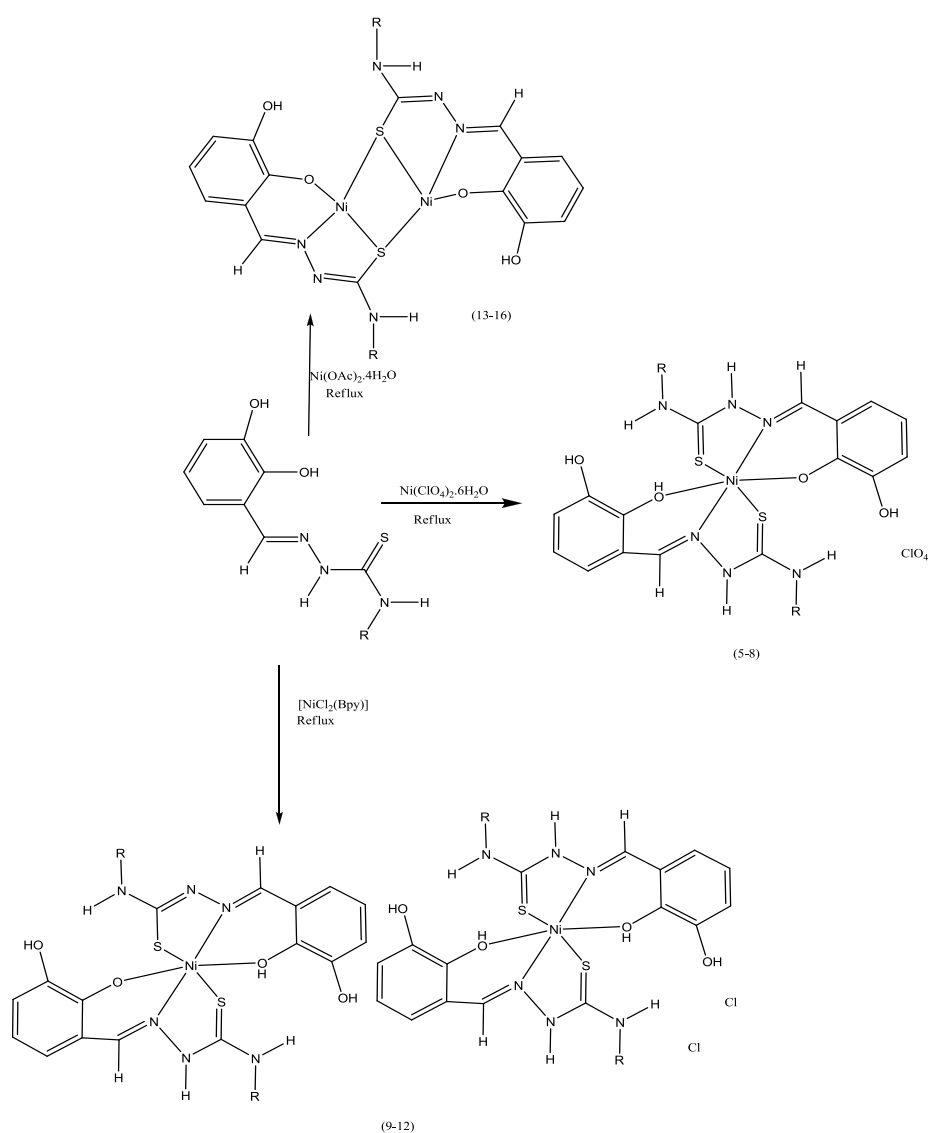
Scheme 2.1: Synthesis of nickel(II) thiosemicarbazone complexes

Table 2.1: Stoichiometries, color and partial elemental analysis of nickel(II) thiosemicarbazone complexes

Complex	Stoichiometries	color	Anal.Calc. (Found)%		
			C	H	N
$[Ni(H_3L^1)(H_2L^1)]ClO_4.2H_2O$ **(5)**	$C_{16}H_{17}N_6O_8S_2ClNi.2H_2O$	Green	31.21	3.44	13.65
			(31.40)	(3.12)	(13.98)
$[Ni(H_3L^2)(H_2L^2)]ClO_4.2H_2O$ **(6)**	$C_{18}H_{21}N_6O_8S_2ClNi.H_2O$	Green	34.55	3.71	13.43
			(34.37)	(4.44)	(13.29)
$[Ni(H_3L^3)(H_2L^3)]ClO_4$ **(7)**	$C_{28}H_{25}N_6O_8S_2ClNi$	Green	45.95	3.44	11.49
			(46.01)	(3.49)	(11.40)
$[Ni(H_3L^4)(H_2L^4)]ClO_4.H_2O$ **(8)**	$C_{20}H_{25}N_6O_8S_2NiCl.H_2O$	Green	36.74	4.16	12.86
			(36.88)	(4.05)	(12.84)
$[Ni(H_2L^1)_2][Ni(H_3L^1)_2]Cl_2.H_2O$ **(9)**	$C_{32}H_{33}N_{12}O_8S_4Cl_2Ni_2.H_2O$	Green	36.01	3.59	15.75
			(36.08)	(3.35)	(15.84)
$[Ni(H_2L^2)_2][Ni(H_3L^2)_2]Cl_2.H_2O$ **(10)**	$C_{36}H_{41}N_{12}O_8S_4Cl_2Ni_2.H_2O$	Green	38.49	4.13	14.96
			(38.68)	(3.11)	(14.87)
$[Ni(H_2L^3)_2][Ni(H_3L^3)_2]Cl_2$ **(11)**	$C_{56}H_{49}N_{12}O_8S_4Cl_2Ni_2$	Green	50.36	3.77	12.58
			(50.58)	(3.74)	(12.65)
$[Ni(H_2L^4)_2][Ni(H_3L^4)_2]Cl_2.H_2O$ **(12)**	$C_{40}H_{49}N_{12}O_8S_4Cl_2Ni_2.H_2O$	Green	40.73	4.61	14.25
			(40.61)	(4.38)	(14.21)
$[Ni_2(HL^1)_2]$ **(13)**	$C_{16}H_{14}N_6O_4S_2Ni_2$	Brownish red	35.86	2.63	15.68
			(35.54)	(2.53)	(15.56)
$[Ni_2(HL^2)_2].H_2O$ **(14)**	$C_{16}H_{18}N_6O_4S_2Ni_2. H_2O$	Brown	37.15	3.46	14.44
			(37.12)	(3.13)	(14.08)
$[Ni_2(HL^3)_2]$ **(15)**	$C_{16}H_{18}N_6O_4S_2Ni_2$	Brown	48.88	3.22	12.21
			(48.76)	(3.80)	(12.12)
$[Ni_2(HL^4)_2]$ **(16)**	$C_{20}H_{22}N_6O_4S_2Ni_2$	Brown	40.58	3.75	14.20
			(40.74)	(3.89)	(14.23)

2.3.2 X-ray crystallography

2.3.2.1 Crystal structure of [Ni(H$_3$L^4)(H$_2$L^4)]$_2$(ClO$_4$)$_2$.2H$_2$O (8a) and [Ni(H$_2$L^1)$_2$][Ni(H$_3$L^1)$_2$]Cl$_2$. H$_2$O (9)

The crystallographic data and structure refinement parameters obtained from X-ray diffraction analysis for complexes **8a** and **9** are contained in Table 2.2. Figure 2.2 shows the molecular structure obtained for complex **8a** and the most significant bond lengths and angles are shown in Table 2.3. This compound crystallizes in the monoclinic space group *P2$_1$/c* with two molecular weight units accommodated per cell. The asymmetric unit of complex **8a** (Figure 2.3) consists of two distorted octahedral [Ni(H$_3$L^4)(H$_2$L^4)]$^+$ cations and two perchlorate counteranion as well as two water molecules of solvation presented in the crystal lattice. In each cation, the nickel center is coordinated to two different 2,3-dihydroxybenzaldehyde-N4-ethylthiosemicarbazone ligands, which is placed approximately perpendicular to each other. One neutral ligand coordinated through the azomethine nitrogen, thione sulfur and phenol oxygen while the other ligand is monoanionic coordinated through the azomethine nitrogen, thione sulfur and phenolate oxygen. This arrangement gives rise to an octahedral environment in such a way that four bicyclic chelate systems are formed.
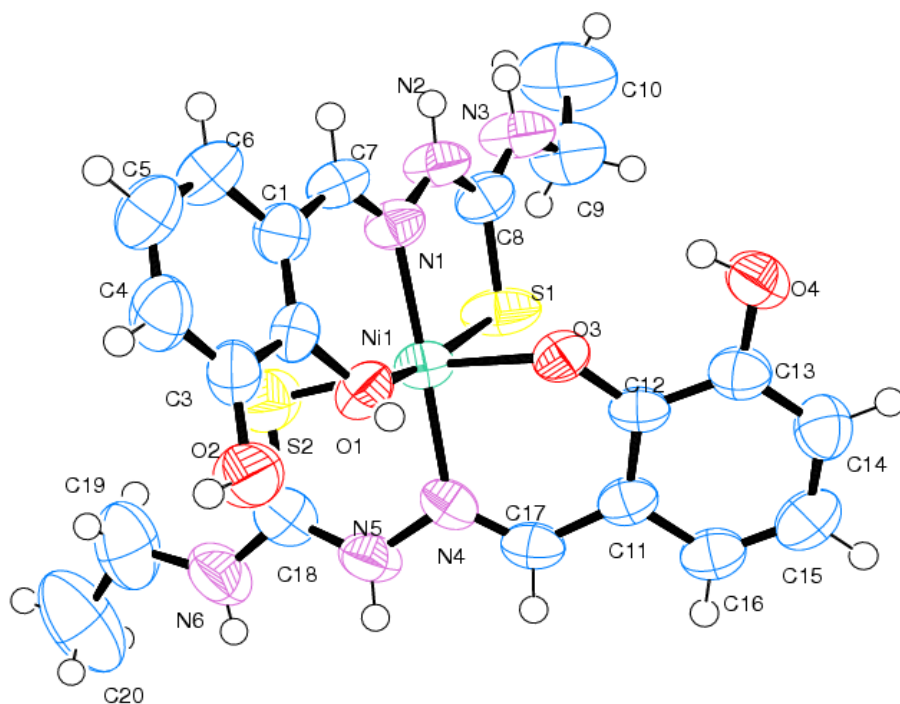
Figure 2.2: Molecular structure of [Ni(H₃L⁴)(H₂L⁴)]ClO₄.2H₂O **(8a)**, displacement ellipsoids are drawn at 70 % probability level, perchlorate ion and water molecule are omitted for clarify
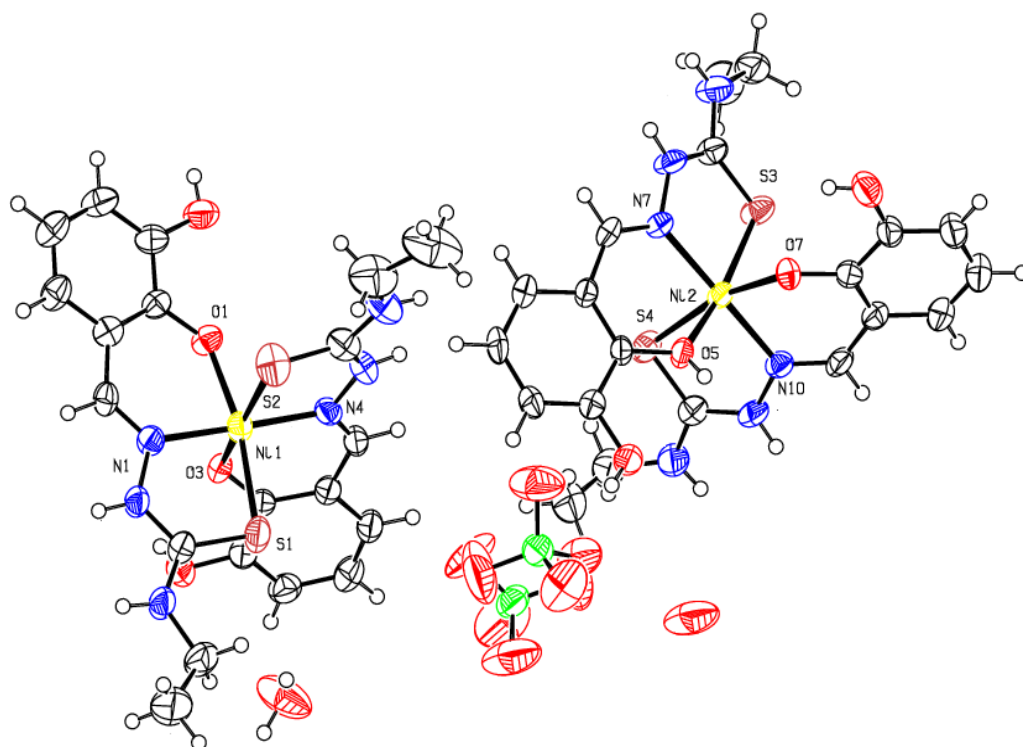
Figure 2.3: View of the asymmetric unit of **8a**. Displacement ellipsoids for non-H atoms are drawn at the 50% probability level

Because of the different character of the atoms forming the environment around the Ni(II) ion, the coordination octahedron is distorted, where the Ni atoms are in a *trans*-N(1)N(4)-*cis*-O(1)O(3)-cis-S(1)S(2) configuration and *trans*-N(7)N(10)-*cis*-O(5)O(7)-*cis*-S(3)S(4) configuration respectively. The *trans* angle involving the two imine nitrogens, N1–Ni1–N4 of 178.46(15)º and N7–Ni2–N(10) of 176.44(13)º are far from 180º. The O1–Ni1–O3 of 83.83(11)º angle and O5–Ni2–O7 of 83.78(10)º, while the S1–Ni1–S2 angle of 98.47(5)º and S3–Ni2–S4 of 98.89(5)º are greater than 90º and reveals that the two thiosemicarbazone ligands in the molecule exert significant steric effects on each other. The bond lengths between each nickel(II) ion and the donor atoms are very unequal, increasing in the order Ni–N < Ni–O < Ni–S (Leovac et al., 2007; Pavlishchuk et al., 1998) as shown in Table 2.3. However, the average Ni–N bond distance of 2.025(3) Å, is in the normal range for Ni–N bond distances of octahedral nickel(II) complexes with thiosemicarbazones (Chattopadhyay et al., 1997; Lobana et al., 2010).

The coordination mode of the oxygens of the 2,3-dihydroxybenzaldehyde moiety in the two ligands around nickel(II) is different. This is suggested by the observation that the average value of bond distances O1–C2, 1.360(5) Å, is only 0.015 Å shorter than the average value of bond O2–C3, 1.375(5) Å, while the average value of bond distances O3–C12, 1.336(4) Å, is 0.038 Å shorter than the average value of O2–C3, 1.375(5) Å. Consequently, the Ni–O bond distances are different and lie in the range 2.049- 2.120 Å. These values are close to the bond distances observed in other nickel salicylaldehyde complexes (Schulte et al., 1991; Shu-Yang et al., 2012). The other values are very similar to those reported for other nickel complexes with ONS-donor thiosemicarbazone (Afrasiabi et al., 2005; Qing et al., 2006). The bicyclic chelate systems Ni1, S2, C18, N5, N4, C17, C11, C12, O3 and Ni1, S1, C8, N2, N1, C7, C1,

C2, O1 are considerably deviated from planarity, as evidenced by the maximum deviation of 0.345(2) Å for O3 and 0.24(3) Å for O1, respectively, from their respective mean planes. Moreover, the bicyclic chelate system Ni2, S3, C28, N8, N7, C27, C21, C22, O5 and Ni2, S4, C38, N11, N10, C37, C31, C32, O7 are deviated from planarity with a maximum mean plane deviation of -0.324(3) Å for O5 and 0.390(2) Å for O7, respectively. The Ni1 is found to be displaced by -0.0135(5) A° from the plane constituting atoms O1, S1, N1, O3, S2, N4 with a maximum least square plane deviation at N1 by 1.938(3) Å. The Ni2 is found to be displaced by -0.0117(5) Å from the plane constituting atoms O5, S3, N7, O7, S4, N10 with a maximum least square plane deviation at N7 by 1.969(3) Å. The dihedral angles between the least squares planes of the two coordinated ligands are 71.36(13)°. The dihedral angles formed by the thiosemicarbazone moieties C7, N1, N2, C8, S1, N3; C17, N4, N5, C18, S2, N6 with the plane containing coordinating atoms are 9.63(15)°, 12.06(15)° respectively, while the phenyl rings C1, C2, C3, C4, C5,C6; C11, C12, C13, C14, C15, C16 have angles of 14.37(18)°, 23.52(18)° to the donor plane indicating that the thiosemicarbazone moieties are not planar with the nickel's coordination plane [Ni1, O1, S1, N1, O3, S2, N4]. Similarly, the thiosemicarbazone moieties C27, N7, N8, C28, S3, N9; C37, N10, N11, C38, S4, N12 are not planar with the nickel's coordination plane [Ni2, O5, S3, N7, O7, S4, N10] where the dihedral angles formed by the thiosemicarbazone moieties with the plane containing coordinating atoms are 10.38(13)°, 16.53(14)° respectively, while the phenyl rings C21, C22, C23, C24, C25,C26; C31, C32, C33, C34, C35, C36 have angles of 12.67(17)°, 13.09(18)° to the donor plane. These factors suggest considerable distortion from an octahedral geometry around the Ni(II) centers in both molecules of the complex.

Table 2.2: Crystal data and structure refinement parameters for complexes **8a** and **9**

Parameters	$[Ni(H_3L^4)(H_2L^4)]_2(ClO_4)_2.2H_2O$ (8a)	$[Ni(H_2L^1)_2][Ni(H_3L^1)_2]Cl_2.H_2O$ (9)
Empirical Formula	$C_{26.67} H_{32} Cl_{1.33} N_8 Ni_{1.33} O_{12} S_{2.67}$	$C_{32} H_{34} Cl_2 N_{12} Ni_2 O_9 S_4$
Formula weight, M	867.64	1047.27
Temperature, T (K)	100	100
Wavelength, Mo Kα (Å)	$\lambda = 0.71073$	$\lambda = 0.71073$
Crystal system	Monoclinic	Monoclinic
Space group	$P2_1/c$	$P2_1/c$
Unit cell dimensions		
a(Å)	12.0076(2)	20.992(6)
b(Å)	26.8576(4)	12.839(3)
c (Å)	17.2286(3)	15.952(4)
α(°)	90.00	90.00
β(°)	101.3100(10)	109.961(4)
γ(°)	90.00	90.00
Volume V (Å^3)	5448.24(15)	4041.1(18)
Z	6	4
Absorption coefficient, μ(mm^{-1})	1.023	1.340
Reflections collected	48139	53059
Density (calculated), (mg m^{-3})	1.587	1.721
F(0 0 0)	2680	2144
Data/ parameters /restraints	11141 /703 /0	10121/551/0
S	0.961	1.082
Independent reflections	11141	10121
	[R(int) = 0.0836]	[R(int) = 0.1556]
$R[F^2 > 2\sigma(F^2)]$	0.1151	0.4260
$wR(F^2)$	0.1011	0.4086
Largest difference peak and hole (e Å^{-3})	0.049 and 0.003	0.033 and 0.005

Table 2.3: Selected bond lengths (Å) and bond angles (°) of complexes **8a** and **9**

Complex 8a		Complex 9	
Bond lengths		**Bond lengths**	
Ni1–N4	2.015(3)	Ni1– N4	2.002(11)
Ni1–N1	2.025(3	Ni1–N1	2.011(12)
Ni2–N7	2.032(3)	Ni2–N10	2.006(12)
Ni2–N10	2.031(3)	Ni2–N7	2.031(13)
Ni1– O3	2.054(3)	Ni1–O3	2.052(11)
Ni1–O1	2.108(3)	Ni1–O1	2.098(10)
Ni2–O7	2.048(3)	Ni2–O7	2.024(11)
Ni2–O5	2.114(3)	Ni2–O5	2.108(9)
Ni1–S2	2.3972(12)	Ni1–S2	2.384(4)
Ni1–S1	2.4073(13)	Ni1–S1	2.398(4)
Ni2–S3	2.3958(11)	Ni2–S4	2.376(4)
Ni2–S4	2.4116(12)	Ni2–S3	2.384(4)
S2–C18	1.682(5)	S2–C16	1.673(14)
S1–C8	1.691(4)	S1–C8	1.690(16)
S4–C38	1.683(4)	S4–C32	1.630(18)
S3–C28	1.680(4)	S3–C24	1.684(17)
N7–C27	1.282(4)	C23–N7	1.283(18)
N10–C37	1.286(5)	N10–C31	1.299(18)
N11–C38	1.344(5)	N11–C32	1.36(3)
N4–C17	1.274(5)	N4–C15	1.284(18)
N8–C28	1.351(5)	N8–C24	1.348(19)
N2–C8	1.347(5)	N2–C8	1.311(19)
N1–C7	1.283(5)	N1–C7	1.277(18)
N5–C18	1.349(5)	N5–C16	1.361(18)
O1– C2	1.360(5)	O1– C1	1.369(17)
O2–C3	1.375(5)	O2–C2	1.36(2)
O4–C13	1.371(4)	O4 –C10	1.379(18)
O3–C12	1.336(4)	O3–C9	1.324(17)
O5–C22	1.358(4)	O5–C17	1.358(16)
O6–C23	1.366(5)	O6–C18	1.365(17)
O7–C32	1.333(4)	O7–C25	1.354(18)

Complex 8a		Complex 9	
Bond angels		Bond angels	
O8–C33	1.365(5)	O8–C26	1.38(2)
N4–Ni1–N1	178.47(14)	N4–Ni1– N1	179.3(5)
N4– Ni1– O3	88.70(11)	N4–Ni1–O3	89.3(4)
N1–Ni1–O3	92.51(11)	N1–Ni1–O3	90.2(4)
N4–Ni1– O1	92.28(13)	N4–Ni1–O1	93.0(5)
N1–Ni1–O1	86.92(13)	N1–Ni1–O1	87.4(4)
O3–Ni1– O1	84.25(12)	O3–Ni1–O1	85.6(4)
N4–Ni1–S1	96.60(9)	N4–Ni1–S1	95.7(4)
N1–Ni1–S1	84.35(10)	N1–Ni1–S1	83.9(3)
O3–Ni1–S1	89.14(8)	O3–Ni1–S1	89.5(3)
O1–Ni1–S1	168.81(10)	O1–Ni1–S1	169.9(3)
N4–Ni1–S2	83.59(10)	N4–Ni1–S2	84.1(4)
N1–Ni1–S2	95.09(10)	N1–Ni1–S2	96.5(4)
O3–Ni1–S2	169.71(8)	O3–Ni1–S2	168.8(3)
O1–Ni1–S2	89.25(10)	O1–Ni1–S2	85.8(3)
S1–Ni1–S2	98.48(5)	S1–Ni1–S2	100.08(15)
N10–Ni2–N7	176.47(13)	N10–Ni2–N7	177.7(5)
N10– Ni2–O7	87.59(11)	N10–Ni2–O7	89.0(5)
N7– Ni2–O7	95.28(11)	N7–Ni2–O7	93.3(5)
N10– Ni2–O5	96.60(11)	N10–Ni2–O5	93.8(4)
N7–Ni2–O5	85.75(11)	N7–Ni2–O5	86.6(4)
N10– Ni2–S3	94.61(9)	N10–Ni2–S3	96.6(4)
N7– Ni2 –S3	83.30(9)	N7 –Ni2–S3	83.2(4)
O7– Ni2– S3	91.31(8)	O7–Ni2–S3	89.7(3)
O5–Ni2– S3	167.64(8)	O5–Ni2–S3	168.4(3)
N10– Ni2– S4	82.65(10)	N10–Ni2– S4	83.7(3)
N7– Ni2–S4	94.85(9)	N7–Ni2–S4	94.0(4)
O7– Ni2–S4	166.38(8)	O7–Ni2–S4	169.5(3)
O5– Ni2–S4	87.71(8)	O5–Ni2–S4	87.7(3)
S3– Ni2–S4	98.90(4)	S3–Ni2–S4	98.63(16)
N10– Ni2–S3	94.61(9)	N10–Ni2–S3	96.6(4)

Table 2.3, continued

The unit cell is viewed along the *a* axis and eight molecules are arranged in the unit volume cell (Figure 2.4). The packing of the molecules is stabilized by hydrogen bonding and π-π interactions. These interactions are given in Table 2.4. The system of hydrogen bonds is shown in Figure 2.5 in which both $[Ni(H_3L^4)(H_2L^4)]^+$ cations act as donors through the nitrogens N2, N3, N5, N6, N8, N9, N11 and N12 and the oxygens O2, O4, O6, and O8, and as acceptors through the oxygen atoms O2, O3, O6 and O7. The two perchlorate anions and water molecules also act as acceptors. The metal chelate ring Cg(1) comprising atoms Nil, S1, C8, N1, N2 is involved in π-π interactions with metal chelate ring Cg(2) comprising of atoms Ni1, S2, C18, N5, N4 of the neighboring ligand with an average distance of 3.322(19) Å. Similar, the metal chelate ring Cg(7) comprising of atoms Ni2, S3, C28, N7, N8 involved in π-π interactions with metal chelate ring Cg(8) comprising of atoms Ni2, S4, C38, N10, N12 of the neighboring ligand with an average distance of 3.339(17) Å. In addition to this, the phenyl ring Cg(5) comprising of atoms C1, C2, C3, C4, C5, C6 is involved in π-π interactions with the phenyl ring Cg(11) comprising of atoms C21, C22, C23, C24, C25, C26 of the neighboring unit at a distance of 3.516 Å.

Since complexes $[Ni(H_3L^1)(H_2L^1)]ClO_4.2H_2O$ (**5**), $[Ni(H_3L^2)(H_2L^2)]ClO_4.2H_2O$ (**6**), $[Ni(H_3L^3)(H_2L^3)]ClO_4$ (**7**) and $[Ni(H_3L^4)(H_2L^4)]ClO_4. H_2O$ (**8**) are analogs with related ligands, differ only in the substitution at N(4), the molecular structures adopted by these complexes are expected to be similar.
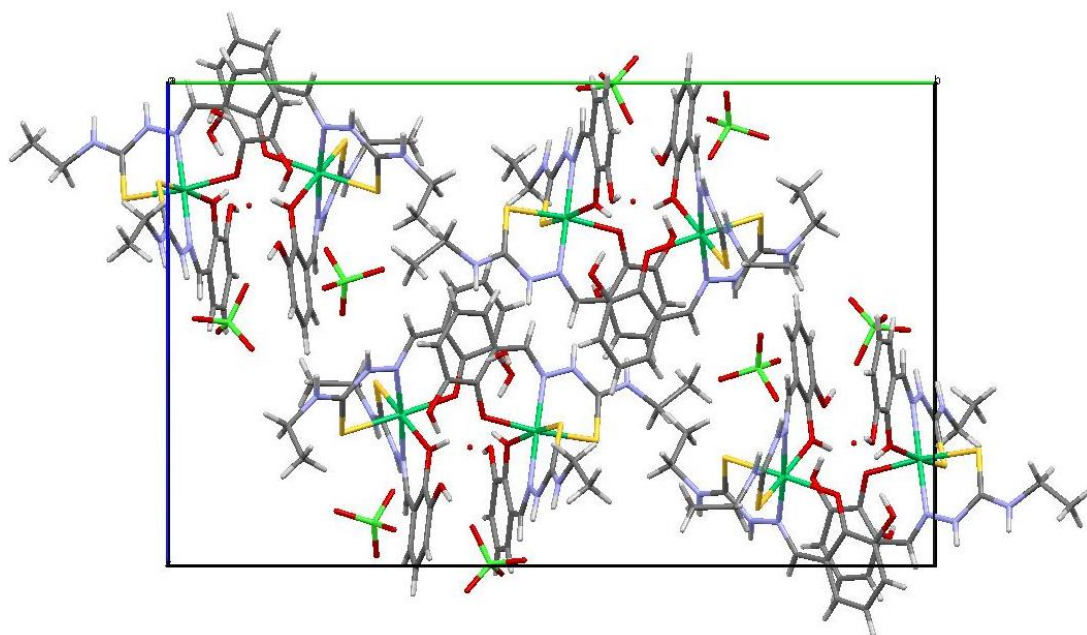
Figure 2.4: Unit cell packing of complex **8a** along *a* axis
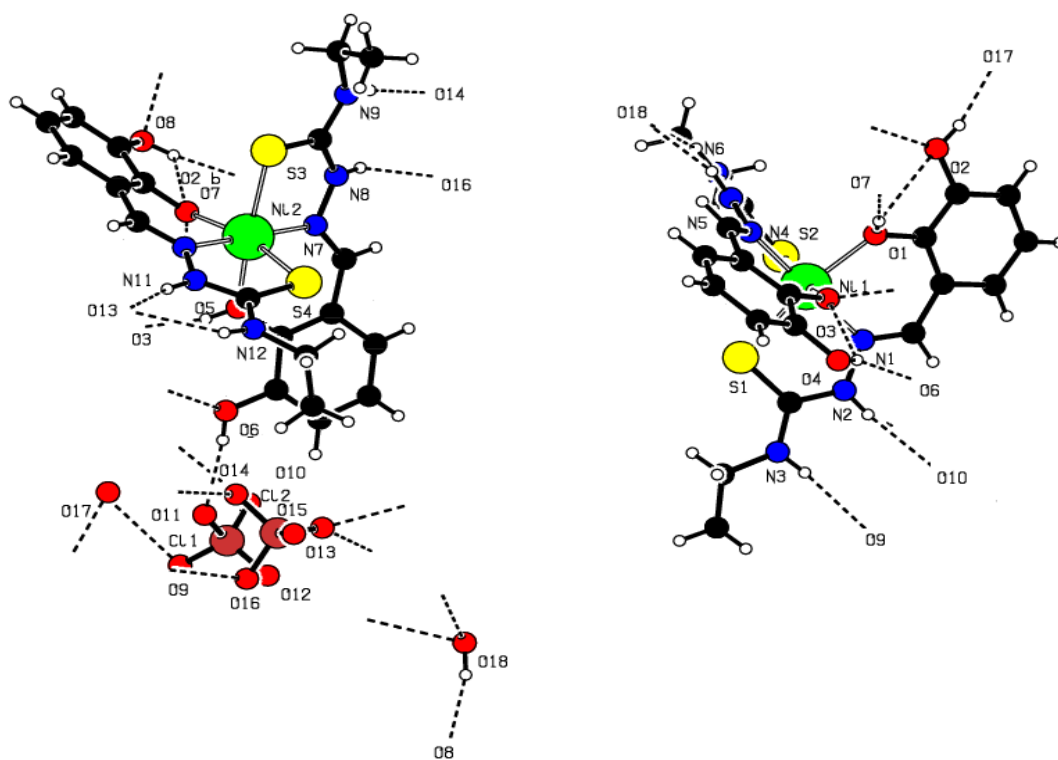
Figure 2.5: Hydrogen bonding interactions in complex **8a**

Table 2.4: Interaction parameters (Å, °) for complex **8a**

π-π interactions

Cg(I)….Cg(J)	Cg—Cg (Å)	α°
Cg(1) —Cg(2)	3.322	3.81
Cg(7) —Cg(8)	3.339	3.81
Cg(5) —Cg(11)	3.516	8.87

Cg(1)= Nil, S1, C8, N1, N2; Cg(2)= Ni1, S2, C18, N5, N4; Cg(7)= Ni2, S3, C28, N7, N8; Cg(8)= Ni2, S4, C38, N10, N12; Cg(5)= C1, C2, C3, C4, C5, C6; Cg(11)= C21, C22, C23, C24, C25, C26

H-bonding

Donor-H….Acceptor	D-H	H….A	D….A	D-H…A
N(2)-H(2A)…..O(10)[a]	0.86	2.32	3.149(6)	163
N(2)-H(2A)…..O(9)[b]	0.86	2.55	3.043(5)	118
O(2)-H(2B)…..O(17)[c]	0.82	1.87	2.673(3)	164
N(3)-H(3A)…..O(9)[a]	0.86	2.30	3.122(5)	160
N(3)-H(3A)…..O(10)[b]	0.86	2.52	3.053(6)	121
O(4)-H(4A)…..O(3)[c]	0.82	2.31	2.754(4)	114
O(4)-H(4A)…..O(6)[a]	0.82	1.95	2.720(4)	155
N(5)-H(5A)…..O(18)[d]	0.86	2.03	2.842(5)	158
O(6)-H(6A)…..O(11)[d]	0.82	2.69	2.903(5)	173
N(6)-H(6B)…..O(18)[d]	0.86	2.53	3.256(6)	143
N(8)-H(8A)…..O(16)[e]	0.86	2.26	3.057(6)	154
O(8)-H(8B)…..O(2)[f]	0.82	1.91	2.685(4)	157
O(8)-H(8B)…..O(7)[f]	0.82	2.33	2.742(4)	112
N(9)-H(9A)…..O(14)[e]	0.86	2.26	3.118(6)	171
N(11)-H(11A)…..O(13)[g]	0.86	2.16	2.977(6)	157
N(12)-H(12A)…..O(13)[g]	0.86	2.44	3.209(6)	149

D = Donor, A = Acceptor, Equivalent position code: a = x, 1+y, z; b = 1-x, 1-y,1-z; c = 1+x,1+y, z; d = 1-x,1/2+y,1/2-z; e = 1+x, y, z; f = x, -1+y, z; g = x,1/2-y,-1/2+z;

Figure 2.6 shows the molecular structure of compound **9** along with the atom numbering scheme and the most significant structural parameters are given in Table 2.2.
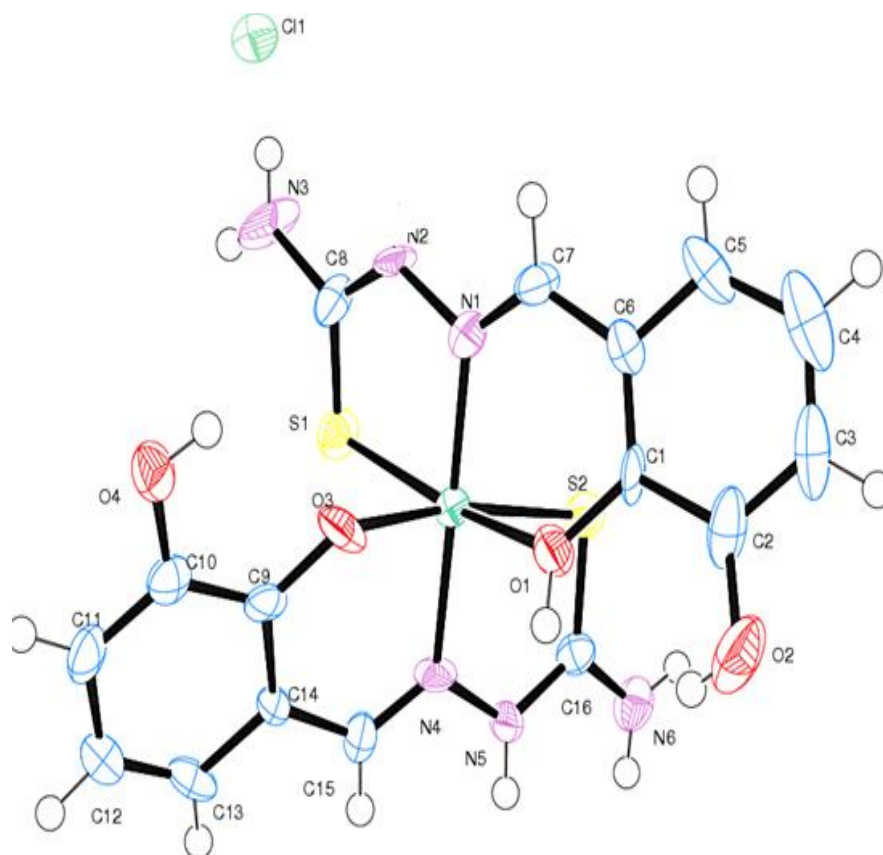
Figure 2.6: Molecular structure of molecule [Ni(H$_2$L^1)$_2$] (A) in complex **9**

Complex **9** crystallizes in the monoclinic space group *P2$_1$/c* and the asymmetric unit (Figure 2.7) is comprised of a molecule [Ni(H$_2$L^1)$_2$] (A) and a cation [Ni(H$_3$L^1)$_2$]$^{2+}$ (B) (A with Ni1 and B with Ni2), two chloride ions to balance the charge and one water molecule of solvate (the water hydrogen's could not be located in the Fourier map).

The two nickel atoms in A and B are in an approximately octahedral coordination environment and the nickel ion in A is bonded to two mononegative tridentate 2,3-dihydroxybenzaldehyde thiosemicarbazone ligands while in B the nickel ion is bounded to two neutral tridentate 2,3-dihydroxybenzaldehyde thiosemicarbazone ligands. Both ligands are coordinated meridionally around the nickel(II) ion, forming a distorted

octahedral NiS2N2O2 core comprising thiol and thione sulfur atoms, two azomethine nitrogen atoms, one phenol oxygen and one phenolic oxygen in A, while in B the octahedron NiS2N2O2 core containing two thione sulfur, two azomethine nitrogen and two phenol oxygen. The two coordinating azomethine nitrogen atoms are *trans* to each other and the other two sets of identical donor atoms are *cis* to each other. This results in formation of four bicyclic chelate rings. Two of them composed by six atoms (from the benzaldehyde moiety), Ni1O1C1C6C7N1, Ni1O3C9C14C15N4 (for A), Ni2O5C17C22C23N7, NI2O7C25C30C31N10 (for B) and the other by five atoms (from the thiosemicarbazone moiety), NiS1C8N2N1, NI1S2C16N5N4 (for A), Ni2S3C24N8N7, Ni2S4C32N11N10 (for B) in the sequence 6:5:6:5.
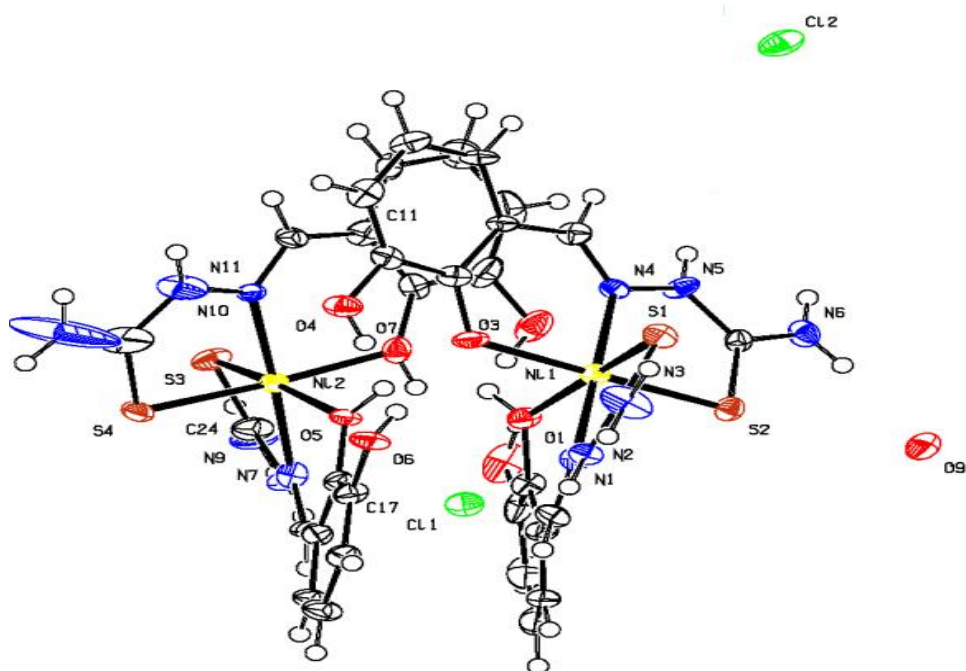
Figure 2.7: View of the two molecules (A with Ni1 and B with Ni2) in the asymmetric unit of **9** with the atom numbering scheme. Displacement ellipsoids for non H atoms are drawn at the 50% probability level.

The perspective view of the complex shows that the ligands with their donor atoms are arranged around the nickel ion in a meridional fashion. In complex **9**, the bicyclic chelate systems Nil, Sl, C8, N2, N1, C7, C6, C1, Ol and Nil, S2, C16, N5, N4, C15, C14, C9,N5 are deviated from planarity as evidenced by the maximum deviation of 0.365(11) Å for O1 and 0.228(15) Å for C14 respectively from their respective mean planes. The dihedral angle formed by the mean planes of the bicyclic chelate rings of each of the ligands is 71.30(3)° which is far from 90º octahedral angle. This value is comparable with complex **8a** but smaller than other reported nickel(II) thiosemicarbazone complexes with distorted octahedral geometry (Saha et al., 2005; Suni et al., 2007). The two thiosemicarbazone moieties in A and B are not planar. This is confirmed by the least square plane formed between the thiosemicarbazone and the phenyl ring. The angle between the least-squares planes of the phenyl rings C1C2C3C4C5C6, C9C10C11C12C13C14 and the thiosemicarbazone moieties C7N1N2C8S1N3, C15N4N5C16S2N6 is 27.7(7)° and 20.1(6)° respectively, while the angle between the least-squares planes of the phenyl rings C17C18C19C20C21C22, C25C26C27C28C29C30 and the thiosemicarbazone moieties C23N7N8C24S3N9, C31N10N11C32S4N12 is 20.4(10)° and 32.2(6)° respectively.

The trans angles N4–Ni1–N1, O1–Nil–S1 and O3–Nil–N2 are 179.3(5), 169.9(3) and 168.8(3)° respectively, while in the other molecule these angles N10– Ni2–N7, O5–Ni2–S3 and O7–Ni2–S4 are 177.7(5), 168.4(3) and 169.5(3)° respectively. These factors are far from 180° suggesting considerable distortion from an octahedral geometry around Ni(II) center in both molecules. The Ni–N and Ni–S bond distances are in the normal range for Ni-thiosemicarbazone type complexes (Castiñeiras et al., 2012). The Ni–N distances are 2.002(11), 2.011(12) Å for molecule A, and 2.006(12), 2.031(13) Å for molecule B and the Ni–S distances are 2.398(4), 2.384(4) Å for

molecule A and 2.384(4), 2.376(4) Å for molecule B. It is interesting to note that, the Ni–S of 2.398(4) Å (thiol) is longer than Ni–S thione bonds by 0.023 (on average) Å. Notably, the bond lengths in complex **9** are slightly smaller compared to that of complex **8a** indicating the higher strength of former bond than the latter. However, the bond lengths Ni–N, Ni–O and Ni–S increase in that order as in similar ONS donor compounds (Afrasiabi et al., 2005; Rodriguez-Argüelles et al., 1999).

Interestingly, in molecule A, the C9–O3 bond length of 1.324 Å is shorter than C1–O1 of 1.369 Å indicating that the O3 is coordinated to nickel(II) as a deprotonated phenolic oxygen while O1coordinates as neutral phenoxy oxygen (Castiñeiras et al., 2012; Wang et al., 2010). However, in molecule B, the C17–O5 bond length of 1.357 Å is similar to C25–O7 of 1.354 Å indicating that both oxygens in molecule B are coordinated to Ni2 centre as neutral phenoxy oxygen (Schulte et al., 1991; Wang et al., 2010). The C–S distances, 1.673(14) Å, 1.684(17) Å, 1.630(18) Å show the thione form of the sulfur atoms which is also indicated by the hydrogen atoms on the hydrazinic nitrogens N(5), N8 and N11, and by the C–N distances [N5–C16, 1.361(18) Å; N8–C24, 1.348(19) Å and N11–C32, 1.36(3) which lie outside the range for C=N double bonds character (Qing et al., 2006) also compared to that in complex **8a**. However, the C—N bond length [1.311(19) Å for N(2)—C(8)] is consistent with partial double bond (Kasuga et al., 2001). These factors confirm the coordination through the thione form for S2, S3, S4 and thiolate form for S1 by deprotonation after enolization of ligand H_3L^1 in complex $[Ni(H_2L^1)_2][Ni(H_3L^1)_2]$ **(9)**.

In complex **9**, when viewed along *b* axis, the molecules are arranged in a parallel manner (Figure 2.8) and the molecules are connected by various hydrogen bonding interactions (Table 2.5). The two molecules A and B are intraconnected through O1(H),

O2(H) and O3 of the molecule A with O7, O8(H) and O5(H) of the nearby molecule B (Figure 2.9). Furthermore the chloride ion is joining the two molecules through O6(H) and N3(H). Intermolecular hydrogen bonding interactions were also observed *i.e.*, O1(H) with O5, N3(H) with O4, N5(H) with S3 and N6(H) with Cl2. The packing of the molecules is shown in Figure 2.10. No obvious π-π and C-H...π interactions were observed in the crystal packing.
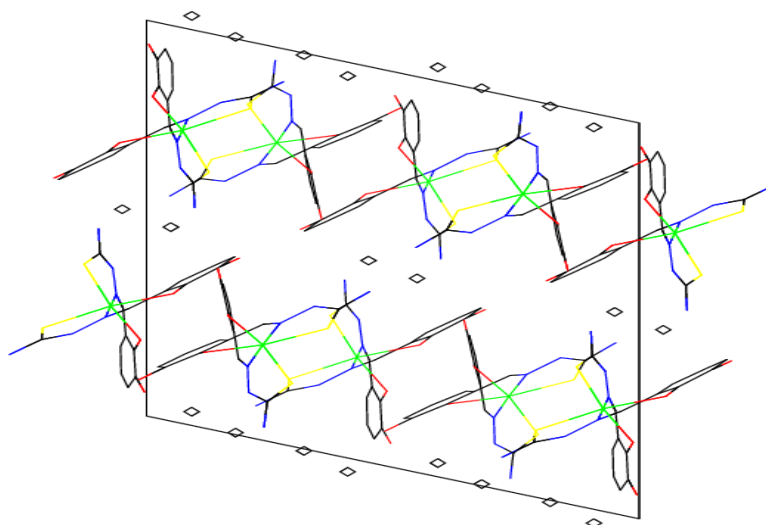
Figure 2.8: Unit cell of $[Ni(H_2L^1)_2][Ni(H_3L^1)_2]$ **(9)** along the *b* axis showing molecules are packed in parallel manner
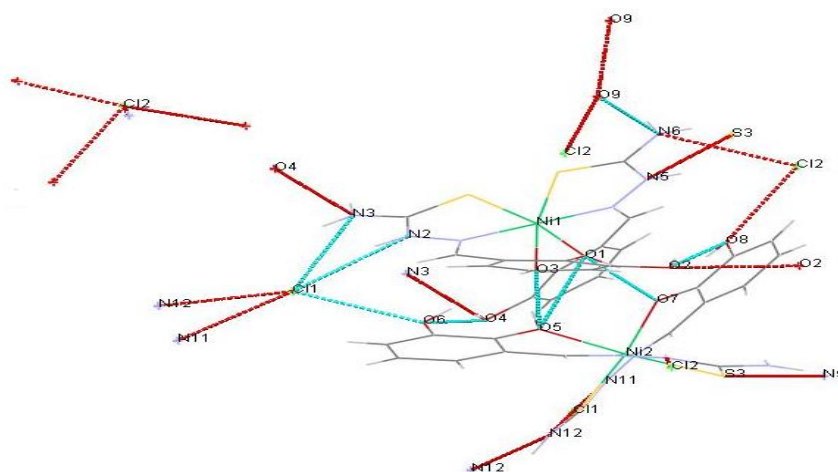
Figure 2.9: Hydrogen bonding interactions for complex **9**. Intramolecular interactions are shown as dotted lines

Table 2.5: Hydrogen bonding (Å, °) for complex **9**

Donor-H….Acceptor	D-H	H….A	D….A	D-H…A
O(1)-H(1A)…..O(7)[a]	0.93	1.61	2.479(15)	153
O(2)-H(2A)…..O(8)[b]	0.82	2.02	2.791(2)	156
N(2)-H(2B)…..Cl(1)[c]	0.86	2.61	3.291(13)	137
N(3)-H(3B)…..Cl(1)[c]	0.86	2.52	3.216(16)	139
N(3)-H(3B)…..O(4)[a]	0.82	2.38	3.07(2)	138
O(4)-H(4B)…..O(6)[c]	0.86	2.99	2.737(15)	142
N(5)-H(5B)…..S(3)[b]	0.86	2.52	3.241(13)	142
N(6)-H(6A)…..Cl(2)[c]	0.86	2.72	3.285(14)	125
N(6)-H(6B)…..O(9)[d]	0.86	2.03	2.867(18)	164
N(8)-H(8A)…..Cl(2)[a]	0.86	2.28	3.103(14)	159
O(8)-H(8B)…..O(2)[e]	0.82	2.08	2.79(2)	145
N(11)-H(11B)…..Cl(1)[d]	0.86	2.48	3.257(16)	150
N(12)-H(12B)…..Cl(1)[d]	0.86	2.33	3.14(3)	159
N(12)-H(12B)…..N(12)[e]	0.86	2.32	2.73(5)	110
O(5)-H(5B)…..O(3)[f]	0.93	1.64	2.531(15)	159
C(7)-H(7A)…..S(4)[g]	0.93	2.62	3.398(15)	142
C(19)-H(19A)…..Cl(1)[g]	0.93	2.76	3.456(18)	133
C(21)-H(21A)…..S(2)[g]	0.93	2.81	3.644(18)	150
C(27)-H(27A)…..Cl(2)[g]	0.93	2.79	3.55(2)	140

D = Donor, A = Acceptor, Equivalent position code: a = 1-x, 1-y, 1-z; b = x, 3/2-y,-1/2+z; c = -1+x, y, z; d = 1-x,1/2+y,3/2-z; e = 1-x, 1-y, 2-z; f = x, 1/2-y, 1/2+z; e = x,1/2-y, -1/2+z; g = x,1/2-y,-1/2+z;
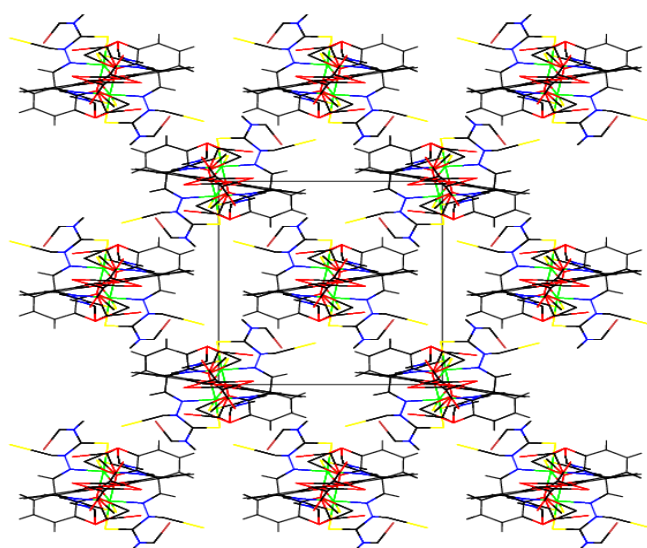
A
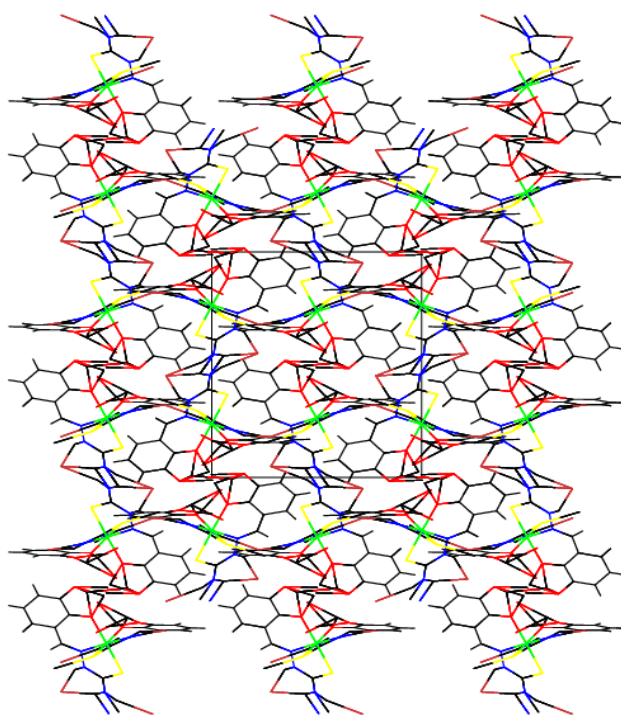
B

Figure 2.10: Packing diagram for A and B in complex **9**

2.3.3 ^{1}H NMR spectra

Proton magnetic resonance spectroscopy is a helpful tool for the identification of the coordination sites in diamagnetic nickel(II) complexes in conjunction with other spectrometric information. The chemical shifts of the functional groups in the thiosemicarbazone ligands and their diamagnetic nickel complexes [Ni$_2$(HL^2)$_2$] **(14)** and [Ni$_2$(HL^3)$_2$] **(15)** are presented in Table 2.6, while the ^{1}H NMR spectra of complexes **14** and **15** are shown in Figures 2.11 and 2.12, respectively.

In both complexes **14** and **15**, the singlet band appeared at 11.41 ppm and 11.78 ppm in the free ligands H$_3$L^2 and H$_3$L^3 respectively, which were assigned to the thioamidic proton N(2)H, has disappeared completely showing that the coordination of the ligands H$_3$L^2 and H$_3$L^3 to nickel(II) is in the thiolate form (Affan et al., 2011). In the spectra of the complex [Ni$_2$(HL^2)$_2$] **(14)** and the complex [Ni$_2$(HL^3)$_2$] **(15)**, the azomethine proton CH=N signal appeared as two singlets, one is upfield shifted while the other is downfield shifted when compared to the free ligands. The more downfield shift for one azomethine proton and the more upfield shift for the other compared to the uncomplexed thiosemicarbazones is probably due to different withdrawing of electron density from the thiosemicarbazone moiety (Casas et al., 2010). The appearance of CH=N as two signals suggested the coordination of two inequivalent azomethine nitrogens in these complexes (Papathanasis et al., 2004). Furthermore, two signals at 9.50 ppm, 8.90 ppm and 9.21 ppm, 9.54 ppm in complexes **14** and **15** respectively, each signal integrates as one hydrogen corresponding to OH present in the thiosemicarbazone moiety. The resonances of these peaks are located either in the same chemical shift as in the free ligands or shifted due to the change in electron density upon coordination with nickel(II).

Table 2.6: ^{1}H NMR spectral assignments for the thiosemicarbazone ligands and their nickel(II) complexes in DMSO-d$_6$

Compound	Chemical shifts, δ (ppm)					
	N(2)H	OH	C=N	N(4)H	Aromatic due to Tsc	Aliphatic due to Tsc
H$_3$L^2 (2)	11.41(s,1H)	9.26(s, 2H)	8.38(s,1H)	8.39(s,1H)	7.38(d,1H)	3.01(d, 3H)
					6.41(dd,1H)	
					6.66(t,1H)	
[Ni$_2$(HL^2)$_2$] (14)	-	9.50(s, 1H)	8.33(s,1H)	6.30(s,1H)	7.33(d,2H)	2.96(d,3H)
		8.90(s, 1H)	8.42(s,1H)		6.75(d,2H)	
					6.61(t,2H)	
H$_3$L^3 (3)	11.78(s,1H)	9.55(s,1H)	8.52(s, 1H)	10.03(s,1H)	7.59(d,1H)	-
		9.04(s, 1H)			7.50(d,2H)	
					7.36(t,2H)	
					7.19(t,1H)	
					6.71(dd,1H)	
					6.69(t,1H)	
[Ni$_2$(HL^3)$_2$] (15)	-	9.54(s, 1H)	8.99(s, 1H)	6.38(s,1H)	7.58-6.63	-
		9.21(s, 1H)	8.47(s, 1H)		(m,13H)	

A small shift occurs for aromatic protons in complex **14** due to the overall loss of electron density. ^{1}H NMR spectrum of **15** shows a multiplet, which integrates as 13 hydrogens at 7.58 – 6.63 ppm due to the aromatic protons of two benzyl rings and the aromatic protons for two equivalent phenyl rings attached at N4.

In the ^{1}H NMR spectra of both complexes **14** and **15**, the N(4)H appears at 6.30 ppm and 6.38 ppm, respectively and has shifted upfield compared to the free H$_3$L^2 and H$_3$L^3 ligands. Perhaps due to the presence of this proton within benzene shielding cone (Ferrari et al., 2001).

Unfortunately, the ^{1}H NMR spectra for complexes $[Ni_2(HL^1)_2]$ **(13)** and $[Ni_2(HL^4)_2]$ **(16)** could not be assigned due to spectral broadening which may be due to the presence of paramagnetic spices formed with solvent in the axial positions (Barber et al., 1992).
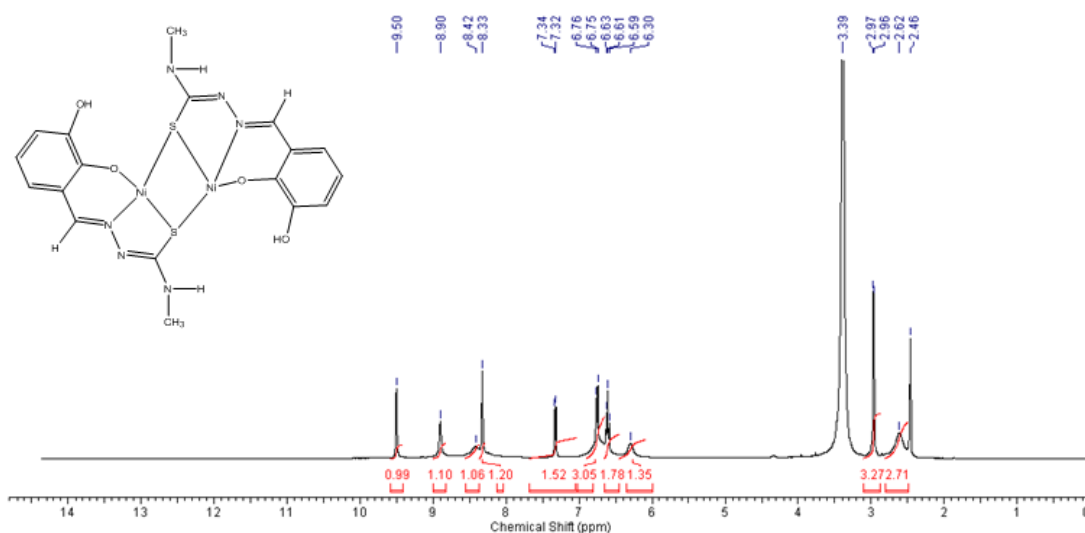
Figure 2.11: ^{1}H NMR spectrum of $[Ni_2(HL^2)_2]$ **(14)**
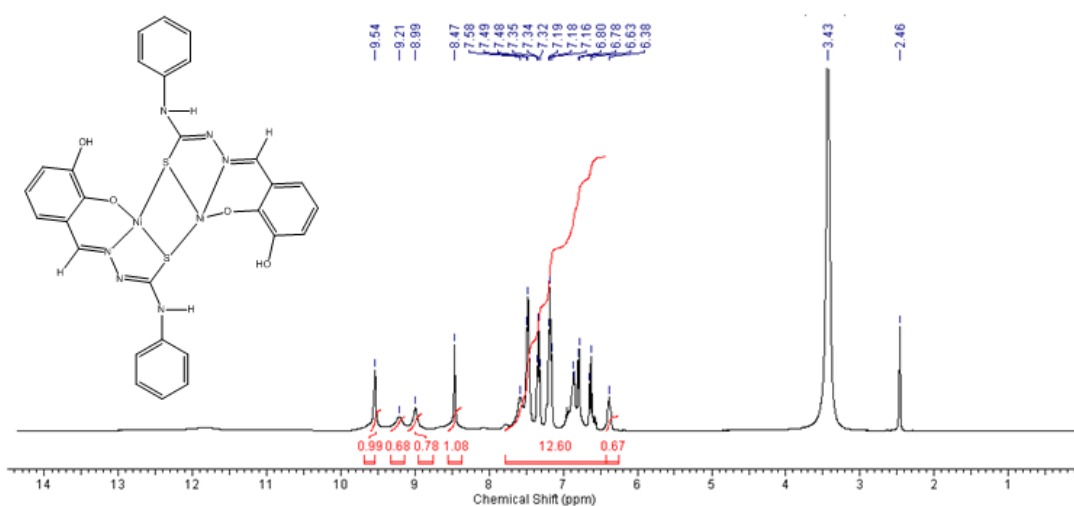
Figure 2.12: ^{1}H NMR spectrum of $[Ni_2(HL^3)_2]$ **(15)**

2.3.4 ^{13}C NMR spectra

The ^{13}C NMR chemical shifts for complexes [Ni$_2$(HL^2)$_2$] **(14)** and [Ni$_2$(HL^3)$_2$] **(15)** in DMSO-d$_6$ are presented in Tables 2.7 and the ^{13}C NMR spectra are showed in Figures 2.13 and 2.14, respectively. The proton decoupled ^{13}C NMR spectra for complexes 14 and 15 show significant shifts compared with the free ligands. The ^{13}C NMR spectra of these complexes showed the presence of 15 carbon atoms in complex **(14)** and 18 carbon atoms in complex **(15)**. These data are coherent with the formulation of each complex containing two ligand molecules and in accordance with the unsymmetric structure of **(14)** and **(15)**.

Table 2.7: ^{13}C NMR spectral assignments for the thiosemicarbazone ligands and their nickel(II) complexes in DMSO-d$_6$

Compound	Chemical shifts, δ (ppm)				
	C=S	C-O	C=N	Aromatic due to Tsc	Aliphatic
H$_3$L^2	178.01	146.09	140.19	121.56 119.54 117.53 116.83	31.38
		145.69			
[Ni$_2$(HL^2)] **(14)**	169.18	150.77	142.69	122.93, 121.84, 119.28,	32.36
		150.03	139.78	118.81, 115.13, 114.65,	
		146.41		111.35, 107.19	
H$_3$L^3	176.20	146.09	141.26	139.67, 128.58, 126.14	-
		145.97		125.70, 121.30, 119.58,	
				118.00, 117.15	
[Ni$_2$(HL^3)$_2$] **(15)**	170.13	151.17	142.01	129.08, 128.73, 126.49,	-
		149.74	139.30	122.36,121.72,121.15	
		146.13		119.58,118.86,118.15	
				117.35,115.84,115.40	

In the ^{13}C NMR spectra of complexes [Ni$_2$(HL^2)$_2$] **(14)** and [Ni$_2$(HL^3)$_2$] **(15)**, the C=S carbon atom resonance is observed in the farest low field and undergoes an upfield shift to 169.18 and 170.13 ppm, from 178.01 and 176.20 ppm in the free H$_3$L^2 and H$_3$L^3

ligands, respectively, resultant of the inductive effect of the metal upon coordination through thiolate sulfur (Rodrìguez-Argnelles et al., 2004). ^{13}C NMR spectra of both complexes **14** and **15** showed three signals in the region 151-146 ppm, the signals at 150.77 ppm and 151.17 ppm in complexes **14** and **15**, respectively, are due the coordinated C–O. These signals have downfield shifted compared with the free ligands as a consequence of the inductive effect of the Ni–O bond. The downfield shift of these signals is in accordance with coordination of the phenolic oxygen to nickel(II). Furthermore, the appearance of another two signals at 150.03 ppm, 146.41 ppm (in complex **14**) and at 149.74 ppm, 146.13 ppm (in complex **15**) propose the presence of two inequivalent phenoxy carbons.

Upon complexation, the signal of C=N group in the free ligands at 140.19 ppm (for H_3L^2) and at 141.26 ppm (for H_3L^3) underwent downfield shift to 142.69 ppm (complex **14**), 142.01 ppm (complex 15) and upfield shift to 139.78 ppm (complex **14**), 139.30 ppm (complex **15**) suggesting coordination of two azomethine nitrogen to nickel(II) (Calatayud et al., 2008). The upfield and downfield shifts of the azomethine carbon suggest variations in the electron density around this group.

The methyl carbon atom in complex **14** is observed at 32.36 ppm. The four different types of aromatic carbons on the benzyl ring are clearly distinguishable in the ^{13}C NMR spectrum. The appearance of each carbon as two signals is in accordance with the presence of two aromatic rings in different chemical environment.
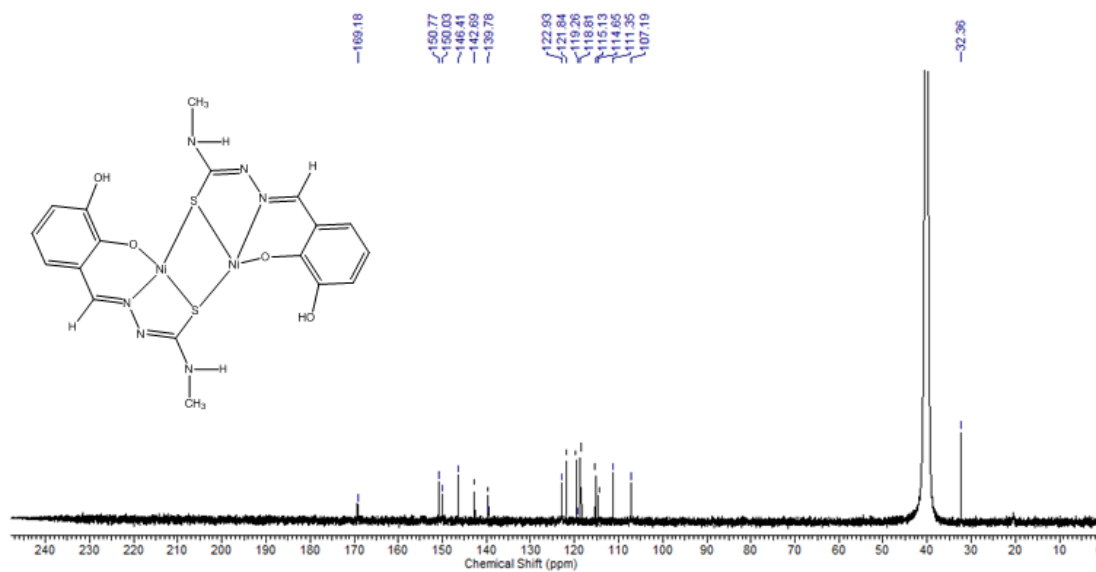
Figure 2.13: ^{13}C NMR spectrum of $[Ni_2(HL^2)_2]$ **(14)**
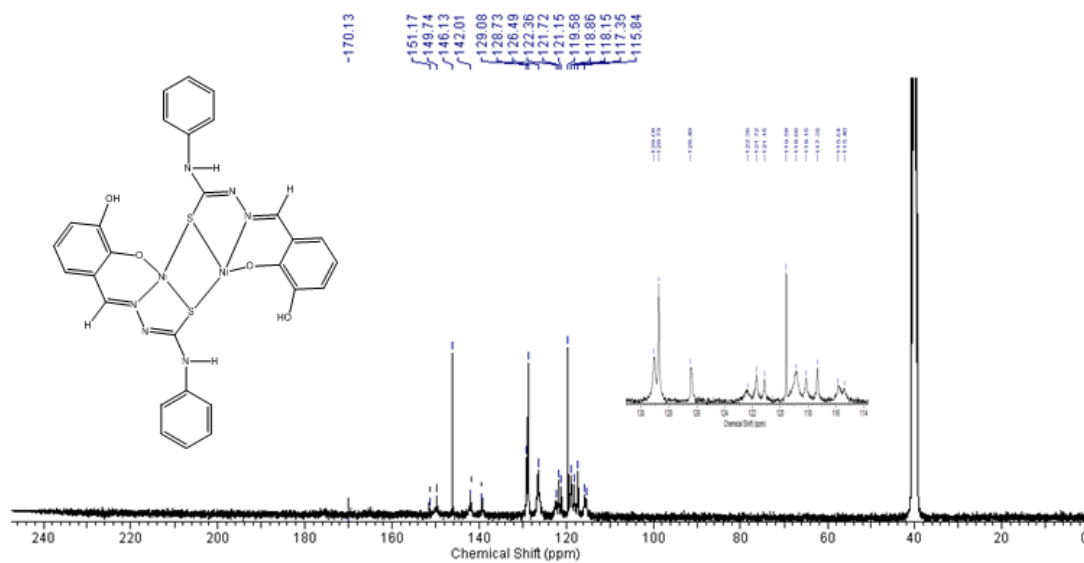
Figure 2.14: ^{13}C NMR spectrum of $[Ni_2(HL^3)_2]$ **(15)**

2.3.5 Infrared Spectra

The most characteristic vibrational frequencies and their tentative assignments for the 2,3-dihydroxybenzaldehyde-N4-substituted thiosemicarbazone ligands H_3L and their nickel(II) complexes are listed in Table 2.8. In the solid state, all the thiosemicarbazones remain in the thione form indicated by the bands found at around 1390-1340 cm^{-1} attributable to $v(C=S)$, asymmetric stretching frequency of the thioamide group is also observed at the region 855-800 cm^{-1} (Chandra & Kumar, 2005). Moreover, $v(S-H)$ band that appears at around 2500-2800 cm^{-1} cannot be seen in the spectra of all ligands and sharp band due to vibration of N^2-H which is observed at 3200-3150 cm^{-1} in the spectra of all H_3L ligands. These results support the existence of thione tautomer in the solid state (Afrasiabi et al., 2004; Bindua et al., 1999). However, the bands at around 3300-3420 cm^{-1} are attributed to v (N^4-H) (Lobana, Sharma, et al., 2009), while the bands in the region 3500- 3370 cm^{-1} are assigned to OH stretching of the polyhydroxybenzaldehyde thiosemicarbazone. Azomethine stretching frequency is observed at 1611- 1542 cm^{-1} and those strong to medium bands that observed in the range 1210-1060 cm^{-1} are assigned to the hydrazinic (N-N) bonds (Chandra & Kumar, 2004; West et al., 1996).

The assignments of the vibrational frequencies of the complexes were made by comparison with vibrational frequencies of the free ligands. The IR spectra obtained for nickel complexes suggested that the coordination of the thiosemicarbazone to nickel(II) ion occurs through azomethine nitrogen, phenolic (phenol) oxygen and thione sulfur. The azomethine $v(C=N)$ vibration mode in the range of 1611-1542 cm^{-1} in the free ligands shows a positive shift to higher frequency 1617-1581 cm^{-1} after complexation, indicating the participation of azomethine group in the coordination to nickel(II) ion where, the electron density on the azomethine link is reduced as expected due to the

coordination of nitrogen to the metal atom and thus cause a shift in the $\nu(C=N)$ group (Ali et al., 2003; Arquero et al., 1996; Sreekanth et al., 2006) . However, this band is not a pure vibrational band of C=N stretching, but it is a combination band of [$\nu(C–N)$ + $\delta(NH)$] stretching vibrations (Chandra & Sharma, 2009; Gambino et al., 2007). Meanwhile, the shift to higher frequency of the $\nu(N–N)$ band, observed in the obtained complexes, has also been related to the electronic delocalization produced as a consequence of coordination through the azomethine nitrogen atom. Further proof for the coordination of the azomethine nitrogen is obtained from the appearance of a new band 520-580 cm^{-1}, assignable to $\nu(Ni\text{-}N)$ for all nickel complexes. The interaction of thiosemicarbazone ligands with nickel(II) through sulfur in all nickel complexes is confirmed by the shift in the vibration bands of thioamide group to lower energies and the decrease in intensity if compared to the corresponding bands of the free ligands (Ali et al., 2011). In complexes **5**-**12**, the bands assigned to the C=S stretching at 1390-1340 cm^{-1} and 855-800 cm^{-1} in the free ligands has shifted to 1342-1330 cm^{-1} and 780-775 cm^{-1}, while the thioamide stretching in complexes **13**-**16** was observed at 1330-1315 cm^{-1} and around 735 cm^{-1}. It has been found that the band at around 735 cm^{-1} is attributed to $C–S_{bridging}$ stretching (Datta et al., 2012). For the studied complexes, the wavenumber shift of the thioamide band of complexes **13**-**16** (thiol coordination) would be larger than in the complexes **5**-**12** (thione coordination), due to the lowering of the C–S bond order owing to deprotonation in the case of thiol coordination. However, the appearance of a new band at around 1525-1559 cm^{-1} in the IR spectra of complexes **13**-**16** due to the newly formed $\nu(N=C)$ supports the above observation. The loss of O-H proton on coordination is difficult to assign in polyhydroxybenzaldehyde thiosemicarbazone due to the presence of more than one OH which engage in complex inter and intra molecular hydrogen bonds (Tan et al., 2012). However, the coordination of phenolic oxygen is indicated by the lowering in the $\nu(C\text{-}O)$ band by 10-30 cm^{-1} when

compared to the ligand. These observations supported by the formation of Ni-O band

which was observed at 480-424 cm^{-1}.

Table 2.8: IR spectral assignments for the thiosemicarbazone ligands and their nickel
complexes (cm^{-1})

Compound	ν(C=N)	ν (C=S)/ ν (C-S)	ν(C-O)	ν(N-N)	ν(Ni-O)	ν(Ni-N)
H$_3$L^1	1611	1342, 824	1279	1068	-	-
[Ni(H$_3$L^1)(H$_2$L^1)](ClO$_4$)$_2$.2H$_2$O (5)	1617	1335, 779	1270	1087	467	523
[Ni(H$_2$L^1)$_2$][Ni(H$_3$L^1)$_2$]Cl$_2$.H$_2$O (9)	1617	1331,778	1266	1094	472	548
[Ni$_2$(HL^1)$_2$] (13)	1601	1320,737	1227	1094	486	545
H$_3$L^2	1543	1389, 853	1290	1043	-	-
[Ni(H$_3$L^2)(H$_2$L^2)] (ClO$_4$)$_2$. H$_2$O (6)	1581	1342, 789	1272	1086	474	581
[Ni(H$_2$L^2)$_2$][Ni(H$_3$L^2)$_2$]Cl$_2$.H$_2$O (10)	1581	1341, 784	1267	1079	474	581
[Ni$_2$(HL^2)$_2$] (14)	1591	1333, 736	1260	1090	447	521
H$_3$L^3	1542	1389, 850	1289	1064	-	-
[Ni(H$_3$L^3)(H$_2$L^3)](ClO$_4$)$_2$ (7)	1607	1324, 773	1264	1061	455	569
[Ni(H$_2$L^3)$_2$][Ni(H$_3$L^3)$_2$]Cl$_2$ (11)	1604	1329, 775	1275	1081	427	578
[Ni$_2$(HL^3)$_2$] (15)	1597	1335, 737	1263	1095	424	520
H$_3$L^4	1542	1384, 807	1307	1051	-	-
[Ni(H$_3$L^4)(H$_2$L^4)](ClO$_4$)$_2$.2H$_2$O (8)	1606	1340, 780	1280	1088	464	569
[Ni(H$_2$L^4)$_2$][Ni(H$_3$L^4)$_2$]Cl$_2$.H$_2$O (12)	1606	1341, 780	1280	1085	473	579
[Ni$_2$(HL^4)$_2$] (16)	1595	1316, 734	1260	1089	445	521
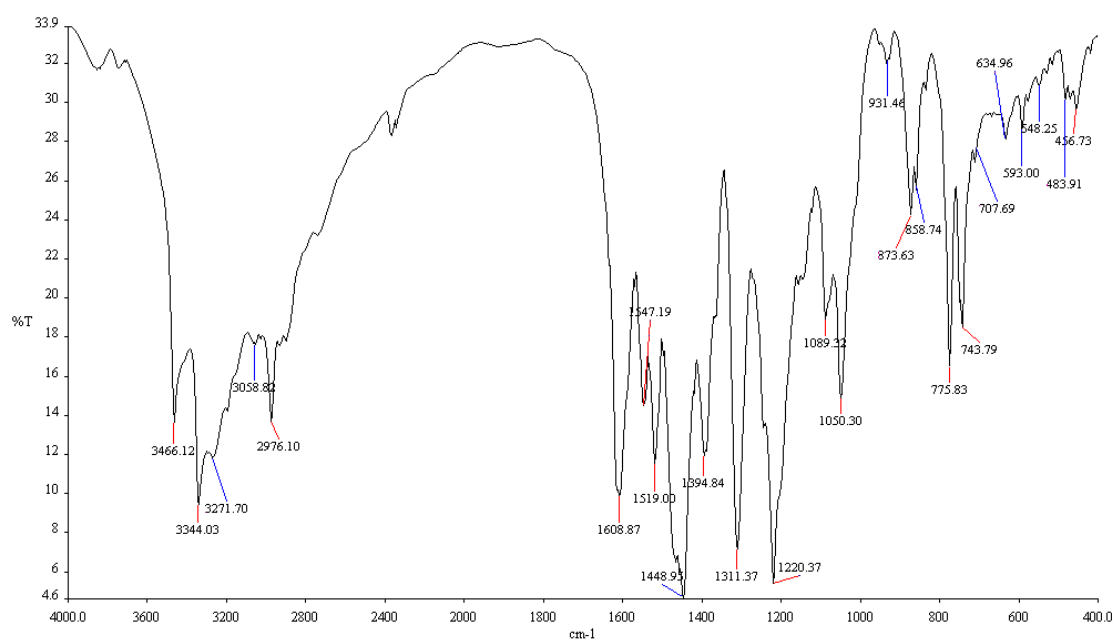
Figure 2.15: IR spectrum of $[Ni(H_3L^1)(H_2L^1)]ClO_4$ **(6)**
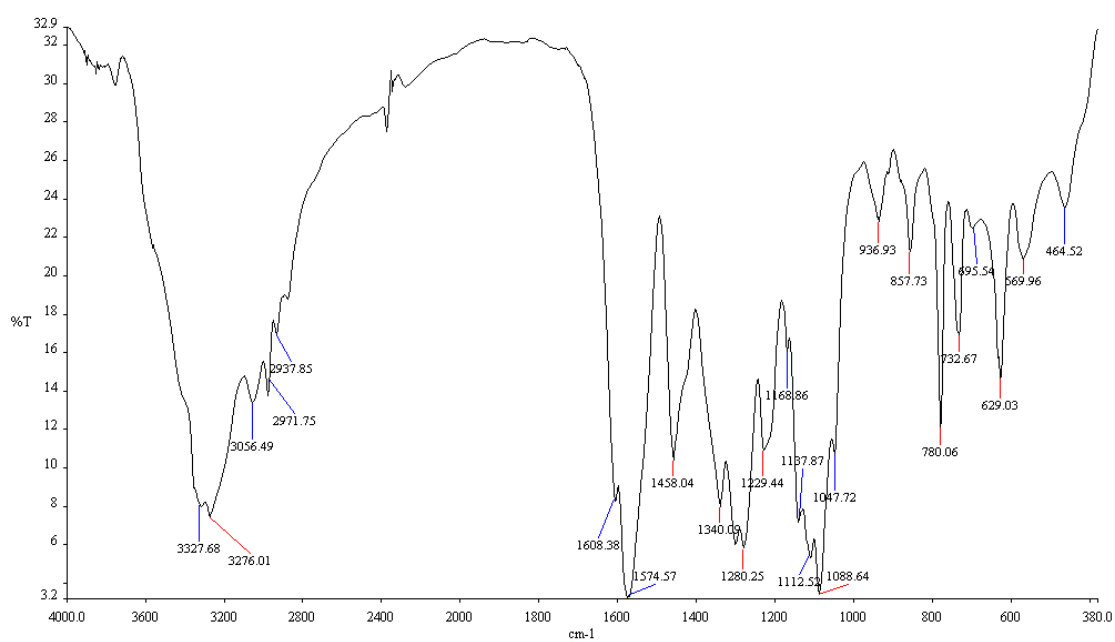
Figure 2.16: IR spectrum of $[Ni(H_3L^4)(H_2L^4)]ClO_4$ **(8)**
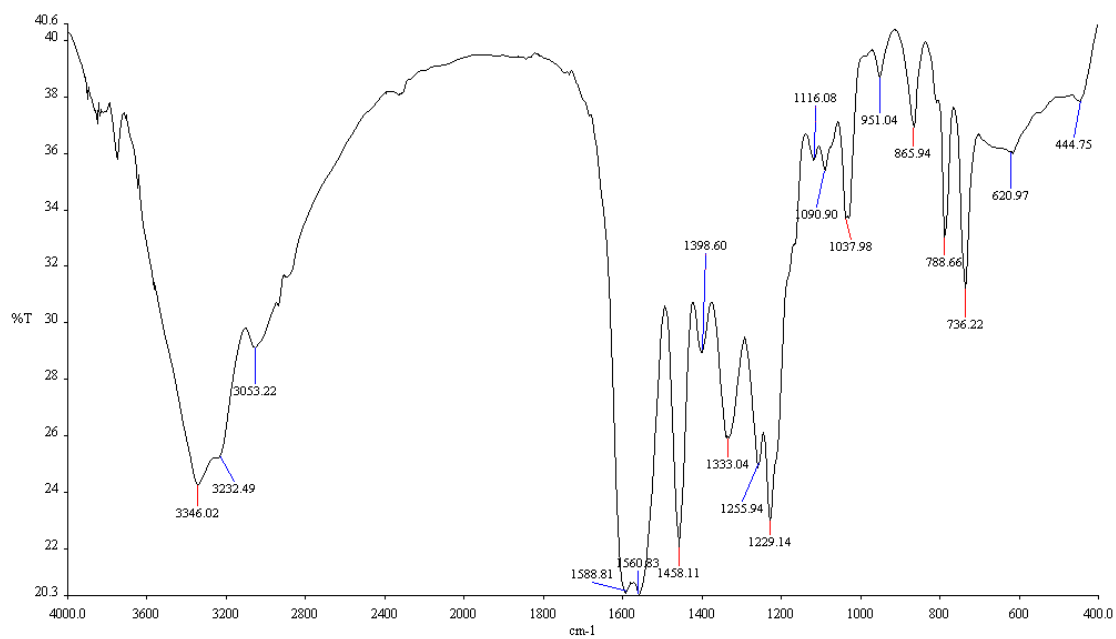
Figure 2.17: IR spectrum of $[Ni_2(HL^2)_2]$ **(14)**
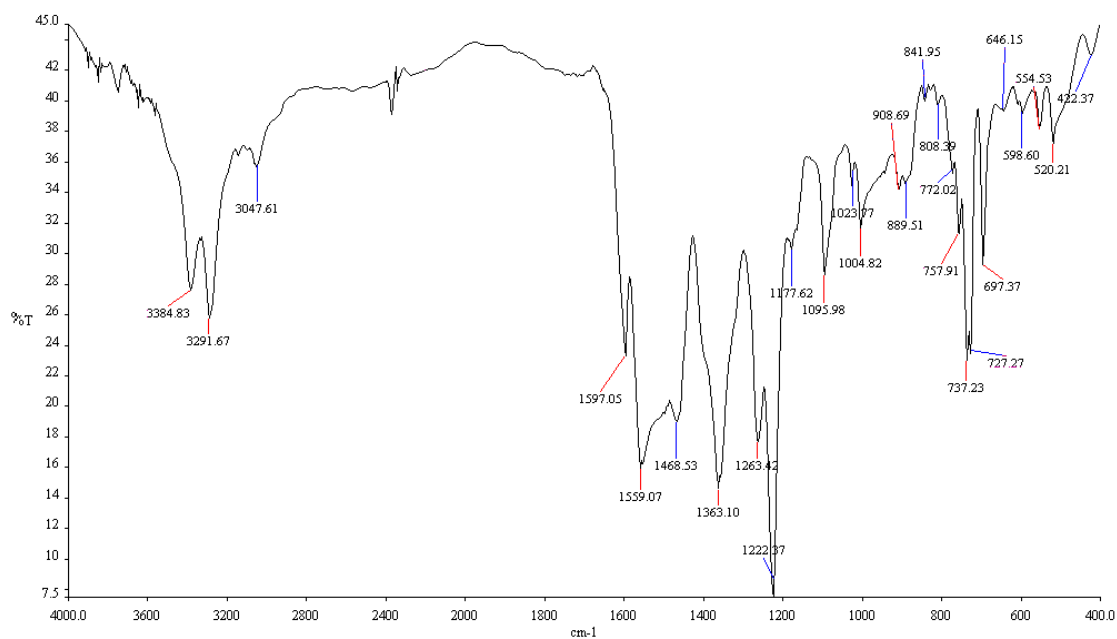
Figure 2.18: IR spectrum of $[Ni_2(HL^3)_2]$ **(15)**

71

2.3.6 Electronic Spectra

Important electronic spectral assignments of 2,3-dihydroxybenzaldeyde N4-thiosemicarbazones and their nickel complexes are presented in Table 2.9. The electronic spectra for the mononuclear nickel(II) complexes (**5-12**) were recorded using solutions in methanol whereas electronic spectra for nickel(II) dinuclear complexes (**13-16**) were recorded by using solutions in DMF. Electronic spectra of thiosemicarbazone ligands H_3L^{1-4} consist of transitions within the thiosemicarbazone moiety, involving a $\pi \rightarrow \pi^*$ band in the range 39,525 - 38,461 cm^{-1} and two n$\rightarrow \pi^*$ bands in the range 27,100-30,233 cm^{-1} mostly due to the azomethine group, the ring transitions and the thioamide group. Upon coordination with nickel(II) ion, these intraligand transitions underwent shifts either to high energy or low energy regions. The $\pi \rightarrow \pi^*$ transition band underwent significant shift to longer wavelength region which indicates coordination via the thioamide sulfur. This shift is a result of the C–S bond being weakened upon coordination (Latheef et al., 2009). Besides, a blue shift in the n$\rightarrow \pi^*$ band has been observed as a result of coordination of azomethine through donation of the lone pairs of electrons on the nitrogen atom. In the spectra of all complexes, one ligand to metal charge transfer (LMCT) band could be located in the range 23,630- 25,125 cm^{-1} which may assigned to S$\rightarrow$Ni LMCT (Manoj & Kurup, 2008).

The energies of the combination d–d bands in the nickel complexes **5** -**12** are in good agreement with octahedral nickel(II) complexes of thiosemicarbazones with ONS donors as well as other complexes (Castiñeiras et al., 2012; Garcìa et al., 2002; Saha et al., 2005). In accordance with these studies, the high energy band which is assigned to $^3A_{2g}$ (F) $\rightarrow$ $^3T_{2g}$ (P) transition is tailing into the visible region and obscured with the high intensity LMCT bands. The solution spectra of the complexes show two bands at 10,869-12,753 cm^{-1} and 15,174-17,006 cm^{-1} that can be assigned to the transitions $^3A_{2g}$

(F) $\rightarrow$ $^3T_{2g}$ (F) and $^3A_{2g}$ (F) $\rightarrow$ $^3T_{1g}$ (F) respectively, which is consistent with octahedral geometry.

On the other hand, the electronic spectra of the nickel(II) complexes **13-16**, show one broad *d-d* band at 20576-21920 cm^{-1}, which can be assigned to the square planar $^1A_{1g}$ $\rightarrow$ $^1B_{1g}$ transition (Gradinaru et al., 2004; Salem et al., 2008) . Normally, the *d-d* bands in diamagnetic nickel(II) complexes are observed as one absorption band due to the presence of four low d orbitals with eight paired electrons and one upper orbital being $d_{x2 - y2}$. The four lower orbitals are often so close in energy hence individual transitions from them to the upper d level cannot be differentiated, resulting in a single absorption band (Gomes et al., 2000; Manoj & Kurup, 2008).

Table 2.9: Electronic spectral assignments (cm^{-1}) for the thiosemicarbazone ligands and their nickel(II) complexes

Compound	$\pi\rightarrow\pi^*$	$n\rightarrow\pi^*$	LMCT	*d-d*
H$_3$L^1	38461	28221 30233	-	-
[Ni(H$_2$L^1)(H$_2$L^1)]ClO$_4$.2H$_2$O **(5)**	36333	31850	25000	12150 15600
[Ni(H$_2$L^1)$_2$][Ni(H$_3$L^1)$_2$]Cl$_2$.H$_2$O **(9)**	36786	31746	25011	12755 15174
[Ni$_2$(H$_3$L^1)$_2$]**(13)**	35842	30945	24173	21505
H$_3$L^2	38759	28328 30120	-	-
[Ni(H$_2$L^2)(H$_2$L^2)]ClO$_4$ **(6)**	36496	31095	24813	12674 16313
[Ni(H$_2$L^2)$_2$][Ni(H$_3$L^2)$_2$]Cl$_2$ **(10)**	36779	31876	24824	10869 16025
[Ni$_2$(H$_3$L^2)$_2$] **(14)**	35664	30545	24850	20576
H$_3$L^3	39525	27100 27932	-	-
[Ni(H$_2$L^3)(H$_2$L^3)]ClO$_4$ **(7)**	36900	29325	24752	11184 17006
[Ni(H$_2$L^3)$_2$][Ni(H$_3$L^3)$_2$]Cl$_2$ **(11)**	36714	28571	25125	11086 16736
[Ni$_2$(H$_3$L^3)$_2$] **(15)**	35087	29154	23364	20741
H$_3$L^4	39062	27700 28089	-	-
[Ni(H$_2$L^4)(H$_2$L^4)]ClO$_4$.H$_2$O **(8)**	36220	28853	24875	11806 16286
[Ni(H$_2$L^4)$_2$][Ni(H$_3$L^4)$_2$]Cl$_2$ **(12)**	36231	29070	24813	12077 16025
[Ni$_2$(H$_3$L^4)$_2$] **(16)**	35158	29069	23630	21920

CHAPTER 3

Synthesis and characterization of mixed nickel(II) complexes of 2,3-dihydroxybenzaldehyde *N*4-substituted thiosemicarbazones with phosphorus-based ligands

3.1 Introduction

The interest in phosphorus based compounds has been receiving significant attention in the last years due to the importance of phosphorus in both industrial and academic spheres. A large majority of the phosphorus compounds, particularly, phosphines have found wide applications as ligands in transition metal complex catalysts owing to their ability to accommodate a wide range of metal oxidation states and the capacity of these ligands to vary the electronic and steric properties (Halpern, 1983). In coordination chemistry, use of phosphorus ligands has been known for a long time (McAuliffe, 1973). However, the interesting property of the metal-phosphorus bonding arises due to the ligand to metal σ bond and metal to ligand π back bond by using the acceptor character of the empty $3d$ orbitals on the phosphorus atom and the filled or partially filled d orbitals of the metal cations. This characteristic leads to a remarkable stability in the phosphorus-metal bond. It has been noted that the behavior of the phosphorus ligands can differ by varying the substituents on phosphorus, which in turn will cause marked changes in their transition metal complexes. Besides the enormous applications diversity exhibited by the metal-phosphorus complexes, they possess a wide range of biological properties such as antiarthritic (Sutton et al., 1972), anticancer (Berners-Price et al., 1987) and antifungal (Dharmaraj et al., 2001).

Nickel complexes with phosphorus ligands represent an important family of compounds that have found uses in catalysis and drug development (Jarrettt & Sadler, 1991; Percec et al., 2004). Thus there is considerable interest in the chemistry of phosphorus based

compounds with nickel. In particular, the catalytic activities of nickel phosphine complexes, such as dichlorobis(triphenylphosphine) nickel(II), are of considerable interest in the cross-coupling of Grignard reagents with aryl and alkyl halides (Palo & Erkey, 1998).

Although research on nickel complexes containing thiosemicarbazones and triphenylphosphine have gained considerable interest (Prabhakaran et al., 2005; Ülküseven et al., 2008), their use in aryl–aryl coupling reaction as well as in medicinal applications are still less studied (Prabhakaran, Sivasamy, et al., 2011; Priyarega et al., 2011).

Guided by the above observations and considering the growing interest in the chemistry of nickel(II)-phosphine complexes of thiosemicarbazones, and to gain insight into the biological activity of these mixed ligand complexes, this chapter will present the synthesis and structural characterization of nickel-phosphine complexes with 2,3-dihydroxybenzaldehyde-N4-subsituted thiosemicarbazone.

3.2 Experimental

3.2.1 Materials and Solutions

Triphenylphosphine and 1,2-bis(diphenylphosphino)ethane were purchased from Merck, nickel(II) chloride hexahydrate, potassium thiocyanate was from Sigma-Aldrich and reagents used were of analytical grade and used without further purification.
The syntheses of the thiosemicarbazone H_3L^1, H_3L^2, H_3L^3 and H_3L^4 have been described in Chapter 2.

Dichlorobis(triphenylphosphine)nickel(II), [$NiCl_2(PPh_3)_2$] was prepared according to the published procedure (Venanzi, 1958): $NiCl_2.6H_2O$ (2.3794 g, 10 mmol) in 2 ml

water was dissolved with glacial acetic acid (50 ml). To this solution PPh$_3$ (5.2474 g, 20 mmol) dissolved in 25 ml glacial acetic acid was added with gentle warming to ensure solution. The olive-green microcrystalline precipitate, when kept in contact with its mother-liquor (glacial acetic) for 24 hours, gave dark blue crystals which were filtered off and washed with warm glacial acetic acid and ether.

Dichloro(1,2-bisdiphenylphosphinoethane)nickel(II), [NiCl$_2$(dppe)] was prepared according to published procedure (Hecke & Horrocks, 1966): NiCl$_2$.6H$_2$O (0.319 g, 1.34 mmol) was dissolved in 30 ml of 2-propanol/methanol and added to a solution of dppe (0.502 g, 0.126 mmol) dissolved in 50 ml warm 2-propanol. The orange precipitate formed was filtered and washed with ether and dried in air.

3.2.2 Physical measurements

IR spectra were recorded as KBr pellets in the frequency range of 400 – 4000 cm^{-1} by using a Perkin-Elmer Spectrum RX-1 spectrophotometer. ^{1}H NMR spectra were recorded in deuterated DMSO-d$_6$ on ECA 400 MHz instrument. ^{13}C NMR and ^{31}P NMR spectra were recorded in deuterated DMSO-d$_6$ on a JEOL ECA 400 MHz instrument. Elemental analyses were performed on a Pelkin-Elmer Analyst 400. UV–visible spectroscopic measurements were recorded with DMF solvent on a Shimadzu UV-1650PC spectrophotometer.

3.2.3 Syntheses of complexes

3.2.3.1 [Ni(H$_2$L^1)(PPh$_3$)]Cl (17)

 [NiCl$_2$(PPh$_3$)$_2$] (0.65 g, 1 mmol) was heated in ethanol (20 mL) for 30 min. The ligand H$_3$L^1 (0.21 g, 1 mmol) in hot methanol (20 mL) was added dropwise and the mixture was refluxed for 2 h. Slow evaporation of the solvent yielded brownish red crystals after

one week. The crystals were filtered, washed with cold ethanol and ether, dried in air and kept in a desiccator over silica gel.

(Yield: 0.11g, 60 %). Anal. Calc. for $C_{26}H_{23}N_3O_2SPNiCl$: C, 55.11; H, 4.09; N, 7.42. Found: C, 55.28; H, 4.60; N, 7.50%. IR (KBr disc, cm^{-1}): 3466 m, 3351 m, 3239 w, 3070 m, 3077m, 1622 s, 1584 m, 1457 s, 1434 m, 1332 w, 1314 m, 1275 m, 1231 s, 1207 w, 1097 m, 1057 w, 870 w, 767 m, 743 m, 710 m, 694 m, 590 w, 534 m, 514 w, 502 w, 483 w (s, strong; m, medium ; w, weak).

Characteristic ^1H NMR signals (DMSO-d_6, TMS, ppm): 11.44 (s,1H, NHCS), 9.51 (s,1H, OH), 8.28 (s,1H, CH=N), 8.01(s,1H, NH$_2$), 7.85(s,1H, NH$_2$), 7.41 - 7.29 (m, 15H, PPh$_3$),   6.76 (d,1H, aromatic, J = 7.3Hz), 6.57 (t,1H, aromatic), 6.25 (s,1H, aromatic). Characteristic ^{13}C NMR signals (DMSO-d_6, TMS, ppm): 172.38 (C=S), 149.79 (C-O), 149.27 (C-O), 147.32 (C=N), 134.98, 134.20, 131.94, 130.69, 129.33 (C - aromatic for triphenylphosphine), 121.47, 119.50, 117.37, 117.13(C-aromatic). Characteristic ^{31}P NMR signals (DMSO-d_6, ppm): 23.90.

3.2.3.2 Synthesis of [Ni(H$_2$L^2)(PPh$_3$)]Cl (18)

[NiCl$_2$(PPh$_3$)$_2$] (0.65 g, 1 mmol) was heated in ethanol (20 ml) for 30 min. The ligand H$_3$L^2 (0.22g, 1 mmol) in hot methanol (20 mL) was added dropwise and the mixture was refluxed for 2 h. Slow evaporation of the solvent yielded brownish red crystals. The crystals were filtered, washed with cold ethanol and ether, dried in air and kept in a desiccator over silica gel.

(Yield: 0.12 g, 58 %). Anal. Calc. for $C_{27}H_{25}N_3O_2SPNiCl$: C, 55.85; H, 4.34; N, 7.24. Found: C, 55.44; H, 4.64; N, 7.67%. IR (KBr disc, cm^{-1}): 3436 s, 3125 m, 3050 w, 2991 m, 1622 s, 1589 w, 1551 w, 1451 m, 1437 m, 1402 m, 1319 m, 1279 m, 1225 s, 1162 m, 1100 m, 871 w, 748 m, 736 m, 696 m, 532 m, 510 m, 486 w, 409 w (s, strong; m, medium ; w, weak).

Characteristic ^{1}H NMR signals (DMSO-d$_6$, TMS, ppm): 11.49 (s, 1H, NHCS), 9.64 (s,1H, OH), 8.82 (s, 1H, N*H*CH$_3$), 8.21 (s,1H, -CH=N), 7.49 - 7.39 (m, 15H, PPh$_3$), 6.85 (d,1H, aromatic, J = 7.3Hz), 6.64 (t,1H, aromatic), 6.38 (s,1H, aromatic), 3.02(s, 3H, -NHC*H$_3$*). Characteristic ^{13}C NMR signals (DMSO-d$_6$, TMS, ppm): 173.37 (C=S), 149.49 (C-O), 148.89 (C-O), 147.24 (C=N), 134.44, 134.14, 131.82, 130.86, 129.33 (C - aromatic for triphenylphosphine), 121.58, 119.43, 117.31, 116.99(C-aromatic), 31.45 (N-*C*H$_2$). Characteristic ^{31}P NMR signals (DMSO-d$_6$, ppm): 24.33.

3.2.3.3 Synthesis of [Ni(HL^3)(PPh$_3$)] (19)

[NiCl$_2$(PPh$_3$)$_2$] (0.65 g, 1 mmol) was heated in ethanol (20 mL) for 30 min. The ligand H$_3$L^3 (0.29 g, 1 mmol) in hot methanol (20 mL) was added dropwise and the mixture was refluxed for 2 h. The red precipitate was filtered, washed with cold ethanol and ether, dried in air and kept in a desiccator over silica gel. Red crystals of this complex were grown by recrystallization from DMF/ ethanol.

(Yield: 0.16 g, 72%). Anal. Calc. for C$_{32}$H$_{26}$N$_3$O$_2$SPNi: C, 59.80; H, 4.23; N, 6.54. Found: C, 60.03; H, 4.54; N, 6.39 %. IR (KBr disc, cm^{-1}): 3416 s, 3210 m, 3066 m, 3070 w, 2942 w, 1590 s, 1559 s, 1494 m, 1457 m, 1418 m,1400 m, 1376 m, 1308 s, 1268 m, 1234 s, 1159 m, 1095 m, 1074 w, 1053 w, 1026 w, 999 w, 866 w, 734 m, 693 m, 565 w, 531 m, 511m, 474 w (s, strong; m, medium ; w, weak).

Characteristic ^{1}H NMR signals (DMSO-d$_6$, TMS, ppm): 9.46 (s,1H, OH), 8.69 (d, 1H, CH=N, J = 8.1Hz), 7.82 (t, 6H, PPh$_3$), 7.77 (d,2H, Ph-aromatic, J = 8.1Hz), 7.59 (m, 9H, PPh$_3$), 7.24 (t, 2H, Ph- aromatic), 7.03 (d,1H, aromatic, J = 7.1), 6.91 (t, 1H, aromatic) , 6.62 (d,1H, Ph-aromatic, J = 6.8Hz), 6.50 (t,1H, Ph-aromatic), 5.43 (s, 1H, N*H*C$_6$H$_5$), Characteristic ^{13}C NMR signals (DMSO-d$_6$, TMS, ppm): 166.23 (C=S), 153.47 (C-O), 149.38 (C-O), 147.20 (C=N), 134.49, 134.39, 131.90, 129.57, 129.54 (C-

aromatic for triphenylphosphine), 141.75, 129.02, 123.17, 121.87, 118.73 , 117.22, 115.99, 113.84(C-aromatic). Characteristic ^{31}P NMR signals (DMSO-d$_6$, ppm): 23.74.

3.2.3.4 Synthesis of [Ni(HL^4)(PPh$_3$)] (20)

Ni(CH$_3$COO)$_2$ (0.12 g, 0.5mmol) , KSCN (0.09 g, 1mmol) and PPh$_3$ (0.26 g, 1mmol) in 10ml methanol were heated under reflux for 15 min. The ligand H$_3$L^4 (0.12 g, 0.5 mmol) in 10 mL methanol was added slowly, the resulting dark red solution was refluxed for 7 h. Dark red crystals were formed after leaving the reaction solution at room temperature for one day.

(Yield: 0.11 g, 64%). Anal. Calc. for C$_{28}$H$_{26}$N$_3$O$_2$SPNi: C, 59.59; H, 4.44; N, 7.72. Found: C, 59.39; H, 4.42; N, 7.78 %. IR (KBr disc, cm^{-1}): 3439 s, 2973 s, 2924 w, 2901 m, 1553 m, 1458 m, 1308 m, 1244 m,1228 s, 1065 m, 1048 s, 948 w, 880 m, 830 w, 740 m, 695 m, 606 w, 531 m, 509 w (s, strong; m, medium ; w, weak).

Characteristic ^{1}H NMR signals (DMSO-d$_6$, TMS, ppm): 8.33 (d,1H, CH=N, J = 8.2), 7.73 (t, 6H, PPh$_3$), 7.53(m, 9H, PPh$_3$), 6.88 (d,1H, aromatic, J = 7.7Hz), 6.51(d, 1H, aromatic, J = 7.2Hz), 6.40 (t, 1H, aromatic), 5.24 (s,1H, N*H*CH$_2$), 3.10 (q, 2H, C*H$_2$*CH$_3$), 0.99 (t,3H,CH$_2$C*H$_3$*). Characteristic ^{13}C NMR signals (DMSO-d$_6$, TMS, ppm): 169.74 (C=S), 150.57 (C-O), 148.56 (C-O), 147.06 (C=N), 134.46, 134.35, 131.78, 129.38, 128.93(C - aromatic for triphenylphosphine), 122.75, 117.49, 115.64, 113.16 (C-aromatic), 39.41 (N-**CH$_2$**-), 15.04 (NCH$_2$**CH$_3$**). Characteristic ^{31}P NMR signals (DMSO-d$_6$, ppm): 23.93.

3.2.3.5 Synthesis of [Ni$_2$(HL^1)$_2$(μ-dppe)] (21)

To a warm solution composed of 30 mL of methanol, 0.124 g (0.0005 mol) Ni(CH$_3$COO)$_2$.4H$_2$O, (0.097 g, 0.001 mol) KSCN and 0. 2 g (0.0005 mol) dppe, were added 10 mL of boiling methanol containing 0.105 g (0.0005 mol) H$_3$L^1. The mixture

was stirred under reflux for 4 h. The resulting orange precipitate was filtered off, washed with ethanol and diethyl ether and dried at room temperature.

(Yield: 0.19 g, 82%). Anal. Calc. for $C_{42}H_{38}N_6Ni_2O_4P_2S_2$: C, 53.99; H, 4.10; N, 9.00. Found: C, 53.76; H, 4.21; N, 9.09 %. IR (KBr disc, cm^{-1}): 3429 s, 3282 s, 3259 s , 3151 s, 2971m, 1584 m, 1593 w, 1553 s, 1531s, 1457 s, 1437m,1411w, 1304s, 1261 w, 1230 s, 1180 w, 1102 m, 1048 w, 982 s, 946 w, 877 m, 843 w, 778 m, 732 m, 722 s, 694 m 592 w, 511 m, 483m (s, strong; m, medium ; w, weak).

Characteristic ^1H NMR signals (DMSO-d_6, TMS, ppm): 8.22 (s, 1H, OH), 7.84 (s, 1H, CH=N), 7.63-7.38 (m, 10H, dppe aromatic), 6.86 (d,1H,aromatic, J = 7.8 Hz), 6.63 (d, 1H,aromatic, J = 7.3 Hz), 6.56 (s, 2H, NH$_2$), 6.43 (t, 1H, aromatic), 2.82(s, 2H, CH2(dppe)). Characteristic ^{13}C NMR signals (DMSO-d6, TMS, ppm): 171.37 (C=S), 149.96 (C-O), 149.40 (C-O), 147.67 (CH=N), 133.08, 132.46, 131.00, 129.39 (C - aromatic for dppe), 122.81, 117.82, 115.52, 113.97 (C-aromatic). Characteristic ^{31}P NMR signals (DMSO-d_6, ppm): 22.03.

3.2.3.6 Synthesis of [Ni$_2$(HL^2)$_2$(μ-dppe)] (22)

Complex **22** was similarly prepared as complex **21** by using 2,3-dihydroxybenzaldehyde 4-methylthiosemicarbazone (0.112 g, 0.0005 mol) as the Schiff base ligand.

(Yield: 0.21 g, 89%). Anal. Calc. for $C_{44}H_{42}N_6Ni_2O_4P_2S_2$: C, 54.92; H, 4.40; N, 8.73. Found: C, 54.89; H, 4.41; N, 8.80 %. IR (KBr disc, cm^{-1}): 3436 s, 3259 s , 3052 s, 2945m, 1590 s, 1555 s, 1530 s, 1531s, 1457 s, 1434 m,1408 m, 1304 m, 1228 s, 1167 m, 1101 m, 1065 w, 1048 w, , 946 w, 872 m, 813 w, 778 w, 732 m, 704 m, 695 m 590 w, 558 w, 525 m, 476 m, 441 w (s, strong; m, medium ; w, weak).

Characteristic ^1H NMR signals (DMSO-d_6, TMS, ppm): 8.30 (s, 1H, OH), 7.71 (s, 1H, CH=N), 7.51-7.34 (m, 10H, dppe aromatic), 6.92 (d,1H, N*H*CH$_3$, J = 7.4 Hz), 6.85(d,

1H, aromatic, J = 7.7 Hz), 6.60 (d, 1H, aromatic, J=7.2), 6.41 (t, 1H, aromatic), 2.79 (s, 2H, CH$_2$(dppe)), 2.66 (d, 3H, NHC$\boldsymbol{H_3}$, J=4.5). Characteristic ^{13}C NMR (DMSO-d$_6$, TMS, ppm): 170.58 (C=S), 150.63 (C-O), 149.39 (C-O), 147.69 (CH=N), 133.12, 132.43, 131.03, 129.39 (C - aromatic for dppe), 122.87, 117.95, 115.52, 114.03 (C-aromatic), 32.34 (N-$\boldsymbol{C}$H3). Characteristic ^{31}P NMR (DMSO-d$_6$, ppm): 21.95.

3.2.3.7 Synthesis of [Ni$_2$(HL^3)$_2$(μ-dppe)] (23)

Complex **23** was similarly prepared as complex **21** by using 2,3-dihydroxybenzaldehyde 4-phenylthiosemicarbazone (0.143 g, 0.0005 mol) as the Schiff base ligand. This complex was also prepared by the following procedure:

Solid [NiCl$_2$(dppe)] (0.19 g; 0.0004 mol) was slowly added to H$_3$L^3 (0.104 g, 0.0004 mol) in ethanol/acetonitrile mixture (30 mL). The mixture was refluxed for 2h. The dark red solution was allowed to stand for 4 days at room temperature. Orange red crystals obtained were washed with methanol and recrystallized from DMSO-d$_6$which afforded suitable crystals for X-crystallographic work.

(Yield: 0.24g, 87%). Anal. Calc. for C$_{54}$H$_{46}$N$_6$Ni$_2$O$_4$P$_2$S$_2$: C, 59.70; H, 4.27; N, 7.74. Found: C, 59.73; H, 4.23; N, 7.79 %. IR (KBr disc, cm^{-1}): 3426 s, 3052 m, 1594 s, 1593 w, 1559 s, 1508 s, 1455 s, 1434 s,1400 m, 1310 s, 1268 m, 1229 s, 1205 m, 1102 m, 1054 w, 982 s, 995 w, 873 m, 833 w, 778 w, 736 m, 717 m, 692 m, 590 w, 556 m, 520 m, 490 m, 447 w (s, strong; m, medium ; w, weak).

Characteristic ^{1}H NMR signals (DMSO-d6, TMS, ppm.): 9.41 (s, 1H, OH), 8.60 (s, 1H, CH=N), 7.69 (t, 6H, dppe aromatic), 7.84 (t, 2H, Ph-aromatic), 7.39 (t, 4H, dppe aromatic), 7.23 (t, 2H, Ph-aromatic), 6.99(d,1H, aromatic, J = 7.1Hz), 6.89 (t, 2H, Ph-aromatic & N$\boldsymbol{H}$C$_6$H$_5$), 6.72 (d, 1H, aromatic, J = 8.8Hz), 6.50 (t, 1H, aromatic), 2.99 (s, 2H, CH$_2$ (dppe)). Characteristic ^{13}C NMR (DMSO-d$_6$, TMS, ppm.): 166.24(C=S), 153.32 (C-O), 150.47 (C-O), 147.96 (CH=N), 133.18, 132.55, 129.41 (C - aromatic for

dppe), 141.80, 129.03, 123.29, 121.76, 118.65, 117.82, 115.78, 114.79 (C- aromatic).

Characteristic ^{31}P NMR (DMSO-d$_6$, ppm): 22.90.

3.2.3.8 Synthesis of [Ni$_2$(HL^4)$_2$(μ-dppe)] (24)

Complex **24** was similarly prepared as complex **21** by using 2,3-dihydroxybenzaldehyde 4-ethylthiosemicarbazone (0.119 g, 0.0005 mol) as the Schiff base ligand.

(Yield: 0.22g, 90%). Anal. Calc. for C$_{46}$H$_{46}$N$_6$Ni$_2$O$_4$P$_2$S$_2$: C, 55.79; H, 4.68; N, 8.49. Found: C, 55.76; H, 4.66; N, 8.45 %. IR (KBr disc, cm^{-1}): 3434 m, 3400 m, 3050 m , 2968 m, 1596 m, 1559 s, 1534 s, 1459 s, 1435m, 1306 m, 1261 m, 1231 s, 1155 w, 1102 m, 1043 w, 998 w, 872 m, 833 w, 777 w, 733 s, 718 s, 702 m 593 w, 556 m, 519 m, 489m, 436 w (s, strong; m, medium ; w, weak).

Characteristic ^{1}H NMR signals (DMSO-d$_6$, TMS, ppm): 8.32 (s, 1H, OH), 7.74 (s, 1H, CH=N), 7.61-7.38 (m, 10H, dppe aromatic), 7.00 (t,1H, -N*H*CH$_2$CH$_3$), 6.89 (d, 1H, aromatic, J = 7.8Hz), 6.64(1H, d, aromatic, J = 7.3Hz), 6.44(t, 1H, aromatic), 3.15(q, 2H, C*H$_2$*CH$_3$), 1.03 (t, 3H, CH$_2$C*H$_3$*), 2.79 (s, 2H, CH$_2$ (dppe)). Characteristic ^{13}C NMR (DMSO-d6, TMS, ppm.): 169.69 (C=S), 150.41 (C-O), 149.39 (C-O), 147.67 (CH=N), 133.12, 132.43, 131.03, 129.39 (C- aromatic dppe), 122.85, 117.97, 115.51, 113.99 (C-aromatic), 15.11 (NH-*C*H$_2$CH$_3$). Characteristic ^{31}PNMR (DMSO-d$_6$, ppm): 22.06.

3.2.4 X-ray crystallography

Block brown crystals of complexes [Ni(H$_2$L^1)(PPh$_3$)]Cl **(17)** and [Ni(H$_2$L^2)(PPh$_3$)]Cl **(18)** were grown from slow evaporation of their methanol/ethanol solutions. While red crystals of compound [Ni(HL^4)(PPh$_3$)] **(20)** were obtained from its methanol mother liquor.   Recrystallization of complex [Ni(HL^3)(PPh$_3$)] **(19)** from a mixture of dimethylformamide/ethanol afforded plate purple   crystals whereas   block purple

crystals of complexes [Ni$_2$(HL^1)$_2$(μ-dppe)] **(21)** and [Ni$_2$(HL^2)$_2$(μ-dppe)] **(22)** were grown by recrystallization of their solids from dimethylformamide (DMF) whereas complex [Ni$_2$(HL^3)$_2$(μ-dppe)] **(23)** was recrystallized from d6-DMSO.

Data were collected on the Bruker SMART APEX CCD area detector diffractometer, equipped with a highly-oriented pyrolytic graphite crystal incident beam monochromator and a molybdenum Kα (λ = 0.71073 Å). The APEX2 software was used for data acquisition and the SAINT software for cell refinement and data reduction (Bruker, 2007). SADABS software was used for Absorption data corrections (Sheldrick, 1996). The structures were solved and refined by SHELXL97 (Sheldrick, 2008). Molecular graphics were drawn by using ORTEP (Farrugia, 1997) and PLATON (Spek, 2003).

3.3 Results and discussion

3.3.1 Synthesis of the complexes

The colors, stoichiometries and partial elemental analyses of mixed nickel(II) complexes of thiosemicarbazone ONS donors with phosphines are listed in Table 3.1 The elemental analyses data of all the complexes are consistent with the molecular formula. All the nickel(II) phosphine complexes of 2,3-dihydroxybenzaldehyde −N4 − substituted thiosemicarbazone are air stable, non hygroscopic in nature, insoluble in water and soluble in common solvents such as dichloromethane, acetone, acetonitrile dimethylformamide and dimethylsulfoxide.

The new nickel(II) complexes of the type [Ni(H$_2$L)(PPh$_3$)]Cl **(17)**, **(18)** were obtained in high yield from the reactions of [NiCl$_2$(PPh$_3$)$_2$] with H$_3$L in 1 : 1 molar ratio (H$_3$L = tridentate ligand derived from 2,3-dihydroxybenzaldehyde and thiosemicarbazide and 4-

methylthiosemicarbazide) in ethanol/methanol, PPh_3 = triphenylphosphine. In the case of N4-phenyl substituted, however, neutral complex of the formula $[Ni(HL^3)(PPh_3)]$ **(19)** were obtained. Synthesis of the nickel-triphenylphosphine complex with 2,3-dihydroxybenzaldehye-4-ethylthiosemicarbazone were not successful from the reaction of $[NiCl_2(PPh_3)_2]$ with this ligand. Instead, $[Ni(HL^4)(PPh_3)]$ **(20)** was obtained by the reaction of nickel(II) acetate $Ni(OAc)_2.4H_2O$ and triphenylphosphine (PPh_3) with the ligand in the presence of potassium thiocyanate. All the complexes were isolated as brown or red crystals from their mother liquor, except the complex with phenyl substitution. The mode of coordination is different for all the four N4-subsituted thiosemicarbazone ligands. They were able to coordinate as dianionic ligands in complexes **(19)** and **(20)** when the thiosemicarbazone moiety has lost both of its thioamide and phenolic protons but coordinate as monoanionic ligands in complexes **(17)** and **(18)** when the thiosemicarbazone moiety has lost only the phenolic proton. In all the reactions with the complex $[NiCl_2(PPh_3)_2]$, it has been observed that the thiosemicarbazones behaved as tridentate ONS chelating ligand by substituting both the chloride ions and one of the triphenylphosphines in the starting complex (Scheme 3.1).

Dinuclear nickel- phosphine complexes of thiosemicarbazone **(21 – 24)** of the general formula $[Ni_2(dppe)(HL)_2]$ (dppe = 1,2-bis(diphenylphosphino)ethane; HL = doubly deprotonated 2,3-dihydroxybenzaldehyde-N4-substituted thiosemicarbazone) were formed in excellent yield by the reaction of the ligands with nickel(II) acetate and dppe in methanolic solution. The acetate anion in this reaction was metathetically displaced by thiocyanate anion. However, the complex $[Ni_2(dppe)(HL^3)_2]$ $(HL^3 = 2,3$-dihydroxybenzaldehyde-4-phenylthiosemicarbazone) was formed by the reaction of the ligand with $[NiCl_2(dppe)]$ in acetonitrile/ethanol mixture (Scheme 3.2).

Table 3.1: Stoichiometries, color and partial elemental analyses of nickel(II)–phosphine thiosemicarbazone complexes

Complex	Stoichiometries	Color	Anal.Calc. (Found)%		
			C	H	N
[Ni(H$_2$L^1)(PPh$_3$)]Cl **(17)**	C$_{26}$H$_{23}$N$_3$O$_2$SPClNi	Brown	55.11	4.09	7.42
			(55.28)	(4.60)	(7.50)
[Ni(H$_2$L^2)(PPh$_3$)]Cl **(18)**	C$_{27}$H$_{25}$N$_3$O$_2$SPClNi	Brown	55.85	4.34	7.24
			(55.44)	(4.64)	(7.67)
[Ni(HL^3)(PPh$_3$)] **(19)**	C$_{32}$H$_{26}$N$_3$O$_2$SPNi	Red	59.80	4.23	6.54
			(60.03)	(4.54)	(6.39)
[Ni(HL^4)(PPh$_3$)] **(20)**	C$_{28}$H$_{26}$N$_3$O$_2$SPNi	Purple	59.59	4.44	7.72
			(59.39)	(4.42)	(7.78)
[Ni$_2$(HL^1)$_2$(dppe)] **(21)**	C$_{42}$H$_{38}$N$_6$Ni$_2$O$_4$P$_2$S$_2$	Purple	53.99	4.10	9.00
			(53.76)	(4.21)	(9.09)
[Ni$_2$(HL^2)$_2$(dppe)] **(22)**	C$_{44}$H$_{42}$N$_6$Ni$_2$O$_4$P$_2$S$_2$	Purple	54.92	4.40	8.73
			(54.89)	(4.21)	(8.80)
[Ni$_2$(HL^3)$_2$(dppe)] **(23)**	C$_{54}$H$_{46}$N$_6$Ni$_2$O$_4$P$_2$S$_2$	Purple	59.70	4.27	7.74
			(59.73)	(4.23)	(7.79)
[Ni$_2$(HL^4)$_2$(dppe)] **(24)**	C$_{46}$H$_{46}$N$_6$Ni$_2$O$_4$P$_2$S$_2$	Purple	55.79	4.68	8.49
			(55.76)	(4.66)	(8.45)

The spectroscopic and crystallographic data show that all these complexes are dinuclear complexes where the two nickel(II) ions are bridged by the bidentate dppe ligand while the thiosemicarbazone ligand is coordinated to each nickel(II) through the azomethine nitrogen, thiolate sulfur and phenolic oxygen.

The magnetic moment values of all nickel(II) phosphine thiosemicarbazone complexes in the crystalline state show diamagnetic nature and the results are in accordance with a square planar geometry for d^8 system (Biittcber et al., 1993).
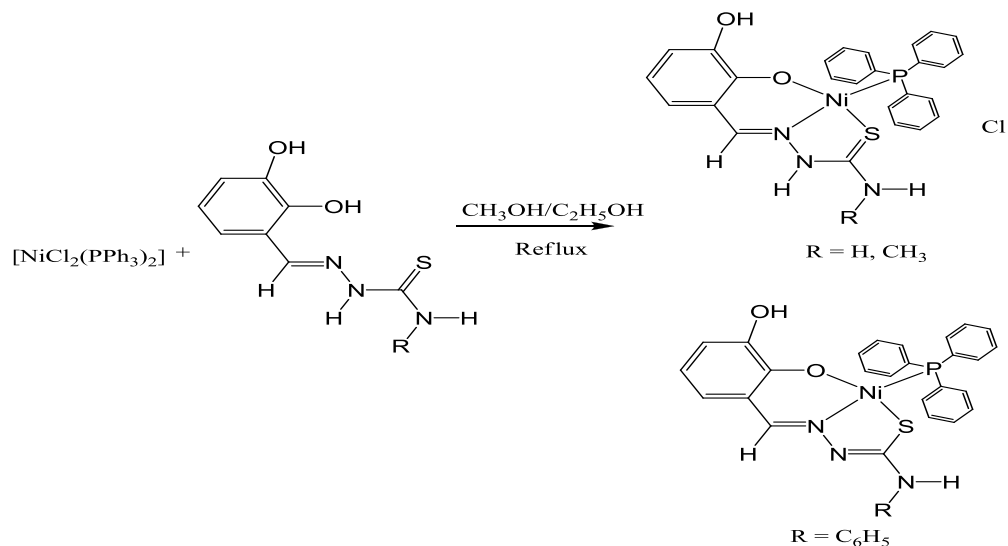
Scheme 3.1: Synthesis of [Ni(H$_2$L^{1,2})(PPh$_3$)]Cl and [Ni(HL^3)(PPh$_3$)]
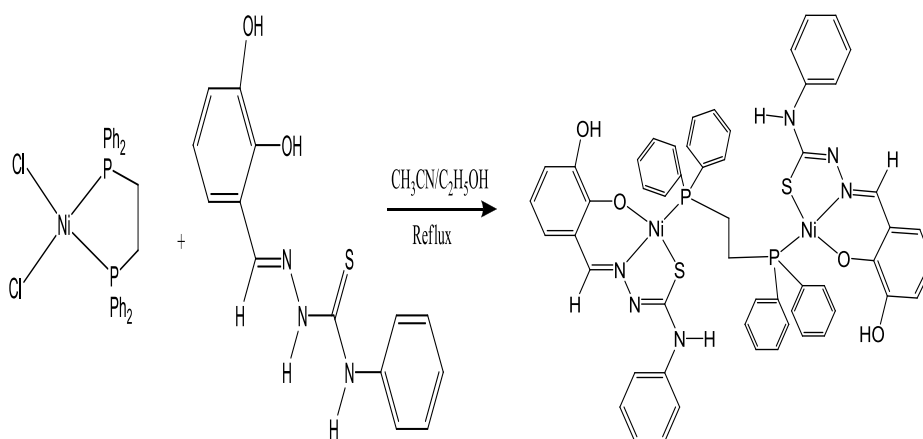
Scheme 3.2: Synthesis of [Ni$_2$(HL^3)$_2$(dppe)]

3.3.2 Crystal structure analysis

3.3.2.1 Crystal structures of [Ni(H$_2$L^1)(PPh$_3$)]Cl (17) and [Ni(HL^4)(PPh$_3$)] (20)

Complex **17** crystallized into an orthorhombic lattice with space group symmetry *P2$_1$2$_1$2$_1$* and Z = 4. A block brown crystal of size 0.35 × 0.25 × 0.20 mm was mounted on a glass fiber for X-ray crystallographic study. Figure 3.1 shows the perspective molecular structure of the compound with numbering scheme. The crystallographic

parameters are summarized in Table 3.2. Selected bond lengths and angles are given in Table 3.3. The structure showed that complex **17** is mononuclear and four-coordinated with one triphenylphosphine and one mono deprotonated 2,3-dihydroxybenzaldehyde thiosemicarbazone as a tridentate ligand coordinating to Ni(II) via azomethine nitrogen (N1), phenolic oxygen (O1) and thione sulfur (S1) forming a six- and five-membered chelate rings with O1–Ni1–N1 and N1–Ni1–S1 bite angles of 94.09 (5)° and 87.90(4)°, respectively. The structure of complex **17** is a distorted square planar geometry with S1–Ni1–O1 and P1–Ni1–N1 bond angels of 176.98(14)° and 176.19(4)°, respectively.
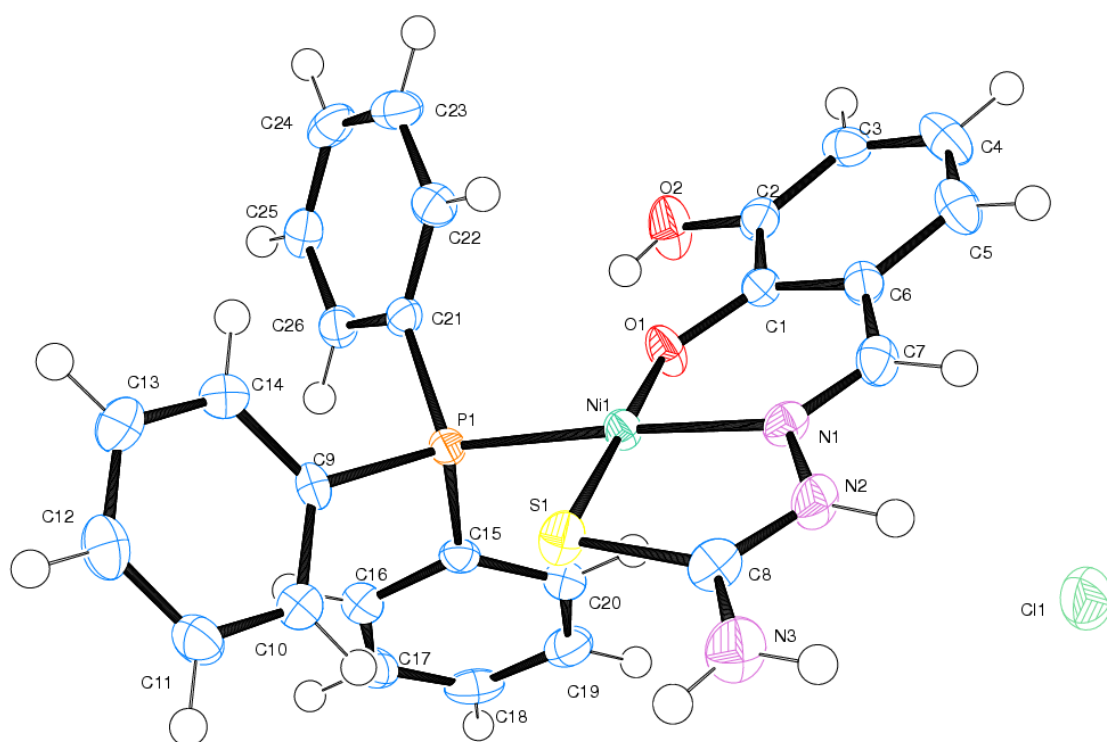
Figure 3.1: ORTEP diagram for [Ni(H$_2$L^1)(PPh$_3$)]Cl **(17)**, displacement ellipsoids are drawn at 70 % probability level and hydrogen atoms are shown as small spheres of arbitrary radii

The Ni(II) ion is found to be displaced by 0.0422 Å from the plane constituted by the atoms O1, N1, S1, P1. The thiosemicarbazone moiety C7, N1, N2, C8, S1, N3, also is almost planar and has a maximum least square plane deviation of 0.0479(13) Å and is at an angle of 12.55(5)° to the plane of the four donor atoms O1, S1, N1 and P1. The

dihedral angle formed by the least square planes Cg(l) comprising atoms Nil, S1, C8, N2, N1 and Cg(2) comprising atoms Nil, O1, C1, C6, C7,N1 is 9.05(5)°. The Ni–O, Ni–N, Ni–S and Ni–P distances were found to be 1.847(1), 1.897(1), 2.1416(4) and 2.1998 (4) Å respectively. This indicates the domination of thiosemicarbazone moiety in the bonding where the nickel atom is closer to thiosemicarbazone moiety than the PPh$_3$. The molecular structure of the complex shows that the ligand is coordinated in its thione tautomer with C8–S1 bond length of 1.724(17) Å, which is shorter than the C8–S1 bond length reported for nickel(II) triphenylphosphine complex with salicylaldehyde N4-phenylthiosemicarbazone (Prabhakaran et al., 2005). Coordination of the phenolic oxygen O1 results in decrease of O1–Cl bond length by 0.04 Å when compared with the uncomplexed O2–C2 bond length.

Table 3.2: Crystal data and structure refinement parameters for complexes **17** and **20**

Parameters	[Ni(H$_2$L^1)(PPh$_3$)]Cl (17)	[Ni(HL^4)(PPh$_3$)] (20)
Empirical Formula	[Ni(C$_8$H$_8$N$_3$O$_2$S)(C$_{18}$H$_{15}$P)]Cl	[Ni(C$_{10}$H$_{11}$N$_3$O$_2$S)(C$_{18}$H$_{15}$P)]
Formula weight, M	566.66	558.26
Temperature, T (K)	100	100
Wavelength, Mo Kα (Å)	λ = 0.71073	λ = 0.71073
Crystal system	Orthorhombic	Orthorhombic
Space group	*P2$_1$2$_1$2$_1$*	*P2$_1$2$_1$2$_1$*
Unit cell dimensions		
a(Å)	7.7902 (4)	10.6015(7)
b(Å)	14.6791 (7)	12.9827(8)
c (Å)	21.7410 (11)	18.2094(11)
α(°)	90.00	90.00
β(°)	90.00	90.00
γ(°)	90.00	90.00
Volume V (Å^3)	2486.2 (2)	2506.3(3)
Z	4	4
Absorption coefficient, μ(mm^{-1})	1.07	0.953
Crystal size (mm)	0.35 × 0.25 × 0.20	0.5 × 0.5 × 0.5
Reflections collected	9879	33868
Density (calculated), (mg m^{-3})	1.514	1.480
F(0 0 0)	1168	1160
Data/ parameters /restraints	5703/332/4	6267/326 /0
S	1.02	1.012
Independent reflections	5703	6267
	[R(int) = 0.028]	[R(int) = 0.0241]
R[F^2 > 2σ(F^2)]	0.021	0.0258
wR(F^2)	0.054	0.0608
Largest difference peak and hole (e Å^{-3})	0.29 and −0.21	0.057 and 0.004

Table 3.3: Selected bond lengths (Å) and angles (°) for complex **17**

Bond lengths		Bond angles	
Ni1—O1	1.847 (1)	O1—Ni1—N1	94.09 (5)
Ni1—N1	1.897 (1)	O1—Ni1—S1	176.98 (4)
Ni1—P1	2.1998 (4)	N1—Ni1—S1	87.90 (4)
Ni1—S1	2.1416 (4)	O1—Ni1—P1	85.66 (4)
S1—C8	1.7240 (17)	N1—Ni1—P1	176.19 (4)
P1—C15	1.8134 (16)	S1—Ni1—P1	92.207 (17)
P1—C9	1.8176 (17)	C8—S1—Ni1	97.58 (6)
P1—C21	1.8211 (16)	C7—N1—N2	116.02 (13)
O1—C1	1.3198 (18)	C7—N1—Ni1	126.64 (12)
O2—C2	1.360 (2)	N3—C8—S1	121.41 (14)
O2—H1	0.839 (10)	N2—C8—S1	118.71 (12)
N1—C7	1.296 (2)		
N1—N2	1.3904 (19)		
N2—C8	1.328 (2)		
N3—C8	1.319 (2)		

Hydrogen bonding interactions for complex **17** is shown in Figure 3.2 and hydrogen bonding parameters are shown in Table 3.4. The molecules of **17** are stabilized by various hydrogen bonding interactions and are packed in the lattice in an offset manner (Figure 3.3). The hydroxy group forms an intramolecular O–H…O hydrogen bond. The two amino groups of the cation are hydrogen-bond donors to the chloride anion and the hydrogen bonds generate a zig-zag chain structure running along the *b* axis as shown in Figure 3.4. No obvious π-π or C–H$\cdots\pi$ interactions were observed in the crystal packing of this complex.
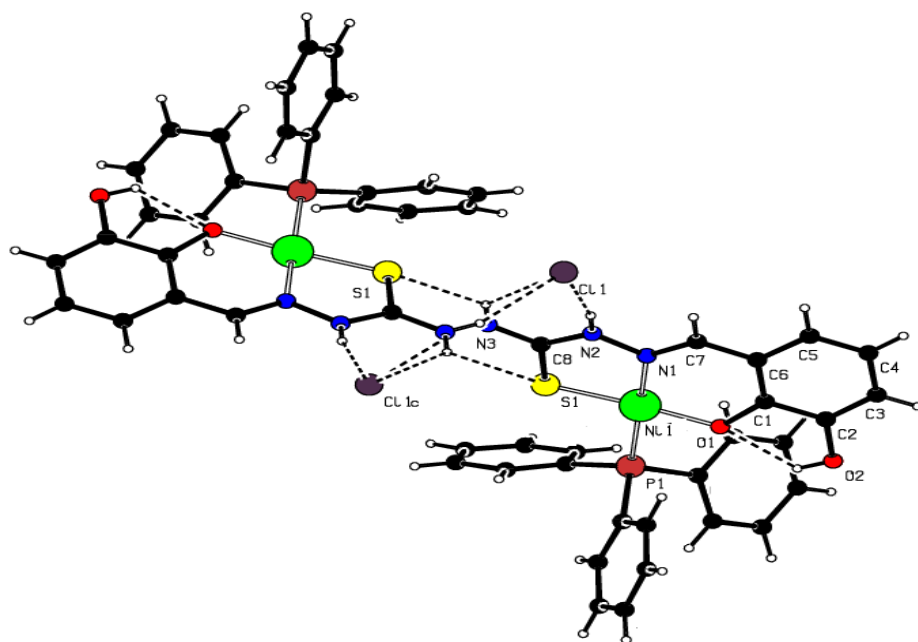
Figure 3.2: Hydrogen bonding interactions in complex **17**

Table 3.4: Hydrogen-bond geometry (Å, °) for complex **17**

D–H⋯A	D—H	H⋯A	D⋯A	D—H⋯A
O2–H1⋯O1	0.84	2.11	2.636(16)	120
N2–H2⋯Cl1	0.86	2.17	3.016(16)	167
N3–H31⋯Cl1	0.85	2.46	3.275(16)	161
N3–H32⋯Cl1	0.85	2.82	3.500(17)	137
N3–H32⋯S1	0.85	2.80	3.441(17)	132
C13–H13⋯S1	0.95	2.85	3.76(17)	161
C16–H16⋯O2	0.95	2.37	3.22(19)	141
C20–H20⋯O1	0.95	2.56	3.22(19)	128

Symmetry codes: x−1/2, −y+1/2, −z+1
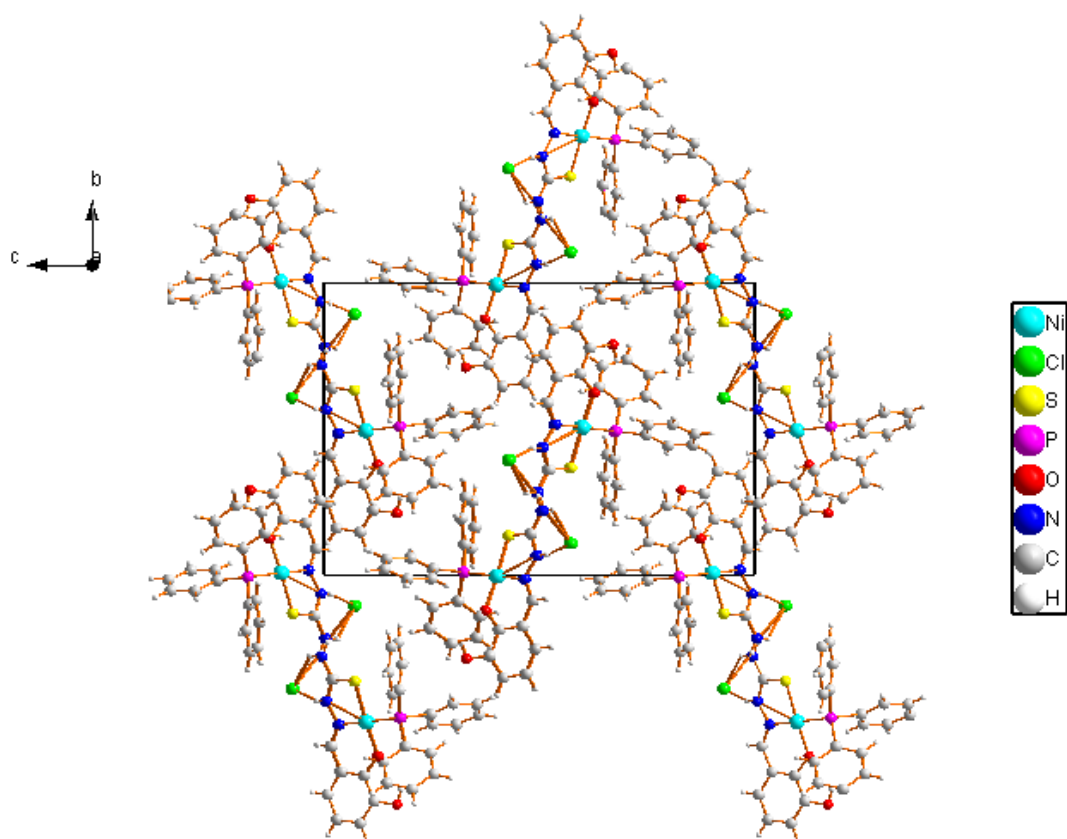
Figure 3.3: Unit cell packing diagram for complex **17** along *a* axis with intermolecular hydrogen bonding interactions
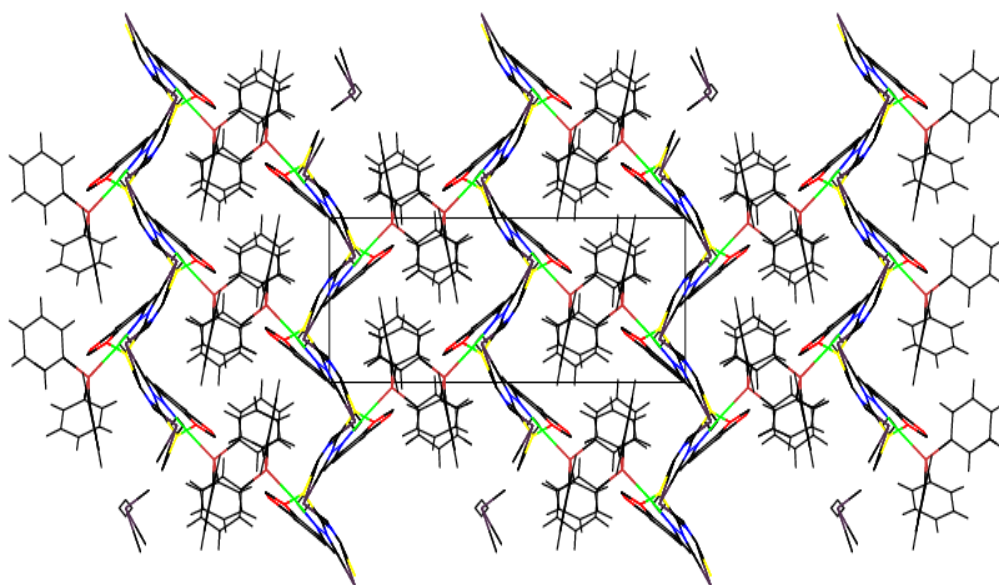
Figure 3.4: Zig zag chain formed from N2–H2···Cl1 and N3–H3···Cl1 hydrogen bonding interactions for complex **17** view down from *b* axis

The complex **20** crystallized into orthorhombic crystal system. The molecular structure of $[Ni(HL^4)(PPh_3)]$ **(20)** is shown in Figures 3.5 while selected bond lengths and bond angles are summarized in Table 3.5. The geometry around nickel atom in this complex is also a distorted square planar as can be seen from the bond angles. The ligand is coordinated as ONS tridentate binegative anion in its deprotonated form as is indicated by the absence of counter ions, through azomethine nitrogen, phenolic oxygen and thiolate sulfur atoms forming one stable six membered (Ni, N1, C7, C1, C2, O1) and another five membered ring (Ni, S1, C8, N2, N1). The fourth coordination position is occupied by a P atom from the PPh$_3$ coligand which is coordinated to Ni *trans* to N1.
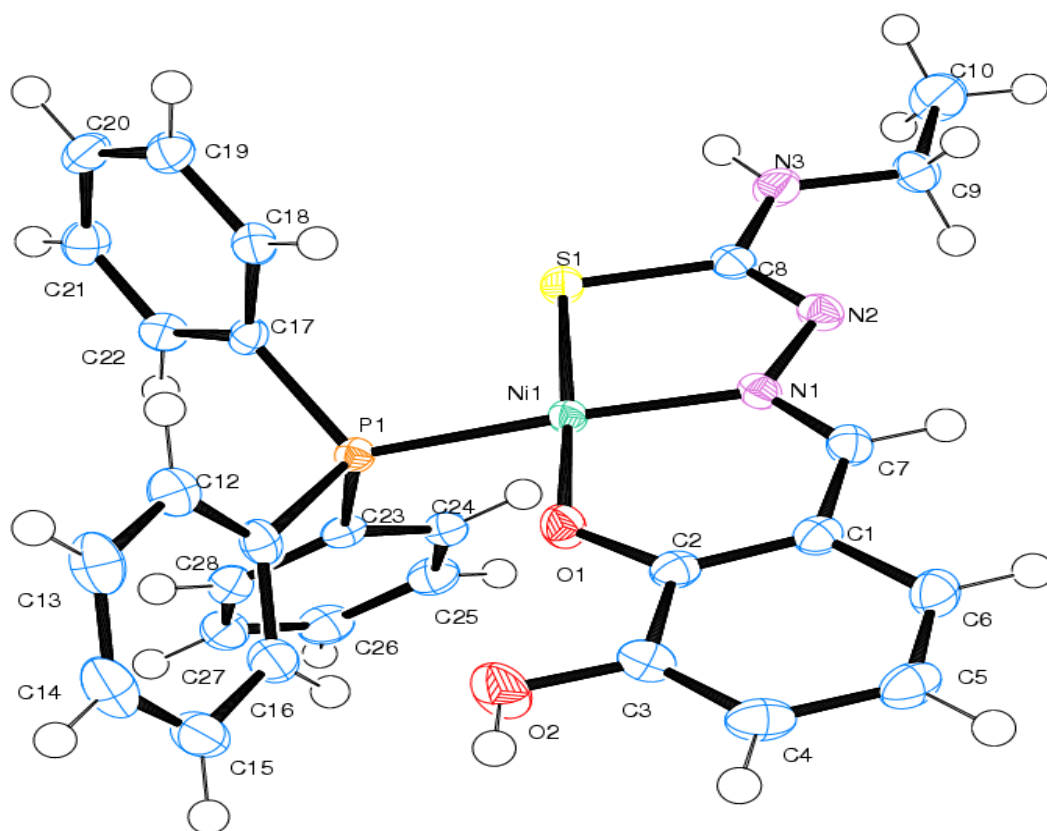
Figure 3.5: ORTEP diagram for $[Ni(HL^4)(PPh_3)]$ **(20)**, displacement ellipsoids are drawn at 70 % probability level and hydrogen atoms are shown as small spheres of arbitrary radii

In the complex **20**, the Ni–N, Ni–P, Ni–S bond lengths of 1.8961(14), 2.2059(5), 2.1488(5), respectively are quite normal as that found in other square planar nickel(II) complexes and Ni–O bond length 1.8510(12), was found to be slightly higher than that of the reported value for other nickel(II) complexes (Güveli et al., 2010; Güveli & Ülküseven, 2011). This slight increase in Ni–O bond length may be due to the presence of hydroxyl group. Considering the plane formed by the O1, N1, S1, P1 set of chelating atoms, the nickel atom sits 0.0170 Å away from them. The thiosemicarbazone fragment C7,N1,N2,C8,S1,N3, also is close to planar has a maximum least square plane deviation from the central metal atom (Ni1) by – 0.084 Å and the dihedral angle formed by the thiosemicarbazone moiety with the plane containing coordinating atoms is 6.62(5)° which denotes a coplanarity of the thiosemicarbazone moiety (Bon et al., 2010). The angles formed between the nickel ion and the coordination sphere O1, N1, S1, P1 show that the nickel is contained within a slightly distorted square-planar environment with the O1–Ni1–S1 of 173.72 (4)° and N1–Ni1–P1 of 171.55(4)° deviate from the linearity. The variations in bond lengths and bond angles in this complex indicate considerable distortion around nickel from its square planar geometry. This is also supported by the dihedral angle formed by the least square plane Cg(1) comprising atoms Ni1, S1, C8, N2, N1 and Cg(2) comprising atoms Ni1, O1, C1, C2, C7,N1] which is 3.44(6)°.

The coordination of the ligand to nickel(II) leads to a lengthening of the S1–C8 bond 1.7529(18) Å (increased single-bond character) and a shortening of the neighboring N2–C8 bond 1.299(2) Å (increased double-bond character) and in accordance to coordination of thiosemicarbazone in the thiolate form (Ferrari et al., 2001; Ketcham et al., 2002).

In compound **20**, there are no obvious classic hydrogen bonds, π-π or C–H···π interactions were observed in the crystal packing of this complex (Figure 3.6).

Higher distortion from ideal square planar geometry is observed for complex **20** in contrast to complex **17**, as reflected in the bond parameters around the metal center in both complexes. The high deviation of complex **20** from regular square planar arrangement may be due to the steric hindrance between the bulky triphenylphosphine group and the ethyl group at N(4) position.

Table 3.5: Selected bond lengths (Å) and angles (°) for complex **20**

Bond lengths		Bond angles	
Ni1–O1	1.8510(12)	O1–Ni1–N1	94.93(6)
Ni1–N1	1.8961(14)	O1–Ni1–S1	173.72(4)
Ni1–P1	2.2059(5)	N1–Ni1–S1	87.03(4)
Ni1–S1	2.1488(5)	O1–Ni1–P1	88.61(4)
S1–C8	1.7529(18)	N1–Ni1–P1	171.55(4)
P1–C17	1.8176(17)	S1–Ni1–P1	90.261(18)
P1–C11	1.8264(18)	C8–S1–Ni1	95.92(6)
P1–C23	1.8249(17)	C7–N1–N2	112.62(14)
O1–C2	1.321(2)	C7–N1–Ni1	125.76(12)
O2–C3	1.368(2)	N3–C8–S1	118.33(13)
O2–H1	0.8400	N2–C8–S1	123.33(13)
N1–C7	1.297(2)	N2– C8– N3	118.32(16)
N1–N2	1.400(2)	C17– P1 –Ni1	114.97(6)
N2–C8	1.299(2)	C11 –P1 –Ni1	114.64(6)
N3–C8	1.359(2)	C23 –P1– Ni1	112.34(6)
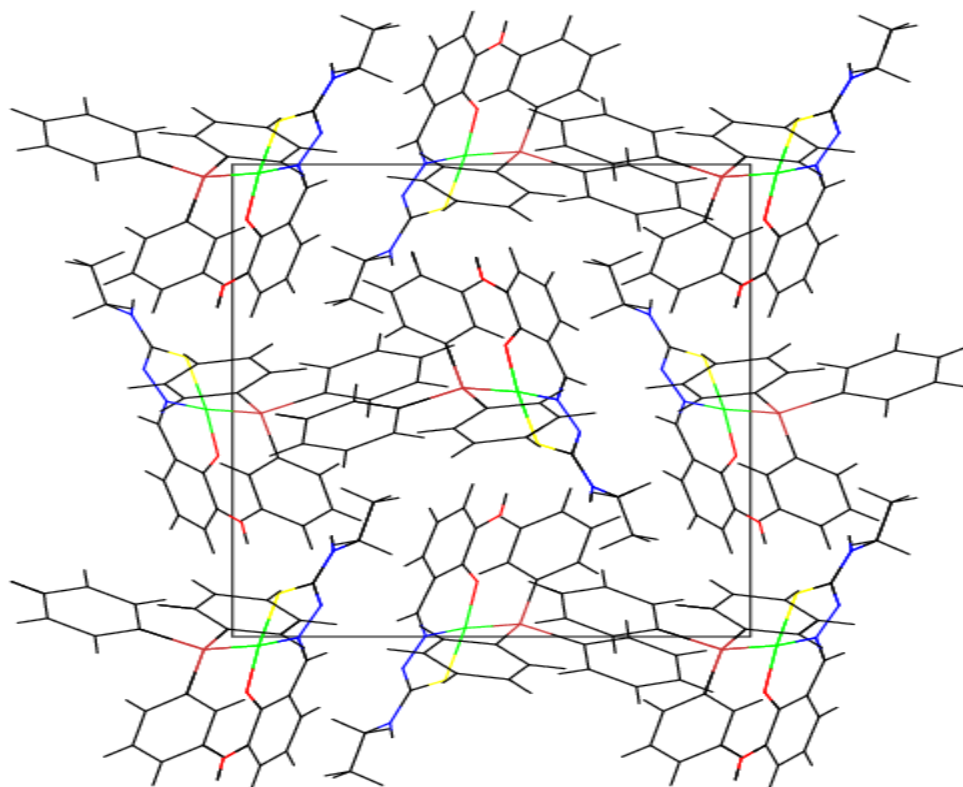
Figure 3.6: Unit cell packing diagram of complex **20** along *a* axis

3.3.2.3 Crystal structures of [Ni$_2$(HL^1)$_2$(dppe)].DMF (21) and [Ni$_2$(HL^2)$_2$(dppe)].DMF (22)

The complex [Ni$_2$(HL^1)$_2$(dppe)].DMF (**21**) and [Ni$_2$(HL^2)$_2$(dppe)].DMF (**22**) crystallized into a triclinic lattice with space group symmetry *P*1. A summary of the crystallographic data for complexes **21** and **22** at 100 K is gathered in Table 3.6. Figures 3.7 and 3.8 illustrate the structural features of complexes **21** and **22**, respectively, for which selected bond lengths and bond angles are listed in Tables 3.7. In both complexes, the asymmetric unit of the crystal of these complexes consists of one Ni(II) ion, one thiosemicarbazone ligand, half a 1,2-bis(diphenylphosphine)ethane,(dppe), as well as a DMF molecule. Thus, the dppe ligand bridges two Ni(II) ions forming dinuclear complex.
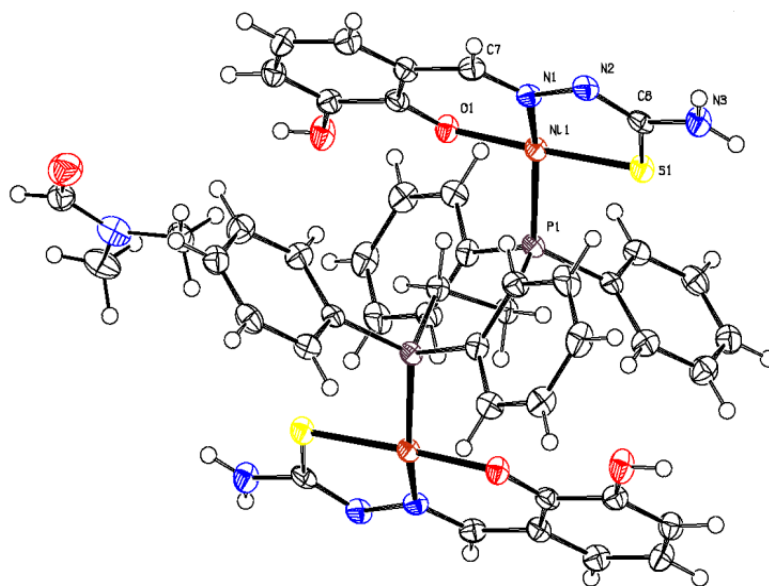
Figure 3.7: Crystal structure of complex **21.** The thermal ellipsoids are plotted at the 30% probability level

The doubly deprotonated thiosemicarbazone ligand behaves as tridentate ligand coordinate to nickel(II) via the thiolate sulfur, azomethine nitrogen atom, as well as phenolic oxygen. In comparison of the bond lengths in the coordinated 2,3-dihydroxybenzaldehyde thiosemicarbazone and 2,3-dihydroxybenzaldehyde-N4-methylthiosemicarbazone ligands with the related free ligands (Farina & Simpson, 2008; Swesi et al., 2006), a shortening of the C8-N2 bond distance, and a lengthening of C7–N1, C8–S1 bond lengths within the five-membered chelate ring are observed, consequent upon dissociation of the hydrazinic proton (Acharyya et al., 2006). The C7–N1 bond length of 1.297(4) Å and 1.306(5) Å, for **21** and **22** respectively, and C8–S1 bond length of 1.753(3) Å and 1.760(4), for **21** and **22** respectively, are similar to those reported for coordinated thiosemicarbazone in the thiolate form (Kolotilov et al., 2007; Lobana et al., 2010). In complex **21** each Ni(II) ion lies in square planar coordination NiSNOP with a P–Ni–N bond angle 155.10(9)° and O–Ni–S bond angles 174.82(8)° which deviate considerably from the ideal angle of 180°. The Ni(II) ion is found to be displaced by 0.175 Å from the plane constituting atoms N1, S1, O1, P1. The ONS

chelation results in a five and six membered planar rings Nil, N1, N2, C8, S1 having a maximum deviation of 0.016(3) Å for C8 and Nil, O1, C2, C1, C7, N1 with a maximum deviation of 0.077(4) Å for Ni1. The dihedral angle between these planar rings is 3.86(11)°. The two thiosemicarbazone ligands in the dimer are approximately *trans* around the Ni(II)-(μdppe)-Ni(II) fragment. The Ni–S bond length of the coordinated thiosemicarbazone ligand of 2.1343(9) Å is shorter than the Ni–P bond length of the dppe 2.1774(9) Å. This indicates that the bonding is dominated by thiosemicarbazone moiety. The Ni–P bond length is longer than the Ni–P of 2.145(1) Å reported for [NiCl$_2$(dppe)] (Bomfim et al., 2003) but similar to Ni–P bond length in other mixed nickel complexes with dppe (Oliveira et al., 2008). The Ni–S, Ni–N and Ni–O distances of 2.1343(9), 1.891(3) and 1.851(2) Å respectively, are comparable with values reported for similar structures (Güveli et al., 2009; Latheef & Kurup, 2008). When the complex [Ni$_2$(HL^1)$_2$(dppe)].DMF **(21)** is compared with [Ni(H$_2$L^1)(PPh$_3$)]Cl **(17)**, some interesting differences can be observed due to the chelation of dppe and its smaller steric effect compared with PPh$_3$. The N1–Ni1–P1 angle in complex **21** [155.10(9)°] is smaller than in complex **17** [176.19(4)°]. The O1–Ni1–P1 angle in **21** [88.28(8)°] is greater than in the triphenylphosphine complex **17** [85.66(4)°] and the Ni–P bond length in **21** [2.177(9) Å] is smaller than Ni–P bonding in the triphenylphosphine complex **17** [2.199(4) Å].

Table 3.6: Crystal data and structure refinement for complexes **21** and **22**

Parameters	[Ni$_2$(HL^1)$_2$(dppe)].DMF (21)	[Ni$_2$(HL^2)$_2$(dppe)].DMF (22)
Empirical Formula	C$_{47.68}$ H$_{52}$N$_8$Ni$_2$O$_{6.60}$P$_2$S$_2$	C$_{50}$ H$_{56}$ N$_8$ Ni$_2$ O$_6$ P$_2$ S$_2$
Formula weight, M	1086.21	1108.51
Temperature, T (K)	100	100
Wavelength, Mo Kα (Å)	$\lambda = 0.71073$	$\lambda = 0.71073$
Crystal system	Triclinic	Triclinic
Space group	$P1$	$P1$
Unit cell dimensions		
a(Å)	10.1334(2)	10.35810(10)
b(Å)	10.1645(2)	10.62240(10)
c (Å)	12.7332(3)	12.5820(2)
α(°)	80.107(2)	101.0720(10)
β(°)	71.727(2)	102.3060(10)
γ(°)	80.387(2)	108.0400(10)
Volume V (Å^3)	1217.87(4)	1235.46(3)
Z	1	1
Absorption coefficient, μ(mm^{-1})	0.983	0.970
Crystal size (mm)	0.14×0.17 × 0.17	0.18× 0.16× 0.12
Reflections collected	10839	11024
Density (calculated), (mg m^{-3})	1.481	1.490
F(0 0 0)	565	578
Data/ parameters /restraints	4981/340/0	5072/318/0
S	0.971	1.059
Independent reflections	[R(int) =0.0660]	[R(int) = 0.0322]
R[F^2 > 2σ(F^2)]	0.0469	0.0644
wR(F^2)	0.1288	0.1496
Largest difference peak and hole (e Å^{-3})	0.001and 0.000	0.141 and 0.003
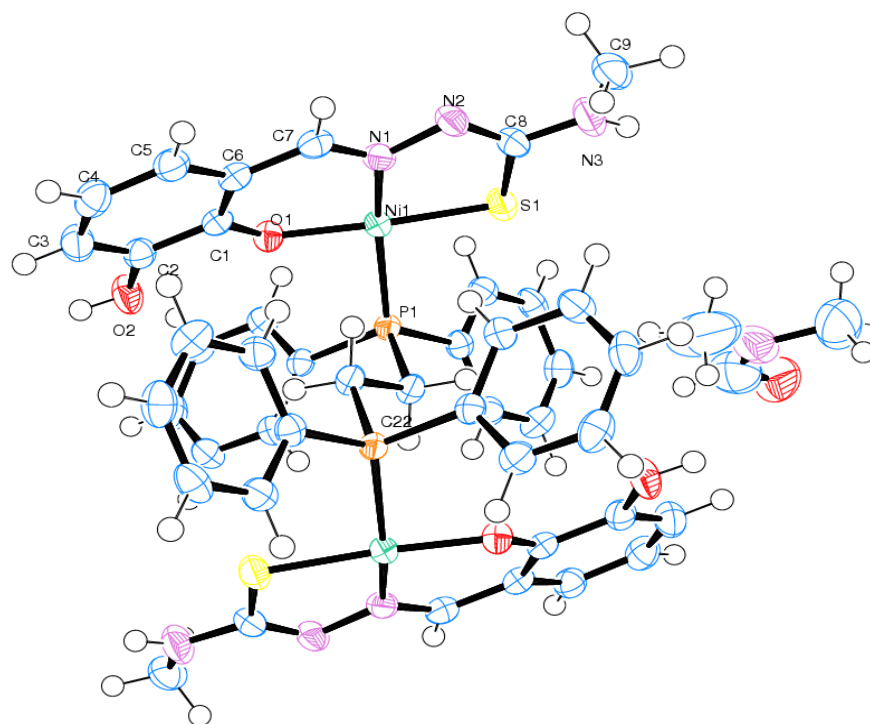
Figure 3.8: Crystal structure of complex **22**. The thermal ellipsoids are plotted at the 70% probability level

Similar to complex **21**, Ni(II) in complex **22** adopts square planar geometry defined by the tridentate ONS donor dianionic ligand and the neutral bidentate dppe ligand which occupy the fourth coordination site and bridge two nickel ions in the dimer. The Ni–O, Ni–N and Ni–S bond lengths [Nil–O1, 1.856(2); Ni1–N1, 1.892(3); Nil–S1, 2.1416(4)); Nil–P1, 2.1722(10)] are in agreement with complex **21** and those found in the related Ni(II) complex (Tamizh et al., 2009). The Ni(II) ion is found to be displaced by 0.128 Å from the plane constituting atoms N1, S1, O1, P1. The ONS chelation results in a five and six membered planar rings Nil, N1, N2, C8, S1 having a maximum deviation of 0.013(3) Å for N2 and Nil, O1, C2, C1, C7, N1 with a maximum deviation of 0.122(3) Å for O1. The dihedral angle between these planar rings is 4.40(14)°. The C7–N1 and N2–C8 bond lengths are comparable to that for C=N bond length. Of these two, N2–C8 bond length is longer due to enolization of the ligand in complex formation. The S1–Ni1–N1 and P1–Ni1–N1 bond angles indicate a slight tilting of the Ni1–S1 bond in the

direction of Ni1–N1 bond and away from the P1–Ni1 bond. The bite angle S1–Ni1–O1 of 173.52(8)º and N–Ni–P of 155.22(9)º defines considerable distortion from the square planar geometry. This deviation from an ideal stereochemistry may be due the restricted bite angle imposed by both the HL^{2-} and dppe ligands.

Table 3.7: Selected bond lengths (Å) and bond angles (°) of complexes **21** and **22**

Complex 21		Complex 22	
Bond lengths		**Bond lengths**	
O1–Ni1	1.851(2)	O1–Ni1	1.856(2)
C7–N1	1.297(4)	C7–N1	1.306(5)
N1–N2	1.398(4)	N1–N2	1.401(4)
Ni1–S1	2.1343(9)	Ni1–S1	2.1416 (4)
N1–Ni1	1.891(3)	N1–Ni1	1.892(3)
N2–C8	1.297(5)	N2–C8	1.308(4)
C8–N3	1.344(5)	C8–N3	1.344(5)
C8–S1	1.753(3)	C8–S1	1.760(4)
Ni1–P1	2.1774(9)	Ni1–P1	2.1722(10)
Bond angles		**Bond angles**	
C2–O1 –Ni1	125.3(2)	C1–O1–Ni1	124.8(2)
O1–C1–C2	125.6(3)	O1–C1–C2	116.1(3)
O1–C2–C3	116.6(3)	O1–C1–C6	125.0(3)
N1– C7– C1	125.9(3)	N1–C7–C6	126.0(3)
C7– N1–N2	113.5(3)	C7–N1–N2	113.9(3)
C7–N1– Ni1	124.9(2)	C7–N1–Ni1	124.2(3)
N2–N1–Ni1	121.4(2)	N2–N1–Ni1	121.6(2)
C8 –N2–N1	112.3(3)	C8 –N2–N1	112.0(3)
N2 –C8–N3	118.9(3)	N2–C8–N3	120.1(4)
N2– C8–S1	122.5(3)	N2–C8–S1	122.9(3)
N3 –C8–S1	118.6(3)	N3 –C8–S1	117.0(3)
C8 –S1–Ni1	96.36(12)	C8 –S1–Ni1	96.13(13)
O1–Ni1–N1	95.51(11)	O1–Ni1– N1	95.30(12)
O1 –Ni1–S1	174.82(8)	O1–Ni1–S1	173.52(8)
N1 –Ni1–S1	87.40(9)	N1–Ni1–S1	87.35(9)
O1 –Ni1–P1	88.28(8)	O1–Ni1–P1	88.08(8)
N1 –Ni1–P1	155.10(9)	N1 –Ni1–P1	155.22(9)
S1– Ni1–P1	90.87(4)	S1–Ni1–P1	91.99(4)
C15–P1–Ni1	122.02(11)	C16–P1–Ni1	123.21(12)
C21–P1–Ni1	99.93(11)	C8–N3–C9	121.9(3)

Hydrogen bonding parameters for complexes **21** and **22** are shown in Table 3.8 and 3.9 respectively. In complexes **21** and **22**, one molecule of DMF moiety is present in the crystal lattice, which is hydrogen bonded to hydrogen atom (H3) of the N(3) amino group of adjacent complex molecule. Moreover, in complex **21**, an intermolecular hydrogen bonding interactions was observed (Figure 3.9) *i.e.*, N3(H) of one molecule with nitrogen atom (N2) of the another molecule forming one dimensional chain as shown in Figure 3.10 . In compound **21** there are 4 molecules in the unit cell packing and the molecules are complement to one another, Figure 3.11. In the case of complex **22,** two molecules are present and two of them are parallel to each other (Figure 3.12).
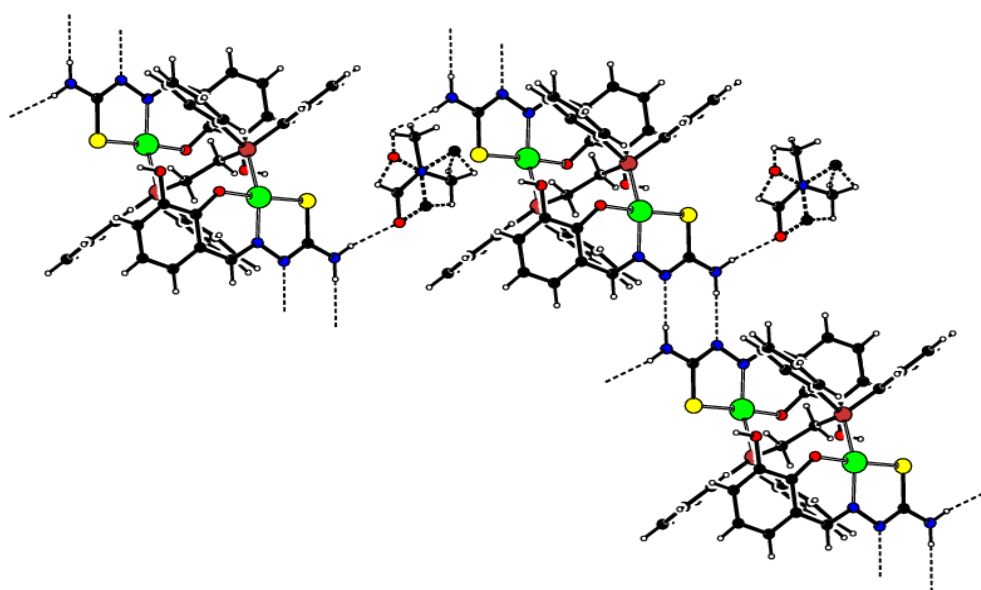
Figure 3.9: Intermolecular hydrogen bonding interactions of **21**

Table 3.8: Hydrogen-bond geometry (Å, °) for complex **21**

D–H⋯A	D—H	H⋯A	D⋯A	D—H⋯A
N3–H3⋯N2[a]	0.88	2.19	3.060 (4)	169
N3–H3⋯O3[b]	0.88	2.10	2.952 (4)	163
C4–H4⋯O2[c]	0.95	2.47	3.330 (5)	150
C22–H20⋯O2[c]	0.98	2.58	3.451 (6)	148
C24–H24⋯S1[d]	0.95	2.86	3.661 (5)	143

Symmetry codes: (a) = 3- x, -y, 2-z; (b) = x, 1+y, -1+z; (c) = 2-x, 1-y, 1-z; (d) = x, -1+y, 1+z
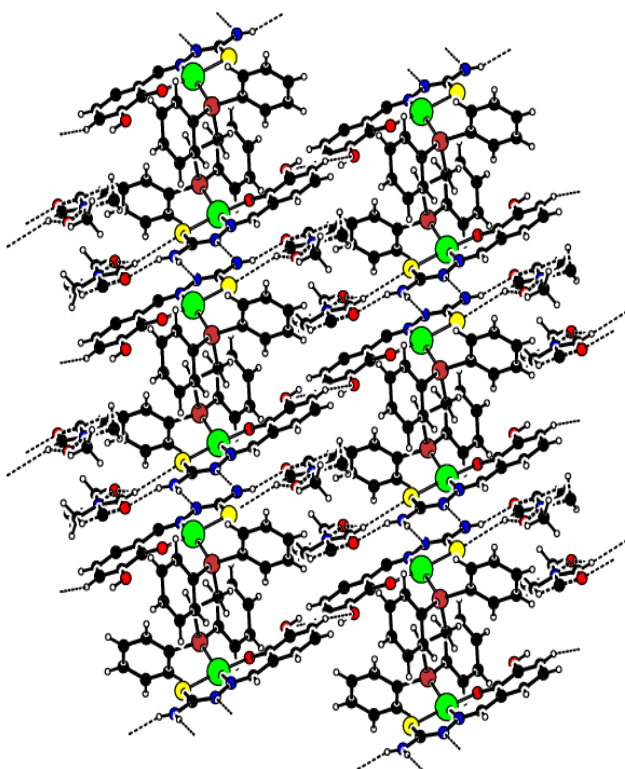
Figure 3.10: One-dimensional chain formed from N3-H3---N2 hydrogen bonding interactions for complex **21**
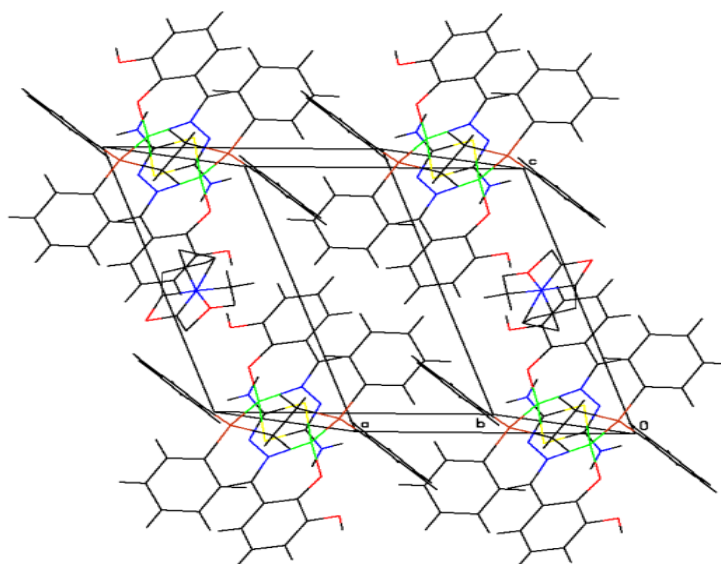
Figure 3.11: Unit cell packing diagram of complex **21** along *b* axis

Table 3.9: Hydrogen-bond geometry (Å, °) for complex **22**

D–H···A	D–H	H···A	D···A	D–H···A
N3–H3···O3[a]	0.88	2.03	2.844 (6)	169
C12–H12···O3[b]	0.95	2.56	3.447 (6)	156
C23–H23···O3[c]	0.98	2.30	2.760 (8)	108
C24–H24···O2[c]	0.98	2.48	3.377 (9)	152

Symmetry codes: (a) = - x, 1-y, 1-z; (b) = x, y, -1+z; (c) = 1-x, 1-y, 2-z
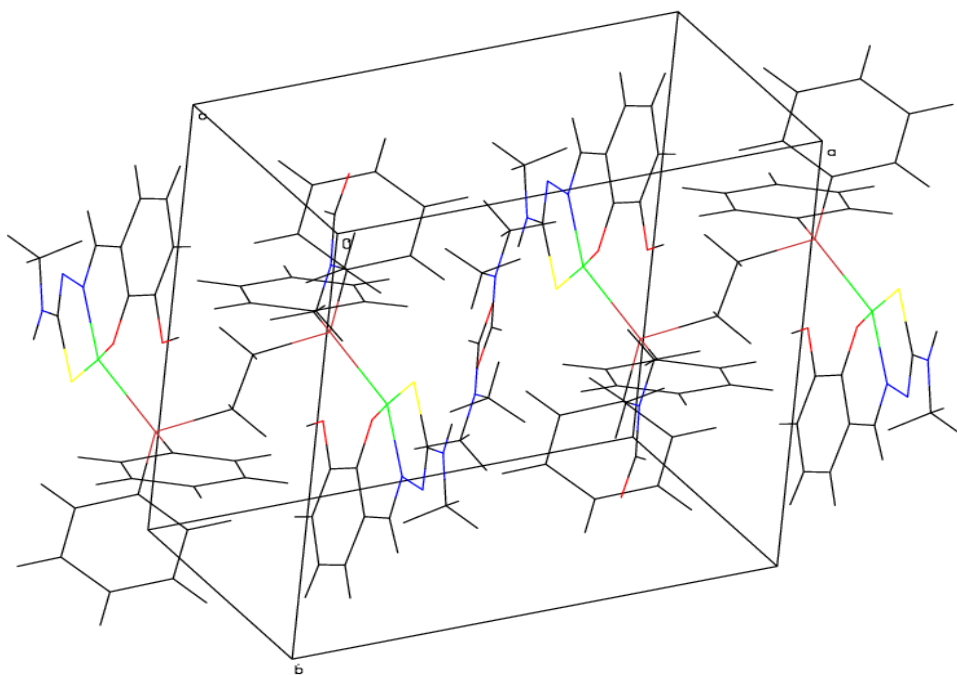
Figure 3.12: Unit cell packing diagram of complex **22** along *b* axis

3.3.3 ^{1}H NMR spectra

Tentative assignments of the ^{1}H NMR spectra of the ligands and their nickel(II) phosphine complexes are given in the Table 3.10. The singlet appeared in the region 11.35 − 11.77 ppm in the free ligands, which was assigned to the N(2)HCS group, was absent in the spectrum of all complexes (except complexes **17** and **18**) indicating the coordination of the ligand under the anionic thiolate form upon deprotonation at N(2) (Lobana et al., 2007). In the spectra of the complex [Ni(H$_2$L^1)(PPh$_3$)]Cl **(17)** and the complex [Ni(H$_2$L^2)(PPh$_3$)] **(18)**, the hydrazinic proton N(2)H signal appeared at 11.45 ppm and 11.43 ppm respectively. The slightly downfield shift of this signal suggested the coordination of the ligand to the metal center in the neutral thione form (Lobana, Sharma, et al., 2009). The coordination of 2,3-dihydroxybenzaldehyde-N4-substituted thiosemicarbazone to nickel(II) through one phenolic oxygen was conformed from the decrease of the integration of phenolic protons from two to one upon complexation for complexes **17**, **18**, **21** and **22** or from the presence of only one phenolic proton signal in the spectrum of complexes **19**, **23** and **24**. However, in complex **20**, this signal could

not be seen which may be due to the –OH exchange with DMSO-d_6 (Crews et al., 1998).

The azomethine proton –CH=N does not show a regular trend in the complexes. The azomethine –CH=N signals which were observed at 8.33–8.52 ppm in the free thiosemicarbazones underwent shift to the high field, thus, indicating coordination of the thiosemicarbazones through the imine nitrogen chelating system. In contrast, the azomethine proton in the complexes with N(4)-phenyl substitution (**19** and **23**), was shifted downfield due to the presence of an electron withdrawing phenyl group (Ferrari et al., 2002; Jayabalakrishnan et al., 2002). Meanwhile, the –CH=N signal in complexes **19** and **20** was present as doublet due to the coupling of the imine proton to the nucleus of the phosphorus atom in triphenylphosphine (Stringer et al., 2009).

In the spectrum of complex **24**, the signal attributed to –CH=N proton was not observed maybe obscured by the ring peaks of the co-ligand (Lobana, Sharma, et al., 2009). The signal for N(4)H appears in the region of 8.85–5.25 ppm in the complexes and its position in respect to the free ligands is highly dependent on the nature of the thiosemicarbazone ligand in the complex. In the spectrum of the complex [Ni(H$_2$L^1)(PPh$_3$)]Cl (**17**), which has the thiosemicarbazone ligand H$_3$L^1 in its mono deprotonated form, the N(4)H signal shows a pair of two broad signals in the range 8.00 – 7.85 ppm. The appearance of this peak as pair in the low field region, is due to the restricted rotation of NH$_2$ group about C(S) N4 bond axis caused by the delocalization of the lone pair of electrons on the N(4)H$_2$ nitrogen.

On the other hand, in the spectrum of the complex [Ni$_2$(HL^1)$_2$(dppe)] (**21**), which has the same ligand H$_3$L^1 but in its doubly deprotonated form, the N(4)H signal appears as

singlet in the high field region, with respect to the free ligand, at 6.56 ppm due to the free rotation of $N(4)H_2$ group caused by the reduction of the double bond character of C(S) N4 bond after deprotonation of N(2)H (Lobana et al., 1998). The dihydroxybenzaldehyde aromatic protons were shifted to the high field environment due to the decrease in the electron density around the thiosemicarbazone moiety as a result of coordination to nickel(II) through sulfur, azomethine nitrogen and phenolic oxygen.

It has been illustrated that the decrease in electron density causes an upfield shift of the aromatic protons, different from aliphatic protons, due to electron withdrawing ability of the metal ion, which in turn decreases the ring current and deshielding of the aromatic protons. For this reason a stronger field is required to take the aromatic protons to resonance (Kolehmainen et al., 1995).

Table 3.10: ^{1}H NMR spectral assignments for the thiosemicarbazone ligands and their nickel(II) - phosphine complexes in DMSO-d_6

Compound	Chemical shifts, δ (ppm)							
	N(2)H	OH	CH=N	N(4)H	Aromatic due to Tsc	Aromatic due to PPh$_3$ or dppe	Aliphatic due to Tsc	Aliphatic due to dppe
H$_3$L^1	11.36 (s, 1H)	9.22 (s, 2H)	8.38 (s, 1H)	8.08 (s, 1H) 7.86 (s, 1H)	7.35 (d, 1H) 6.80 (d, 1H) 6.63 (t,1H)	-	-	-
[Ni(H$_2$L^1)(PPh$_3$)]Cl (17)	11.44 (s, 1H)	9.51 (s, 1H)	8.28 (s, 1H)	8.00 (s, 1H) 7.85 (s,1H)	6.76 (d,1H) 6.57 (t,1H) 6.25 (s, 1H)	7.41- 7.29 (m,15H)	-	-
[Ni$_2$(HL^1)$_2$(dppe)] (21)	-	8.22 (s, 1H)	7.84 (s, 1H)	6.56 (s, 2H)	6.86 (d, 1H) 6.63 (d, 1H) 6.43 (t, 1H)	7.63- 7.38 (m, 10H)	-	2.82 (s, 2H)
H$_3$L^2 (2)	11.41 (s,1H)	9.26 (s, 2H)	8.38 (s,1H)	8.39 (s,1H)	7.38 (d,1H) 6.81 (dd,1H) 6.66 (t,1H)	-	3.01 (d,3H)	-

Compound	Chemical shifts, δ (ppm)							
	N(2)H	OH	CH=N	N(4)H	Aromatic due to Tsc	Aromatic due to PPh₃ or dppe	Aliphatic due to Tsc	Aliphatic due to dppe
[Ni(H₂L²)(PPh₃)]Cl (**18**)	11.49 (s,1H)	9.64 (s,1H)	8.21 (s,1H)	8.82 (s,1H)	6.85 (d,1H) 6.64 (t,1H) 6.38 (s,1H)	7.49- 7.39 (m, 15H)	3.02 (s,3H)	-
[Ni₂(HL²)₂(dppe)] (**22**)	-	8.30 (s,1H)	7.71 (s,1H)	6.92 (d, 1H)	6.85 (d, 1H) 6.60 (d, 1H) 6.40 (t, 1H)	7.51- 7.34 (m, 10H)	2.66 (d, 3H)	2.79 (s, 2H)
H₃L³ (**3**)	11.78 (s,1H)	9.55 (s,1H) 9.06 (s, 1H)	8.52 (s, 1H)	10.03 (s,1H)	7.59 (d,2H) 7.51 (d,1H) 7.37 (t,2H) 7.20 (t,1H) 6.85 (dd,1H) 6.68 (t,1H)	-	-	-

Table 3.10, continued

Compound	Chemical shifts, δ (ppm)							
	N(2)H	OH	CH=N	N(4)H	Aromatic due to Tsc	Aromatic due to PPh₃ or dppe	Aliphatic due to Tsc	Aliphatic due to dppe
[Ni(HL³)(PPh₃)] **(19)**	-	9.46 (s,1H)	8.69 (d,1H)	5.43 (s,1H)	7.77 (d,2H) 7.24 (t,2H) 7.03 (d, 1H) 6.91 (t, 1H) 6.62 (d, 1H) 6.50 (t,1H)	7.82 (t, 6H) 7.59 (m, 9H)	-	-
[Ni₂(HL³)₂(dppe)] **(23)**	-	9.41 (s,1H)	8.60 (s,1H)	6.89 (t, 1H)	7.84 (t, 2H) 7.23 (t, 2H) 6.99 (d, 1H) 6.89 (t, 1H) 6.72 (d, 1H) 6.50 (t, 1H)	7.69 (m, 6H) 7.39 (t, 4H)	-	2.99 (s, 2H)

Table 3.10, continued

	N(2)H	OH	CH=N	N(4)H	Aromatic	Aromatic	Aliphatic	Aliphatic

Compound	Chemical shifts, δ (ppm)							
	N(2)H	OH	CH=N	N(4)H	Aromatic due to Tsc	Aromatic due to PPh$_3$ or dppe	Aliphatic due to Tsc	Aliphatic due to dppe
H$_3$L^4	11.36(s, 1H)	9.52(s, 1H) 8.95(s, 1H)	8.38 (s,1H)	8.41 (t,1H)	7.37 (d,1H) 6.81 (dd,1H) 6.66 (t,1H)	-	3.58 (q,2H) 1.14 (t, 3H)	-
[Ni(HL^4)(PPh$_3$)] (20)	-	-	8.33 (d,1H)	5.24 (s, 1H)	6.88 (d, 1H) 6.51 (d,1H) 6.40 (t, 1H)	7.73 (t, 6H) 7.53 (m, 9H)	3.10 (q,2H) 0.99 (t, 3H)	-
[Ni$_2$(HL^4)$_2$(dppe)] (24)	-	8.32 (s, 1H)	Overlap with dppe	7.00 (s, 1H)	6.89 (d, 1H) 6.64 (d, 1H) 6.45 (t, 1H)	7.74-7.38 (m, 10H)	3.15 (q, 2H) 1.02 (t,3H)	2.79 (s, 2H)

Table 3.10, continued

However, the coordination of nickel(II) to the phosphorus atom of PPh$_3$ and dppe is confirmed by the downshift of the phenyl protons of PPh$_3$ and dppe in the spectrum of all complexes when compared to the free PPh$_3$ and dppe due to the change in the molecular environment as a result of complexation with the metal ion (Lobana et al., 2004; Oliveira et al., 2002). ^{1}H NMR spectra of the complexes **19**, **20**, **22** and **23** are given in Figures 3.13 – 3.16, while the ^{1}H NMR spectra for the other complexes are shown in Appendix B.
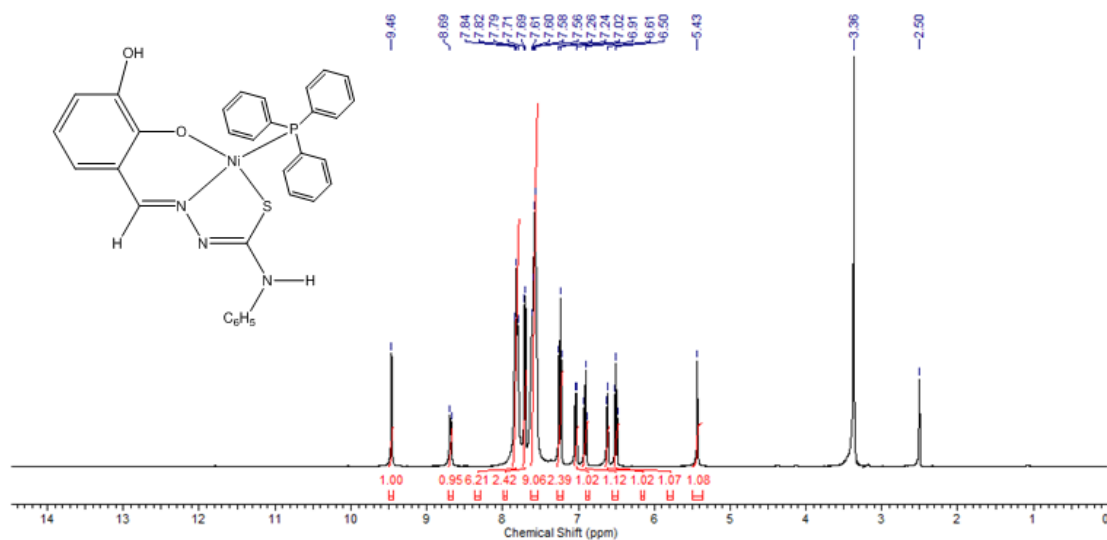
Figure 3.13: ^{1}H NMR spectrum of [Ni(HL^3)(PPh$_3$)] **(19)**

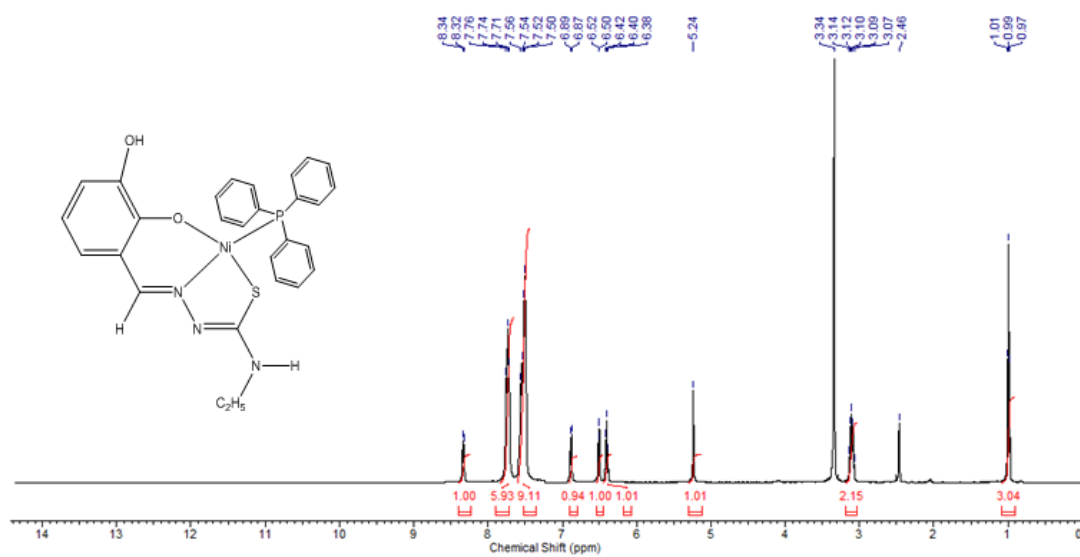**Figure 3.14:** ^{1}H NMR spectrum of [Ni(HL^4)(PPh$_3$)] **(20)**
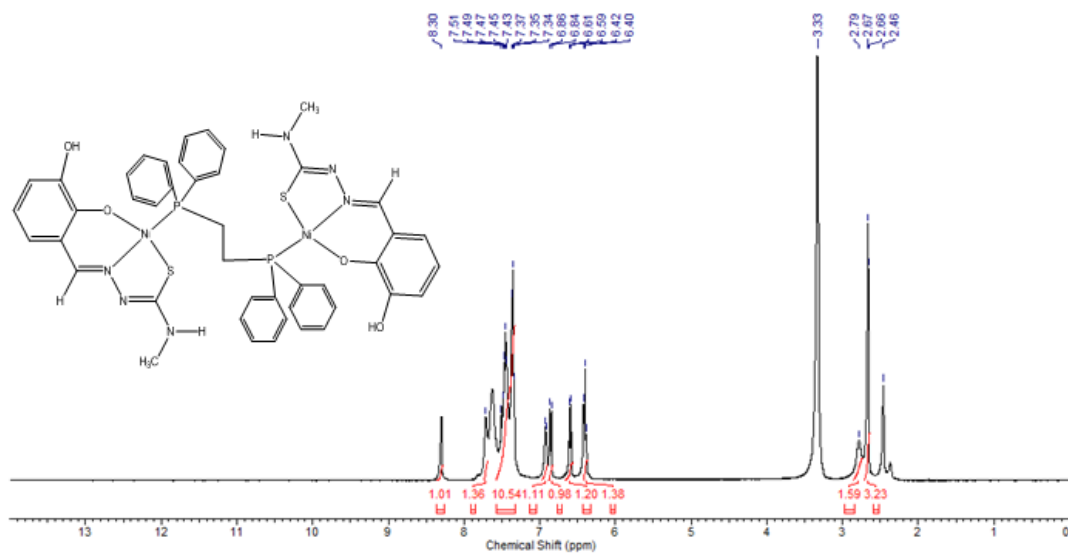
Figure 3.15: ^{1}H NMR spectrum of [Ni$_2$(HL^2)$_2$(dppe)] **(22)**
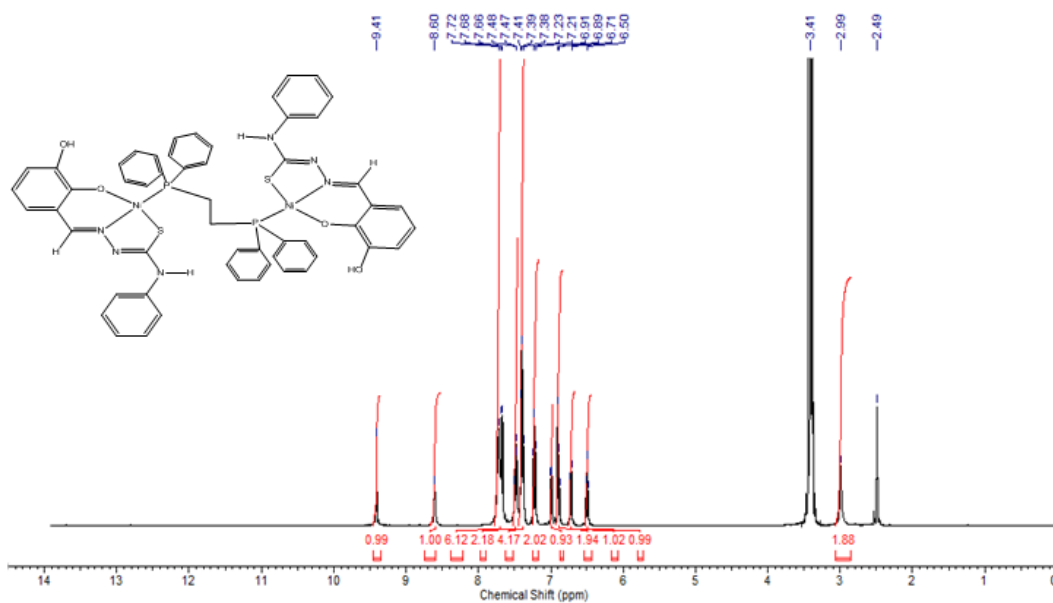
Figure 3.16: ^{1}H NMR spectrum of [Ni$_2$(HL^3)$_2$(dppe)] **(23)**

3.3.4 ^{13}C NMR spectra

Tentative assignment of different resonance peaks to respective carbon atoms in thiosemicarbazone ligands and their nickel(II)-phosphine complexes are presented in Table 3.11. The C=S carbon atom resonance was observed in the farthest low field at 178.00 – 176.20 ppm in the ^{13}C NMR spectrum of the free ligands, resultant of the conjugative effect of the –N(1)–N(2)–CS–N(4)– thiosemicarbazone skeleton. This signal underwent upfield shift to 173.37 – 166.23 ppm in all complexes which may be due to the electron delocalization induced from the coordination of nickel(II) with the ligand through the thiolate sulfur (Castiñeiras et al., 2012; Lobana et al., 1997). The considerable shifts in the positions of the carbon atoms adjacent to the phenolic oxygen from 146.69 – 145.31 ppm and the protonated carbon atom of CH=N from 139.90 – 141.26 ppm in the free ligands to 146.69 – 145.31 ppm and 147.06 – 147.97 ppm, respectively, in nickel complexes support the proposed coordination in the complexes. This downfield shift in the C–O and CH=N peaks in the complexes is due to the decrease in electron density resulting from the presence of electronegative atom and an electron delocalization on the C=N bond (Hanif & Chohan, 2013). The shifts in the positions of carbon atoms adjacent to the coordinating atoms clearly indicate the bonding of the sulfur, the phenolic oxygen and the azomethine nitrogen to nickel atom. The carbon atoms of the phenyl rings in triphenylphosphine and 1,2-bis(diphenylphosphino)ethane are observed in the 134.49 – 129.30 ppm. In the N(4)-substituted phenyl thiosemicarbazone complexes, the carbon atom adjacent to the more electronegative nitrogen atom N(4) was shifted farther downfield of δ = 141.75 when compared to the neighboring carbon atoms. Meanwhile, the aromatic carbons of the benzaldehyde ring were observed in the more upfield region in respect to the free ligands.

Table 3.11: ^{13}C NMR spectral assignments for the thiosemicarbazone ligands and their nickel(II)- phosphine complexes in DMSO-d_6

Compound	Chemical shifts, δ (ppm)						
	C=S	C-O	C=N	Aromatic due to Tsc	Aromatic due to PPh₃	Aromatic Due to dppe	Aliphatic
H3L[1]	178.06	146.04	140.81	121.41	-	-	-
		145.76		119.61			
				117.60			
				116.94			
[Ni(H₂L[1])(PPh₃)]Cl (17)	172.38	149.79	147.32	121.47	134.98	-	-
		149.27		119.50	134.20		
				117.37	131.94		
				117.13	130.69		
					129.33		
[Ni₂(HL1)₂(dppe)] (21)	171.37	149.96	147.67	122.39	-	133.08	-
		149.40		117.82		132.46	
				115.52		131.00	
				113.97		129.39	
H₃L[2]	178.01	146.09	140.19	121.56	-	-	31.38
		145.69		119.54			
				117.53			
				116.83			
[Ni(H₂L[2])(PPh₃)]Cl (18)	173.37	149.49	147.24	121.58	134.44	-	31.54
		148.89		119.43	134.14		
				117.31	131.82		
				116.99	130.86		
					129.33		
[Ni₂(HL[2])₂(dppe)] (22)	170.58	150.63	147.69	122.87	-	133.12	32.34
		149.39		117.95		132.43	
				115.52		131.03	
				114.03		129.39	

Compound	Chemical shifts, δ (ppm)						
	C=S	C-O	C=N	Aromatic due to Tsc	Aromatic due to PPh₃	Aromatic Due to dppe	Aliphatic
H₃L³	176.20	146.09	141.26	139.67	-	-	-
		145.97		128.58			
				126.14			
				125.70			
				121.30			
				119.58			
				118.00			
				117.15			
[Ni(HL³)(PPh₃)]	166.23	153.47	147.20	141.75	134.49	-	-
(19)		149.38		129.02	134.39		
				123.17	131.90		
				121.87	129.57		
				118.73	129.47		
				117.22			
				115.99			
				113.84			
[Ni₂(HL³)₂(dppe)]	166.24	153.32	147.97	141.80	-	133.18,	-
(23)		150.47		129.03		131.55,	
				123.29		129.41	
				121.76			
				118.65			
				117.82			
				115.76			
				114.79			
H₃L⁴	176.64	145.69	139.90	121.10	-	-	38.28
		145.31		119.09			14.62
				117.17			
				116.43			

Table 3.11, continued

Compound	C=S	C-O	C=N	Aromatic due to Tsc	Aromatic due to PPh$_3$	Aromatic Due to dppe	Aliphatic
[Ni(HL^4)(PPh$_3$)] **(20)**	169.61	150.54 148.54	147.04	122.75 117.48 115.69 113.19	134.43 134.32 131.79 129.47 129.38	-	39.33 15.04
[Ni$_2$(HL^4)$_2$(dppe)] **(24)**	169.69	150.41 149.39	147.67	122.85 117.97 115.51 113.99	-	133.12 132.43 131.03 129.38	15.12

Table 3.11, continued

Complexes **18** and **22** have an additional peak due to N-**CH$_3$** at 31.45 and 32.34 ppm respectively while complexes **20** and **24** have peaks due to NCH$_2$**CH$_3$** at 15.04 and 15.12 ppm respectively, which present in C$_2$H$_5$ group attached to NH. However, the peaks attributed to N**CH$_2$**- in the C$_2$H$_5$ group and the CH$_2$ in the dppe ligand were obscured in the ^{13}C NMR spectra. However, the ^{13}C NMR spectrum observed for nickel(II) complexes provides direct information about the carbon skeleton of the compounds where the total numbers of the signals in the ^{13}C NMR spectra of the complexes are in good accordance with the proposed structures. ^{13}C NMR spectra of the complexes **17**, **19**, **20**, **22** and **23** are given in Figures 3.17 – 3.21, while the ^{13}C NMR spectra for the other complexes are shown in Appendix B.
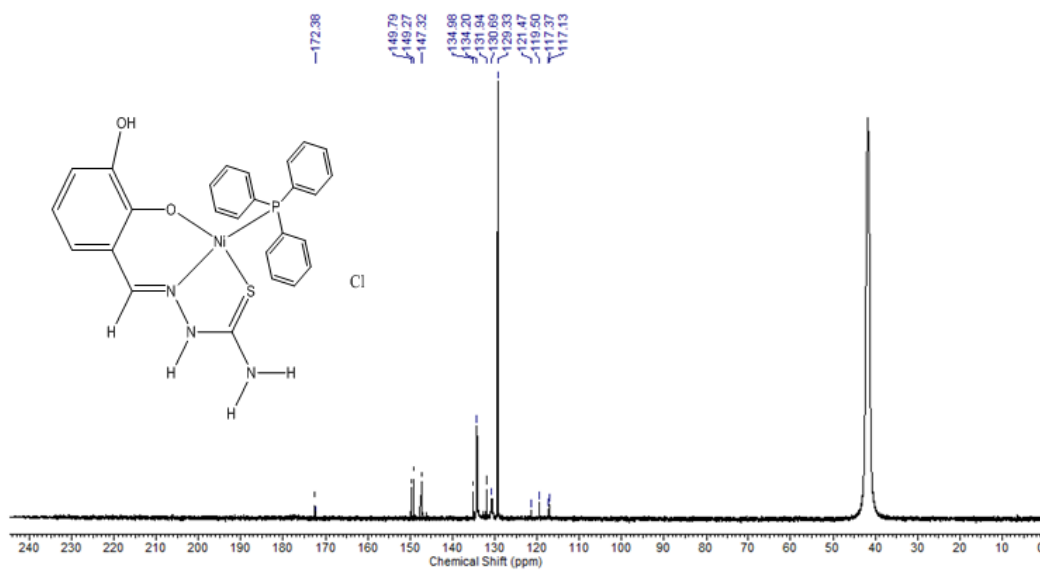
Figure 3.17: ^{13}C NMR spectrum of [Ni(H$_2$L^1)(PPh$_3$)]Cl (**17**)
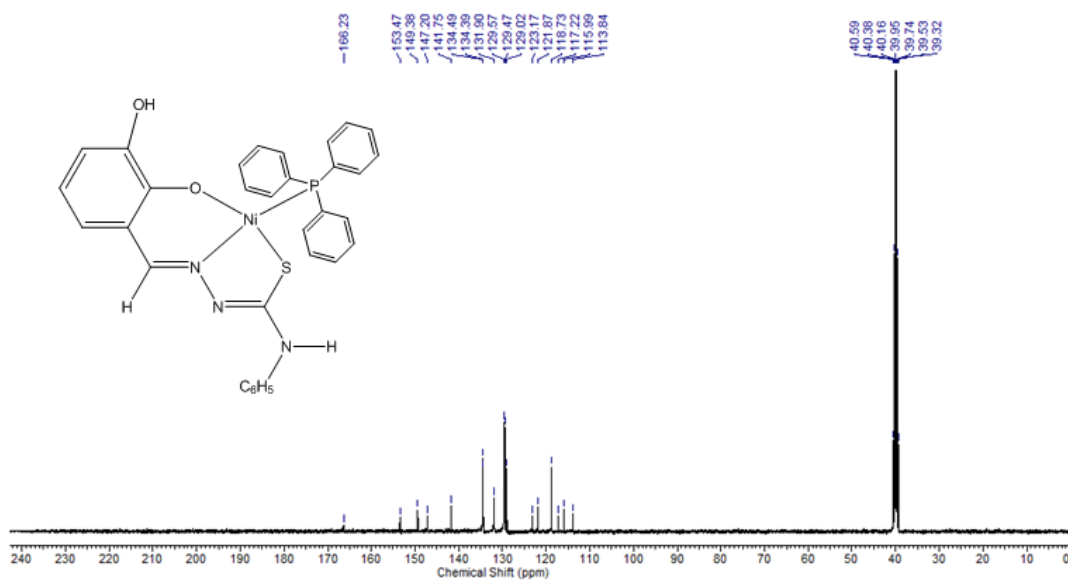
Figure 3.18: ^{13}C NMR spectrum of [Ni(HL^3)(PPh$_3$)] (**19**)
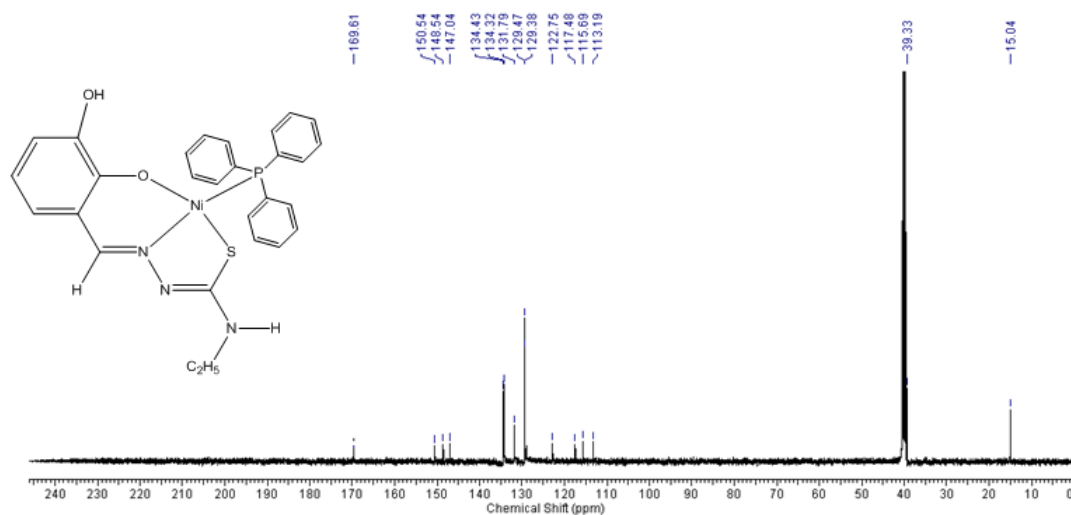
Figure 3.19: ^{13}C NMR spectrum of [Ni(HL^4)(PPh$_3$)] **(20)**
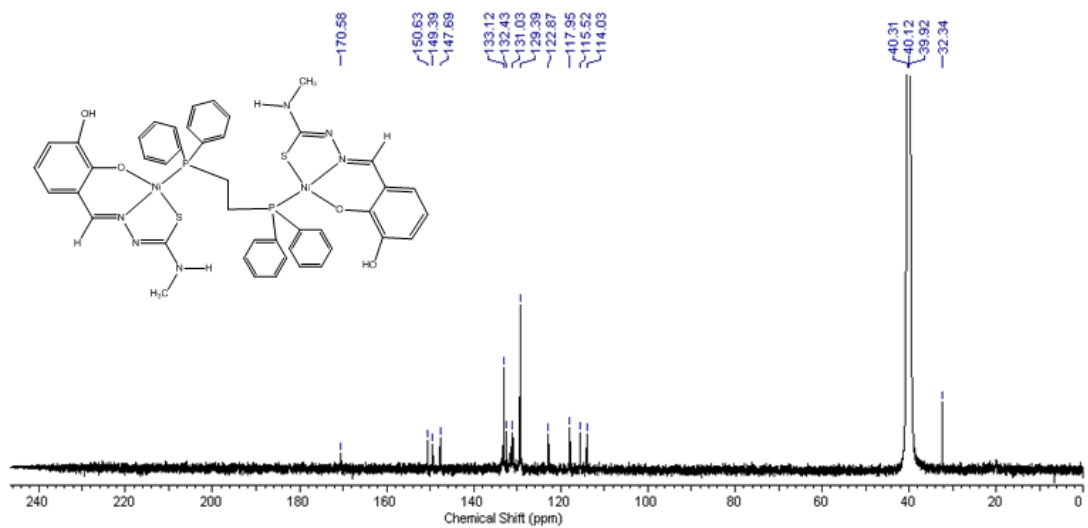
Figure 3.20: ^{13}C NMR spectrum of [Ni$_2$(HL^2)$_2$(dppe)] **(22)**
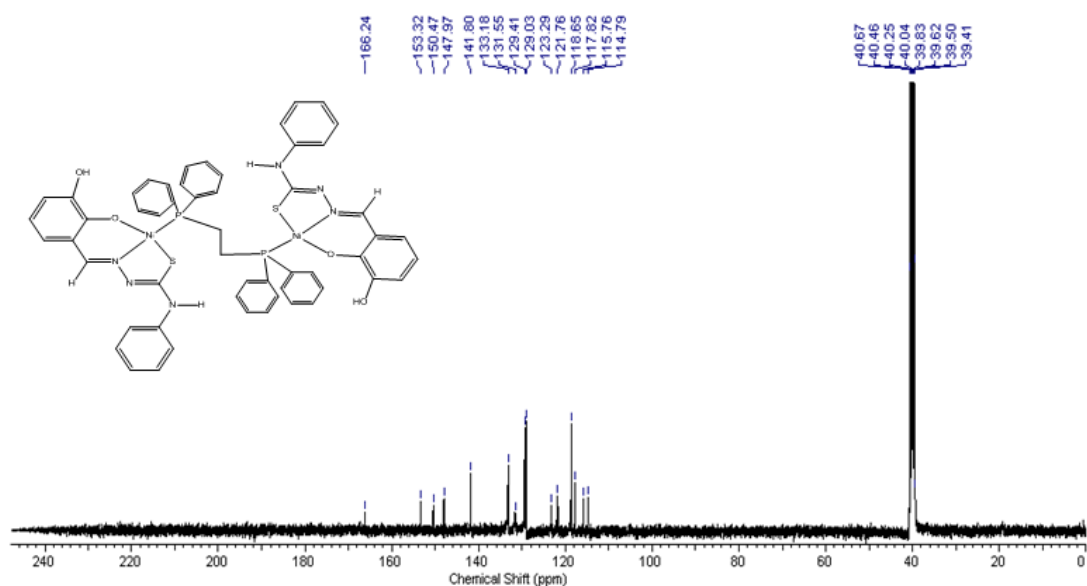
Figure 3.21: ^{13}C NMR spectrum of $[Ni_2(HL^3)_2(dppe)]$ **(23)**

3.3.5 ^{31}P NMR spectra

The ^{31}P signals for nickel(II)-phosphine complexes of thiosemicarbazones are presented in Table 3.12. The ^{31}P NMR spectrum of mixed triphenylphosphine complexes in DMSO exhibited only one signal at around 23.93 ppm indicating the presence of one coordinated triphenylphosphine where the free PPh_3 phosphorus resonates at the more upfield region of 6.23 ppm. The very high deshielding for the coordinated phosphorus in the nickel complexes compared with the free phosphines indicates the drift of electron density from the phosphorus towards the nickel centre (Tamizh et al., 2009). In the ^{31}P NMR spectrum of thiosemicarbazones with 1,2-bis(diphenylphosphine)ethane, one signal was observed for all complexes indicating that both phosphorus atoms in the dinuclear complexes are magnetically equivalent (Oliveira et al., 2002). ^{31}P NMR spectra of the complexes 17, **20**, **21** and **23** are given in Figures 3.22 - 3.25, while the other ^{31}P NMR spectra are shown in Appendix B.

Table 3.12: ^{31}P NMR spectral assignments for nickel(II)- phosphine complexes of thiosemicarbazone in DMSO

Complex	Chemical shifts, δ (ppm)
[Ni(H$_2$L^1)(PPh$_3$)]Cl **(17)**	23.90
[Ni(H$_2$L^1)(PPh$_3$)]Cl **(18)**	24.33
[Ni(HL^3)(PPh$_3$)] **(19)**	23.74
[Ni(HL^4)(PPh$_3$)] **(20)**	23.93
[Ni$_2$(HL^1)$_2$(dppe)] **(21)**	23.03
[Ni$_2$(HL^2)$_2$(dppe)] **(22)**	21.95
[Ni$_2$(HL^3)$_2$(dppe)] **(23)**	22.90
[Ni$_2$(HL^4)$_2$(dppe)] **(24)**	22.06
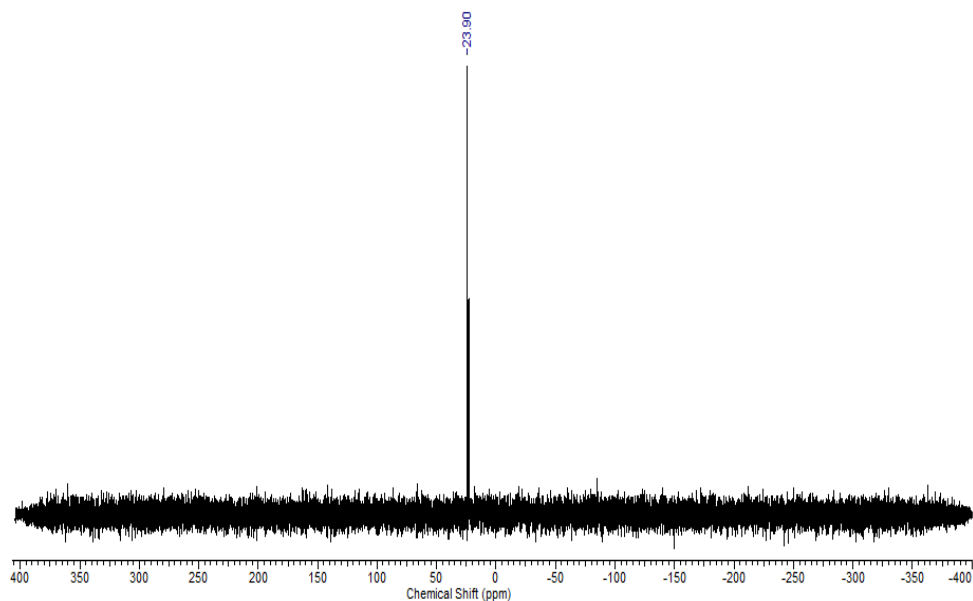
Figure 3.22: ^{31}P spectrum of [Ni(H$_2$L^1)(PPh$_3$)]Cl **(17)**
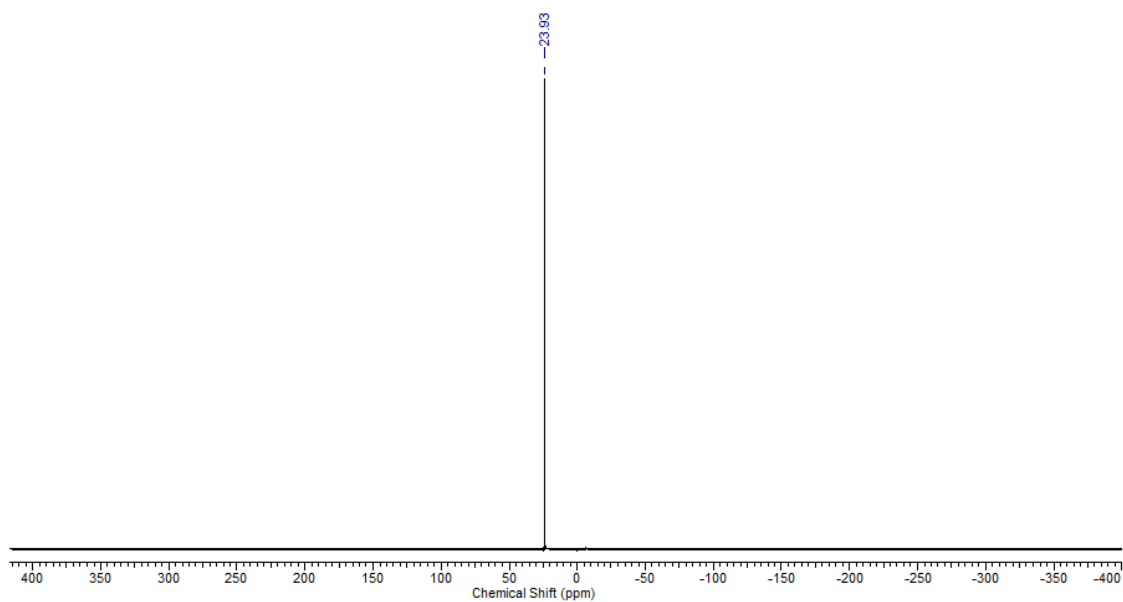
Figure 3.23: ^{31}P spectrum of the complex [Ni(HL^4)(PPh$_3$)] **(20)**
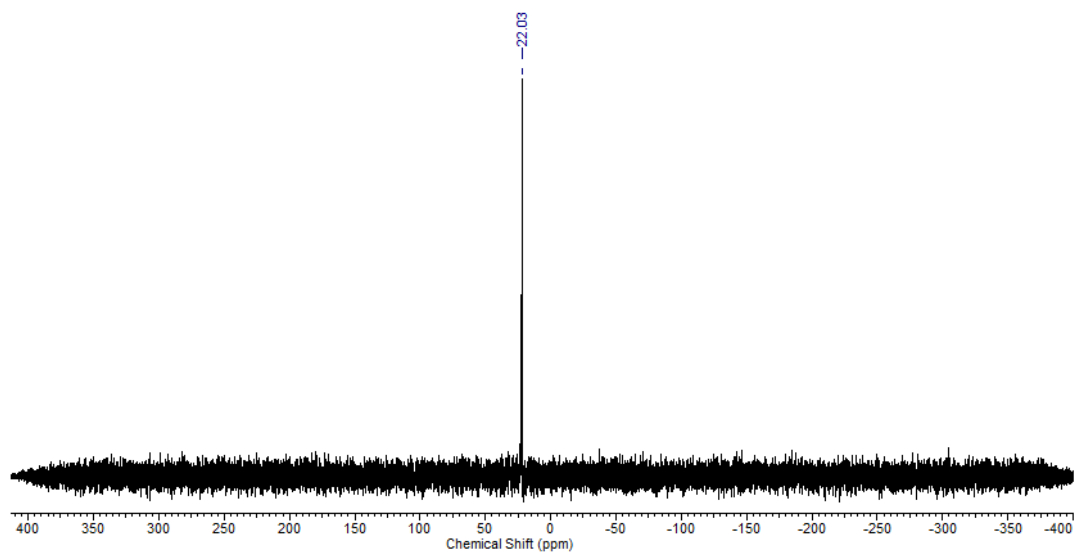
Figure 3.24: ^{31}P spectrum of [Ni$_2$(HL^1)$_2$(dppe)] **(21)**
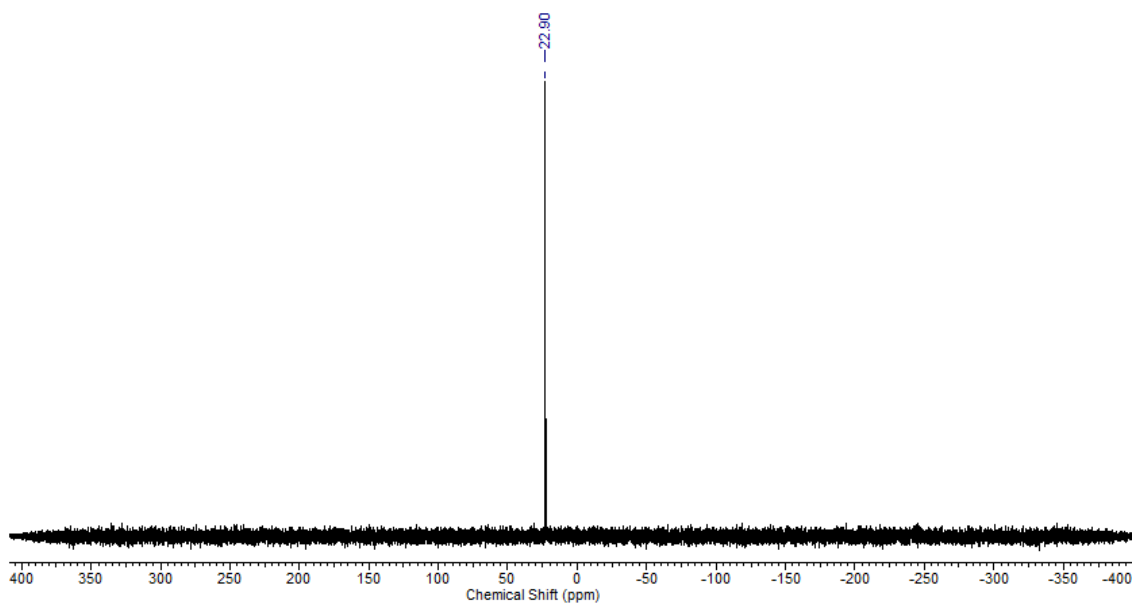
Figure 3.25: ^{31}P spectrum of $[Ni_2(HL^3)_2(dppe)]$ **(23)**

3.3.6 Infrared spectra

The most significant IR bands for nickel(II) phosphine mixed complexes of 2,3-dihydroxybenzaldehyde-N4-subsituted thiosemicarbazone are presented in Table 3.13 with their tentative assignments. The coordination of thiosemicarbazone ligands with nickel(II) is confirmed by comparing IR spectra of the free ligands with those of the complexes.

The chelation of the thiosemicarbazone ligands can be easily detected by monitoring the position of the ligand bands which have shifted to lower or high energy upon complexation. Absorption due to phenolic O-H can still be observed in the IR spectra of all the complexes at around 3450 - 3400 cm^{-1} due to polyhydroxy groups in the thiosemicarbazone ligands. This indicates that only one of the phenolic oxygen atoms from each thiosemicarbazone ligand is deprotonated and involved in coordination with Ni(II) (Kobakhidze et al., 2010; Tan et al., 2012). In addition, the band appeared in the region 1307–1270 cm^{-1} due to phenolic C–O stretching in the free thiosemicarbazone

ligands has been shifted downward to 1268-1230 cm^{-1} in the IR spectra of the complexes indicating the coordination through phenolic oxygen atom (Tamizh et al., 2010). The presence of another hydroxy group, which is considered as an electron donor may increase the electron density on the OH to become acidic by resonance and facilitates the deprotonation (El-Asmya & Al-Hazmi, 2009). The involvement of phenolic oxygen in bonding is supported by the appearance of a new band for ν (Ni–O) at 520-510 cm^{-1} region (Liu et al., 2006).

In all complexes, the ν(C=N) underwent a change in wavenumber and intensity, caused by complexation and upshifted by 20-50 cm^{-1} to higher wavenumber. Quite a number of thiosemicarbazones which undergo similar shift of the ν(C=N) bands to higher wavenumbers upon coordination has also been reported (Ali et al., 2011; Baligar & Revankar, 2008). The coordination of azomethine nitrogen to Ni(II) is further corroborated with the appearance of a new band at around 565 - 532 cm^{-1} region due to a ν(Ni—N) stretch in the spectra of all complexes. The spectra of all complexes exhibited an increase in the frequency of ν(N–N) bands, which found in the region 1070-1043 cm^{-1} of the free ligands (Ali et al., 2011; Youssef et al., 2009). This blue shift is due to the decrease in the repulsion between the lone pairs on the two nitrogen atoms. The decrease in repulsion led to the strengthening of the bond between nitrogen and nitrogen.

The IR spectrum of complex [Ni(H$_2$L^1)(PPh$_3$)]Cl **(17)** (Figure 3.26) and the complex [Ni(H$_2$L^2)(PPh$_3$)]Cl **(18)**, exhibited broad medium intensity band in the 2700–2560 cm^{-1} range which is assigned to the H-bonding vibrations (N–H … Cl) (Garg & Kumar, 2003). On this basis, it can be hypothesized that complexes **17** and **18** would form, during the crystallization, coupled dimers stabilized by an intermolecular hydrogen

bond (N(2)-H···Cl···N(4)H), as found by the X-ray analysis. The ν (N2-H) vibration is still seen in the spectra at 3170-3070 cm^{-1} indicates that the ligand is coordinated to Ni(II) in the thione form (Lobana et al., 2008).

In contrast, the spectral band v(N2-H) of the free thiosemicarbazones in the IR spectrum of complex [Ni(HL^3)(PPh$_3$)] **(19)** (Figure 3.27) and the complex [Ni(HL^4)(PPh$_3$)] **(20)**, disappeared providing strong evidence for ligand coordination around the Ni(II) ion in its deprotonated thiolate form (Chellan et al., 2010). A new band was found at 1560 cm^{-1}, 1554 cm^{-1} in complexes **19** and **20** respectively, which is due to the formation of a new –N=C bond formed during the enolization of the thiosemicarbazone ligands. Similar observation was found in complexes **(21-24)**, where the vibration of the newly –N=C- band appeared in the range 1559-1553 cm^{-1}.

However, the coordination of thiosemicarbazone sulfur to Ni(II) either in its thione or thiol form is confirmed by the downward shift of 10-80 cm^{-1} for υ(C=S) in the spectra of all complexes. It has been observed from the IR spectra of all complexes that the down shift in the υ (C=S) band is larger in the complexes with doubly deprotonated ligands (complexes **19**, **20**, **21**, **22**, **23** and **24**) than the mono deprotonated ligands (complexes **17** and **18**), which could be due the lowering of C-S order owing to deprotonation (Fostiak et al., 2003; Liu et al., 1999). Moreover, all complexes exhibited weak bands between 490-436 cm^{-1} which are due to v(Ni-S) (Elfetoh et al., 1998).

Additionally, the IR spectra of the complexes **17**, **18**, **19** and **20** shows bands characteristic of coordinated triphenylphosphine in the expected region (Carty, 1967; Karvembu et al., 2003; Lobana, Khanna, et al., 2009), while complexes **21**, **22**, **23** and **24** exhibit strong two bands with almost equal intensity assigned to bridging dppe in the

region 740 – 690 cm^{-1} (Vijayshree et al., 1993). However, the bands attributed to ν (Ni-P) cannot be assigned since the appearance of this band occurs in the far infrared spectra.

Table 3.13: IR spectral assignments for the thiosemicarbazone ligands and their nickel(II)-phosphine complexes

Compound	ν(C=N)	ν(C=S)/ ν(C-S)	ν(C-O)	ν(N-N)	ν(Ni-S)	ν(Ni-O)	ν(NiN)	Bands due to dppe	Bands due To PPh$_3$
H$_3$L^1	1611	1342 824	1279	1068	-	-	-	-	-
[Ni(H$_2$L^1)(PPh$_3$)]Cl (17)	1622	1332 777	1231	1097	483	514	534	-	1434 1057 694
[Ni$_2$(HL^1)$_2$(dppe)] (21)	1617	1304 733	1263	1101	483	511	555	1457 722 694	-
H$_3$L^2	1543	1389 853	1290	1043	-	-	-	-	-
[Ni(H$_2$L^2)(PPh$_3$)]Cl (18)	1622	1375 781	1279	1100	486	510	532	-	1437 1048 696
[Ni$_2$(HL^2)$_2$(dppe)] (22)	1590	1303 739	1267	1100	476	522	565	1474 704 695	-
H$_3$L^3	1542	1389 850	1289	1064	-	-	-	-	-
[Ni(HL^3)(PPh$_3$)] (19)	1590	1308 734	1268	1095	474	511	565	-	1457 1074 693
[Ni$_2$(HL^3)$_2$(dppe)] (23)	1594	1310 736	1268	1102	490	520	556	1455 717 692	-
H$_3$L^4	1542	1384 807	1307	1051	-	-	-	-	-
[Ni(HL^4)(PPh$_3$)] (20)	1592	1308 740	1246	1098	-	510	531	-	1458 1050 695
[Ni$_2$(HL^4)$_2$(dppe)] (24)	1596	1306 733	1261	1102	436	519	556	1459 718 702	-
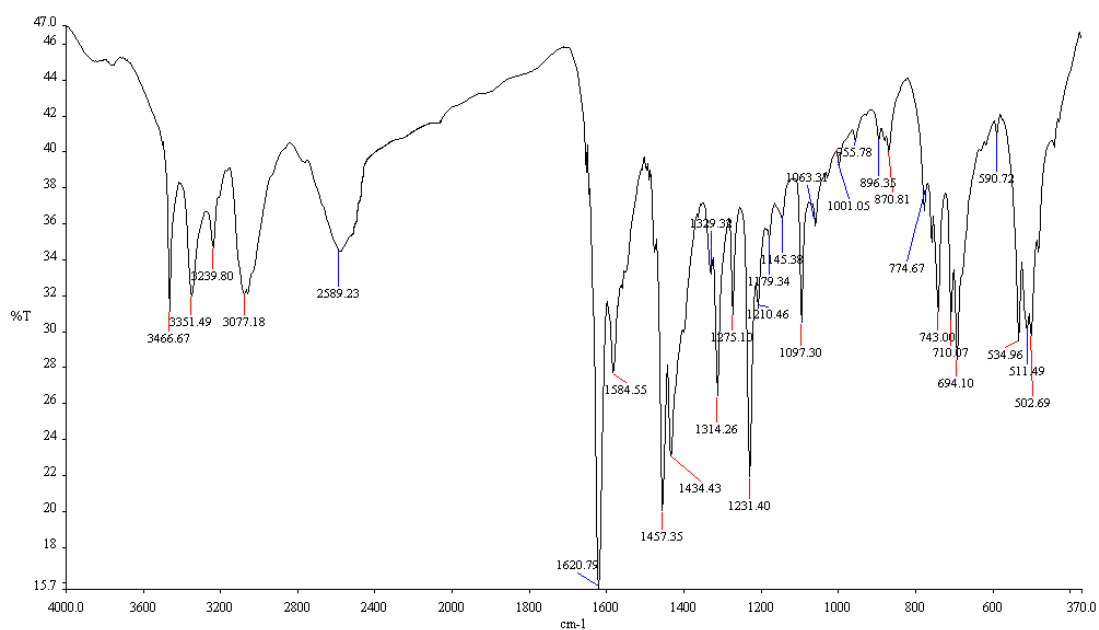
Figure 3.26: IR spectrum of [Ni(H$_2$L^1)(PPh$_3$)]Cl **(17)**
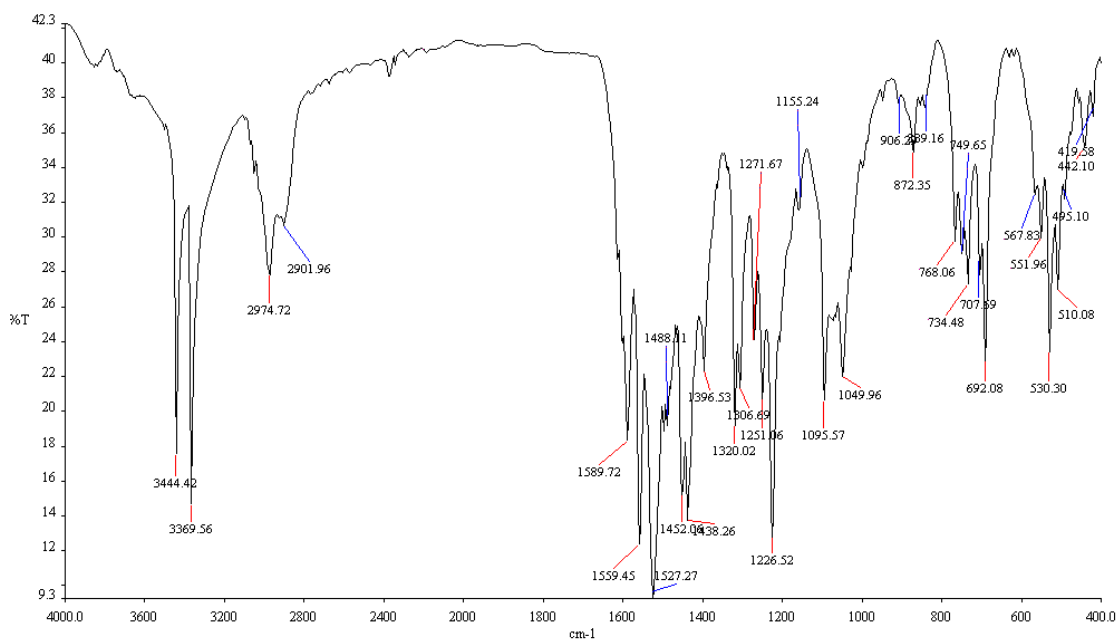
Figure 3.27: IR spectrum of [Ni(HL^3)(PPh$_3$)] **(19)**
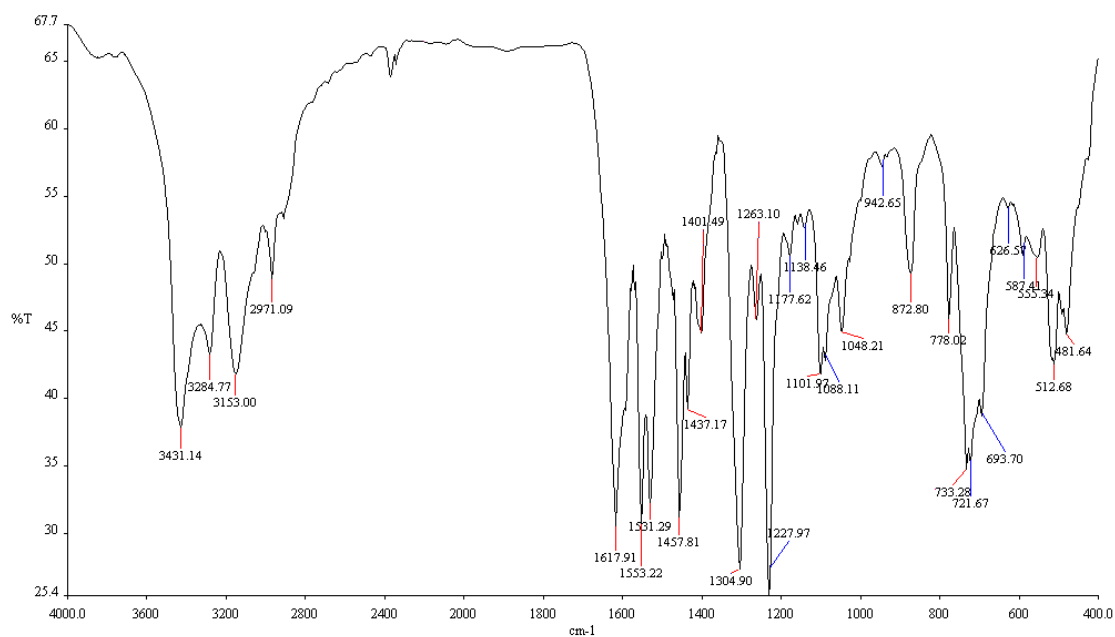
Figure 3.28: IR spectrum of $[Ni_2(HL^1)_2(dppe)]$ **(21)**
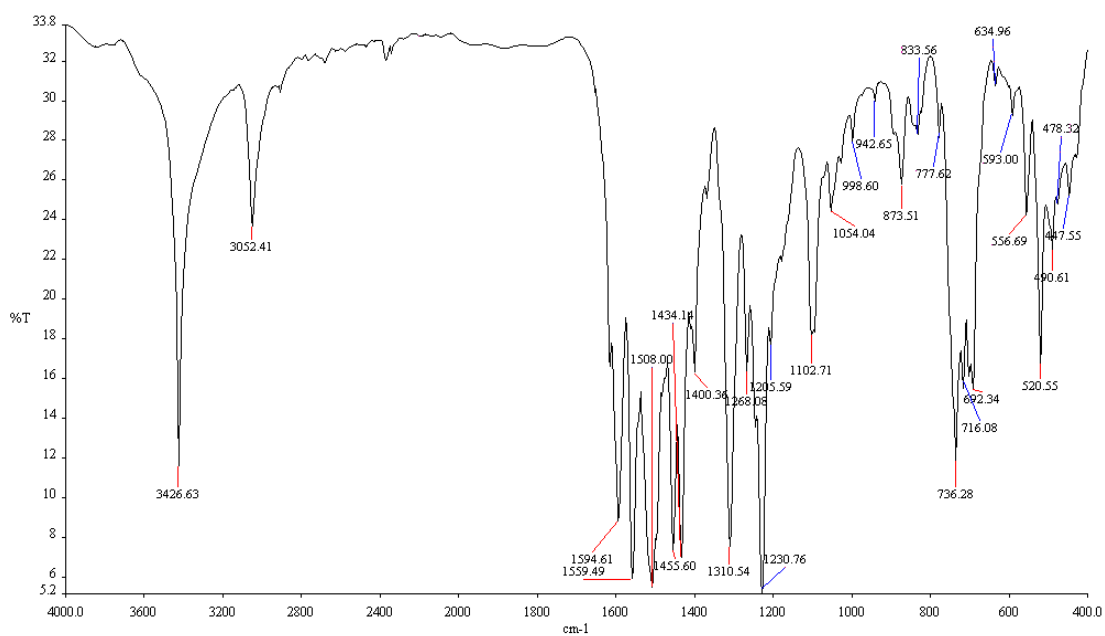
Figure 3.29: IR spectrum of $[Ni_2(HL^3)_2(dppe)]$ **(23)**

131

3.3.7 Electronic spectra

Electronic spectral assignments for the ligands 2,3-dihydroxybenzaldehyde N(4)-substituted thiosemicarbazones and their nickel(II) phosphine complexes in DMF are summarized in Table 3.14. All the ligands have a $\pi \rightarrow \pi^*$ band at around 39,525 - 38,461 cm^{-1} due to azomethine, thioamide and ring transitions (Bindu & Kurup, 1997). Significant shift to lower energy is observed for this band upon complexation with nickel(II). The shift of the $\pi \rightarrow \pi^*$ bands to longer wavelength region in nickel complexes is that the coordination with metal ion causes weakening of the C=S bond and enhances the conjugation system CH=N-N=CS (Latheef et al., 2008). Furthermore, all the thiosemicarbazone ligands have two bands at around 27,100-30,233 cm^{-1} attributed to $n \rightarrow \pi^*$ transition of azomethine and thioamide group. Upon complexation, the $n \rightarrow \pi^*$ band in the complex have suffered a blue shift owing to the donation of azomethine lone pair of electrons to the nickel indicating that the azomethine nitrogen is involved in coordination to the nickel ion (Offiong et al., 2000; Siji et al., 2010). Two moderately intense bands in the range 24,630-23,980 cm^{-1} and 23,866-21,881 cm^{-1} are found only in the spectra of the complexes and allocated for ligand to metal charge transfer transitions (LMCT) (Kalaivani et al., 2012). The same behavior has been observed in the electronic spectra of other similar square planar nickel(II) complexes (Gradinaru et al., 2004; Prabhakaran, Palaniappan, et al., 2011).

Additionally, nickel complexes show a broad d-d band around 18,000-20,000 cm^{-1} which attributed to $^1A_{1g} \rightarrow {}^1B_{1g}$ transitions characteristic of four coordinate nickel(II) complexes with square planar geometry (Güveli et al., 2010; Hecke & Horrocks, 1966). The absence of d–d transitions at lower energy (i.e. no absorption below 15000 cm^{-1}) point out a square-planar geometry for mixed nickel(II) thiosemicarbazone complexes

with phosphines. However, the planarity of these complexes was also confirmed from

the diamagnetism and the X-ray diffraction studies.

Table 3.14: Electronic spectral assignments (cm^{-1}) for the thiosemicarbazone ligands and their nickel(II) phosphine complexes in DMF

Compound	$\pi\rightarrow\pi^*$	$n\rightarrow\pi^*$	LMCT	*d-d*
H_3L^1	38461	28221, 30233	-	-
$[Ni(H_2L^1)(PPh_3)]Cl$ **(17)**	35335	29761	23980 22935	18590
$[Ni_2(HL^1)_2(dppe)]$ **(21)**	34602	29901	24630 23866	20115
H_3L^2	38759	28328, 30120	-	-
$[Ni(H_2L^2)(PPh_3)]Cl$ **(18)**	35352	28764	24330 22573	18187
$[Ni_2(HL^2)_2(dppe)]$ **(22)**	34863	28759	24570 22075	20476
H_3L^3	39525	27100, 27932	-	-
$[Ni(HL^3)(PPh_3)]$ **(19)**	36363	28653	24038 22727	18241
$[Ni_2(HL^3)_2(dppe)]$ **(23)**	35211	28735	23980 22172	19613
H_3L^4	39062	27700, 28089	-	-
$[Ni(HL^4)(PPh_3)]$ **(20)**	35219	28735	24154 22573	19017
$[Ni_2(HL^4)_2(dppe)]$ **(24)**	35108	28818	24630 21881	19820

CHAPTER 4

Synthesis and characterization of nickel(II) complexes of thiourea derivatives of

diamines

4.1 Introduction

Over the last two decades, the number of studies concerning metal-containing thiourea

has increased rapidly (Bott et al., 1998; Henderson et al., 2002; Lipowska et al., 1996)

as thioureas and their derivatives constitute an important class of N,S-donor ligands

which show heterodentate chelation in complex formation. Even though the low

basicity of thiourea ligands militates against the formation of nitrogen-metal bond, they

can coordinate to metal ions in different coordination modes. However, the chelation

flexibility of thioureas is based on the tautomerism between the thione and thiol forms,

Figure 4.1.
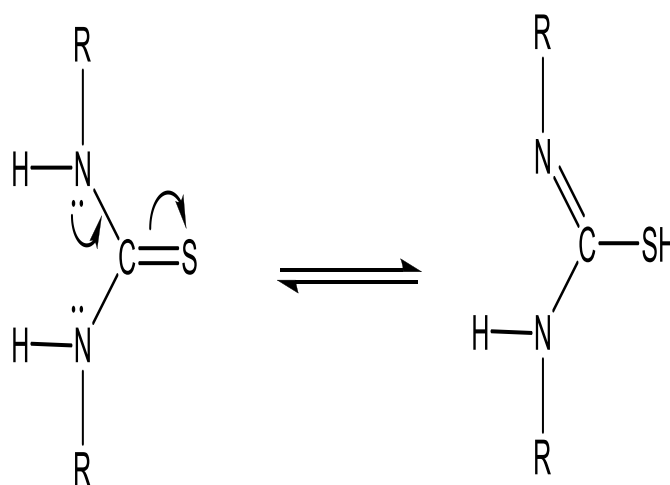
Figure 4.1: Thione - thiol tautomerism in thiourea ligands

Thioureas and their complexes are associated with diverse applications in

pharmaceutical chemistry for potential therapeutic agents as antibacterial, antifungal,

antiallergic, antineoplastic, anticancer and anti-HIV (D'Cruz et al., 2003). Additionally,

they play major contribution in analytical, environmental and industrial chemistry as

selective colorimetric and fluorescent anion sensors (Evans et al., 2006), analytical agents for detecting heavy metals (Unterreitmaier & Schuster, 1995) and as homogeneous catalysis for several chemical reactions (Cauzzi et al., 2000; Yalalov et al., 2008). Consequently, several thioureas and their metal complexes have been the subject of chemical and structural studies (Moloto et al., 2003).

Tetrahedral, square planar as well as octahedral nickel(II) complexes of thioureas and N-substituted thioureas, in which the ligands are known to be bidentate, have been reported (Arslan et al., 2003; Campo et al., 2002; Eaton & Zaw, 1972). On the other hand, ligands, such as N,N-dialkylthiourea are found to be monodentate in their nickel(II) complexes (Asif et al., 2010; El-Bahya et al., 2003). In addition, di, tri and oligonuclear nickel(II) complexes with thioureas and bisthioureas have been elucidated (Beyer et al., 2008; Du & Liu, 2008; Hoyer et al., 1986).

N,N-disubstituted thioureas derivatives of diamines have been extensively used as anion binding site in receptors due to the relatively acidic thiourea NH protons with a strong hydrogen-bond donor capability in the thiourea moiety (Benito et al., 2001; Kumar et al., 2007; Li et al., 2010). Furthermore, thiourea derivatives of diamines are a well known class of excellent catalysts (Dai et al., 2003; Fuerst & Jacobsen, 2005). An important feature of thiourea diamine derivatives is that these thioureas can be converted to heterocyclic compounds such as 2-aminobenzimidazoles (Wan et al., 2011) and imidazole-2-thione (Yella & Patel, 2010). However, the cyclization reaction requires catalyst to promote the reaction. The widely used catalyst for this reaction is transition metal ions (often Pd or Cu catalysts) with ligand in presence of base (Wang et al., 2004).

Indeed, most of these studies have been centered on the preparation and investigation of their analytical properties, very little is known of their ligational behavior (Lipowska et al., 1996). Moreover, examples in the literature of diamines thiourea derivatives as ligands of nickel(II) are rather rare (Cheresova et al., 1997; Hosny & Mostafa, 2010).

Details regarding the synthesis and characterization of nickel(II) complexes of diamines thiourea ligands, N-(2-aminophenyl)-N'-phenylthiourea **(25)**, N-(4-aminophenyl)-N'-phenylthiourea **(26)** and N-(2-aminopyridin-3-yl)-N'-phenylthiourea **(27)** are presented in this chapter.

4.2 Experimental

4.2.1 Materials and solutions

The 1,2-phenylenediamine (Merck), 1,4-phenylenediamine (Merck), 1,10-phenanthroline (Merck), 2,3-diaminopyridine (Aldrich), phenyl isothiocyanate (Merck), 2,2'-bibyridine (Alpha) and nickel(II) nitrate hexahydrate (Aldrich) were used as received. The potassium thiocyanate (Merck) and nickel(II) chloride hexahydrate (Merck) were dried under high vacuum before use. All solvents employed in this study were of analytical grade and used as received.

4.2.2 Physical measurements

The details of spectroscopic measurements and elemental analysis for the characterization of the thioureas ligands and their nickel complexes were similar to the details described in Chapter 3.

4.2.3 Syntheses

4.2.3.1 Synthesis of thioureas ligands

4.2.3.1.1 Synthesis of N-(2-aminophenyl)-N'-phenylthiourea (25) and N-(4-aminophenyl)-N'-phenylthiourea (26)

These ligands were prepared by known published procedures (Deohate et al., 2004; Galabov et al., 1980). 1,2-phenylenediamine or 1,4-phenylenediamine (1.018 g, 10 mmol) was dissolved in absolute ethanol (20 mL) with stirring. The phenylisothiocyanate (1.2 ml, 10 mmol) was added dropwise, then immediately a white precipitate (in the case of 25) or white gray precipitate (in the case of **26**) was obtained. The suspended solution was stirred for a further 2 h. This precipitate was filtered and washed with ethanol (100 mL), dried in air and kept in a desiccator over silica gel.

PhTUPho-NH$_2$ **(25)** (Yield: 2.11 g, 87%). Anal. Calc. for C$_{13}$H$_{13}$N$_3$S: C, 64.17; H, 5.39; N, 17.42. Found: C, 63.93; H, 5.35; N, 17.42 %. IR (KBr disc, cm^{-1}): 3211 s, 2999 m, 1614s, 1534 s, 1503 s, 1449 m, 1335 s, 1316 s, 1242 m, 1151 w, 1133 m, 1072 w s, 1025 w, 930 w, , 856 w, 725 s, 698 s, 688 s, 634 m, 615 w, 551 w, 476 w(s, strong; m, medium ; w, weak).

Characteristic ^{1}H NMR signals (DMSO-d$_6$, TMS, p.p.m.): 9.57 (s, 1H, NHCS), 9.07 (s, 1H, CSNH), 7.52 (d, 2H, aromatic), 7.33 (t, 2H, aromatic), 7.11 (t, 2H, aromatic), 6.96 (t, 1H, aromatic), 6.76 (d, 1H, aromatic), 6.57 (t, 1H, aromatic), 4.92 (s, 2H, NH$_2$). Characteristic ^{13}C NMR signals (DMSO-d$_6$, TMS, p.p.m.): 180.60 (C=S), 144.52, 140.18, 128.86, 128.66, 127.65, 124.80, 124.59, 124.14, 116.87, 116.43 (C-aromatic).

PhTUPhp-NH$_2$ **(26)**

(Yield: 2.06 g, 84%). Anal. Calc. for C$_{13}$H$_{13}$N$_3$S: C, 64.17; H, 5.39; N, 17.42; S, 13.18. Found: C, 64.08; H, 5.65; N, 17.15; S, 12.98%. IR (KBr disc, cm^{-1}): 3431s, 3351s, 3326s, 3213 s, 3171m, 2959 m, 1625m, 1601m, 1538 s, 1511 s, 1449 m, 1363 w,

1300m, 1276s, 1228m, 1197m, 1166 m, 1072 m, 1051 m, 948 w, 924w, 826 m, 775 w, 747m, 708m, 696 m, 634 m, 558 m, 518m,474 m(s, strong; m, medium ; w, weak).

Characteristic ^{1}H NMR signals (DMSO-d$_6$, TMS, p.p.m.): 9.38 (s, 1H, NHCS), 9.34 (s, 1H, CSNH), 7.45 (d, 2H, aromatic), 7.28 (t, 2H, aromatic), 7.09 (t, 1H, aromatic), 7.00 (d, 2H, aromatic), 6.53 (d, 2H, aromatic), 4.92 (s, 2H, NH$_2$). Characteristic ^{13}C NMR signals (DMSO-d$_6$, TMS, p.p.m.): 179.60 (C=S), 146.53, 146.53, 139.73, 128.24, 127.37, 126.17, 124.11, 123.72, 113.46 (C-aromatic).

4.2.3.1.2 Synthesis of N-(2-aminopyridin-3-yl)-N'-phenylthiourea (27)

Phenyl isothiocyanate (1.2 mL, 10 mmol) was added to ethanolic solution (20 mL) of 2,3-diaminopyridine (1.09 g, 10 mmol). The reaction mixture was heated for 7 h at 60C°. The light brown solid was filtered, washed with cold ethanol and ether, dried in air and kept in a desiccator over silica gel.

PhTUPhPyo-NH$_2$ (**27**) (Yield: 1.92 g, 79%). Anal. Calc. for C$_{12}$H$_{12}$N$_4$S: C, 58.99; H, 4.95; N, 22.93; S, 13.12. Found: C, 59.08; H, 4.95; N, 22.93; S, 13.07%. IR (KBr disc, cm^{-1}): 3448 m, 3337 s, 3147 s, 2974 s, 1616 s, 1593 m, 1535 s, 1498 s, 1362 m, 1292 m, 1247 m, 1205 s, 1077 w, 1027 w, 927 w, 818 m, 781 m, 761 m, 727m, 694 m, 646 m, 612 w, 503 w, 468 m, 418 w(s, strong; m, medium ; w, weak).

Characteristic ^{1}H NMR signals (DMSO-d$_6$, TMS, p.p.m.): 9.78 (s, 1H, NHCS), 9.03 (s, 1H, CSNH), 7.84 (d, 1H), 7.53 (d, 2H), 7.42 (d, 1H), 7.33 (t, 2H), 7.13 (t, 1H), 6.58 (t, 1H), 5.74 (s, 2H, NH$_2$). Characteristic ^{13}C NMR signals (DMSO-d$_6$, TMS, p.p.m.): 180.95 (C=S), 156.22, 146.15, 140.00, 136.30, 128.95, 124.94, 124.10, 120.03, 112.89 (C-aromatic).

4.2.3.2 Synthesis of thioureas complexes

4.2.3.2.1 Synthesis of [Ni(PhTUPh*o*-NH$_2$)$_2$] (28)

NiCl$_2$.6H$_2$O (0.24 g, 1mmol) in 10 mL methanol was added to a hot solution of N-(2-aminophenyl)-N'-phenylthiourea (0.48 g, 2 mmol) and KOH (0.11g, 2 mmol) in 30 ml methanol in which dark green precipitate was formed after 5 minutes. The mixture was heated under reflux for further 1 h. The green solid was filtered, washed thoroughly with methanol and ether, dried in air and kept in a desiccator over silica gel.

(Yield: 0.41 g, 82%). Anal. Calc. for C$_{26}$H$_{24}$N$_6$S$_2$Ni.2H$_2$O: C, 55.63; H, 4.67; N, 14.97. Found: C, 55.52; H, 4.70; N, 14.99%. IR (KBr disc, cm^{-1}): 3459 m, 3328 s, 3195 m, 3059 m, 3022w, 1610m, 1588 m, 1558 s, 1491 s, 1457 w, 1395 m, 1320s, 1224 s, 1155 m, 1135w, 1070 m, 1024 m, 1003 w, 943 m, 868 w, 754 s, 695 s, 634 m, 612 w, 543 w, 492 w, 449 m (s, strong; m, medium ; w, weak).

4.2.3.2.2 Synthesis of [Ni$_2$(PhTUPh*o*-NH$_2$)$_2$(Phen)$_2$]NO$_3$.H$_2$O (29)

Ni(NO$_3$)$_2$.6H$_2$O (0.29 g, 1 mmol) and 1,10-phenanthroline (0.18 g, 1 mmol) were heated in methanol (20 mL) for 1h followed by addition of N-(2-aminophenyl)-N'-phenylthiourea (0.24 g, 1 mmol) and KOH (0.056g, 1 mmol) in hot methanol (15 mL) and the mixture was refluxed for another 3 h. The resulting green solution was concentrated. Dark green crystals were collected after standing the solution at room temperature for two days. The crystals were filtered, washed thoroughly with ethanol and then methanol and ether, dried in air and kept in a desiccator over silica gel.

(Yield: 0.24 g, 74%). Anal. Calc. for C$_{50}$H$_{40}$N$_{11}$O$_4$S$_2$Ni$_2$: C, 57.72; H, 3.88; N, 14.81. Found: C, 57.89; H, 3.28; N, 15.06 %. IR (KBr disc, cm^{-1}): 3316 m, 3229 w, 3057 m, 1575 s, 1518 w, 1502 w, 1425 m,1384 s, 1319 m, 1294 s, 1251 m, 1142 w, 1050 m 1032 m, 931 m, 845 m, 762 m, 726 m, 697 m, 527 m, 424 w (s, strong; m, medium ; w, weak).

4.2.3.2.3 Synthesis of [Ni$_2$(PhTUPh*o*-NH$_2$)$_2$(bpy)$_2$]NO$_3$ (30)

Ni(NO$_3$)$_2$.6H$_2$O (0.29 g, 1 mmol) and 2,2'-bipyridine (0.16 g, 1 mmol) were heated in methanol (20 mL) for 1 h followed by addition of N(2-aminophenyl)-N'-phenylthiourea (0.24g, 1 mmol) and KOH (0.056 g, 1 mmol) in hot methanol (15 mL) and the mixture was refluxed for another 3 h. Dark green precipitate was filtered, washed thoroughly with methanol and ether, dried in air and kept in a desiccator over silica gel.

(Yield: 0.37 g, 80%). Anal. Calc. for C$_{46}$H$_{38}$N$_{11}$O$_3$S$_2$Ni$_2$: C, 56.70; H, 3.93; N, 15.81. Found: C, 56.33; H, 3.71; N, 15.65%. IR (KBr disc, cm^{-1}): 3407 m, 3331 S, 3109 m, 3065m, 1578 s, 1502 m, 1475 m, 1444 m,1384 s, 1319 m, 1295 s, 1251 m, 1154 w, 1090 m, 1050 m, 1033m, 931 m, 830 w, 812 w, 764 s, 736 m, 695 m, 670m, 526 m, 450w, 419 w (s, strong; m, medium ; w, weak).

4.2.3.2.4 Synthesis of [Ni(PhTUPh*p*-NH$_2$)$_2$] (31)

Complex **31** was similarly prepared as complex **28** by using N(4-aminophenyl)-N'-phenylthiourea (0.48 g, 2 mmol) as the thiourea ligand.

(Yield: 0.44 g, 83%)Anal. Calc. for C$_{26}$H$_{24}$N$_6$S$_2$Ni.2H$_2$O: C, 55.63; H, 4.67; N, 14.97. Found: C, 55.45; H, 4.51; N, 14.95%. IR (KBr disc, cm^{-1}): 3427 m, 3330 m, 3233 m, 3039 m, 1591 m, 1561 s, 1514 s, 1400 m, 1322 s, 1286 s, 1232 m, 1169 m, 1075 w, 1026 w, 926 w, 830 m, 764 m, 735 w, 697 m, 670 w, 623 w, 594 m, 527 m, 503m, 418 w, 378m (s, strong; m, medium ; w, weak).

4.2.3.2.5 Synthesis of [Ni$_2$(PhTUPh*p*-NH$_2$)$_2$(Phen)$_2$]NO$_3$.2H$_2$O (32)

To a solution of 1-(4-aminophenyl)-N'-phenylthiourea (0.48 g, 2 mmol) and KOH (0.056g, 1 mmol) in hot methanol (20 mL) was added NiCl$_2$.6H$_2$O (0.24 g, 1 mmol) followed by 1,10-phenanthroline (0.18 g, 1 mmol) .The mixture was heated at reflux for 2 h. Slow evaporation of the solution afforded green precipitate that was filtered,

washed thoroughly with methanol and then ether, dried in air and kept in a desiccator over silica gel. Recrystallization of the solid by slow diffusion of hexane into THF solution of the complex gave small crystals.

(Yield: 0.19 g, 66%). Anal. Calc. for $C_{50}H_{42}N_{11}O_5S_2Ni_2$: C, 56.74; H, 4.00; N, 14.56. Found: C, 56.90; H, 4.23; N, 14.83 %. IR (KBr disc, cm^{-1}): 3417 w, 3336 m, 3221 m, 3030 w, 1591 m, 1560 s, 1514 m, 1322 s, 1285 m, 1231 m, 1169 w, 1124 w, 1072 w, 1026 w, 927 w, 869 m, 828 m, 765 m, 623 w, 503 m (s, strong; m, medium ; w, weak).

4.2.3.2.6 Synthesis of [Ni$_2$(PhTUPh*p*-NH$_2$)$_2$(bpy)$_2$]NO$_3$.H$_2$O (33)

Ni(NO$_3$)$_2$.6H$_2$O (0.29g, 1 mmol) and 2,2'-bipyridine (0.16 g, 1 mmol) were heated in methanol (20 mL) for 1 h followed by addition of 1-(4-aminophenyl)-N'-phenylthiourea (0.24g, 1 mmol) and KOH (0.056 g, 1 mmol) in hot methanol (15 mL) and the mixture was refluxed for another 3 h. The solution was concentrated; the dark green precipitate that formed was filtered, washed thoroughly with methanol and ether, dried in air and kept in a desiccator over silica gel.

(Yield: 0.40 g, 84%). Anal. Calc. for $C_{46}H_{40}N_{11}O_4S_2Ni_2$: C, 55.67; H, 4.06; N, 15.53. Found: C, 55.53; H, 4.23; N, 15.66 %. IR (KBr disc, cm^{-1}): 3344 m, 3233 m, 3042 m, 1596 m, 1542 s, 1515 s, 1475 m, 1384 s, 1314 s, 1258 m, 1225 m, 1170 w, 1090 m, 1025 w, 931 w, 830 w, 761 m, 736 m, 695 m, 670m, 526 w, 517 w (s, strong; m, medium ; w, weak).

4.2.3.2.7 Synthesis of [Ni(PhTUPy*o*-NH$_2$)$_2$] (34)

Complex **34** was similarly prepared as complex **28** by using N-(2-aminopyridin-3-yl)-N'-phenylthiourea (0.50 g, 2 mmol) as the thiourea ligand.

(Yield: 0.56 g, 87%). Anal. Calc. for $C_{24}H_{21}N_8S_2Ni.H_2O$: C, 51.26; H, 4.12; N, 19.93. Found: C, 51.29; H, 4.20; N, 19.77%. IR (KBr disc, cm^{-1}): 3462 m, 3357 s, 3162 m,

3049 m, 2927w, 1605w, 1594 m, 1578 w, 1552s, 1496 m, 1465 s, 1451 m, 1422 m, 1322 s, 1306 m, 1255 m, 1221 s, 1185 m, 1135w, 1070 w, 1026 w, 943 m, 831 w, 786 w, 761 s, 739 m, 695 s, 631 m, 602 w, 563 w, 496 w, 464 w (s, strong; m, medium ; w, weak).

4.2.3.2.8 Synthesis of [Ni$_2$(PhTUPyo-NH$_2$)$_2$(Phen)$_2$]Cl (35)

NiCl$_2$.6H$_2$O (0.24 g, 1 mmol) and 1,10-phenanthroline (0.18 g, 1 mmol) were heated in methanol (20 mL) for 1h followed by addition of N-(2-aminopyridin-3-yl)-N'-phenylthiourea (0.25 g, 1 mmol) and KOH (0.056 g, 1 mmol) in hot methanol (15 mL) and the mixture was refluxed for another 3 h. Complex **35** precipitated as a dark green crystalline solid, which was collected by filtration, washed thoroughly with ethanol and then dried in air and kept in a desiccator over silica gel.

(Yield: 0.36 g, 77%). Anal. Calc. for C$_{48}$H$_{36}$N$_{12}$S$_2$Ni$_2$Cl: C, 57.78; H, 3.64; N, 16.84. Found: C, 57.74; H, 3.78; N, 16.88%. IR (KBr disc, cm^{-1}): 3462 m, 3358 w, 3166 m, 3051 m, 2931 m,1594 s, 1552 s, 1497 w, 1425 m,1466 s, 1332 s, 1250 s, 1250 w, 1183 w, 1130 w, 1076 w, 1028 w, 924 w, 827 w, 762 m, 735 m, 697 m, 632 m, 603w, 502 w (s, strong; m, medium ; w, weak).

4.2.3.2.9 Synthesis of [Ni$_2$(impytH)$_4$].H$_2$O (36)

NiCl$_2$.6H$_2$O (0.24 g, 1mmol) in 10 mL methanol was added dropwise to a mixture of N-(2-aminopyridin-3-yl)-N'-phenylthiourea (0.50 g, 2 mmol) and KOH (0.11g, 2 mmol) in hot methanol (40 mL). The green solution was heated under reflux for 2 h. To this solution, 1,10-phenanthroline (0.18 g, 1 mmol) or 2,2'-bipyridine (0.16 g, 1 mmol) was added, the color of the green precipitate was changed to gray. The solution was further refluxed for 3 h. The gray precipitated was filtered, washed thoroughly with methanol and then ether, dried in air and kept in a desiccator over silica gel.

(Yield: 0.11 g, 87%). Anal. Calc. for $C_{24}H_{18}N_{12}S_2Ni_2O$: C, 39.16; H, 2.46; N, 22.83. Found: C, 39.34; H, 2.48; N, 22.75%. IR (KBr disc, cm^{-1}): 3179 s, 2969 w, 2928 w, 1655 s, 1620 m, 1490 m, 1420 s,1364 s, 1305 s, 1263 s, 1193 m, 1122 w, 1099 w, 1039 m, 980 m, 937 w, 840 m, 791 m, 769 s, 654 w, 622 w, 589 w, 530 m, 465 w, 431 m (s, strong; m, medium ; w, weak).

4.2.3.2.10 Synthesis of [Ni$_2$(PhTUPyo-NH$_2$)$_2$(Bpy)$_2$]Cl (37)

$NiCl_2.6H_2O$ (0.24 g, 1 mmol) and 2,2'-bipyridine (0.16 g, 1 mmol) were heated in methanol (20 mL) for 1 h followed by addition of 1-(2-aminopyridin-3-yl)-N'-phenylthiourea (0.25g, 1 mmol) and KOH (0.056g, 1 mmol) in hot methanol (15 mL) and the mixture was refluxed for another 3 h. Dark green crystalline solid that precipitated, was filtered, washed thoroughly with ethanol and then dried in air and kept in a desiccator over silica gel.

(Yield: 0.14 g, 82%)Anal. Calc. for $C_{44}H_{36}N_{12}S_2Ni_2Cl$: C, 55.64; H, 3.86; N, 17.70. Found: C, 55.78; H, 3.80; N, 17.79 %. IR (KBr disc, cm^{-1}): 3462 m, 3358 m, 3159 m, 3050 m, 2928 m, 2823 w, 1611 m, 1594 s, 1578 m, 1552 s, 1497 m, 1465 m,1418 w, 1331 s, 1256 w, 1220 m, 1185 w, 1076 w, 1027 w, 924 w, 830 w, 761 m, 738 m, 696 m, 631 m, 603w, 501 w (s, strong; m, medium ; w, weak).

4.2.4 X-ray crystallography

Block green crystals of compound **29**, suitable for X-ray diffraction studies were obtained by slow evaporation of its solution in methanol. A crystal having approximate dimensions 0.16 x 0.13 x 0.10 mm^3 was sealed in a glass capillary and intensity data was measured at room temperature. Gray crystals of compound **36** were grown by recrystallization from a mixture of DMF and ethanol. The X-ray diffraction data was measured at room temperature and data acquisition and cell refinement was done using

a Bruker SMART APEX CCD diffractometer equipped with graphite monochromated Mo Ka (A = 0.71073 Å) radiation. The Bruker SAINT software were used for data reduction (Bruker, 2007). The structure was solved by direct methods with the program SHELXS-97 and refined by full matrix least squares on F2 using SHELXL-97 (Sheldrick, 2008). The graphical tool used was ORTEP (Farrugia, 1997), DIAMOND (Brandenburg, 2006) and PLATON (Spek, 2003).

4.3 Results and discussion

4.3.1 Synthesis of the ligands and complexes

Thiourea ligands namely N-(2-aminophenyl)-N'-phenylthiourea **(25)**, N-(4-aminophenyl)-N'-phenylthiourea **(26)** and N-(2-aminopyridin-3-yl)-N'-phenylthiourea **(27)** were prepared following the published procedures (Galabov et al., 1980) by the reaction of phenylisothiocyanate with 1,2-phenylenediamine, 1,4-phenylenediamine and 2,3-diaminopyridine, respectively, in a simple reaction include transfer of an amino proton from the diamine to the isothiocyanate group whereby no by-products are formed, and thus purification is simple. The general structures of N-phenylthiourea derivatives of diamines are shown in Figure 4.2. The microanalysis data, infrared bands and NMR chemical shifts data for the ligands are in good agreement with the published procedures.
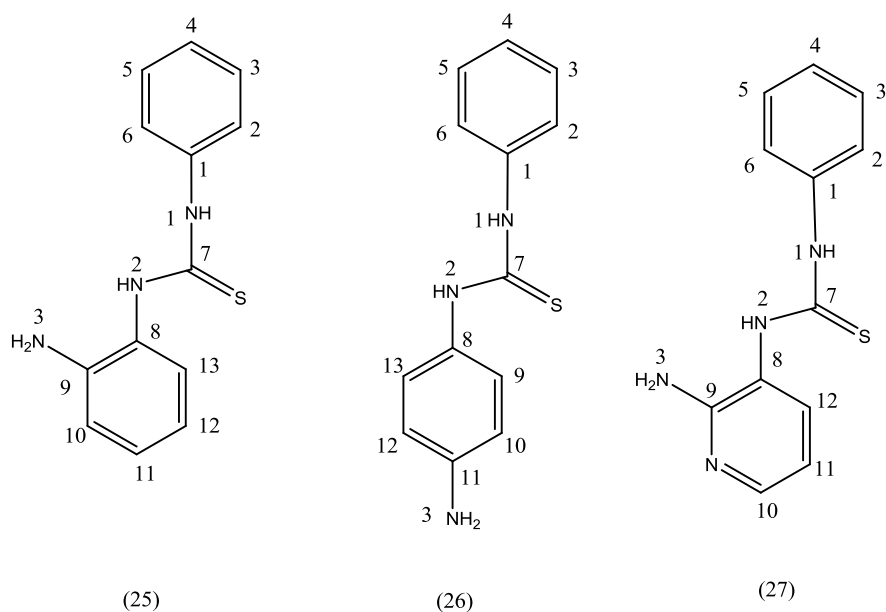
Figure 4.2: Schematic representation of N-(2-aminophenyl)-N'-phenylthiourea **(25)**, N-(4-aminophenyl)-N'-phenylthiourea **(26)** and N-(2-aminopyridin-3-yl)-N'-phenylthiourea **(27)**

Nickel(II) complexes [Ni(PhTUPh*o*-NH$_2$)$_2$] **(28)**, [Ni(PhTUPh*p*-NH$_2$)$_2$] **(31)** and [Ni(PhTUPy*o*-NH$_2$)$_2$] **(34)** were isolated as green microcrystalline solids by the reaction of thiourea ligands with nickel(II) chloride hexahydrate in 2 : 1 ligand : metal molar ratio in methanol, accompanied by addition of base to facilitate deprotonation of the phenylthiourea ligand and bidentate chelation. The magnetic susceptibility measurements revealed that these complexes are diamagnetic complexes. The analytical data of the complexes are given in Table 4.1 and are consistent with the stoichiometries proposed. These complexes are air stable, insoluble in common organic solvents such as chloroform, benzene, acetonitrile, ethanol, and methanol but partially soluble in tetrahydrofuran and dichloromethane and soluble in dimethylformamide and dimethylsulfoxide. All the prepared complexes were obtained in reasonable yields but attempts to grow crystals were unsuccessful.

Attempts to prepare mixed nickel(II) complexes of thiourea diamine derivatives with 1,10-phenanthroline and 2,2'-bipyridine by the reaction of complexes **28**, **31** and **34** with

phen or bpy *in situ* did not produce the desired complexes. However, the yield of the reaction is dependent on the thiourea ligand. Addition of the appropriate co-ligand to the reaction mixture which comprise Ni(II) salt with the thiourea ligands N-(2-aminophenyl)-N'-phenylthiourea (**25**), N-(4-aminophenyl)-N'-phenylthiourea (**26**) or N-(2-aminopyridin-3-yl)-N'-phenylthiourea (**27**), resulted in color change from green to grey in the case of N-(2-aminopyridin-3-yl)-N'-phenylthiourea only. The resulting mixture was stirred for 3 hours and the solvent removed while in the case of ligands **25** and **26**, the reaction mixture remained green even though the reaction time was increased up to 6 hours. On the basis of the spectral and chemical data, it is very likely that the thiourea ligand N-(2-aminopyridin-3-yl)-N'-phenylthiourea (**27**) in complex **34** has undergone an oxidative cyclization to 1H-imidazo[4,5-b]pyridine-2-thiol in the presence of phen or bpy in which a new dinuclear complex, compound **36** could be isolated (Scheme 4.1) (Murru et al., 2009; Sahu et al., 2011). The probable explanation for this pattern is the initial nucleophilic attack of diamine nitrogen on the thiocarbonyl of the thiourea moiety leading to the formation of a cyclic intermediate, which is further oxidized to afford the heterocyclic ligand (Scheme 4.2). Oxidative cyclization reactions have been reported for a number of pyridyl thiourea derivatives especially in the presence of copper (Che et al., 2000; Li et al., 2002; Tadjarodi et al., 2007; West et al., 2003). On the other hand, in the case of thiourea ligands **25** and **26**, characterization of the reaction mixture revealed that only [Ni(PhTUPh*o*-NH$_2$)$_2$] (**28**), [Ni(PhTUPh*p*-NH$_2$)$_2$] (**31**) complexes were obtained, respectively. It follows that by adding 1,10-phenanthroline or 2,2'-bipyridine to the nickel complex of thiourea diamine derivatives, only the thiourea ligand **27** undergoes an intramolecular cyclization which might be ascribed to the effect of electron withdrawing nitrogen present in PhTUPy*o*-NH$_2$ ligand, which with the catalytic effect of Ni/Phen in aerobic conditions facilitates easier

cyclization to a five-membered ring than other PhTUPh*o*-NH$_2$ and PhTUPh*p*-NH$_2$ ligands.

However, the mixed thiourea nickel complexes with 1,10-phenanthroline and 2,2'-bipyridine, compounds **29**, **30**, **32**, **33**, **35** and **37** were obtained as binuclear species bridged by thiourea ligands from the reaction of 1,10-phenanthroline or 2,2'-bipyridine with Ni(II) salt in 1 : 1 molar ratio in refluxing methanol followed by the addition of thiourea ligand (Scheme 4.3). The analytical and spectroscopic data are consistent with the proposed formulation of the complexes. These ionic compounds are green in color and air stable in the solid state. Spectroscopic and crystallographic data show that the thiourea ligands are coordinated to nickel(II) in the thiolate form and bridging two nickel atoms through the sulfur. The deprotonation of the ligands was ensured by the addition of a strong base such as potassium hydroxide.

Table 4.1: Stoichiometries, color and partial elemental analyses of nickel(II) complexes with thiourea

Complex	Stoichiometries	color	Anal.Calc. (Found)%		
			C	H	N
[Ni(PhTUPho-NH$_2$)$_2$] **(28)**	C$_{26}$H$_{24}$N$_6$S$_2$ONi	Dark Green	57.47	4.45	15.47
			(57.20)	(4.31)	(15.63)
[Ni(PhTUPhp-NH$_2$)$_2$].H$_2$O **(31)**	C$_{24}$H$_{24}$N$_6$S$_2$ONi	Dark Green	55.63	4.67	14.97
			(55.45)	(4.51)	(14.95)
[Ni(PhTUPyo-NH$_2$)$_2$].H$_2$O **(34)**	C$_{24}$H$_{24}$N$_8$S$_2$ONi	Dark Green	51.17	4.29	19.89
			(51.29)	(4.40)	(19.77)
[Ni$_2$(PhTUPhoNH$_2$)$_2$(Phen)$_2$]NO$_3$. H$_2$O **(29)**	C$_{50}$H$_{40}$N$_{11}$O$_4$S$_2$Ni$_2$	Green	57.72	3.88	14.81
			(57.89)	(3.28)	(15.06)
[Ni$_2$(PhTUPho-NH$_2$)$_2$(bpy)$_2$]NO$_3$ **(30)**	C$_{46}$H$_{38}$N$_{11}$O$_3$S$_2$Ni$_2$	Green	56.70	3.93	15.81
			(56.33)	(3.71)	(15.65)
[Ni$_2$(PhTUPhpNH$_2$)$_2$(Phen)$_2$]NO$_3$. 2H$_2$O **(32)**	C$_{50}$H$_{42}$N$_{11}$O$_5$S$_2$Ni$_2$	Green	56.74	4.00	14.56
			(56.90)	(4.23)	(14.83)
[Ni$_2$(PhTUPhpNH$_2$)$_2$(Bpy)$_2$]NO$_3$. H$_2$O **(33)**	C$_{46}$H$_{40}$N$_{11}$O$_4$S$_2$N$_{i2}$	Green	55.67	4.06	15.53
			(55.53)	(4.23)	(15.66)
[Ni$_2$(PhTUPyo-NH$_2$)$_2$(Phen)$_2$]Cl **(35)**	C$_{48}$H$_{36}$N$_{12}$S$_2$Ni$_2$Cl	Green	57.78	3.64	16.48
			(57.74)	(3.78)	(16.88)
[Ni$_2$(PhTUPyo-NH$_2$)$_2$(Bpy)$_2$]Cl **(37)**	C$_{44}$H$_{36}$N$_{12}$S$_2$Ni$_2$Cl	Green	55.64	3.82	17.70
			(55.78)	(3.80)	(17.79)
[Ni$_2$(impytH)$_4$].H$_2$O **(36)**	C$_{24}$H$_{16}$N$_{12}$S$_2$Ni$_2$O	Gray	39.16	2.46	22.83
			(39.34)	(2.48)	(22.75)
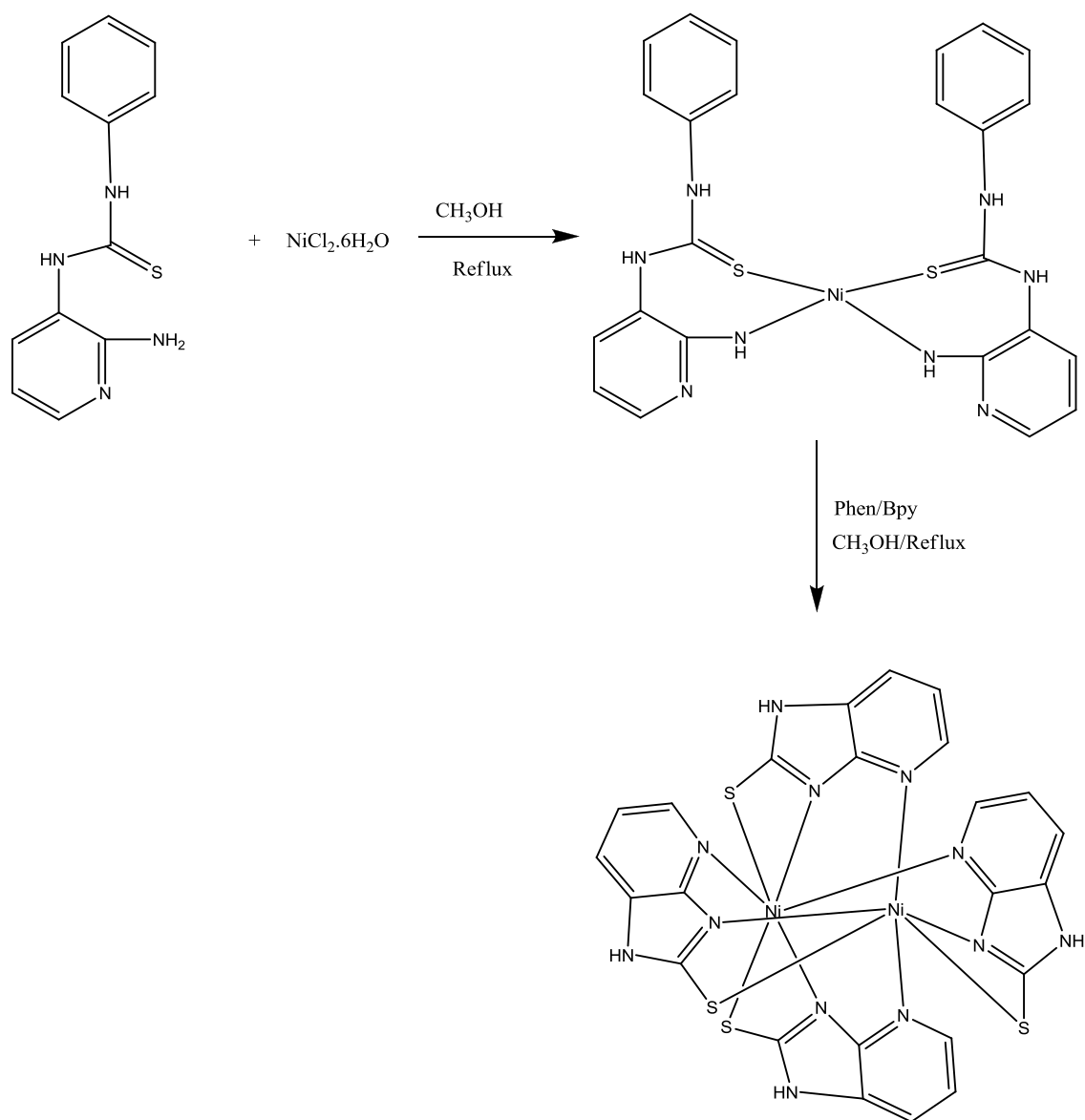
Scheme 4.1: Synthesis of [Ni(PhTUP*yo*-NH$_2$)$_2$] **(34)** and [Ni$_2$(impytH)$_4$] **(36)**
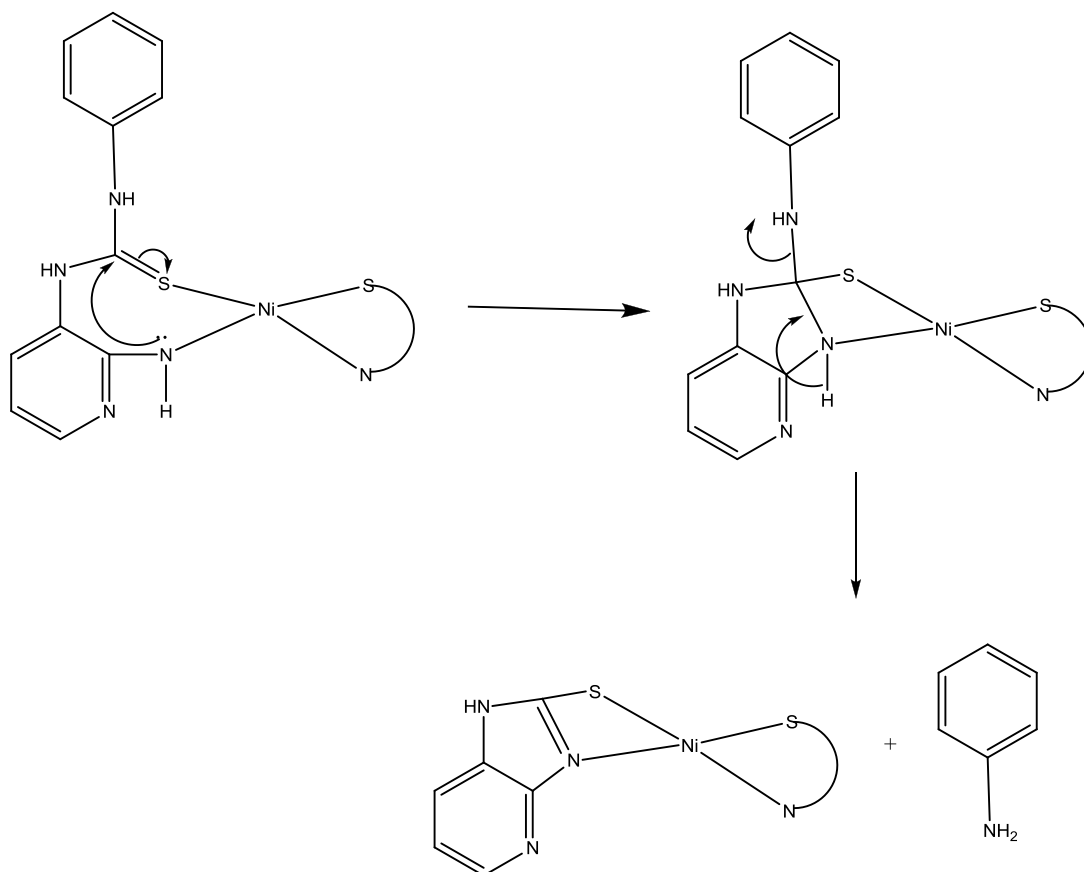
Scheme 4.2: Proposed cyclization mechanism for N-(2-aminopyridin-3-yl)-N'-phenylthiourea in the complex [Ni(PhTUP*yo*-NH$_2$)$_2$] **(34)**

4.3.2 Crystal structure analysis

4.3.2.1 Crystal structure of [Ni$_2$(PhTUPh*o*-NH$_2$)$_2$(Phen)$_2$]NO$_3$.H$_2$O (29)

The crystal structure of compound **29** has been determined and confirms the geometry predicted from spectroscopic studies. Crystallographic data and selected interatomic distances and angles are listed in Tables 4.2 and 4.3, respectively while the molecular structure is shown in Figure 4.3. Compound **29** crystallizes in the triclinic space group *P*1, and the asymmetric unit comprises of a cation involving one NiL unit, one 1,10-phenanthroline as well as one nitrate anion and a water solvate.
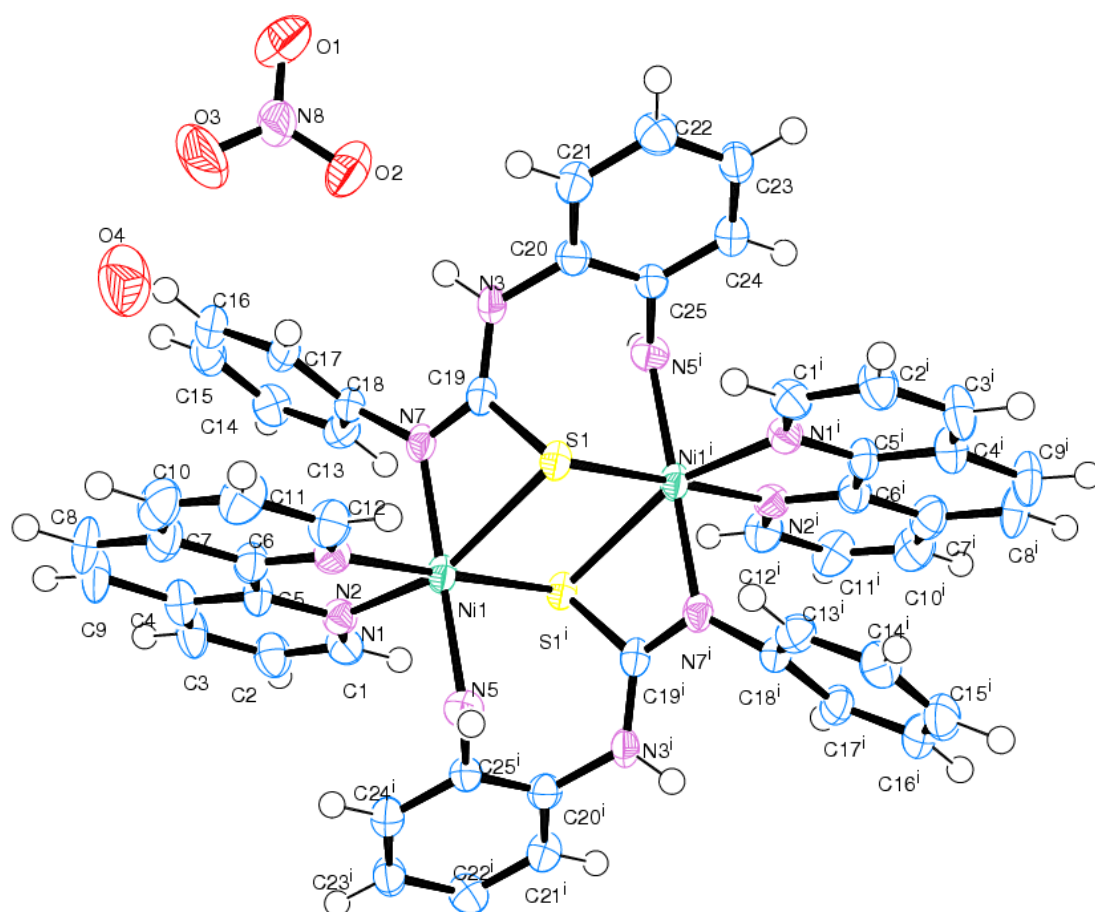
Figure 4.3: An ORTEP view of complex [Ni$_2$(PhTUPh*o*-NH$_2$)$_2$(phen)$_2$]NO$_3$.H$_2$O **(29)**

It can be seen from the crystal structure that the title complex is a binuclear species built by two nickel(II) moieties [Ni$_2$-(μ-S$_2$)] in which each nickel(II) center is bonded to two monoanionic N-(2-aminophenyl)-N'-phenylthiourea through the NNS atoms resulting in four bicyclic chelate systems, and N,N- bidentate chelate of 1,10-phenanthroline. This arrangement gives rise to an octahedral environment in such a way that the dimer is formed by two octahedral and with an intramolecular Ni⋯Ni distance of 3.778 A° which lies in the expected range for a metal–metal bond. This is greater than other structural data obtained for nickel binuclear complexes (Kersting et al., 1999; Latheef et al., 2009) but is lower than other nickel binuclear complexes (Mahendrasinh et al., 2011). Within the cation, a distorted octahedral coordination geometry is found for both Ni(II) and which is defined by two bridged thiolate-sulfur atoms (S1 and S2), two

nitrogen atoms of 1,10-phenanthroline (N1 and N2), and two amino nitrogen atoms (N5 and N7) of two thiourea ligands. The apical positions are taken up by the N5 and N7, while the basal positions are occupied by the remaining N1, N2, S1 and S2 donor atoms. The bond lengths and angles within the 1,10-phenanthroline ligand are similar to those found in other 1,10-phenanthroline complexes. The coordinative pyridyl nitrogens (N1 and N2) bond lengths [Nil–Nl, 2.054(3) and Nil-N2, 2.083(3)] are similar to other complexes with octahedral 1,10-phenanthroline coordination (Tabatabaee et al., 2011; Tian et al., 1997). The Nphen–Ni–Nphen angles of 80.76(13)° is similar to those reported for other bidentate complexes of 1,10-phenanthroline (Baggio et al., 2000).

)The *trans* angles N5–Ni1–N7, 173.39(13)°; and N2–Ni1–S1, 178.33(9)°; are close to linearity while N1–Ni1–S2, 159.06(10)° deviate considerably from linearity. Further distortion is provided by the deviation of the bite angle N7–Ni1–S1, 66.28(9)° from the classic 90° angle. The Ni–S bond lengths; Nil–S1, 2.4510(12); and Nil–S2, 2.5885(l2) are in agreement with those found in the thiolate bridging complexes (Demoro et al., 2012; Henderson et al., 2002). The Nil–N7 bond length of 2.042(3) A° is shorter than Nil–N5 of 2.136(3) A° which indicates that the nitrogen atom N7 of the thiourea moiety coordinates more strongly to the Ni center than the amino nitrogen N5. The N7–C19 bond distance of 1.290(5) ° is shorter than N3–C19 of 1.361(5) and almost equal to the N–C double bond length (Dan et al., 2012; Hemamalini et al., 2005). The formation of thiolate sulfur is supported by the decrease in the bond length of N7–C19, 1.361(5) A° and the lengthening in the C19–S1 bond as reported for other thiolate bond (Takjoo et al., 2011) . The deviations from the least-square plane through the S1, N1, N2,N5, N7 and S1a atoms comprising the octahedron are -0.9933(11), 1.278(4), -0.569(4), -1.518(4), 1.201(4) and 0.6429 Å, respectively, and the Ni1 atom is deviated by -0.0415(6) Å in the direction of the S1a atom.

Table 4.2: Crystal data and structure refinement parameters for complexes **29** and **36a**

Parameters	[Ni$_2$(PhTUPho-NH$_2$)$_2$(Phen)$_2$]NO$_3$.H$_2$O (29)	[Ni$_2$(impytH)$_4$] (36a)
Empirical Formula	C$_{50}$H$_{38}$N$_{12}$Ni$_2$O$_7$S$_2$	C$_{108}$ H$_{84.25}$ N$_{52}$ Ni$_8$ O$_8$ S$_{16}$
Formula weight, M	1100.46	3221.16
Temperature, T (K)	100	100
Wavelength, Mo Kα (Å)	λ = 0.71073	λ = 0.71073
Crystal system	Triclinic	Monoclinic
Space group	P1	$C2/c$
Unit cell dimensions		
a(Å)	9.123(3)	32.361(2)
b(Å)	9.853(3)	20.9130(14)
c (Å)	15.049(4)	21.5926(15)
α(°)	100.483(4)	90.00
β(°)	93.100(4)	121.8730(10)
γ(°)	114.307(4)	90.00
Volume V (Å^3)	1199.6(6)	12409.8(15)
Z	1	4
Absorption coefficient, μ(mm^{-1})	0.939	-
Crystal size (mm)	0.16× 0.13 × 0.10	0.4 × 0.3 × 0.4
Reflections collected	7156	15420
Density (calculated), (mg m^{-3})	1.523	1.536
F(0 0 0)	566	6561
Data/ parameters /restraints	7156 /335 /0	15420/907/0
S	1.012	1.023
Independent reflections	7156	15420
	[R(int) = 0.0836]	[R(int) =0.0979]
R[F^2 > 2σ(F^2)]	0.1151	0.0522
wR(F^2)	0.1739	0.1151
Largest difference peak and hole (e Å^{-3})	-	4.891and0.014

Table 4.3: Selected bond lengths (Å) and angles (°) for complex **29**

Bond lengths		Bond angles	
Ni1–N7	2.042(3)	N7–Ni1–N1	92.78(13)
Ni1–N1	2.054(3)	N7–Ni1–N2	85.29(13)
Ni1–N2	2.083(3)	N1–Ni1–N2	80.76(13)
Ni1–N5	2.136(3)	N7–Ni1–N5	173.39(13)
Ni1–S1	2.4510(12)	N1–Ni1–N5	91.41(13)
Ni1–S1	2.5885(12)	N2–Ni1–N5	90.34(13
S1–C19	1.766(4)	N7– Ni1–S1	93.23(9)
C19–N7	1.290(5)	N1–Ni1–S1	98.57(10)
C19–N3	1.361(5)	N2–Ni1–S1	178.33(9)
C18–N7	1.434(5)	N5–Ni1–S1a	91.20(9)
C25–N5	1.436(5)	N7–Ni1–S1	66.28(9)
C20–N3	1.420(5)	N1–Ni1–S1	159.06(10)
C1–N1	1.334(5)	N2–Ni1–S1	97.15(9)
C12–N2	1.327(5)	N5–Ni1–S1	109.47(9)
N2–C6	1.367(5)	S1–Ni1–S1	82.93(4)
N1–C5	1.362(5)	C19 –S1–Ni1	98.17(13)
O1–N8	1.251(5)	C19–S1–Ni1	73.94(13
O2–N8	1.235(5)	Ni1–S1–Ni1	97.07(4)
O3–N8	1.214(5)	C12–N2–Ni1	130.1(3)
		C6–N2–Ni1	110.9(3)
		C25–N5–Ni1	113.5(2)

The unit cell packing diagram of complex **29** viewed along the *b* axis is given in Figure 4.4. It can be seen that four molecules are present in which each two are parallel to each other. In the unit cell π–π, C–H$\cdots\pi$ and hydrogen bonding interactions were observed. The diverse π–π stacking are of ring Cg(9) with Cg(8) [D(Cg-Cg) = 3.772 Å; Cg(9) = C13, C14, C15, C16, C17, C18; Cg(8) = C4, C5, C6, C7, C8, C9] , ring Cg(9) with Cg(6) [D(Cg-Cg) = 3.779 Å; Cg(6) = N1, C1, C2, C3, C4, C6 and ring Cg(9) with metal chelate ring Cg(1) [D(Cg-Cg) = 3.938 Å; Cg(1) = Ni1, N7, C19, S1]. In addition to this,

two C–H⋯π interactions are shown in the unit cell and that are C13–H13 of the phenyl ring in thiourea moiety with phenanthroline ring Cg(6) [Cg(6) = N1, C1, C2, C3, C4, C6; dH---Cg = 3.28 Å] and C1a–H1a of the phenanthroline with Cg(10) [Cg(10) = C20, C21, C22, C23, C24, C25; dH---Cg = 3.21 Å] which also contribute stability to the unit cell packing. Furthermore, two intramolecular hydrogen bonding interactions are observed i.e., N3(H) with O2 of the nitrate counterion and with N7 as shown in Figure 4.5. Intermolecular hydrogen bonding interactions were also observed *i.e.*, N5(H) with O1 and C3(H) with O4 and C16(H) with O4 and C21(H) with O4as illustrated in Table 4.4.
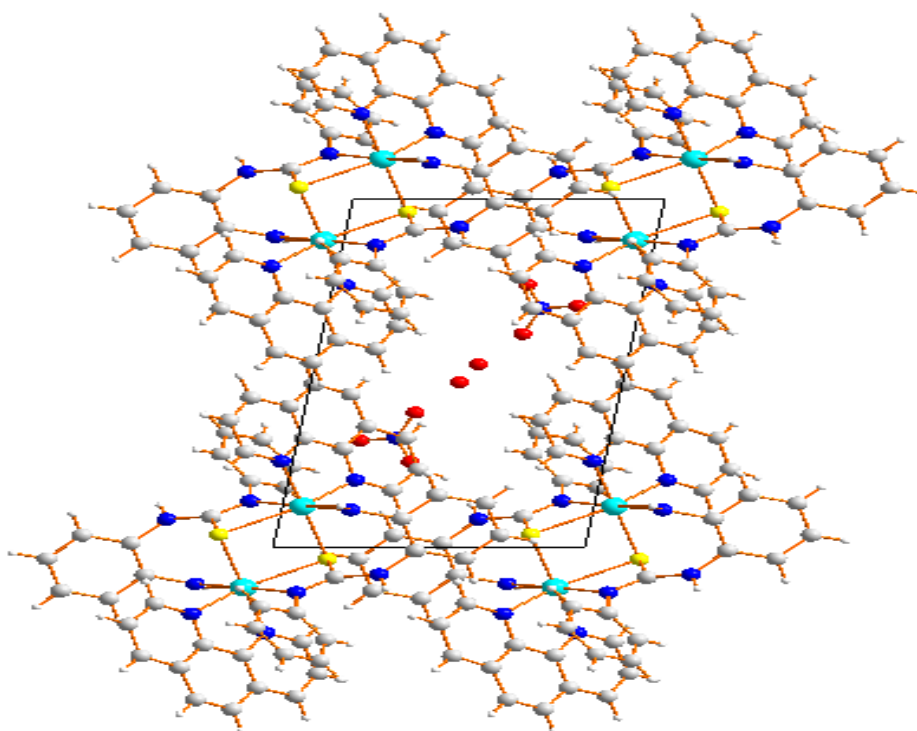

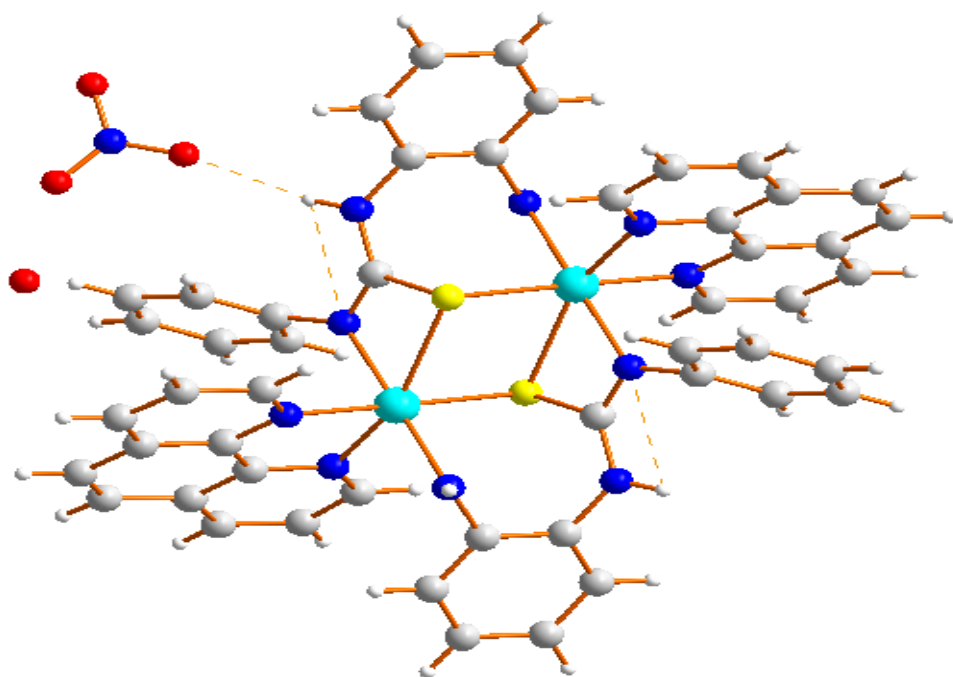**Figure 4.4:** Unit cell packing of complex **29** along *b* axis

Figure 4.5: Hydrogen bonding interactions of complex **29**

Table 4.4: Interaction parameters of the complex **29**

π–π interactions		
Cg(I)···Cg(J)	Cg–Cg (Å)	α °
Cg(9)···Cg(8)	3.772	21.8
Cg(9)···Cg(6)	3.779	14.9
Cg(9)···Cg(1)	3.938	16.2

Cg(9) = C13, C14, C15, C16, C17, C18; Cg(8) = C4, C5, C6, C7, C8, C9; Cg(6) = N1, C1, C2, C3, C4, C6; Cg(1) = Ni1, N7, C19, S1

C–H···π interactions			
X–H···Cg(J)	H···Cg (Å)	X–H···Cg (°)	X···Cg (Å)
C13–H13···Cg(6)	3.28	83	3.292(5)
C1a–H1a ···Cg(10)	3.21	107	3.602(5)

Cg(6) = N1, C1, C2, C3, C4, C6; Cg(10) = C20, C21, C22, C23, C24, C25

H bonding				
Donor-H….Acceptor	D–H	H….A	D….A	D–H…A
N3–H3A…..O(2)[a]	0.88	2.47	3.055(5)	125
N3–H3A…..N(7)[a]	0.88	2.56	2.361(5)	67
N5–H5A…..O(1)[a]	0.88	2.81	3.040(5)	96
C3–H3B…..O(4)[a]	0.95	2.29	3.228(10)	168
C16–H16A…..O(4)[b]	0.95	2.52	3.405(9)	155
C21–H21A…..O(2)[b]	0.95	2.52	3.276(5)	136

D=donor, A= Acceptor, Equivalent position code: a= -1+x, y, z; b= 1-x, 1-y, 1-z
Cg=Centroid, α=dihedral angles between planes I & J, β= angle between Cg-Cg and Cg(J) perp.

4.3.2.2 Crystal structure of $Ni_2(impytH)_4.2H_2O.3DMF$ (36a)

Spectroscopic and microanalysis data showed that complex **36a** is a nickel complex with 1H-imidazo[4,5-b]pyridine-2-thiol not with N-(2-aminopyridin-3-yl)-N'-phenylthiourea. This evidence was corroborated by the crystal structure obtained for this complex. Table 4.2 list relevant crystallographic data and the details of data collection and refinement while selected bond lengths and angles for compound **36a** are given in Table 4.5. $[Ni_2(impytH)_4]$ (**36a**) crystallizes in the monoclinic space group C2/c with two molecules and three molecules of DMF solvate as well as two water molecules in the asymmetric unit. The molecular structure of $[Ni_2(impytH)_4]$ is shown in Figure 4.6 with the solvated molecules omitted. $[Ni_2(impytH)_4]$ structure is a dinuclear complex containing N–C–N bridges with an intramolecular Ni···Ni distance at 3.713A°. One nickel ion is coincident with a crystallographic center of inversion and the complex has an octahedral geometry. The molecule contains two similar types of Ni(II) atoms with four bridging N–C–N fragments, and each nickel ion has a N_4S_2 coordination environment consisting of two thiolate sulfurs, two imidazole nitrogens and two pyridyl nitrogens. In each ligand, the sulfur and imidazole nitrogen are coordinated to one nickel ion while the pyridyl nitrogen is coordinated to the other one.

The coordination of sulfur from the imidazopyridinethiol ligand occurs through deprotonation after enolization, confirmed by the partial single and double bond nature of C1–S1 [1.705(4)Å] and N1–C1 [1.333(5)Å] bond lengths (Lo'pez-Torres et al., 2004). In the case of this nickel complex, Ni–S bond distances are Ni1–S1, 2.5660(11) Å; Ni1–S2, 2.5377(11) Å; Ni2–S3, 2.5383(11) Å; Ni2–S4, 2.5553(11) Å and agree well with values observed for Ni–S bonds in octahedral complexes (Vetter et al., 2006).
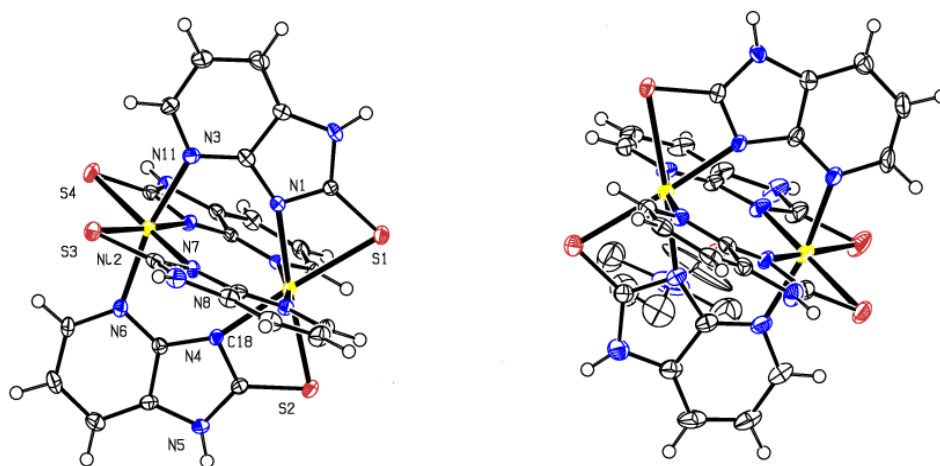
Figure 4.6: Crystal structure of complex **36a**

The Ni1–N bond distances are Ni1–N1, 2.097(3) Å; Ni1–N4, 2.120(3) Å; Ni1–N9, 2.074(3) Å and Ni1–N12, 2.073(3) Å whereas the Ni2–N bond distance are Ni2–N3, 2.069(3) Å; Ni2–N10, 2.102(3)Å; Ni2–N6, 2.075(3) Å and Ni2–N7, 2.104(3)Å. The Ni–N(imidazole) bond lengths are slightly larger than the Ni–N(pyridyl) bond distances, which indicate the higher strength of the Ni-N(pyridyl) bond. The Ni–N(pyridyl) bond lengths are close to those in other structurally characterized complexes containing Ni-N(pyridyl) bonds (Deoghoria et al., 2002; Panja & Eichhorn, 2012; Sharma et al., 2011). The *trans* angles, N12–Ni–N9 of 168.84(13)° and N1–Ni1–N4 of 116.27(12)° indicate that complex **36a** has large distortion from octahedral geometry (Manoj & Kurup, 2008). Other indications of distorted octahedral geometry are the bond angles of N4–Ni1–S2, 67.68(8)°; N9–Ni1–N1, 85.20(12)°; N12–Ni1–N1, 88.63(12). The Ni2N3C3N1Ni1 and Ni2N7C15N9Ni1 fragments are planar with nickel atoms deviate from the least square plane comprising Ni2,N3,C3,N1,Ni1 (plane 1) by 0.012(5) Aº (both Ni1 and Ni2), whereas the deviation from the least square plane comprising Ni2,N7,C15,N9,Ni1 (plane 2) is 0.0142(5) Aº for Ni1 and 0.0285(5) Aº for Ni2. The plane containing Ni1, N12, C21, N10, Ni2 (plane 3) is deviated from the

central metal atoms Ni1 by 0.0230(5) Å and Ni2 by 0.0296(5) Å. However, Ni1 and Ni2 do not deviate significantly from the least square plane comprising Ni1, N4, C9, N6, Ni2 (plane 4) [0.0094(5) Å for Ni1 and 0.0070(5) Å for Ni2]. The dihedral angle formed by the planes 1 and 2 is 87.78 (4)º and by the planes 3 and 4 is 89.09 (9)º, consistent with a nearly 90º octahedral angle.

The unit cell packing diagram of the complex **36a** viewed along the *c* axis is given in Figure 4.7. The diverse π–π stacking and C–H$\cdots\pi$ interactions give rise to polymeric chains in the unit cell (Figure 4.8). The shortest π–π interactions (Table 4.6) are observed at 3.801 Å for Cg(9) $\cdots$ Cg(4) [Cg(9) = N3, C4, C5, C6, C2, C3; Cg(4) = Ni2, S4, C19, N10]. The C–H$\cdots\pi$ interactions present in the unit cell are C(18)–H(18)$\cdots$Cg(7) [dH---Cg = 3.22 Å; Cg(7) = N7, C13, N8, C14, C15] and C(24)–H(24)$\cdots$Cg(8) [dH---Cg = 3.21 Å; Cg(8) = N10, C19, N11, C20, C21]. Hydrogen bonding interactions for compound **36a** is shown in Figure 4.9 and hydrogen bonding parameters are shown in Table 4.6. The two water molecules in the unit cell link the adjacent molecules by N8–H8$\cdots$O1$\cdots$S7 and N17–H17 $\cdots$O2$\cdots$S2 hydrogen bonds and leads to 3D dimensional network (Figure 4.10). The stability of the unit cell packing is built by these π-π,   C–H$\cdots\pi$ and hydrogen bonding interactions.

Table 4.5: Selected bond lengths (Å) and angles (°) for complex **36a**

Bond lengths		Bond angles	
Ni1–N12	2.073(3)	N2– Ni1– N9	168.84(13)
Ni1–N9	2.074(3)	N12–Ni1–N1	88.63(12)
Ni1–N1	2.097(3)	N9– Ni1–N1	85.20(12)
Ni1–N4	2.120(3)	N12–Ni1–N4	85.30(12)
Ni2 –N3	2.069(3)	N9–Ni1–N4	89.10(12)
Ni2–N10	2.102(3)	N1–Ni1–N4	116.27(12)
Ni2–N6	2.075(3)	N12–Ni1–S2	90.46(9)
Ni2–N7	2.104(3)	N9–Ni1–S2	96.34(9)
Ni3–N24	2.060(4)	N1–Ni1–S2	175.84(9)
Ni3–N21	2.062(3)	N4– Ni1–S2	67.68(8)
Ni3–N13	2.092(3)	N12–Ni1–S1	93.96(9)
Ni3–N16	2.097(4)	N9–Ni1–S1	92.30(9)
Ni4–N18	2.058(3)	N1–Ni1–S1	67.78(9)
Ni4–N19	2.108(3)	N4–Ni1–S1	175.83(9)
Ni4–N22	2.109(3)	S2–Ni1–S1	108.24(4)
Ni1–S1	2.5660(11)	C2–Ni1–S1	73.79(13)
Ni1–S2	2.5377(11)	N3–Ni2–N6	168.87(13)
Ni2–S3	2.5383(11)	N3–Ni2–N10	86.69(12)
Ni2–S4	2.5553(11)	N6–Ni2–N10	87.84(12)
Ni3–S5	2.5449(13)	N3–Ni2–N7	86.05(12)
Ni3–S6	2.5458(13)	N6–Ni2–N7	87.65(12)
Ni4–S7	2.6005(11)	N10–Ni2–N7	116.01(12)
Ni4–S8	2.5664(12)	N3–Ni2–S3	93.80(10)
S1–C1	1.705(4)	N6–Ni2–S3	92.40(9)
C1–N1	1.333(5)	N10–Ni2–S3	175.62(9)
C1–N2	1.373(5)	N7–Ni2–S3	68.37(9)
C3–N1	1.365(5)	N3–Ni2–S4	91.21(10)
C2 –N2	1.376(5)	N6–Ni2–S4	95.72(9)
C3–N3	1.330(5)	N10–Ni2–S4	68.02(9)
C4–N3	1.348(5)	N7–Ni2–S4	174.92(9)

Table 4.6: Interaction parameters of the complex **36a**

π–π interactions		
Cg(I)···Cg(J)	Cg–Cg (Å)	α °
Cg(4)···Cg(9)	3.801	56.85(4)
Cg(4)···Cg(5)	4.221	1.05(3)
Cg(10)···Cg(7)	4.716	39.51(3)
Cg(10)···Cg(3)	3.866	36.21(3)

Cg(9) = N3, C4, C5, C6, C2, C3; Cg(4) = Ni2, S4, C19, N10; Cg(5) = N1, C3, C2, N2, C1; Cg(7) = N7, C13, N8, C14, C15; Cg(10) = N6, C10, C11, C12, C9

C–H···π interactions			
X–H···Cg(J)	H···Cg (Å)	X–H···Cg (°)	X···Cg (Å)
C18–H18···Cg(7)	3.22	40	2.573(5)
C24–H24 ···Cg(8)	3.21	40	2.564(4)

Cg(7) = N7, C13, N8, C14, C15; Cg(8) = N10, C19, N11, C20, C21

H bonding				
Donor-H….Acceptor	D-H	H….A	D….A	D-H…A
O1–H1C…..S(7)[a]	0.97	2.30	3.228(5)	162
O2–H1D…..O(5)[i]	1.12	2.12	3.236(6)	175
N2–H2A…..S(7)[j]	0.88	2.84	3.566(3)	141
O1–H2E…..S(3)[f]	0.84	2.63	3.437(4)	162
N5–H5B…..O(5)[i]	0.88	2.58	3.093(5)	118
N5–H5B…..O(2)[a]	0.88	2.32	3.147(6)	157
N8–H8A…..O(1)[h]	0.88	1.93	2.790(5)	165
N11–H11B…..S(5)[b]	0.88	2.72	3.436(4)	139
N14–H14A…..S(4)[b]	0.88	2.77	3.446(5)	135

Donor–H….Acceptor	D–H	H….A	D….A	D-H…A
N17-H17B…..O(2)[l]	0.88	1.98	2.831(6)	164
N20–H20A…..O(3)[g]	0.88	2.02	2.747(6)	138
N23–H23B…..N(23)[b]	0.88	2.58	3.079(7)	117
N23–H23B…..O(4)[m]	0.88	2.37	3.101(7)	141
C10–H10A…..S(7)[h]	0.95	2.85	3.760(5)	160
C30–H30A…..S(8)[e]	0.95	2.86	3.739(5)	154
C34–H34A…..S(3)[d]	0.95	2.87	3.819(5)	177
C41–H41A…..O(1)[b]	0.95	2.58	3.526(7)	174
C48–H48A…..S(2)[k]	0.95	2.68	3.530(6)	149
C50–H50A…..O(3)[c]	0.98	2.42	2.835(7)	105

D = donor, A = Acceptor, Equivalent position code: a = 1/2-x, ½ -y, 1 –z; b = - x, y, ½ -z; c = 1/2 -x, 1/2 +y, ½ -z; d = x, 1 –y, 1/2 +z; e = -x, 1 –y, 1-z; f = 1/2 -x, - 1/2 +y, 1/2-z; g = x, -y, 1/2 +z; h = x, 1 –y, - 1/2 +z; i = 1/2 +x, 1/2 +y, z; j = x, y, -1 +z; k = -1/2 +x,1/2 –y, 1/2 +z; l = -x, -y, 1-z; m = -1/2 +x, 1/2 +y, z
Cg = Centroid, α = dihedral angles between planes I & J, β = angle between Cg-Cg and Cg(J) perp.

Table 4.6, continued
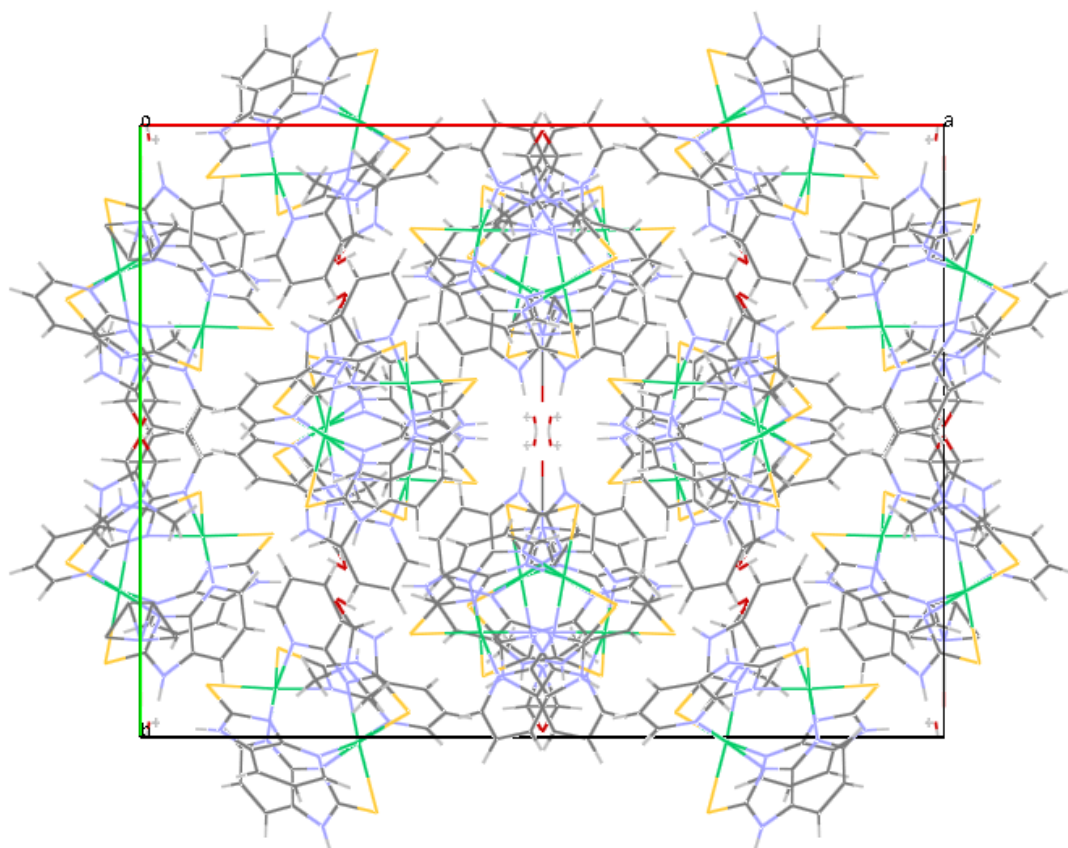
Figure 4.7: Unit cell packing diagram of the complex **36a** viewed along the *c* axis
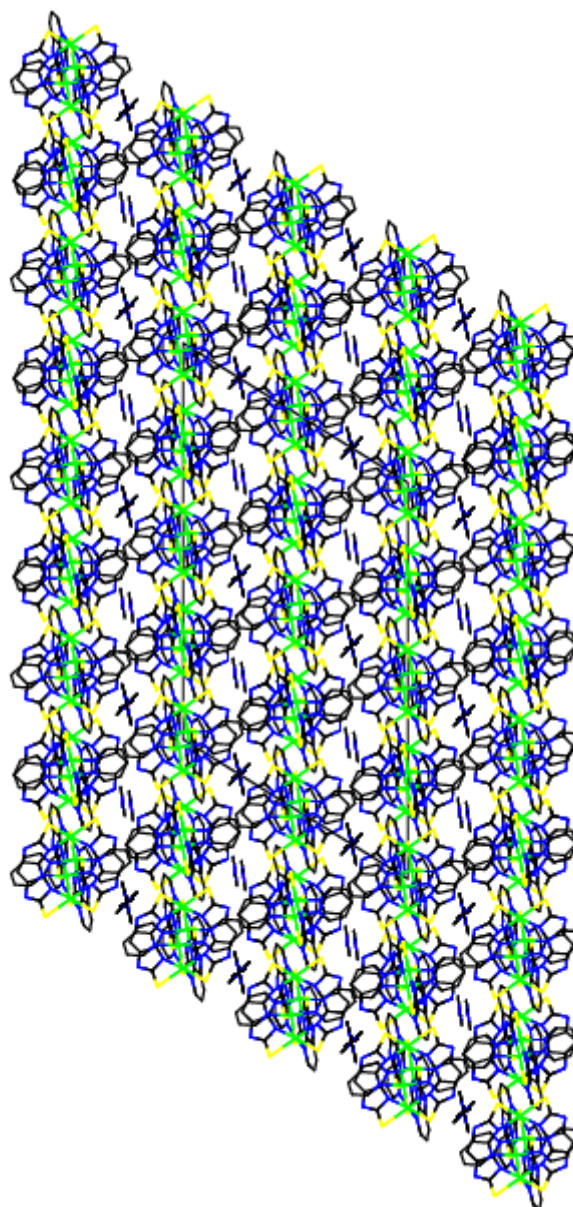
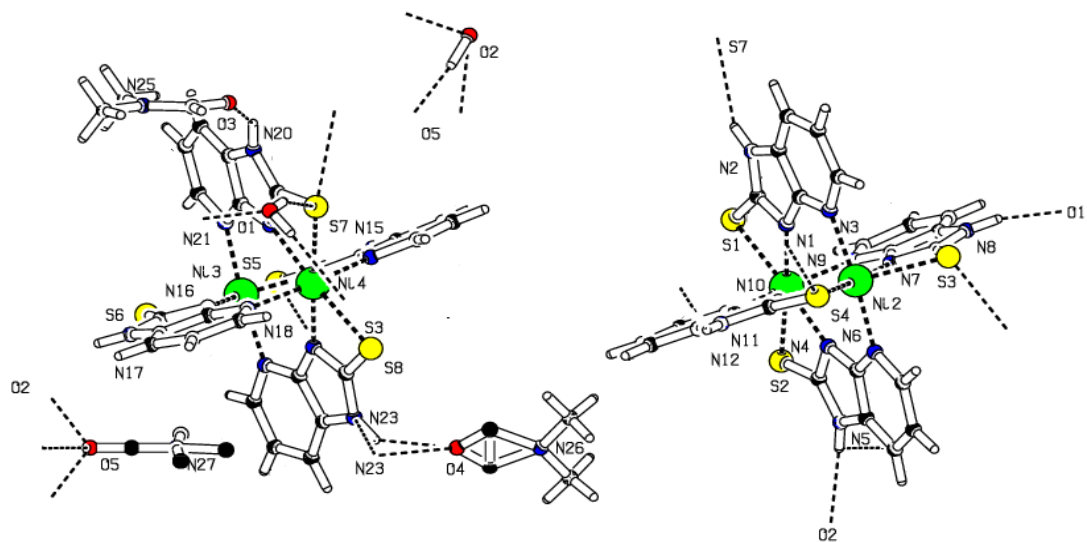**Figure 4.8:** Polymeric chains in the unit cell for complex **36a**

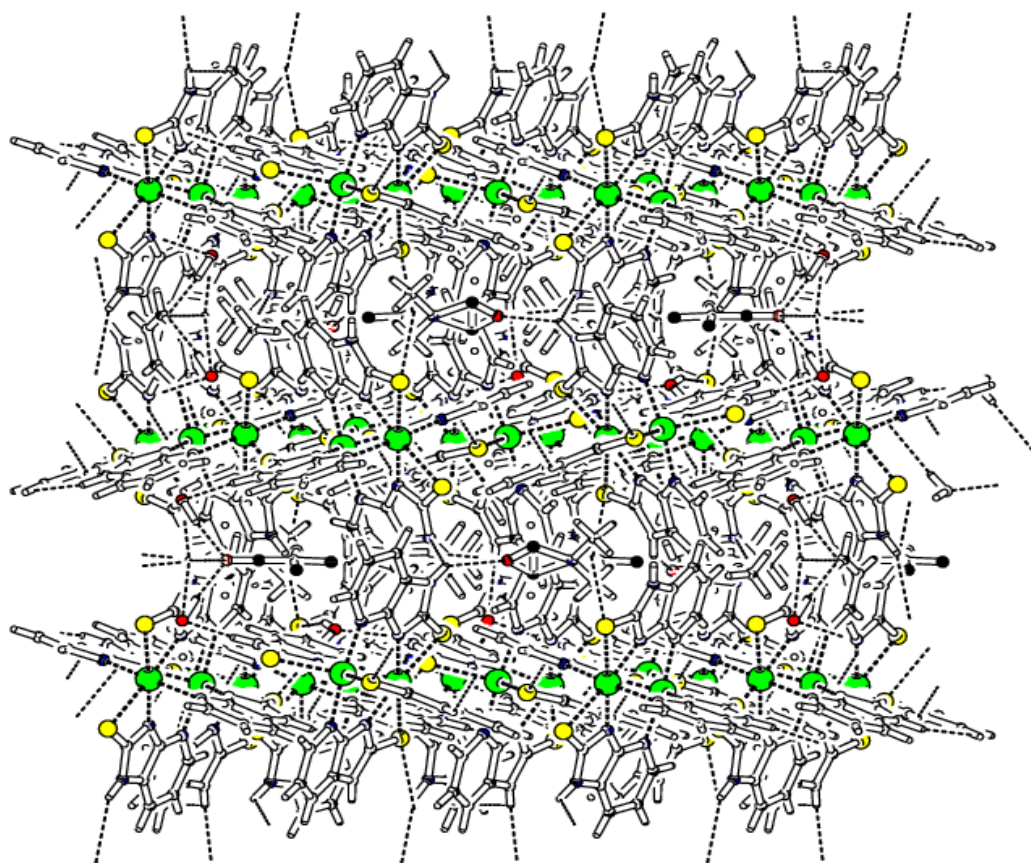**Figure 4.9:** Hydrogen bonding interactions for complex **36a**

Figure 4.10: 3Dimensional network formed from hydrogen bonding interactions for complex **36a**

4.3.3 ^{1}H NMR

The ^{1}H NMR spectra of [Ni[(II)]L$_2$] were recorded in DMSO-d$_6$ and showed the diamagnetic character of the complexes which is compatible with the assumed square-planar geometry in the solid state. The ^{1}H NMR chemical shift data for the diamagnetic nickel(II) thiourea complexes are summarized in Table 4.7. The ^{1}H NMR spectra are allocated according to the numbering scheme given in Figure 4.2. In the ^{1}H NMR spectra of all complexes, there were a collapse in the multiplicity signals of aromatic protons which are connected to the nitrogen atoms (Moloto et al., 2003). In the ^{1}H NMR spectrum of the complex [Ni(PhTUPh*o*-NH$_2$)$_2$] (**28**) (Figure 4.11), three broad NH peaks in the down field region at 9.55, 9.04 ppm and 8.68 ppm were observed. The signals at 9.55 ppm and 9.04 ppm in the complex, which have been assigned to N(1)H and N(2)H respectively, appeared at the same chemical shifts in the free PhTUPh*o*-NH$_2$ ligand (at 9.58 and 9.07 ppm) (Figure 4.12) indicating non-involvement of the NH groups in coordination and the presence of the ligand in its thione form (Koch et al., 1999; Rotondo et al., 2012). However, another N(2)H signal was observed in the spectrum of this complex at 8.68 ppm, which is consistent with the presence of two N(2)H in different conformational isomers (Babashkina et al., 2011; Koch, 2001). Noteworthy, the NH signals were broad in nature which implies the occurrence of hydrogen bonding (R.Koch et al., 1995; Yuan et al., 1997).

Despite the poor resolution of the aromatic protons signals, the integration corresponding to 18 protons clearly showed the establishment of two isomers in the solution (Moloto et al., 2003; Sokolov et al., 2006). Furthermore, only a single resonance for the N(3)H group was observed at 4.82 ppm that appears slightly broadened, was upfield relative to the free ligand (δ 4.92 ppm). The shielding of N(3)H proton is related with the increase of the unshared electron on nitrogen atom upon

deprotonation followed by coordination to nickel(II). However, this negative shift is very common in metal–bound nitrogen atoms (Cornago et al., 2005).

The ^{1}H NMR spectrum of [Ni(PhTUPhp-NH$_2$)$_2$] (**31**) (Figure 4.13), showed an unsymmetrical binding mode which is expected to be through both sulfur and nitrogen atoms. In the ^{1}H NMR spectrum of this complex, the PhTUPhp-NH$_2$ ligand is coordinated to nickel(II) in its thiol form as evidenced by the disappearance of N(1)H signal which was appeared at 9.39 ppm in the free ligand (Figure 4.14) (Binzet et al., 2009 ; Gomes et al., 2011). The peak corresponding to N(2)H at 9.35 ppm in the free ligand has shifted to the high region (at 8.92 ppm) in complex **31** which can be explained by the delocalization of π - electrons as a result of participation of the metal ion in back π-bonding with sulfur atom (Jambi & Kandil, 2012; Kanjan & Dikshit, 2000). Moreover, the appearance of N(2)H as a single signal integrated for two protons indicates that the nickel is coordinated to two unsymmetrical PhTUPhp-NH$_2$ ligands. However, the appearance of only one resonance peak reveals that the two N(2)H protons could be on the same side (*syn*) of the molecule. This is further confirmed by the split in N(3)H$_2$ peak located at 5.05 ppm in the free ligand to two signals at 5.00 and 4.95 ppm in the complex. The integration of 18 aromatic protons in this complex showed that the two ligands coordinated to nickel are chemically nonequivalent (Ahmad et al., 2002).

In the ^{1}H NMR spectrum of the complex [Ni(PhTUPyo-NH$_2$)$_2$] (**34**) (Figure 4.15), the presence of N(1)H and N(2)H signals at 9.73 and 9.01 ppm in the same chemical shifts as in the free ligands (9.76 ppm and 9.02 ppm) (Figure 4.16) clearly indicate the non involvement of nitrogen atoms of thiourea moiety in coordination with Ni(II). Consequently, the appearance of the N(1)H and N(2)H signals shows that the thiourea

ligand PhTUPyo-NH$_2$ is coordinated to nickel(II) in the thione form. The broadness of the N(2)H peak suggests that the N(2)H proton is engaged in a hydrogen bonding interaction with the pyridyl nitrogen atom (Lenthall et al., 2007). Furthermore, the singlet at 5.72 ppm which is attributed to N(3)H signal in the free ligand PhTUPym-NH$_2$, has splitted and shifted to the higher field (at 5.65 and 4.84 ppm) upon coordination. The upfield shifting of the N(3)H signal when compared to that of the free ligand could be associated to a substantial increase in the electron density around the nitrogen atom, suggesting the Ni–N(3) bond formation. However, the split in this signal is an evidence that the nickel(II) is coordinated to two N(3) atoms in which the N(3)H protons are chemically inequivalent due to the rigid thiourea ligand and give rise to two absorptions (Bierbach et al., 1998).

The proportion of protons observed by integration exactly matches with the proposed stoichiometry of the complexes. Therefore, the data mentioned above show that each of PhTUPho-NH$_2$ and PhTUPyo-NH$_2$ ligands are coordinated in a bidentate manner via the thioamidic sulfur and N(3) nitrogen atoms while the PhTUPhp-NH$_2$ ligand is coordinated to through thioamidic sulfur and N(1) nitrogen atoms. It can be concluded that the coordination of the thiourea diamine derivatives to nickel(II) is influenced by the position of the amino group on the aromatic ring due to the effect of the amino group in different positions on inter and intra hydrogen bonding interactions of N(1)H and N(2)H of thiourea moiety (Babashkina et al., 2009 ; Tadjarodi et al., 2007).

Table 4.7: ^{1}H NMR assignments of thiourea diamine derivatives and their nickel(II) complexes

Compound	Chemical Shifts, δ(p.p.m)			
	N(1)H	N(2)H	NH₂	Aromatic due to TU
PhTUPh*o*-NH₂ (**25**)	9.58	9.07	4.92	7.53 (d,2H)
	(s, 1H)	(s, 1H)	(s, 2H)	7.32 (t, 2H)
				7.11 (t, 2H)
				6.98 (t, 1H)
				6.77 (d,1H)
				6.58 (t, 1H)
[Ni(PhTUPh*o*-NH₂)₂] (**28**)	9.55	9.04	4.82	7.70 – 6.41
	(s, 1H)	(s, 1H)	(s, 2H)	(m, 18H)
		8.68		
		(s, 1H)		
PhTUPh*p*-NH₂ (**26**)	9.39	9.35	5.05	7.46 (d, 2H)
	(s, 1H)	(s, 1H)	(s, 2H)	7.30 (t, 2H)
				7.09 (t, 1H)
				7.01 (d, 2H)
				6.53 (d, 2H)
[Ni(PhTUPh*p*-NH₂)₂] (**31**)	-	8.92	5.00 (s, 2H)	7.41 – 6.31
		(s, 2H)	4.98 (s, 2H)	(m, 18H)
PhTUPy*o*-NH₂ (**27**)	9.76	9.02	5.70	7.82 (d, 1H)
	(s,1H)	(s,1H)	(s, 2H)	7.50 (d, 2H)
				7.39 (d, 1H)
				7.30 (t, 2H)
				7.09 (t, 1H)
				6.55 (t, 1H)
[Ni(PhTUPy*o*-NH₂)₂] (**34**)	9.73	9.01	5.65	7.84 – 6.40
	(s, 1H)	(s,1H)	(s, 1H)	(m, 8H)
			4.84	
			(s,1H)	
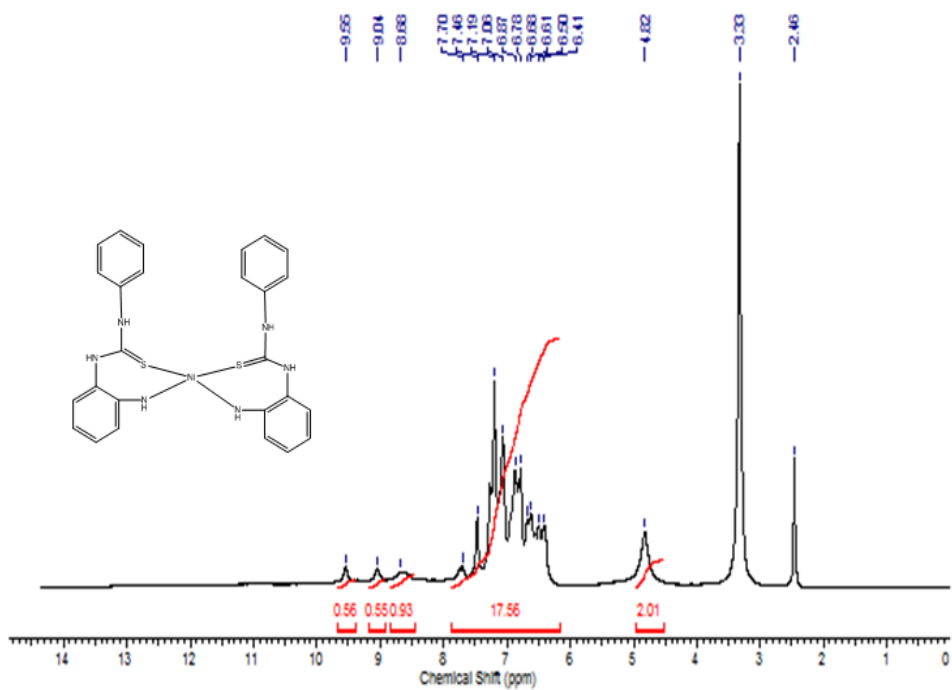
Figure 4.11: ^{1}H NMR spectrum of [Ni(PhTUPh*o*-NH₂)₂] **(28)**
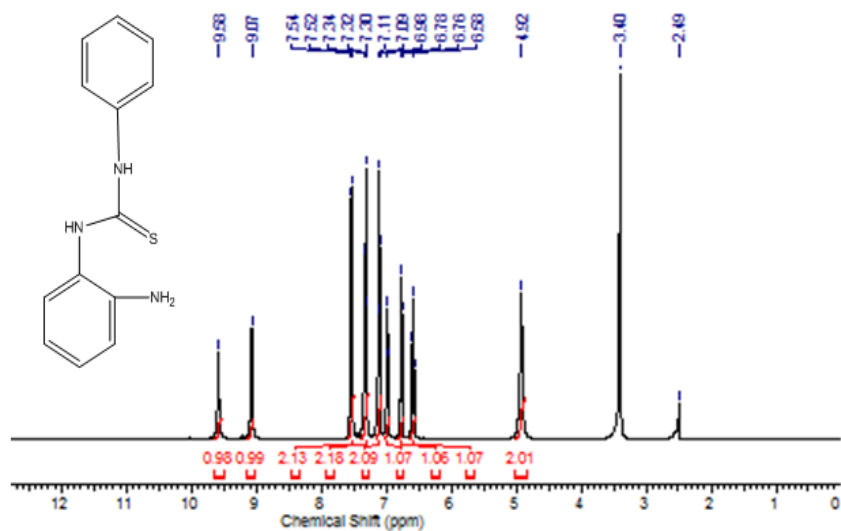
Figure 4.12: ^{1}H NMR spectrum of PhTUPh*o*-NH₂ **(25)**
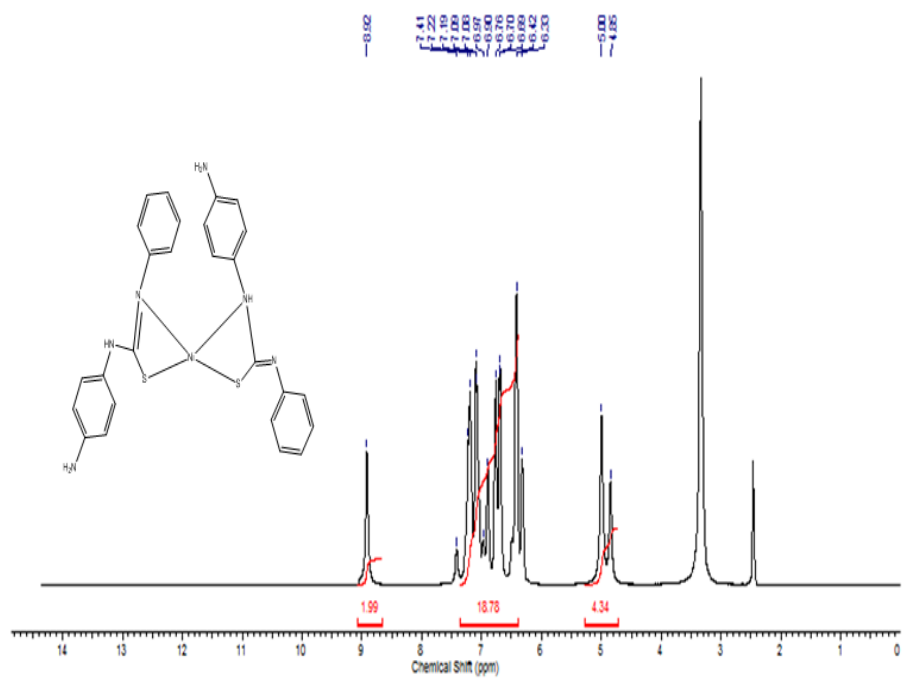
Figure 4.13: ^{1}H NMR spectrum of [Ni(PhTUPh*p*-NH$_2$)$_2$] **(31)**
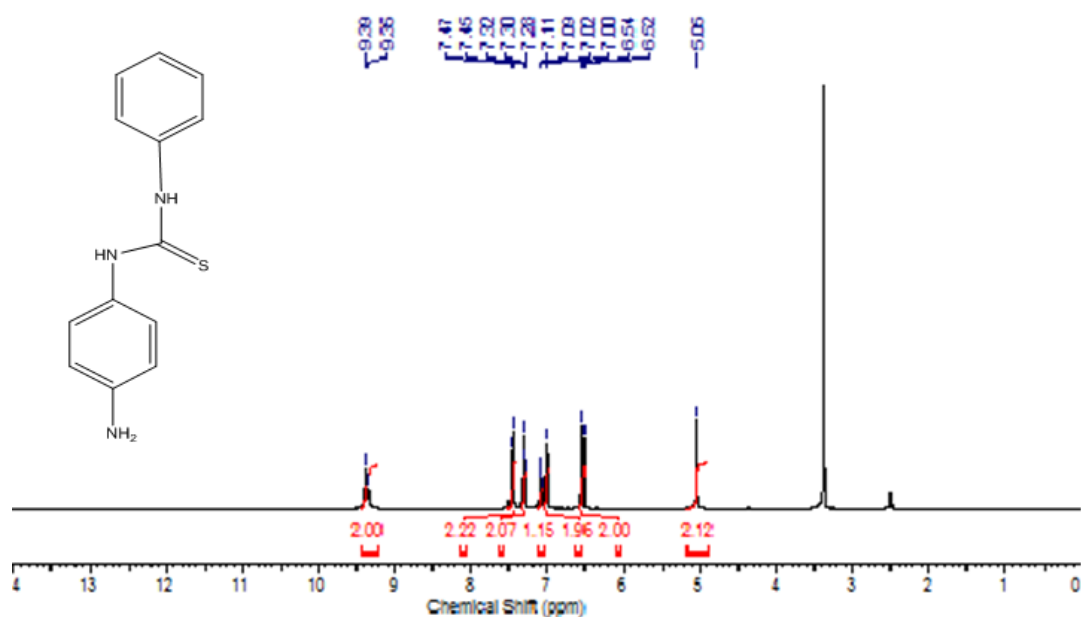
Figure 4.14: ^{1}H NMR spectrum of PhTUPh*p*-NH$_2$ **(26)**
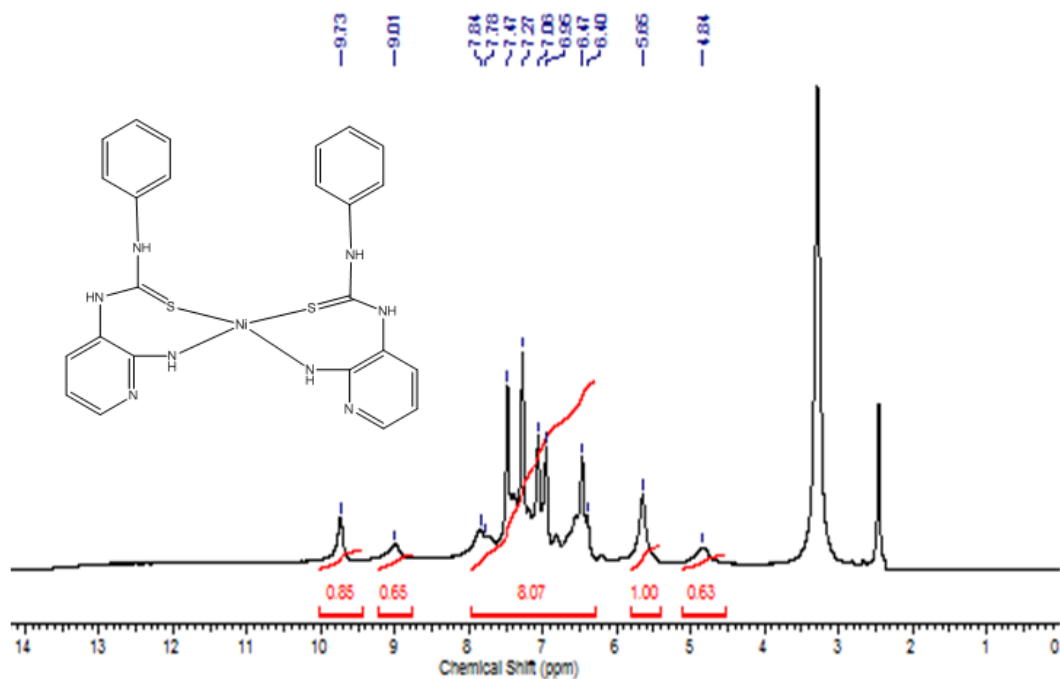
Figure 4.15: ^{1}H NMR spectrum of [Ni(PhTUPyo-NH$_2$)$_2$] **(34)**
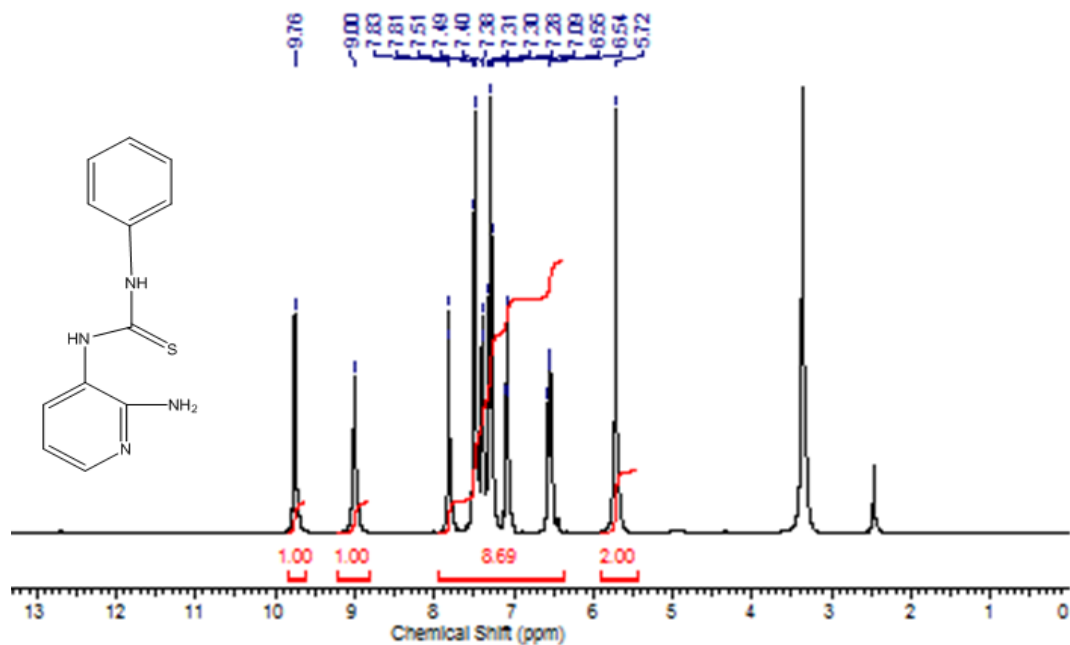
Figure 4.16: ^{1}H NMR spectrum of PhTUPyo-NH$_2$ **(28)**

4.3.4 ^{13}C NMR spectra

The ^{13}C NMR spectra of thiourea derivatives of diamines and the corresponding nickel(II) complexes recorded in DMSO showed all the expected signals. The ^{13}C assignments of the thiourea free ligands and their nickel complexes are summarized in Table 4.8. The spectrum of the complex [Ni(PhTUPh*p*-NH$_2$)$_2$] **(31)**, (Figure 4.17), displayed two C=S resonance at 173.85 and 171.09 ppm, respectively, suggesting that both PhTUPh*p*-NH$_2$ ligands which present in the coordination sphere with nickel(II) ion are not chemically equivalent. However, the substantial upshift in the carbon resonances of C=S bond when coordinated to nickel(II) is related to the lowering of the C=S bond order upon coordination and a shift of N–C electron density producing partial double bond character in the C–N bond and in accordance with the data observed for other metal complexes of thioureas (Kandil et al., 2007; Nadeem et al., 2009). It should be noted that [Ni(PhTUPh*p*-NH$_2$)$_2$] **(31)** gave two signals for both C=S and aromatic carbons showing that the two ligands coordinated to nickel(II) are nonequivalent. Small shielding as well as deshielding effects were observed in these aromatic carbon atoms, which may be related to the strength of metal-sulfur bond.

In the ^{13}C NMR spectrum of the complex [Ni(PhTUPy*o*-NH$_2$)$_2$] **(34)** (Figure 4.19), notable are the relatively large displacements observed for the ^{13}C shifts of the thiocarbonyl C=S, on going from unbound ligand (180.97 ppm) (Figure 4.20) to the nickel complex (207.15 ppm). Thus, the C(S) carbon resonance underwent relatively large average downfield displacement of 26.18 ppm. The large shift in this complex is consistent with extensive delocalization of the electron density within the chelate ring (Mautjana et al., 2003). Furthermore, an upfield shift in the aromatic carbons resonance was observed.

Because of the low solubility of [Ni(PhTUPh*o*-NH$_2$)$_2$] **(28)**, no dynamic ^{13}C NMR study has been carried out.

Table 4.8: ^{13}C NMR spectral assignments for the thiourea ligands and their nickel(II) complexes in DMSO-d$_6$

Carbons	Compound/ Chemical Shifts, (δ ppm)	
	PhTUPh*p*-NH$_2$ (26)	**[Ni(PhTUPh*p*-NH$_2$)$_2$] (31)**
C7	180.25	173.85, 171.09
C11	147.06	147.37, 143.84
C8	140.21	140.26, 137.42
C1	128.82	129.29, 128.86
C10	127.93	128.80, 127.28
C9	126.75	127.16, 124.81
C2,6	124.74	124.69, 124.33
C3,5	124.34	124.21, 124.17
C4	114.24	114.60, 114.03
	PhTUPy*o*-NH$_2$ (27)	**[Ni(PhTUPy*o*-NH$_2$)$_2$] (34)**
C7	180.97	207.15
C9	156.23	140.02
C12	146.16	129.35
C8	140.01	129.06
C10	136.31	129.03
C11	128.96	125.02
C1	124.95	124.23
C2,6	124.11	124.14
C3,5	120.04	116.31
C4	112.90	112.54
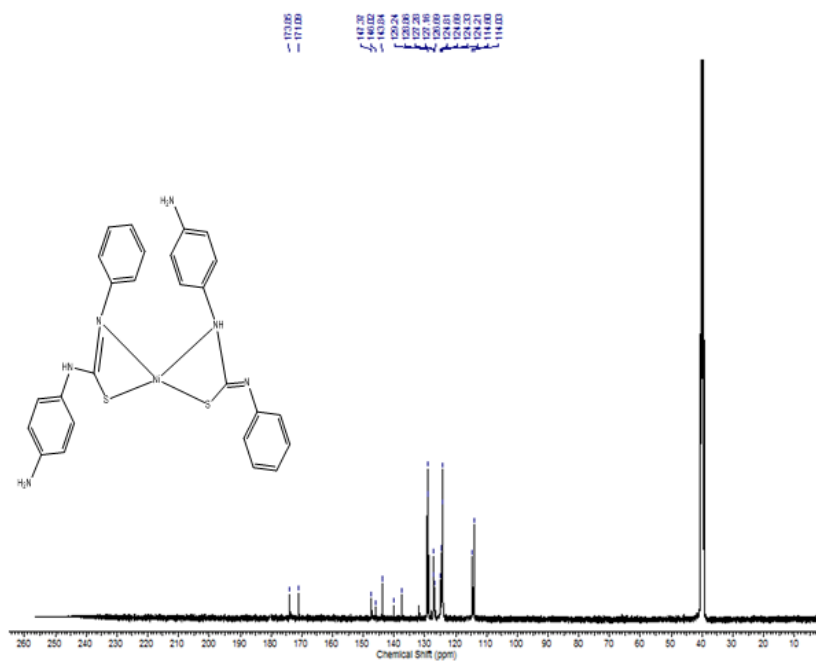
Figure 4.17: ^{13}C NMR spectrum of [Ni(PhTUPh*p*-NH$_2$)$_2$] (**31**)
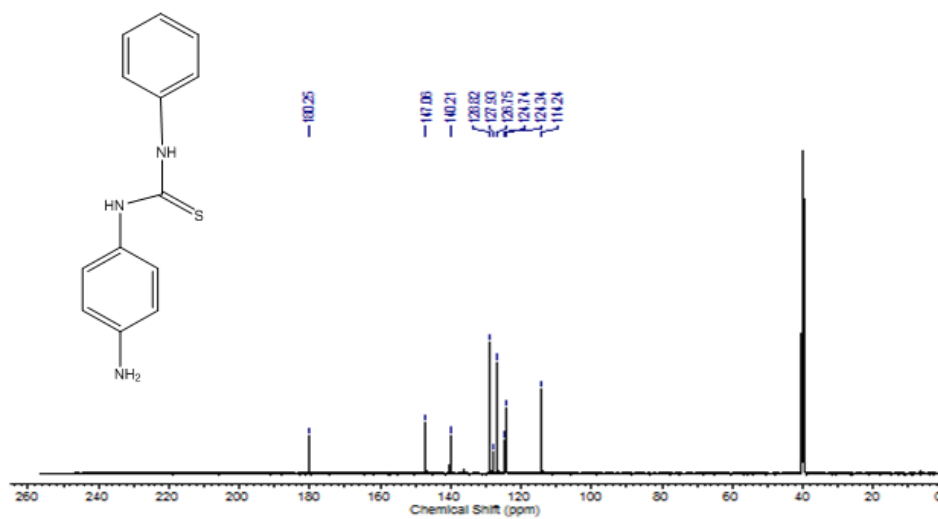
Figure 4.18: ^{13}C NMR spectrum of PhTUPh*p*-NH$_2$ (**26**)
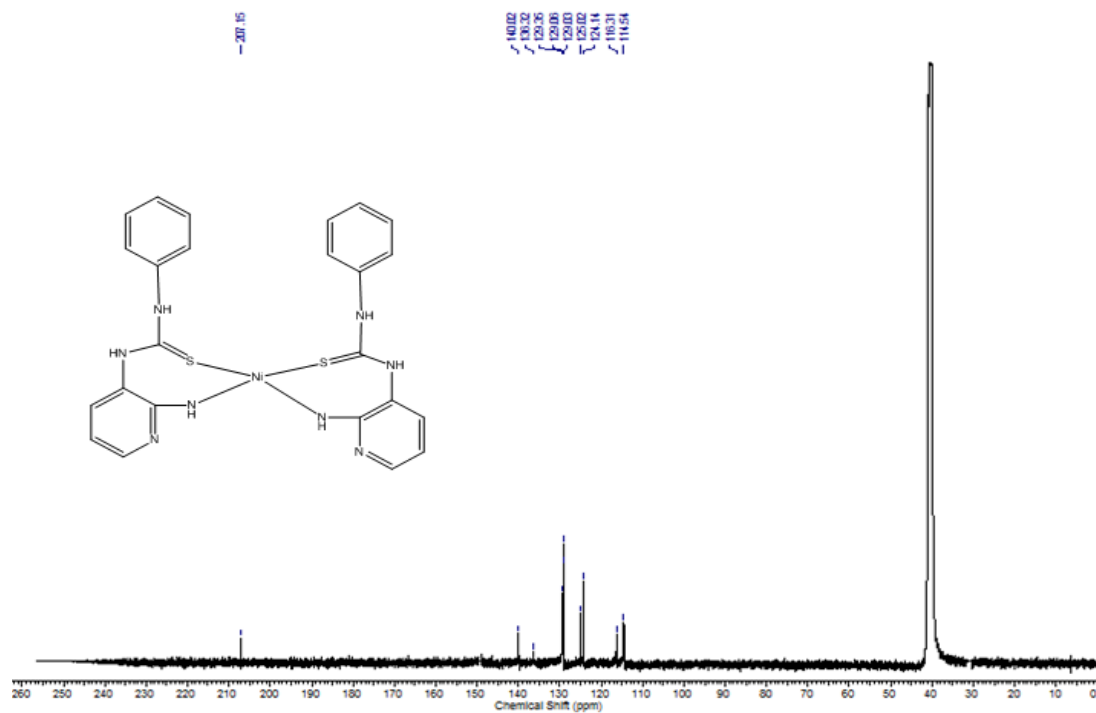
Figure 4.19: ^{13}C NMR spectrum of [Ni(PhTUPy*o*-NH$_2$)$_2$] **(34)**
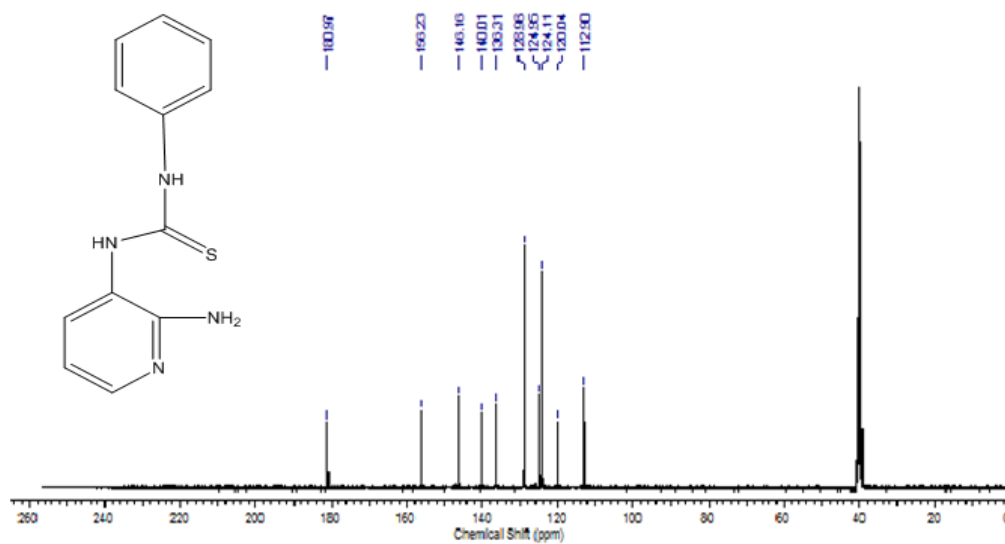

Figure 4.20: ^{13}C NMR spectrum of PhTUPy*o*-NH$_2$ **(27)**

4.3.5 Infrared spectra

Table 4.9 represents the most useful IR assignments bands of the free ligands and their nickel complexes for the establishment of the coordination mode of thiourea ligands in their nickel(II) coordination complexes. The IR spectra of complexes **26**, **28**, **29, 27**, **34** and **36** are shown in Figures 4.21-4.26, respectively, while the spectra of the ligands and other complexes are shown in Appendix C. The IR spectra of the free ligands showed strong bands in the 3350–3200 cm^{-1} regions, attributable to NH stretching modes. All the three ligands adopt the thione form in the solid state. This is evident by the absence of the $\nu(SH)$ band in the 2600 -2500 cm^{-1} region (Tadjarodi et al., 2007).

In nickel complexes [Ni(PhTUPh*o*-NH$_2$)$_2$] **(28)** and [Ni(PhTUPy*o*-NH$_2$)$_2$] **(34)**, the stretching frequencies of N-H vibrations shifted to higher frequency in the region 3328 – 3162 cm^{-1} and is consistent with the complexation of thiourea ligands which are not nitrogen-bonded (Barnes et al., 2008). Consequently, the PhTUPh*o*-NH$_2$ and PhTUPy*m*-NH$_2$ ligands are coordinated to nickel(II) in the thione form. The existence of both uncoordinated N(1)H and N(2)H in complexes **28** and **34** is also supported by ^{1}HNMR (Section 4.3.3). In contrast, the $\nu(NH)$ vibration due to N(1)H in the free ligand PhTUPh*p*-NH$_2$ at 3213 cm^{-1} was absent in the spectrum of complex [Ni(PhTUPh*p*-NH$_2$)$_2$] (**31**). This indicates that deprotonation of the C=S group has occurred and therefore the PhTUPh*p*-NH$_2$ ligand is coordinated in the thiolate form. This conclusion is supported by the absence of NH signal at 9.39 ppm in the ^{1}HNMR spectra. Moreover, the $\nu(NH)$ vibration due to N(2)H at 3326 cm^{-1} in the free PhTUPh*p*-NH$_2$ has shifted to lower wavenumber (3233 cm^{-1}). The downfield shift of this vibration in nickel(II) complex can be attributed due to the withdrawing effect of nickel(II) ion which in turn decrease the electron density around the C-N bond. It can also be noticed that the broadness and weakness in the NH bands may be due to the intermolecular and

intramolecular hydrogen bonding which have been reported in numerous structural studies (West et al., 2001).

In the free ligands, the four characteristic thioamide bands which have contributions from the thioamide group HN-C=S, namely I ν(C-N) + δ(N-H) at about 1600 - 1500 cm-1, II ν(C=S) + ν(C=N) + ν(C–H) at about 1400 - 1200 cm^{-1}, III ν(C–N) + ν(C–S) at about 1250 - 1000 cm^{-1} and 1V ν(C–S) at about 800 - 700 cm^{-1}, have considerable changes in frequency upon coordination with nickel(II). In complexes [Ni(PhTUPho-NH$_2$)$_2$] (28), [Ni(PhTUPhp-NH$_2$)$_2$] (31) and [Ni(PhTUPyo-NH$_2$)$_2$] (34), the thioamide band I having contributions from ν(C-N) + δ(N-H), shifted by 15 - 30 cm^{-1} towards the higher frequency region (Yamaguchri et al., 1958). This blue shift is attributed to the delocalization of π electrons on the chelate ring, resulting in a considerable change in the nature of the N–C bond as well as of the C=S bond upon metal–sulfur bond formation. The thioamide band II which has more contribution from ν(C=S), underwent downfield shift or was split and intense bands were observed. In the case of the complex [Ni(PhTUPho-NH$_2$)$_2$] (28), this band is red shifted to lower wavenumber from 1335 cm^{-1} to 1322 cm^{-1}, while in the complex   [Ni(PhTUPhp-NH$_2$)$_2$] (31), the thioamide band II of the ligand PhTUPhp-NH$_2$ at 1363 cm^{-1} and 1276 cm^{-1} was split into three bands at 1322, 1275 and 1205 cm^{-1} on complexation. In the complex [Ni(PhTUPyo-NH$_2$)$_2$] (34), the broad thioamide band II of the ligand PhTUPyo-NH$_2$ observed at 1362 cm^{-1} showed a downward shift and was split into two bands at 1322 and 1306 cm^{-1} as the result of coordination to nickel (Gunasekaran et al., 2011; Saad et al., 2012). It is worth noticing that the thioamide band III in the thiourea ligands which appear at 1228 – 1134 cm^{-1} in the free ligands, was shifted to higher wave number (Duquey et al., 2009; Gunasekaran et al., 2011). The changes, which range from 4-21 cm^{-1} are

attributed to the change in the bond character of both C-N and C=S bonds upon coordination with metal ion.

The coordination of thioamide sulfur to nickel(II) in the above complexes is further supported by the observed lowering of ν(C=S) frequencies due to the decrease in electron density around CS bond upon complexation of sulfur to nickel(II). These observations were consistent with the literature values (El-Bahya et al., 2003; Kanjan & Dikshit, 2000; Zhang et al., 2008), thus confirming the coordination through sulfur atom.

In mixed nickel(II) complexes of phenylthiourea ligands with 1,10-phenanthronline and 2,2'-bipyridine, complexes **29**, **30**, **32**, **33**, **35** and **37**, the thioamide band I having contributions from ν(C–N) + δ(N–H) was shifted to higher frequency (1577 -1541 cm^{-1}) in accordance with the free ligands, suggesting that one of the coordination sites of the ligand to the nickel(II) is through a nitrogen atom of the thiourea moiety (Cheresova et al., 1997; Fuks et al., 2005 ; Yuen et al., 2011). The bands appearing in the range 1363 – 1276 cm^{-1} (thioamide band II) in the spectra of ligands have been shifted to lower frequencies (1332 - 1295 cm^{-1}) in mixed thiourea complexes with 1,10-phenanthroline and 2,2'-bipyridine indicating coordination of the sulfur to nickel(II). The lowering in the vibration frequency of thioamide band II can be explained by the formation of a greater single C–S bond character via loss of hydrogen from one of the NH groups and participation of the sulfur atom of the C=S group in the bridging bonds between two nickel atoms, resulting in a decrease of the electronic density in the conjugated chelate cycle. However, this trend of coordination is found to be consistent with other reports (Alia et al., 1999; Muthu & Meenakashisundaram, 2012). A conspicuous difference in the spectra of both nickel(II) complexes (i.e. between complexes **28**, **31**, **34** and their

analogs mixed complexes) appears in the vibration of thioamide band IV, shift of this band is the largest for mixed complexes, where its absorption intensity is also lowered, in accordance with the single bond formation (Bombicza et al., 2004).

The IR spectrum of the complex $[Ni_2(impyt)_4].H_2O$ showed the characteristic $\nu(NH)$ stretching vibration required by the presence of the heterocyclic thione ligands at 3171 cm^{-1} (Beheshti et al., 2011; Liu et al., 2010), but did not show the $\nu(NH)$ band attributed to NH_2, which in the free ligand appeared at 3448 cm^{-1}. Moreover, the strong sharp bands in the region 1535 - 1593 cm^{-1} in the free ligand, which is a characteristic band for the phenyl group (Jensen & Nielsen, 1966) were absent in this complex. These observations reveal the elimination of PhNH during complexation, thus, suggesting cyclization of the thiourea ligand.

In mixed thiourea complexes of 1,10-phenanthroline, complexes **29** and **32** the bands at 1425, 1384 and 845cm^{-1} and in complex **35** at 1465 and 761 cm^{-1} corresponding to symmetric and asymmetric stretching vibrations of the 1,10-phenanthroline co-ligand and are consistent with the presence of a bidentate phen ligand (Tang et al., 1998). Similarly, the bands at 1445, 1384 and 764 cm^{-1} in complexes **30** and **33**, and in complex **37** at 1466 and 761 cm^{-1} are indicative for the presence of bidentate 2,2-bipyridne ligand.

Table 4.9: IR spectral assignments for the thiourea ligands and their nickel(II) complexes (cm^{-1})

Compound	ν(NH)	ν(NH$_2$)	Thioamide bands				Bands due to Phen/bpy
			I	II	III	IV	
PhTUPh*o*-NH$_2$ **(25)**	3215	-	1533	1335	1243	793	-
PhTUPh*p*-NH$_2$ **(26)**	3326	3431	1538	1363	1228	797	-
	3213			1276			
PhTUPy*o*-NH$_2$ **(27)**	3337	3448	1535	1362	1205	781	-
	3147						
[Ni(PhTUPh*o*-NH$_2$)$_2$] **(28)**	3328	3445	1560	1322	1264	755	-
[Ni(PhTUPh*p*-NH$_2$)$_2$] **(31)**	3233	3427	1561	1322	1232	764	-
				1275			
				1205			
[Ni(PhTUPy*o*-NH$_2$)$_2$] **(34)**	3162	3462	1552	1322	1221	761	-
	3357			1306			
[Ni$_2$(PhTUPh*o*NH$_2$)$_2$(phen)$_2$]NO$_3$.H$_2$O **(29)**	3229	3316	1575	1319	1251	726	1425
							1384
							845
[Ni$_2$(PhTUPh*o*-NH2)$_2$(bpy)$_2$] NO$_3$ **(30)**	3221	3316	1577	1295	1251	736	1444
							1384
							764
Ni$_2$(PhTUPh*p*-NH$_2$)$_2$(Phen)$_2$]NO$_3$ .2H$_2$O **(32)**	3233	-	1541	1317	1259	726	1424
							1384
							843
[Ni$_2$(PhTUPh*p*-NH$_2$)$_2$(bpy)$_2$]NO$_3$.H$_2$O **(33)**	3233	3344	1542	1314	1258	735	1445
							1384
							761
[Ni$_2$(PhTUPy*o*-NH$_2$)$_2$(Phen)$_2$]Cl **(35)**	3166	3358	1552	1332	1220	738	1466
				1320			761
[Ni$_2$(PhTUPy*o*-NH$_2$)$_2$(Bpy)$_2$]Cl **(37)**	3159	3358	1552	1331	1220	735	1465
				1322			761
[Ni$_2$(impytH)$_4$].H$_2$O **(36)**	3179	-	1620	1364	1263	769	-

182
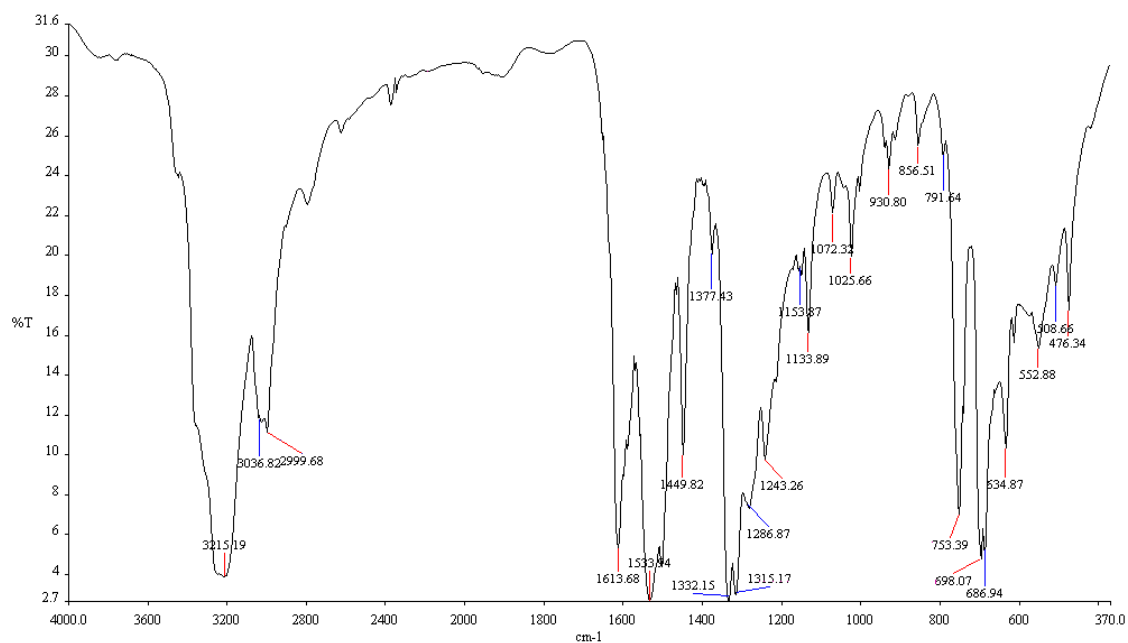
Figure 4.21: IR spectrum of PhTUPh*o*-NH$_2$ **(25)**
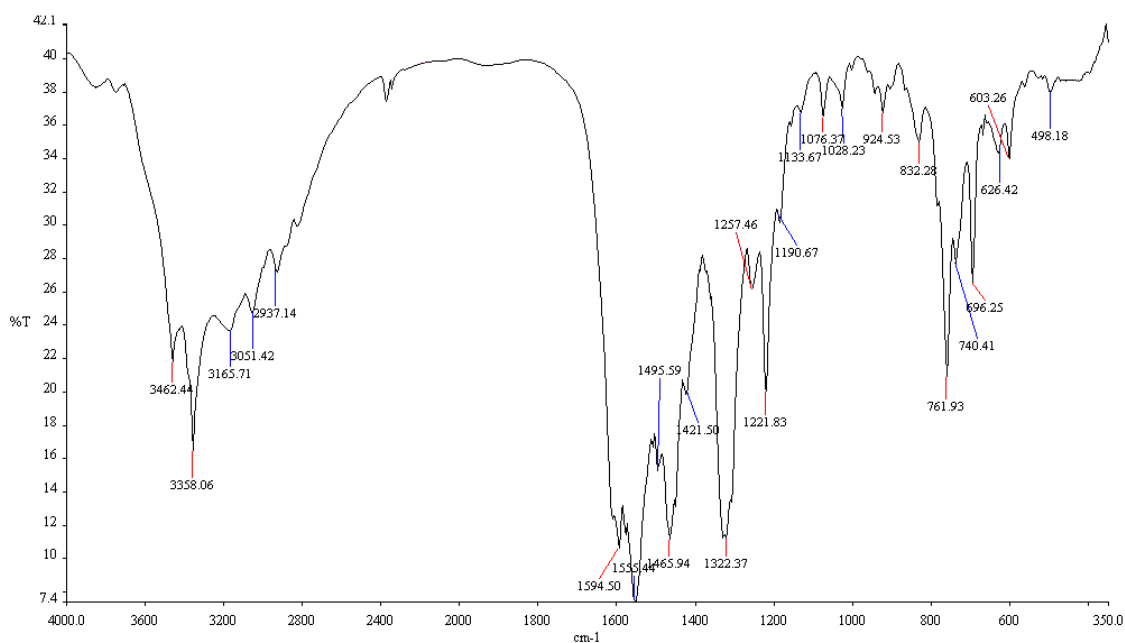
Figure 4.22: IR spectrum of [Ni(PhTUPh*o*-NH$_2$)$_2$] **(28)**
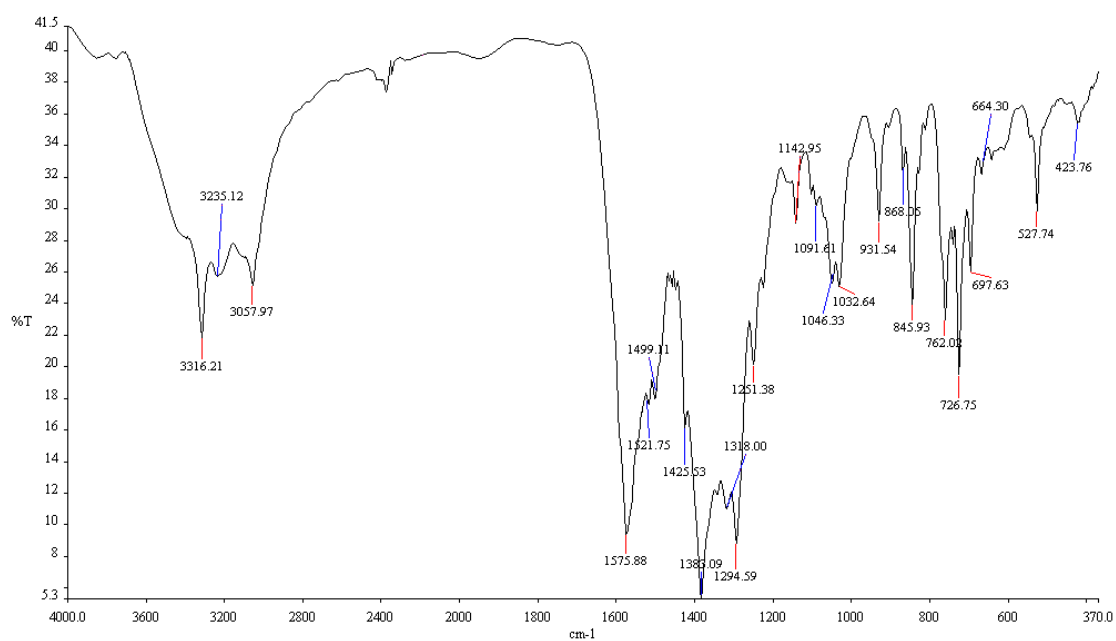
Figure 4.23 IR: spectrum of [Ni$_2$(PhTUPhoNH$_2$)$_2$(phen)$_2$]NO$_3$.H$_2$O **(29)**
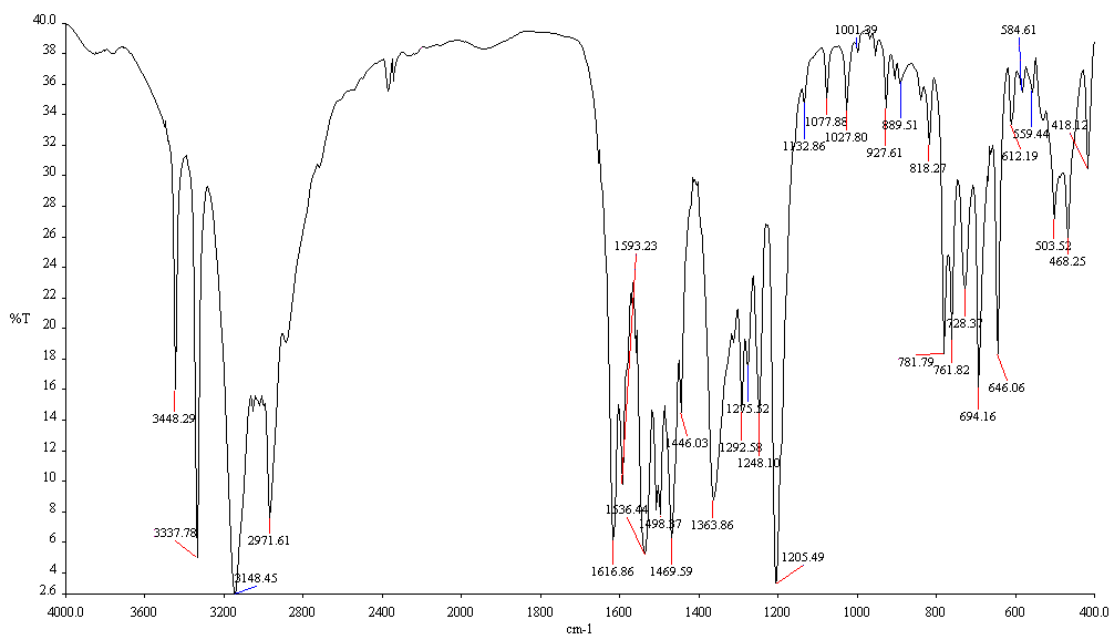
Figure 4.24: IR spectrum of PhTUPyo-NH$_2$ **(27)**
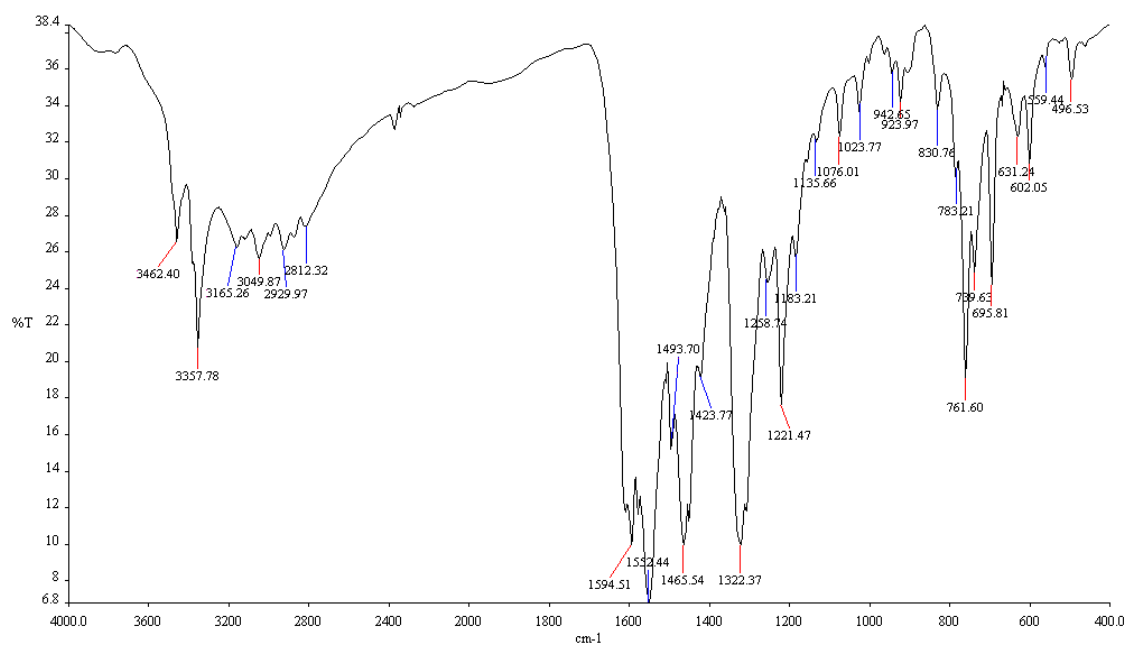
Figure 4.25: IR spectrum of [Ni(PhTUPy*o*-NH$_2$)$_2$] **(34)**
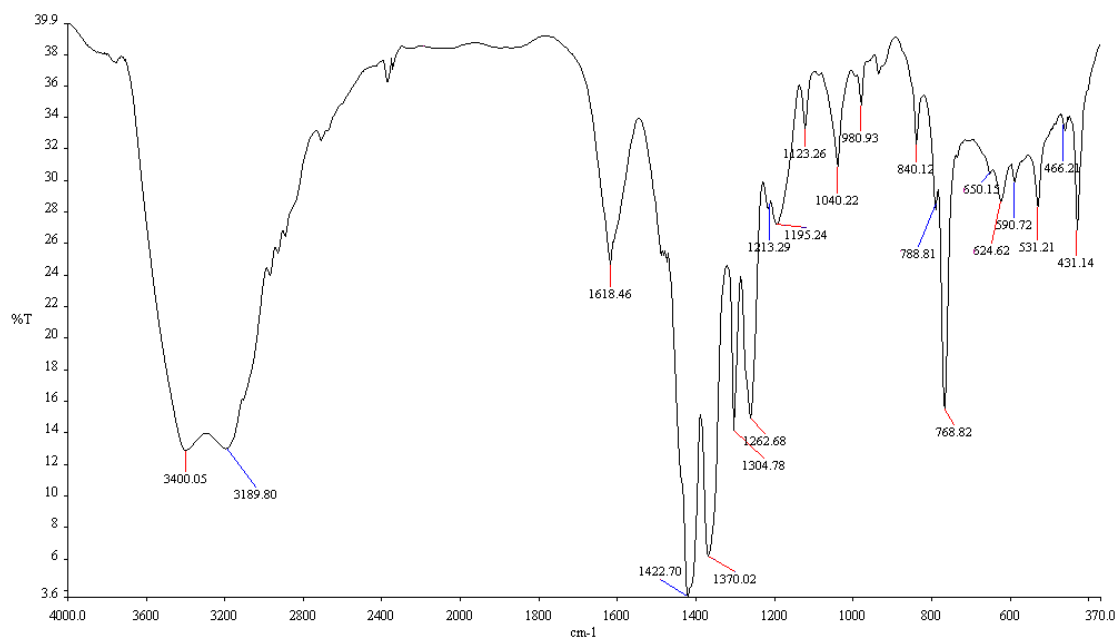
Figure 4.26: IR spectrum of [Ni$_2$(impytH)$_4$].H$_2$O **(36)**

CHAPTER 5

Biological Applications

5.1 Introduction

Since the serendipitously discovery of the anticancer activities of cisplatin by Barnett Rosenberg, extensive researches have been done on studying the cytotoxic activities of inorganic compounds. It has been found that DNA is the main target for cisplatin as an anticancer drug (Pizarro & Sadler, 2009). Thus, in order to find new compounds with anticancer activities, studying the interactions of the new compounds with DNA is critical to the rational design and development of new anticancer agents. The interactions between DNA and metal complexes drugs can be done in different ways through electrostatic interactions, DNA intercalation, DNA cleavage, covalent binding and non-covalent binding to minor groove. Metal complexes as effective anticancer drugs can combine two or more interaction types depending on their ligand, metal ion, geometry and their ability to form stacking and hydrogen bonding interactions with the base pairs of DNA (Zeglis et al., 2007).

Normally, cancer cells have an elevated level of particular enzymes or metal ions compared to normal cells, thus, in order to design new anticancer drugs that can be selective between healthy and cancer cells, many studies have centered on development of metal complexes as anticancer agents that target protein and enzymes instead of targeting DNA (Gopal et al., 2002; Meggers et al., 2007). One of these biological targets is topoisomerases. Topoisomerases are enzymes that catalyze the winding and unwinding of DNA during replication and transcription. The catalytic activity of topoisomerases is based on the cleavage of the DNA strands and the passage of either individual DNA strands through a break in the opposing strand or the passage of double helices through a double stranded break in the same or different molecule (Wang,

1996). Based on their functional mechanisms, topoisomerases have been classified into two types; topoisomerases that cleave only one strand of the DNA are classed as type I, while those that cleave both strands are defined as type II subfamily members of topoisomerases (Champoux, 2001). The two kinds of topoisomerases carry out the passage by reversibly cleaving one or both strands of the DNA. The reversibility of the reaction is ensured by the covalent attachment of the enzyme to a DNA end through a phosphodiester linkage involving a tyrosine residue in the enzyme. Topoisomerases are good targets for antibacterial agents and anticancer drugs owing to their important roles in many genetic processes including DNA replication, recombination, transcription, chromosome condensation and the maintenance of genome stability (Liu, 1989). The activity of topoisomerase I does not change with different phases of cell growth, therefore, it is a more attractive cellular target for anticancer drug development than topoisomerase II (Sinha, 1995). Moreover, topoisomerase I does not require a nucleotide cofactor or any other energy source to relax supercoiled DNA while topoisomerase II family cannot relax supercoiled DNA without ATP (Chen & Hwang, 1999). Diverse numbers of metal complexes have been reported to interact with DNA topoisomerases and their inhibition activities on topoisomerase are considered to be relevant from their ability to prevent topoisomerase binding to DNA and/or preventing the cleavage activity of the enzyme, resulting in the inhibition of DNA relaxation. However, there are several indications showing that the amount of inhibition mostly depends on the nature of the metal ion, the complexes and the ligands involved (Chin et al., 2011; Singh et al., 2007). Although the mechanism of action for inhibiting topoisomerase I and II by complexes of several transition metal ions has been well established (Che & Siu, 2010; Sinha, 1995), few studies about the activities of nickel complexes that inhibit topoisomerase enzymes have been reported (Afrasiabi et al., 2004; Hall et al., 1997; Prabhakaran, Sivasamy, et al., 2011).

5.2 Topoisomerase I inhibition

5.2.1 Materials and solutions

The pBR322, gene ruler 1 kb DNA ladder, 6x loading buffer and Tris-(hydroxymethyl)aminomethane (Tris) were procured from BioSyn Tech (Fermentas). Analytical grade agarose powder was obtained from Promega. Sodium chloride, E coli DNA topoisomerase I and ethidium bromide were purchased from Sigma Chemical Co. (USA). The aqueous solutions for DNA experiments were prepared with ultra-pure water from an Elga PURELAB ULTRA Bioscience water purification system with a UV light accessory. The Tris-NaCl (TN) buffer was prepared from the combination of Tris-(hydroxymethyl)aminomethane (Tris) base and NaCl dissolved in water and its pH was adjusted with hydrochloric acid (HCl) solution to pH 7.5. The Tris-NaCl buffer pH 7.5 contains Tris at 5 mM and NaCl at 50 mM. All the test compounds in *N,N*-dimethylformamide (DMF) were freshly prepared daily.

5.2.2 Topoisomerase I inhibition assay

The DNA topoisomerase I inhibitory activity assay is based on the conversion of a supercoiled plasmid substrate to its relaxed form by the catalytic activity of the topoisomerase I enzyme. The supercoiled substrate and its relaxed product can be easily distinguished using agarose gel electrophoresis, since the relaxed topological isomers of DNA migrate more slowly than supercoiled species. The inhibition of the topoisomerase I enzyme by nickel complexes was determined by measuring the relaxation of supercoiled plasmid DNA pBR322 in the presence of varying concentrations of the complexes and the products were analyzed by agarose gel electrophoresis. Each reaction mixture contained 0.25 μg plasmid DNA pBR322, 0.25 unit of *E.coli* DNA topoisomerase I, and the nickel complex at final concentration of 500 μM. These mixtures were prepared on ice with total volume of each reaction

mixture 20 μl. These reaction mixtures were incubated for 30 min at 37 ℃. The mixtures were applied to 1.25 % agarose gel and electrophoresed for 3 hours at 40 V with running buffer of Tris-acetate EDTA (TAE) at pH 8.1. The gel was stained, destained, and photographed under UV light using a Syngene Bio Imaging system and the digital image was viewed with Gene Flash software.

5.2.3 Results and discussion

The gel electrophoresis diagrams for the concentration dependent experiments of thiosemicarbazone ligands H_3L^1 and H_3L^3 and nickel complexes **5**, **7**, **13**, **15**, **17**, **19**, **21** and **24** are shown in Figures 5.1- 5.10 while the gel electrophoresis diagrams for the other compounds are shown in Appendix D. The capacity of the complexes to change the catalytic activity of topoisomerases I was studied by a DNA relaxation assay in which supercoiled plasmid DNA was treated with topoisomerase I in the presence of varying concentrations of the complex (5 – 500 μM) and the results were analyzed by gel electrophoresis on agarose gel. Supercoiled plasmid DNA pBR322 is a one strand DNA cutter. Enzyme activity is characterized by conversion of DNA pBR322 from the supercoiled conformation (Form I; Figure 5.1, L2) to the fully relaxed conformation (Form II; Figure 5.1, L4). The supercoiled pBR322 (Form I) is very compressed and can migrate faster in the gel during electrophoresis. When one strand of the supercoiled DNA is cut, the DNA become unwinded, and more relaxed open circular pBR322 (Form II) is formed and this nicked DNA migrates slower in the gel. The species migrating between the two forms are the various topoisomers indicating that the enzyme was causing relaxation. In these topoisomerase DNA relaxation assay experiments, it was found that 0.25 of *E.coli* topoisomerase I could completely convert all plasmid pBR322 to fully relaxed DNA or topoisomers (Figures 5.1& 5.2, lane 4). As can be seen from Figures 5.1 & 5.2 (L6 – L13), the ligands H_3L^1 and H_3L^3 did not inhibit

topoisomerase I activity in the concentration range 5–500 μM, as the DNA bands are the same as those observed for DNA incubated with topoisomerase I alone (L4). The same results were observed for ligands H_3L^2 and H_3L^4 (Appendix D).
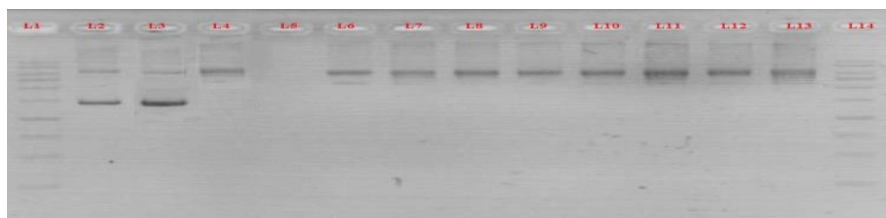

Figure 5.1: Topoisomerase I inhibition assay by gel electrophoresis for H_3L^1

Electrophoresis results of incubating *E.coli* topoisomerase I (0.25unit/21μL) with pBR322 in the absence or presence of varying concentration of the ligand H_3L^1 : Lane 1&14 Gene Ruler 1-kb DNA ladder, lane 2 DNA alone, lane 3 DNA + 500 μM ligand (control), lane 4 DNA +0.25 U topoisomerase I (control), lane 5 empty, Lane 6-13 Topoisomerase I with increasing concentration of ligand: lane 6, 5 μM; lane 7, 10 μM; lane 8, 20 μM; lane 9, 40 μM; lane 10, 80μM; lane 11, 160μM; lane 12 250μM; lane 13, 500μM .
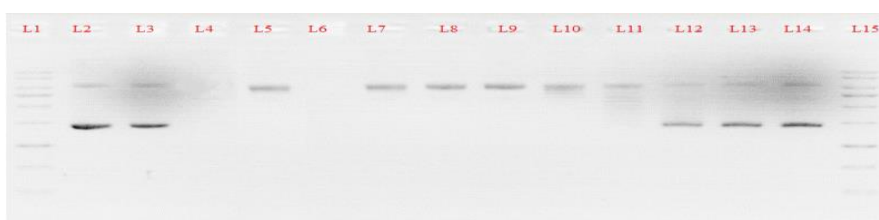

Figure 5.2: Topoisomerase I inhibition assay by gel electrophoresis for H_3L^3

 Electrophoresis results of incubating *E.coli* topoisomerase I (0.25unit/21μL) with pBR322 in the absence or presence of varying concentration of the ligand H_3L^3 : Lane 1&14 Gene Ruler 1-kb DNA ladder, lane 2 DNA alone, lane 3 DNA + 500 μM ligand (control), lane 4 DNA +0.25 U topoisomerase I (control), lane 5 empty, Lane 6-13 Topoisomerase I with increasing concentration of ligand: lane 6, 5 μM; lane 7, 10 μM; lane 8, 20 μM; lane 9, 40 μM; lane 10, 80μM; lane 11, 160μM; lane 12 250μM; lane 13, 500μM

However, incubating DNA pBR322 with topoisomerase I and increasing concentration of nickel(II) thiosemicarbazone complexes presented in chapter 2, namely, the series

[[Ni(H$_3$L^1)(H$_2$L^1)]ClO$_4$.2H$_2$O **(5),** [Ni(H$_3$L^2)(H$_2$L^2)]ClO$_4$.2H$_2$O **(6),** [Ni(H$_3$L^3)(H$_2$L^3)] ClO$_4$ **(7)** and [Ni(H$_3$L^4)(H$_2$L^4)]ClO$_4$.H$_2$O **(8)]** and the series [[Ni$_2$(HL^1)$_2$] **(13),** [Ni$_2$(HL^2)$_2$].H$_2$O **(14),** [Ni$_2$(HL^3)$_2$] **(15)** and [Ni$_2$(HL^4)$_2$] **(16)]**, gave rise to the increasing reduction of the nicked band, which contain nicked and fully relaxed DNA, and formation of various faster moving bands of topoisomers with different degree of relaxation (Figure 5.3, L10 – L13; Figure 5.4, L9 – L10; Figure 5.5, L9 – L11; Figure 5.6, L9 – L11).

Figure 5.3: Topoisomerase I inhibition assay by gel electrophoresis for [Ni(H$_3$L^1)(H$_2$L^1)]ClO$_4$.2H$_2$O **(5)**

Electrophoresis results of incubating *E.coli* topoisomerase I (0.25unit/21μL) with pBR322 in the absence or presence of varying concentration of complex **5** : Lane 1&15 Gene Ruler 1-kb DNA ladder, lane 2 DNA alone, lane 3 DNA + 500 μM complex (control), lane 4 empty, lane 5 DNA +0.25 U topoisomerase I (control), lane 6 empty, Lane 7-14 topoisomerase I with increasing concentration of complex: lane 7, 5 μM; lane 8, 10 μM; lane 9, 20 μM; lane 10, 40 μM; lane 11, 80μM; lane 12, 160μM; lane 13, 250 μM; lane 14, 500 μM
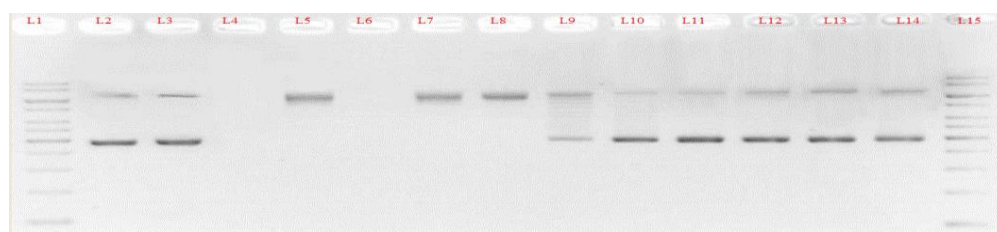
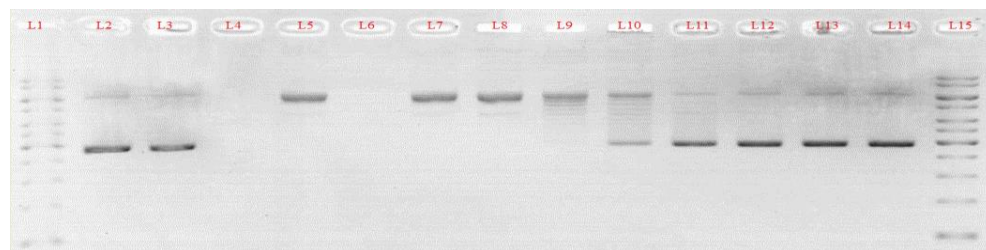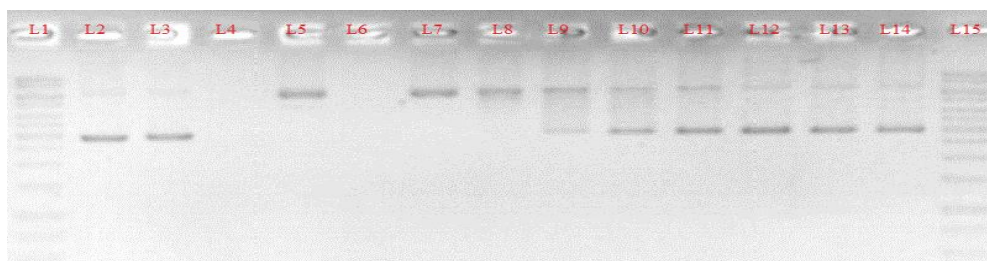**Figure 5.4:** Topoisomerase I inhibition assay by gel electrophoresis for
Ni(H$_3$L^3)(H$_2$L^3)]ClO$_4$ **(7)**

Electrophoresis results of incubating *E.coli* topoisomerase I (0.25unit/21μL) with pBR322 in the absence or presence of varying concentration of complex **7** : Lane 1&15 Gene Ruler 1-kb DNA ladder, lane 2 DNA alone, lane 3 DNA + 500 μM complex (control), lane 4 empty, lane 5 DNA +0.25 U topoisomerase I (control), lane 6 empty, Lane 7-14 topoisomerase I with increasing concentration of the complex: lane 7, 5 μM; lane 8, 10 μM; lane 9, 20 μM; lane 10, 40 μM; lane 11, 80 μM; lane 12, 160 μM; lane 13 250 μM; lane 14, 500 μM

Figure 5.5: Topoisomerase I inhibition assay by gel electrophoresis for [Ni$_2$(HL^1)$_2$] **(13)**

Electrophoresis results of incubating *E.coli* topoisomerase I (0.25unit/21μL) with pBR322 in the absence or presence of varying concentration of complex **13** : Lane 1&15 Gene Ruler 1-kb DNA ladder, lane 2 DNA alone, lane 3 DNA + 500 μM complex(control), lane 4 empty, lane 5 DNA +0.25 U topoisomerase I (control), lane 6 empty, Lane 7-14 topoisomerase I with increasing concentration of the complex: lane 7, 5 μM; lane 8, 10 μM; lane 9, 20 μM; lane 10, 40 μM; lane 11, 80 μM; lane 12, 160 μM; lane 13 250 μM; lane 14, 500 μM

Figure 5.6: Topoisomerase I inhibition assay by gel electrophoresis for $[Ni_2(HL^3)_2]$ **(15)**

Electrophoresis results of incubating *E.coli* topoisomerase I (0.25unit/21µL) with pBR322 in the absence or presence of varying concentration of complex **15** : Lane 1&15 Gene Ruler 1-kb DNA ladder, lane 2 DNA alone, lane 3 DNA + 500 µM complex (control), lane 4 empty, lane 5 DNA +0.25 U topoisomerase I (control), lane 6 empty, Lane 7-14 topoisomerase I with increasing concentration of the complex: lane 7, 5 µM; lane 8, 10 µM; lane 9, 20 µM; lane 10, 40 µM; lane 11, 80µM; lane 12, 160µM; lane 13 250 µM; lane 14, 500 µM

The formation of faster moving bands of less relaxed topoisomers was observed with increasing concentration of the nickel(II) thiosemicarbazone complexes. These results demonstrated that these complexes were capable of inhibiting the function of topoisomerase I in relaxing the supercoiled pBR322. Also, these results showed that the degree of inhibition by nickel(II) thiosemicarbazone complexes is concentration dependent. In addition, all eight nickel(II) thiosemicarbazones complexes (except complex **15**) posses similar amount of inhibition effect on topoisomerase I activity, in which the initial inhibitory effect started from 20 - 40 µM complex concentration and the inhibitory effect is enhanced with the increasing complex concentration from 20 – 500 µM. However, complex **15** shows the highest inhibition activity among the complexes presented in chapter 2, which could induce the inhibition of *E.coli* topoisomerase I activity starting from low concentration (10 µM). Possibly, due to the existence of phenyl substituent, which is more hydrophobic compared with the other substituents. Moreover, the inhibitory effect of complex **15** (complex with N4-phenyl substituent) is larger than of complex **7** (complex with N4-phenyl substituent also). This

may be related to the coordinatively unsaturated square planar geometry in complex **15**, giving the opportunity for easy binding of DNA to metal centre through the available unoccupied sites (Prabhakaran, Sivasamy, et al., 2011).
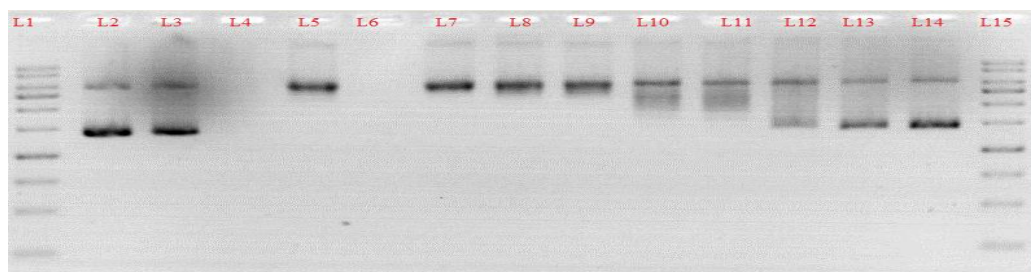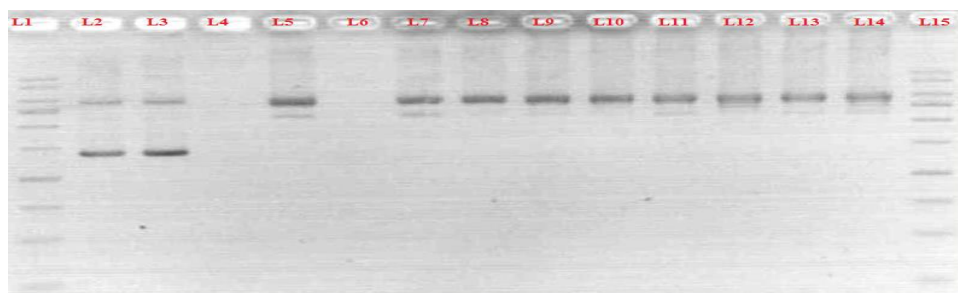

Figure 5.7: Topoisomerase I inhibition assay by gel electrophoresis for $[Ni(H_2L^1)(PPh_3)]Cl$ **(17)**

Electrophoresis results of incubating *E.coli* topoisomerase I (0.25unit/21μL) with pBR322 in the absence or presence of varying concentration of complex **17** : Lane 1&15 Gene Ruler 1-kb DNA ladder, lane 2 DNA alone, lane 3 DNA + 500 μM complex (control), lane 4 empty, lane 5 DNA +0.25 U topoisomerase I (control), lane 6 empty, Lane 7-14 topoisomerase I with increasing concentration of the complex: lane 7, 5 μM; lane 8, 10 μM; lane 9, 20 μM; lane 10, 40 μM; lane 11, 80μM; lane 12, 160 μM; lane 13, 250 μM; lane 14, 500 μM
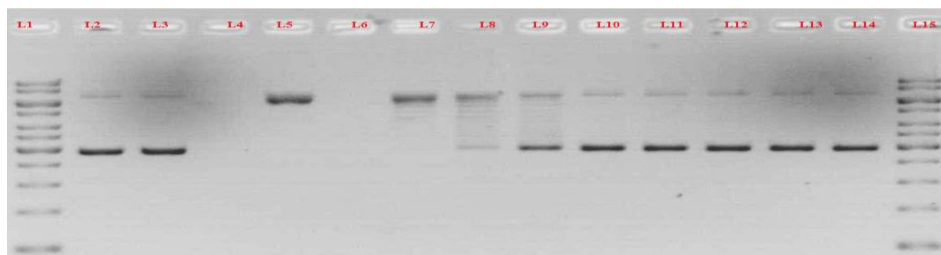

Figure 5.8: Topoisomerase I inhibition assay by gel electrophoresis for $[Ni(HL^3)(PPh_3)]$ **(19)**

Electrophoresis results of incubating *E.coli* topoisomerase I (0.25unit/21μL) with pBR322 in the absence or presence of varying concentration of complex **19** : Lane 1&15 Gene Ruler 1-kb DNA ladder, lane 2 DNA alone, lane 3 DNA + 500 μM complex (control), lane 4 empty, lane 5 DNA +0.25 U topoisomerase I (control), lane 6 empty, Lane 7-14 topoisomerase I with increasing concentration of the complex: lane 7, 5 μM; lane 8, 10 μM; lane 9, 20 μM; lane 10, 40 μM; lane 11, 80μM; lane 12, 160 μM; lane 13, 250 μM; lane 14, 500 μM

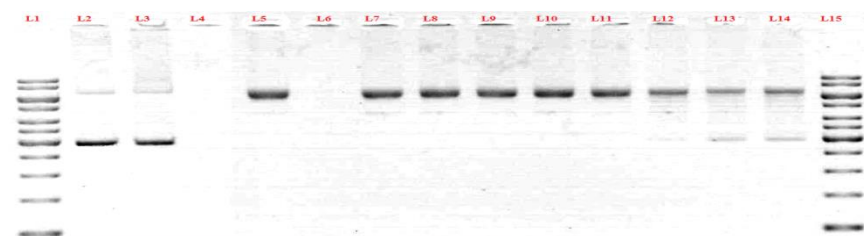**Figure 5.9:** Topoisomerase I inhibition assay by gel electrophoresis for [Ni$_2$(HL^1)$_2$(dppe)] **(21)**

Electrophoresis results of incubating *E.coli* topoisomerase I (0.25unit/21µL) with pBR322 in the absence or presence of varying concentration of complex **21** : Lane 1&15 Gene Ruler 1-kb DNA ladder, lane 2 DNA alone, lane 3 DNA + 500 µM complex (control), lane 4 empty, lane 5 DNA +0.25 U topoisomerase I (control), lane 6 empty, Lane 7-14 topoisomerase I with increasing concentration of the complex: lane 7, 5 µM; lane 8, 10 µM; lane 9, 20 µM; lane 10, 40 µM; lane 11, 80µM; lane 12, 160µM; lane 13, 250 µM; lane 14, 500 µM

Figure 5.10: Topoisomerase I inhibition assay by gel electrophoresis for [Ni$_2$(HL^4)$_2$(dppe)] **(24)**

Electrophoresis results of incubating *E.coli* topoisomerase I (0.25unit/21µL) with pBR322 in the absence or presence of varying concentration of complex **24** : Lane 1&15 Gene Ruler 1-kb DNA ladder, lane 2 DNA alone, lane 3 DNA + 500 µM complex (control), lane 4 empty, lane 5 DNA +0.25 U topoisomerase I (control), lane 6 empty, Lane 7-14 topoisomerase I with increasing concentration of the complex: lane 7, 5 µM; lane 8, 10 µM; lane 9, 20 µM; lane 10, 40 µM; lane 11, 80 µM; lane 12, 160µM; lane 13, 250 µM; lane 14, 500 µM

As can be seen from Figures 5.7 – 5.10, by incubating the pBR322 with the highest concentration (500 μM) of the complexes presented in chapter 3, (i.e. the series [Ni(H$_2$L^1)(PPh$_3$)]Cl **(17),** [Ni(H$_2$L^2)(PPh$_3$)]Cl **(18),** [Ni(HL^3)(PPh$_3$)] **(19),** [Ni(HL^4)(PPh$_3$)] **(20),** and the series [Ni$_2$(HL^1)$_2$(dppe)] **(21),** [Ni$_2$(HL^2)$_2$(dppe)] **(22),** [Ni$_2$(HL^3)$_2$(dppe)] **(23)**, [Ni$_2$(HL^4)$_2$(dppe)] **(24)**), no cleavage or unwinding of the DNA was observed as the banding model is the same as the control without any added complex (L3). The gel electrophoresis results for these series of nickel(II) thiosemicarbazone mixed complexes clearly show that all complexes (except **19** and **20**) are potent topoisomerase I inhibitors displaying different degree of inhibition.   In complex **17**, the initial inhibition of the catalytic activity of TopoI is observed at 40 μM (Figure 5.7, L10) while the complete inhibition of TopoI action is at 250 μM (Figure 5.7, L13). On the hand, complex **21**, partially inhibited Topo I at 5 μM as evidenced by the presence of a smear of faster moving, overlapping bands of less relaxed topoisomers (Figure 5.9, L 7) while at 20 μM (Figure 5.9, L9) almost totally inhibited Topo I as the DNA pattern now appeared as a mainly closed circular, supercoiled DNA band and a thin nicked open circular DNA band, as was observed for the untreated DNA (Figure 5.9, L2). Comparing the gel electrophoresis results of complexes **19** and **24**, Figure 5.8 and 5.10 respectively, show that the DNA relaxation effects caused by TopoI were partially inhibited by complex **24** at 160 μM (Figure 5.10, L12) concentrations as evidenced by the reduction in the number of the topoisomers but a fully relaxed conformation is not observed. In contrast, complex **19** failed to inhibit topo I in the concentration range 5 – 500 μM (Figure 5.8, L7- L14). The substituents on N4 nitrogen have significant effect on the inhibitory activities of thiosemicarbazone complexes. It has been found that complexes bearing ligands with larger substituents on N4 have greater activity on inhibiting the topoisomerases activity (Zeglis et al., 2011). However, the influence of nickel(II) mixed complexes of 2,3-dihydroxybenzaldehyde N4-

thiosemicarbazones with phosphines on the enzyme activity has different sequence. The gel electrophoresis results suggested that the nickel(II) mixed complexes bearing small group on N4 had greater activity, most likely, due to the small steric hindrance between the thiosemicarbazone with small N4 substituent and the bulky phosphine ligand.

The gel electrophoresis diagrams for the topoisomerase I inhibition experiments of thiourea ligands PhTUPho-NH$_2$ (**25**) and PhTUPmy-NH$_2$ (**27**) presented in chapter 4 and their nickel(II) complexes **28**, **34**, **29** and **35** are shown in Figures 5.11- 5.16 while the gel electrophoresis diagrams for the other compounds are shown in Appendix D.

The thiourea ligands **25** (Figure 5.11) and **27** (Figure 5.12) did not cause any significant inhibition on *E.coli* topoisomerase I activity. However, complexation of the thiourea diamine ligand **25** (thiourea ligand with the amine group *ortho* to thiourea moiety) with nickel(II), complex [Ni(PhTUPho-NH$_2$)$_2$] (**28**), has enhanced its inhibitory effect. This complex could inhibit the *E.coli* topo I activity at 250 µM and 500 µM (Figure 5.13; L13 and L14, respectively). Besides that, the inhibitory effect of ternary nickel complexes of this ligand (the complex [Ni$_2$(PhTUPho-NH$_2$)$_2$(Phen)$_2$]NO$_3$.H$_2$O (**29**)) was much better, as can seen in Figure 5.15, complex **29** showed to initiate the inhibition on *E.coli* topo I activity at 80 µM (Figure 5.15; L11) in a concentration dependent manner.

On the other hand, nickel(II) complexes of the thiourea ligand **27** showed to aggregate DNA at higher complex concentration. Complex [Ni(PhTUPyo-NH$_2$)$_2$].H$_2$O (**34**) could inhibit *E.coli* topo I activity at 10 µM (Figure 5.14; L8), but further increased in the complex concentration has reduced its inhibitory effect and various form of DNA (supercoiled and relaxed) were barely seen (Figure 5.14; L9-14). Similar behavior was seen for the ternary nickel complex with this ligand, complex [Ni$_2$(PhTUPyo-

NH$_2$)$_2$(Phen)]Cl **(35)**. Although this complex could induce slight inhibition on *E.coli* topo I activity at 20 μM (Figure 5.16; L9), additional raised in complex concentration has reduced the degree of supercoiled and relaxed forms of DNA. Additionally, the intensity of DNA in lane 3 (Figures 5.14 and 5.16) (negative control, DNA+250 μM of the complexes **34** and **35**) was also reduced. It may be suggested that these complexes were able to aggregate DNA into large clump which prevent DNA from traveling further in the gel. This performance has been reported for molecules that non covalently interact with DNA (Bergeron et al., 2009).
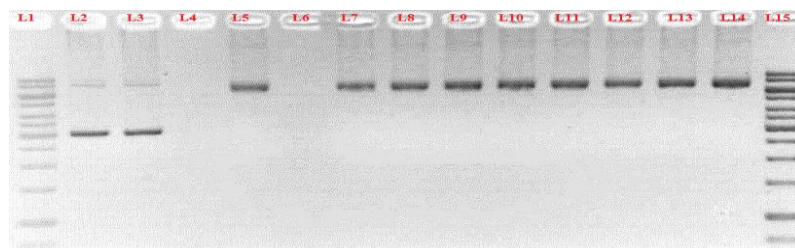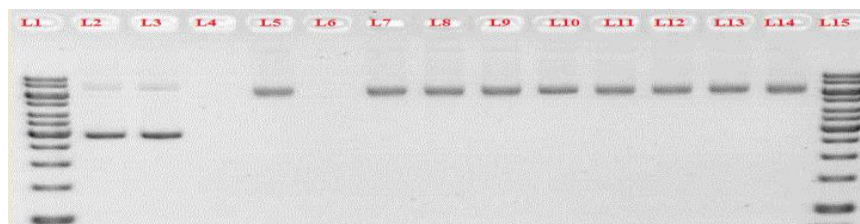
Figure 5.11: Topoisomerase I inhibition assay by gel electrophoresis for PhTUPh*o*-NH$_2$ **(25)**

Electrophoresis results of incubating *E.coli* topoisomerase I (0.25unit/21μL) with pBR322 in the absence or presence of varying concentration of ligand **25** : Lane 1&15 Gene Ruler 1-kb DNA ladder, lane 2 DNA alone, lane 3 DNA + 500 μM complex (control), lane 4 empty, lane 5 DNA +0.25 U topoisomerase I (control), lane 6 empty, Lane 7-14 topoisomerase I with increasing concentration of ligand: lane 7, 5 μM; lane 8, 10 μM; lane 9, 20 μM; lane 10, 40 μM; lane 11, 80 μM; lane 12, 160 μM; lane 13, 250 μM; lane 14, 500μM
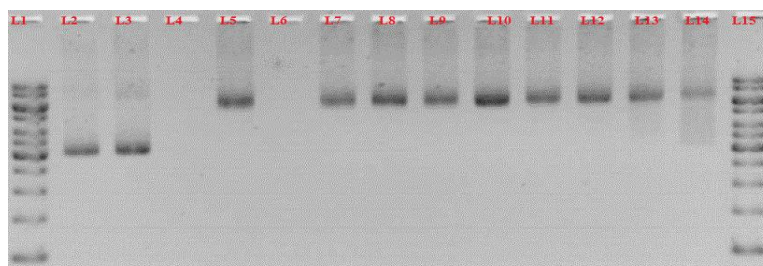

Figure 5.12: Topoisomerase I inhibition assay by gel electrophoresis for PhTUP*yo*-NH$_2$ **(27)**

Electrophoresis results of incubating *E.coli* topoisomerase I (0.25unit/21μL) with pBR322 in the absence or presence of varying concentration of ligand **27** : Lane 1&15 Gene Ruler 1-kb DNA ladder, lane 2 DNA alone, lane 3 DNA + 500 μM ligand (control), lane 4 empty, lane 5 DNA +0.25 U topoisomerase I (control), lane 6 empty, Lane 7-14 topoisomerase I with increasing concentration of the ligand: lane 7, 5 μM; lane 8, 10 μM; lane 9, 20 μM; lane 10, 40 μM; lane 11, 80 μM; lane 12, 160 μM; lane 13, 250 μM; lane 14, 500 μM

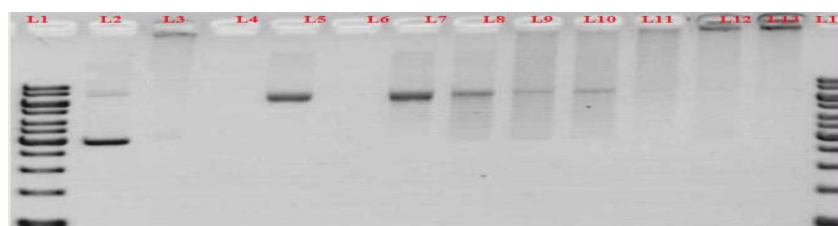**Figure 5.13:** Topoisomerase I inhibition assay by gel electrophoresis for [Ni(PhTUPh*o*-NH$_2$)$_2$] **(28)**

 Electrophoresis results of incubating *E.coli* topoisomerase I (0.25unit/21μL) with pBR322 in the absence or presence of varying concentration of complex **28** : Lane 1&15 Gene Ruler 1-kb DNA ladder, lane 2 DNA alone, lane 3 DNA + 500 μM complex (control), lane 4 empty, lane 5 DNA +0.25 U topoisomerase I (control), lane 6 empty, Lane 7-14 topoisomerase I with increasing concentration of the complex: lane 7, 5 μM; lane 8, 10 μM; lane 9, 20 μM; lane 10, 40 μM; lane 11, 80 μM; lane 12, 160μM; lane 13, 250 μM; lane 14, 500 μM
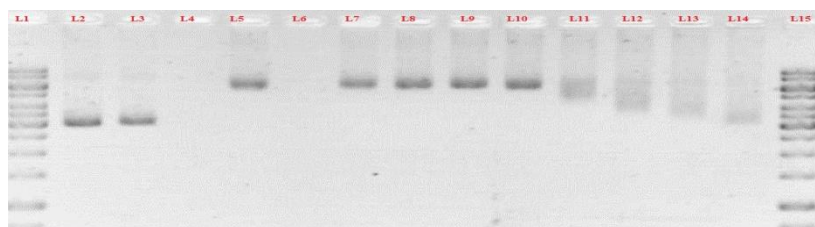

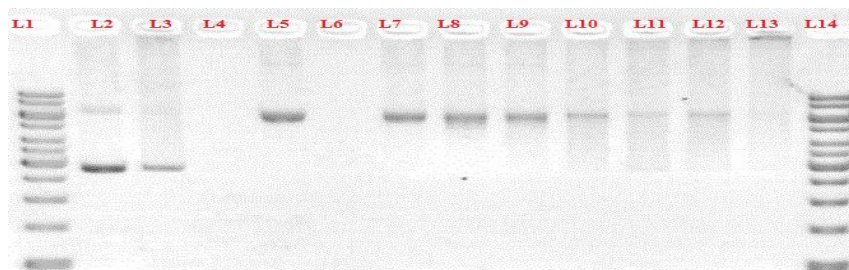**Figure 5.14:** Topoisomerase I inhibition assay by gel electrophoresis for [Ni(PhTUP*yo*-NH$_2$)$_2$].H$_2$O **(34)**

 Electrophoresis results of incubating *E.coli* topoisomerase I (0.25unit/21μL) with pBR322 in the absence or presence of varying concentration of complex **34** : Lane 1&14 Gene Ruler 1-kb DNA ladder, lane 2 DNA alone, lane 3 DNA + 500 μM complex (control), lane 4 empty, lane 5 DNA +0.25 U topoisomerase I (control), lane 6 empty, Lane 7-13 topoisomerase I with increasing concentration of the complex: lane 7, 5 μM; lane 8, 10 μM; lane 9, 20 μM; lane 10, 40 μM; lane 11, 80 μM; lane 12, 160μM; lane 13, 250 μM

Figure 5.15: Topoisomerase I inhibition assay by gel electrophoresis for [Ni$_2$(PhTUPho-NH$_2$)$_2$(Phen)$_2$]NO$_3$.H$_2$O **(29)**

Electrophoresis results of incubating *E.coli* topoisomerase I (0.25unit/21μL) with pBR322 in the absence or presence of varying concentration of complex **29** : Lane 1&15 Gene Ruler 1-kb DNA ladder, lane 2 DNA alone, lane 3 DNA + 500 μM complex (control), lane 4 empty, lane 5 DNA +0.25 U topoisomerase I (control), lane 6 empty, Lane 7-14 topoisomerase I with increasing concentration of the complex: lane 7, 5 μM; lane 8, 10 μM; lane 9, 20 μM; lane 10, 40 μM; lane 11, 80 μM; lane 12, 160μM; lane 13, 250 μM; lane 14, 500 μM

Figure 5.16: Topoisomerase I inhibition assay by gel electrophoresis for [Ni$_2$(PhTUPyo-NH$_2$)$_2$(Phen)$_2$]Cl **(35)**

Electrophoresis results of incubating *E.coli* topoisomerase I (0.25unit/21μL) with pBR322 in the absence or presence of varying concentration of complex **35** : Lane 1&15 Gene Ruler 1-kb DNA ladder, lane 2 DNA alone, lane 3 DNA + 500 μM complex (control), lane 4 empty, lane 5 DNA +0.25 U topoisomerase I (control), lane 6 empty, Lane 7-14 topoisomerase I with increasing concentration of the complex: lane 7, 5 μM; lane 8, 10 μM; lane 9, 20 μM; lane 10, 40 μM; lane 11, 80 μM; lane 12, 160μM; lane 13, 250 μM; lane 14, 500 μM

CHAPTER 6

Conclusion

6.1 Syntheses and characterizations of nickel(II) complexes

This thesis describes the synthesis, structural and spectral characterization of nickel(II) complexes of N/S donor ligands which incorporate an additional donor atom. Four well known thiosemicarbazone ligands (H_3L^1 (**1**), H_3L^2 (**2**) H_3L^3 (**3**) H_3L^4 (**4**)) have been used to coordinate with nickel(II) ion. Five new series of nickel(II) complexes of the general formulation [Ni(H_3L)(H_2L)]ClO$_4$ (**5-8**), [Ni(H_2L)][Ni(H_3L)]Cl$_2$ (**9-12**), [Ni$_2$(HL)$_2$] (**13-16**), ([Ni(H_2L)(PPh$_3$)]Cl (**17,18**), [Ni(HL)(PPh$_3$)] (**19,20**)) and [Ni$_2$(HL)$_2$(dppe)] (**21-24**) have been prepared by the reaction of 2,3-dihydroxybenzaldehyde N(4)-thiosemicarbazones with various nickel(II) compounds. These complexes have been characterized by elemental analyses, IR, UV, NMR, magnetic susceptibility. The structures for some of the complexes (**8**, **9**, **17**, **19**, **21** and **22**) have been solved by single crystal X-ray crystallography. Results from spectroscopic data and crystal structure analysis show that the complexes **5-8** are mononuclear six coordinated with two ONS tridentate thiosemicarbazone ligands, in which one ligand is coordinating through the phenol oxygen, azomethine nitrogen and thione sulfur atoms and the other ligand is coordinating through the phenolic oxygen, azomethine nitrogen and thione sulfur, while complexes **9-12** are dimers and the two thiosemicarbazones are coordinated as ONS donor ligands as neutral H_3L and monodeprotonated H_2L ligands.

Complexes **13-16**, **17-20** and **21-24** are four coordinated with the ONS tridentate doubly deprotonated thiosemicarbazone ligand bounded to nickel(II) through phenolic oxygen, azomethine nitrogen and thiolate/thione sulfur. The binuclear complexes **13-16** are diamagnetic due to square planar nature of the complexes. Elemental analysis and IR

spectral data suggest that two thiosemicarbazone ligands are coordinated to two nickel ions as sulfur bridging ligands. Attempts to prepare the single crystals of these complexes were unsuccessful due to the low solubility of these complexes in common solvents. In the mononuclear complexes **17**-**20**, NMR spectroscopic data and X-ray studies show that the coordination mode of the thiosemicarbazone ligand to nickel(II) ion depends on the substituent on N4. In complexes with the unsubstituted thiosemicarbazone (**17**) and its N4-methyl substituent (**18**), ionic complexes are formed with the monodeprotonated thiosemicarbazone ligand, while in the complexes with N4 ethyl and phenyl substituents (**19** and **20**), neutral complexes are formed with the doubly deprotonated thiosemicarbazone ligands bounded to nickel(II) through phenolic O, azomethine N and thiolate S. Spectral studies of all the complexes support the presence of PPh$_3$ as coligand to complete the forth coordination site.

Single crystal diffraction studies for complexes **21**-**24** have shown that these complexes are binuclear complexes and bridged with the coligand dppe while the thiosemicarbazone ligand is bounded to nickel(II) as tridentate ligand also through phenolic O, azomethine N and thiolate S.

Three thiourea diamine derivatives (PhTUPh*o*-NH$_2$ (**25**), PhTUPh*p*-NH$_2$ (**26**) and PhTUP*yo*-NH$_2$ (**27**) have been employed in this study. Three series of nickel(II) complexes have been prepared and characterized using elemental analysis, IR, UV, NMR and X-ray diffraction. The reaction of thiourea diamine ligands with nickel(II) chloride in basic solution yields mononuclear diamagnetic complexes (**28**, **31** and **34**) with the thiourea ligand coordinates to nickel(II) as N/S bidentate donor ligand as evidenced by the spectroscopic studies. On the other hand, the reaction of these ligands with the methanolic solution of nickel(II) salts and   1,10-phenanthroline or 2,2-

bipyridine affords binuclear complexes (**29**, **30**, **32**, **33**, **35** and **37**) with the thiourea ligands bridge two nickel ions and coordinate as NNS donors while the coligand 1,10-phen or 2,2'-bpy coordinates as bidentate NN ligand. A single crystal X-ray diffraction study of one of these complexes has been carried out in details. However, the reaction of the ligand PhTUP*yo*-NH$_2$ (**27**) with nickel(II) chloride in basic solution followed by the addition of 1,10-phenanthroline affords binuclear nickel(II) complex but with the thiourea ligands converted to heterocyclic ligand and the coligand is not in the coordination sphere. The X-ray diffraction study of this complex shows that the heterocyclic ligand is coordinated through bridging two nickel ions via NCN coordination core.

6.2 Biological applications

The results from topoisomerase inhibition assay described in Chapter 5 show that all nickel complexes with ONS and NNS donor ligands (except complexes **19** and **20**) are able to inhibit the function of DNA topoisomerase I, but none of the free ligands are active. The influence of nickel(II) complexes of 2,3-dihydroxybenzaldehyde N4-thiosemicarbazones on the enzyme activity has different sequence which is dependent on the N(4) substituent, presence of co-ligands and the coordination environment around nickel ion. The gel electrophoresis results suggested that in the absence of the auxiliary ligand, the ability of a nickel complex to inhibit Topo I enzyme is found to be dependent on the N(4) substituent. In this matter, nickel(II) complexes bearing phenyl group (complexes **7** and **15**) on N4 have greater activity. This can be assumed to be due to the higher affinity phenyl group has towards DNA intercalation. The higher ability of complex **15** compared to complex **7** to inhibit the topoisomerase I activity is most likely due to its square planar geometry which can bind to more molecules than the bulky octahedral complex **7**. However, in the existence of a bulky coligand the complex

with the phenyl substituent on N(4) is smaller. This may be attributed to the large steric hindrance between the thiosemicarbazone with phenyl substituent and the bulky phosphine ligand. The topoisomerase inhibition of nickel thiourea complexes is increased by the presence of 1,10-phenanthroline or 2,2'-bipyridine as co-ligands. Another important observation is that in the case of complexes **34** and **35**, the inhibition ability of these complexes is reduced by increasing the complex concentration.

6.3 Future work

The original goal of this thesis was accomplished, new nickel(II) complexes of nitrogen/Sulfur donor ligands with properties capable of inhibition the function of topoisomerase I enzyme were successfully designed, synthesized and characterized. Among the nickel(II) complexes studied, complexes $[Ni(H_3L^3)(H_2L^3)]ClO_4$ (**7**) and $[Ni_2(HL^3)_2]$ (**17**) deserve further study owing to their good topoisomerase I inhibition activity. Future work will focus on cytotoxicity assays which can be carried out to evaluate the potential anticancer properties of these complexes that can effectively inhibit topoisomerase I.

As noted in Chapter 2, the series complexes $[Ni_2(HL)_2]$ did not form crystals to carry out the single X-ray diffraction studies, accordingly, the synthesis of these complexes by another alternative route, could lead to pure crystals, and thus to a further improved X-ray structure determination of the complexes. Additionally, it would be of interest to extend the characterization study to quantitatively analyze nickel(II) in all complexes by using atomic absorption of gravimetric analysis. Further study on the IR spectroscopy to include the region $400 - 200$ cm^{-1} would be of interest since this region can provide a good information about nickel-oxygen, nickel-nitrogen and nickel-phosphine stretching vibrations.

In the case of the nickel(II) thiourea complexes series, the inhibition ability of the mixed complexes is not yet fully understood. It may be advantageous to further study the precise mechanism by which these complexes produce their potent inhibition effect.

Since the complexation reaction of nickel(II) salts with 1,10-phenanthroline/2,2'-bipyridine and thiourea ligands yielded dinuclear complexes in which the thiourea ligands is bridging two nickel ions through its thiolate sulfur in the axial position and the co-ligand is taking the other two axial positions (see Chapter 4, Figure 4.3), it is of interest to try the reactions of nickel(II) salts with thiourea ligands in presence of potential bridging ligands, such as imidazole, pyrazine or 4,4'-dipyridyl. Interacting of these ligands with the nickel(II) solution, will substitute the two labile axial water molecules in the starting material $[Ni(H_2O)_6]^{2+}$ and hopefully bridge adjacent nickel(II) centers producing polymers (Figure 6.1). Since the mixed nickel(II) thiourea complex is paramagnetic, more work will be done in order to measure the magnetic susceptibility and investigate any potential magnetic coupling across the various bridges.
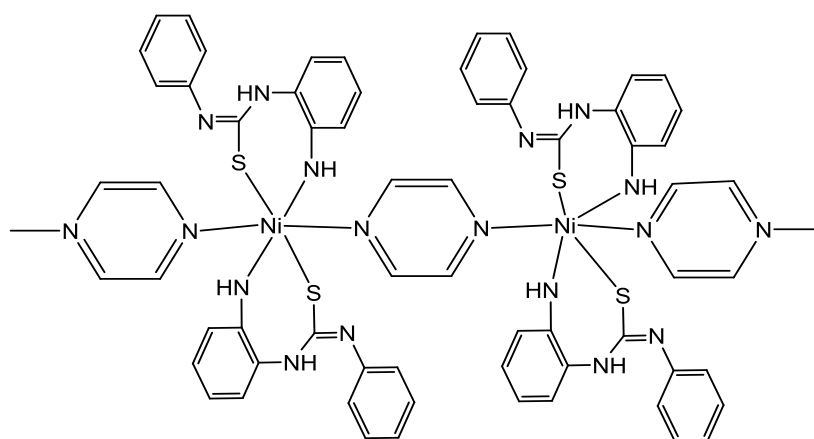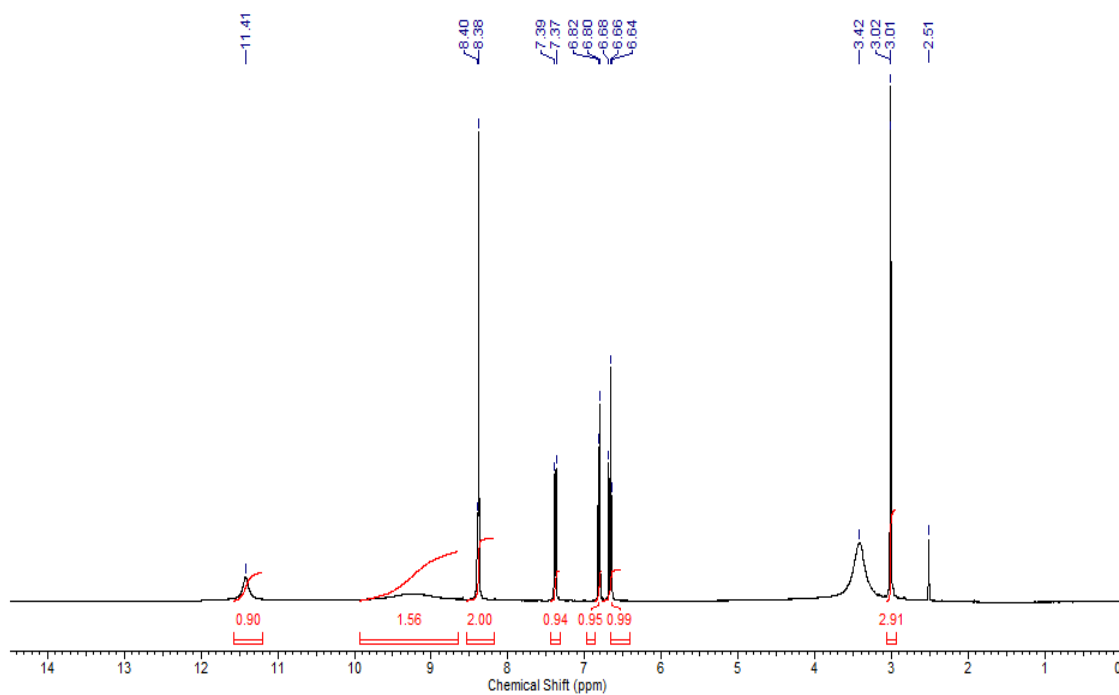

Figure 6.1: Proposed structure of a mixed nickel(II) thiourea complex with pyrazine
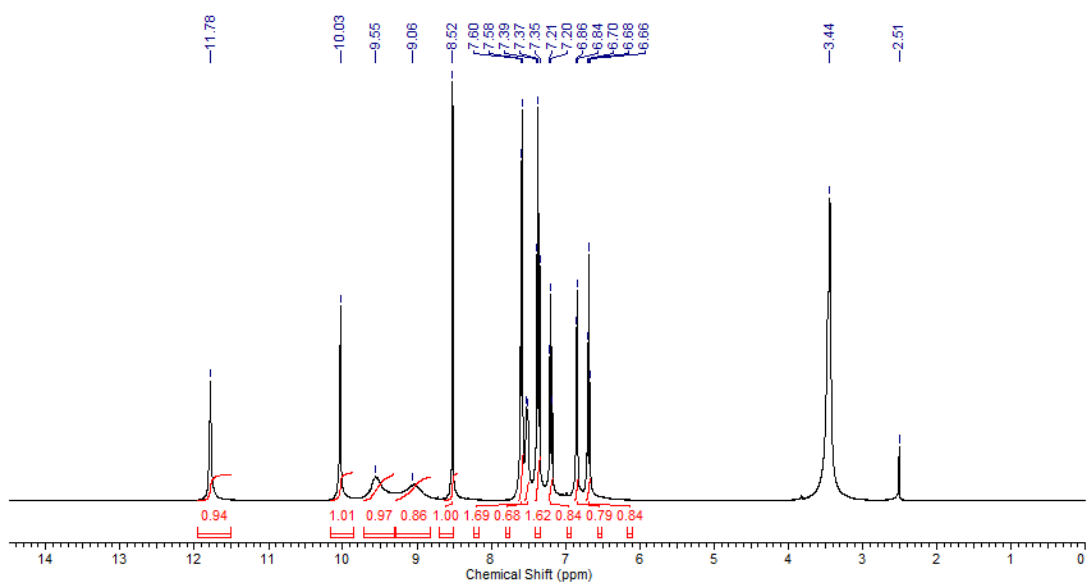
APPENDIX A

Spectra of compounds in chapter 2
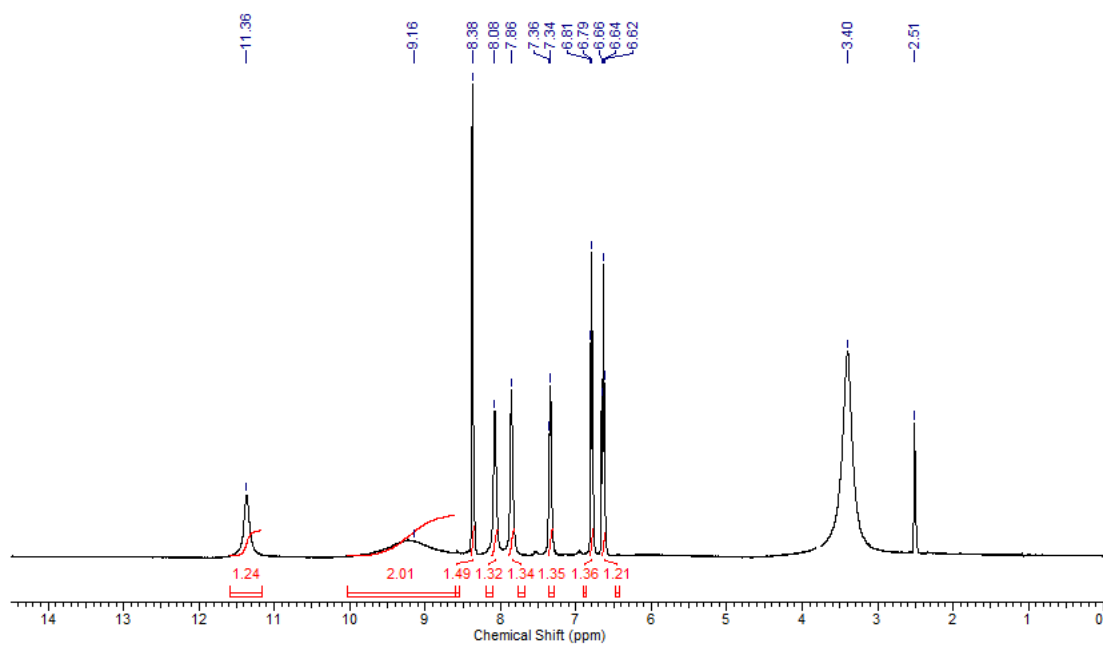
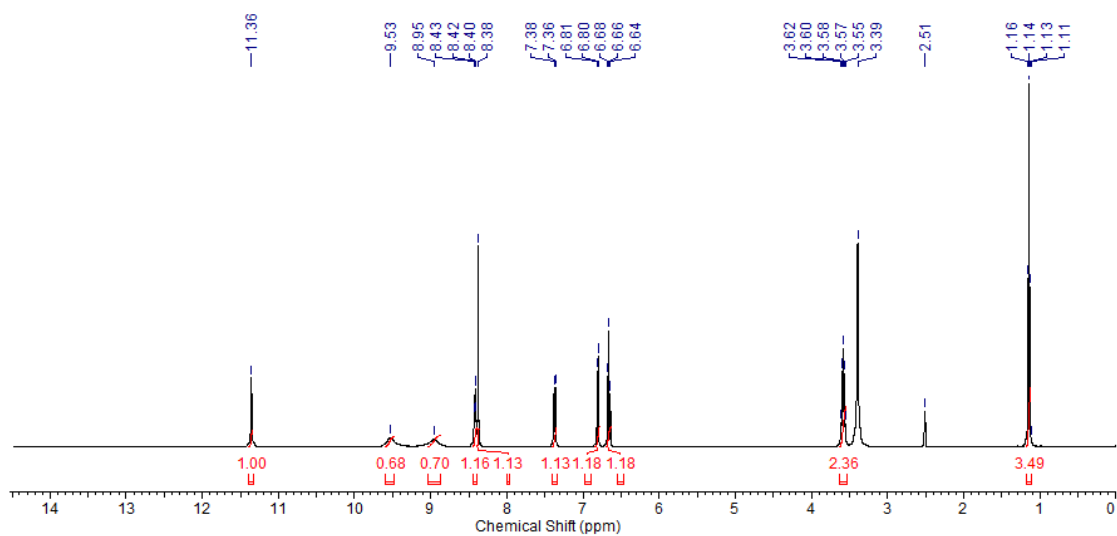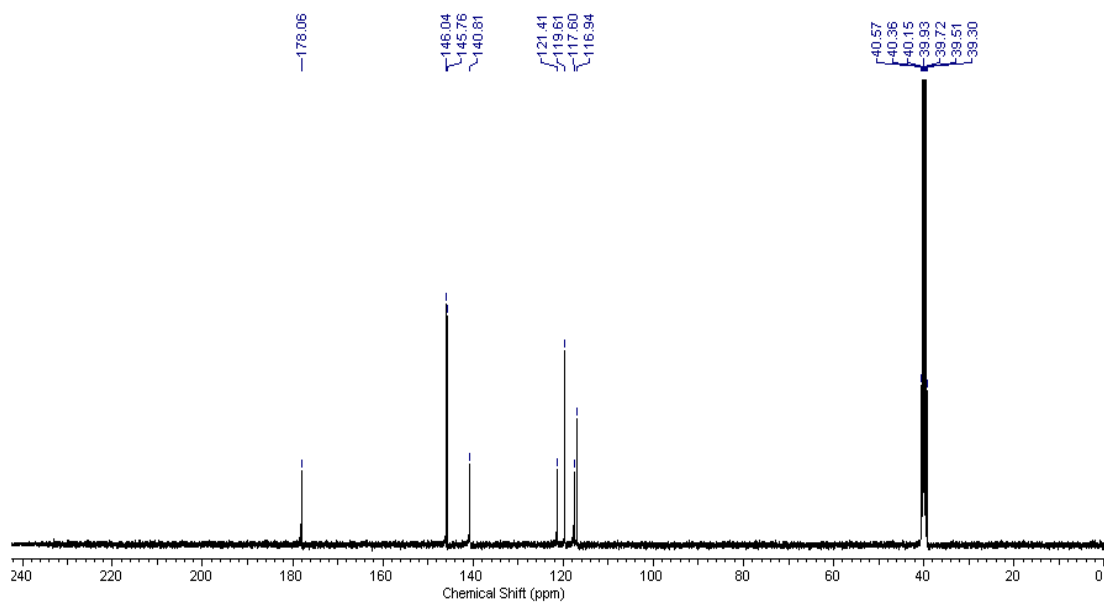**A1:** ^{1}H NMR spectrum of H_3L^1

A2: ^{1}H NMR spectrum of H_3L^2

A3: ^{1}H NMR spectrum of H_3L^3

A4: ^{1}H NMR spectrum of H_3L^4

A5: ^{13}C NMR spectrum of H_3L^1
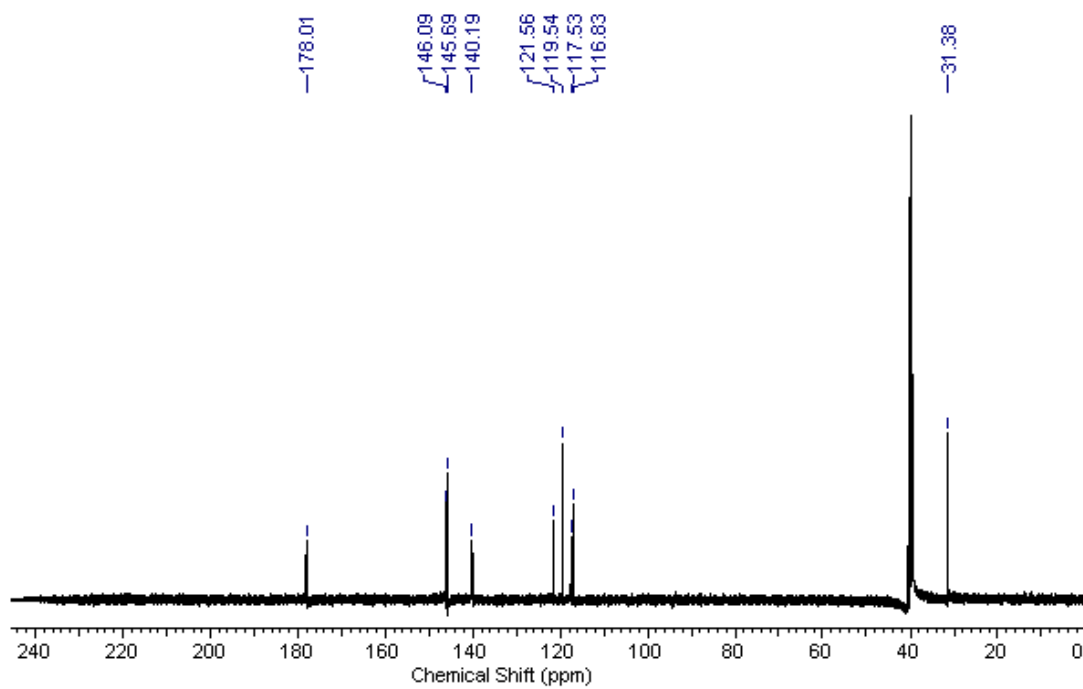
A6: ^{13}C NMR spectrum of H_3L^2
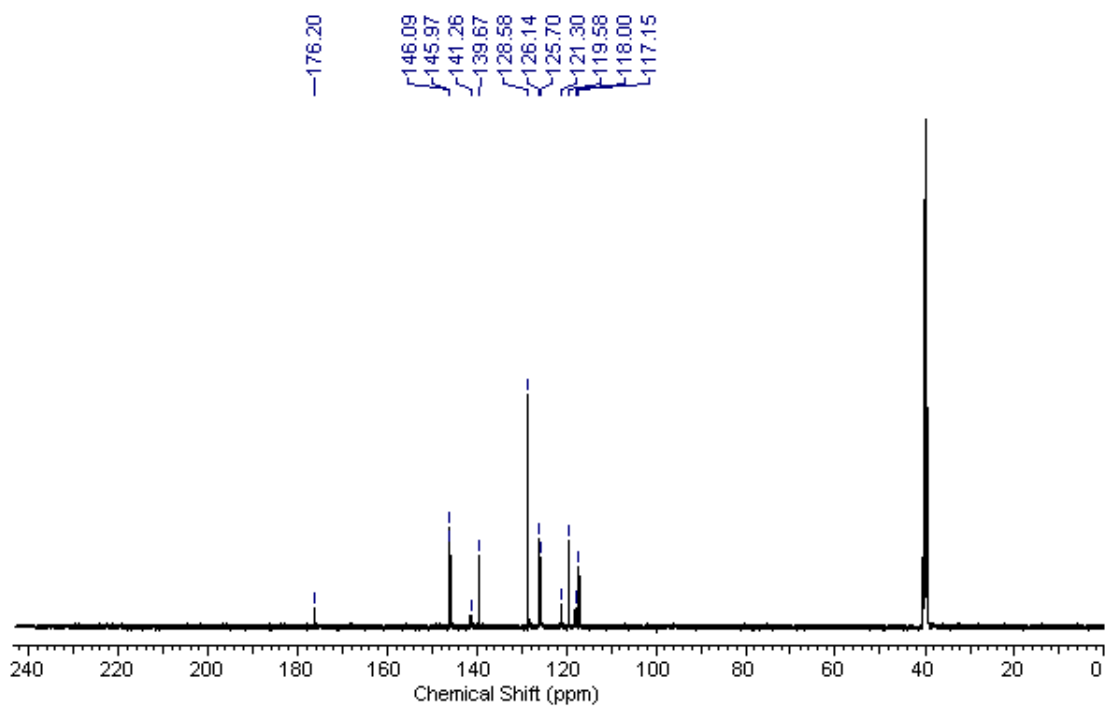
A9: ^{13}C NMR spectrum of H_3L^3
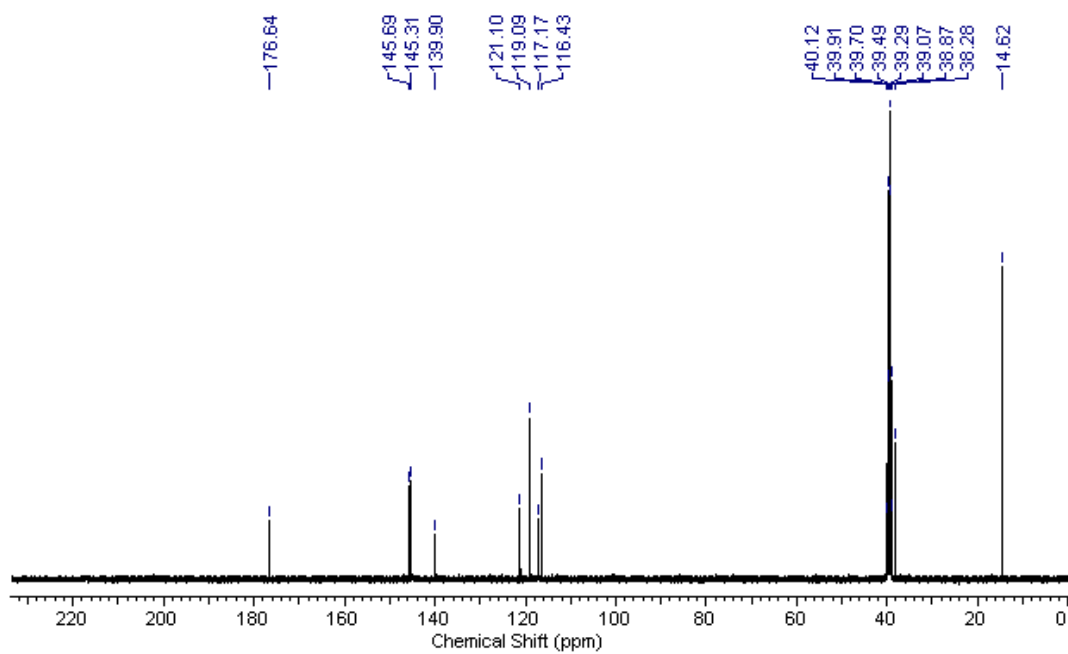
A10: ^{13}C NMR spectrum of H_3L^4
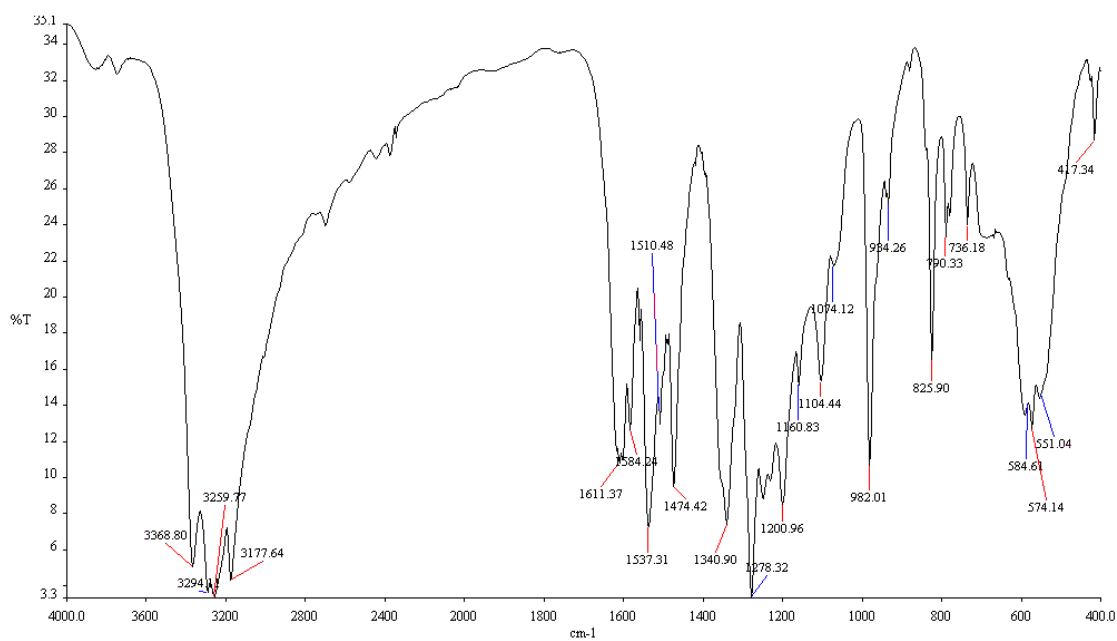
A11: IR spectrum of H_3L^1
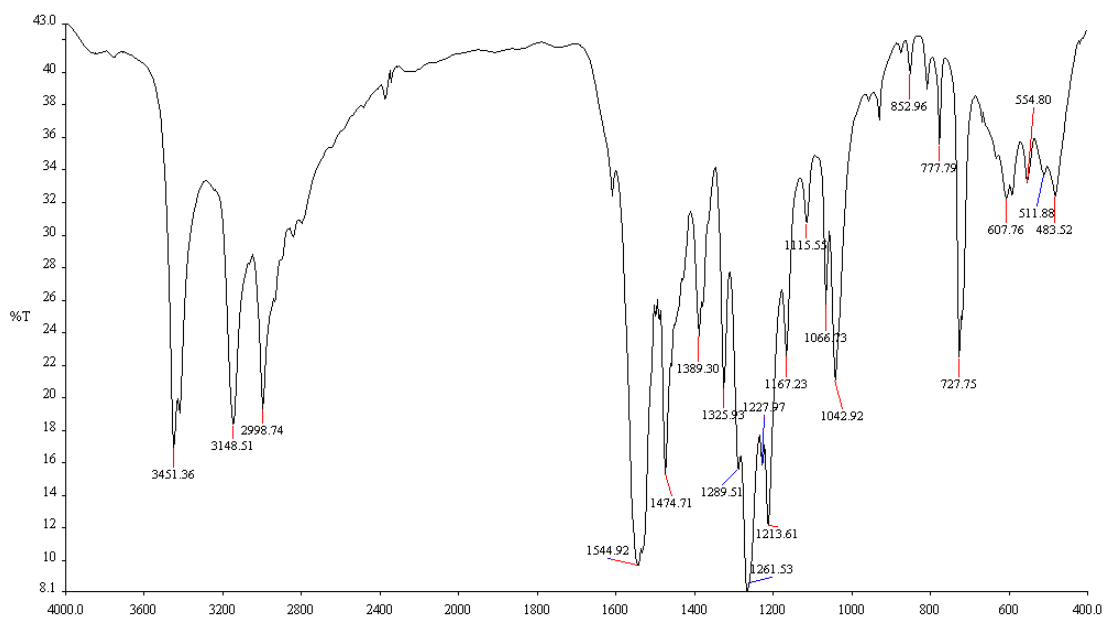
A12: IR spectrum of H_3L^2
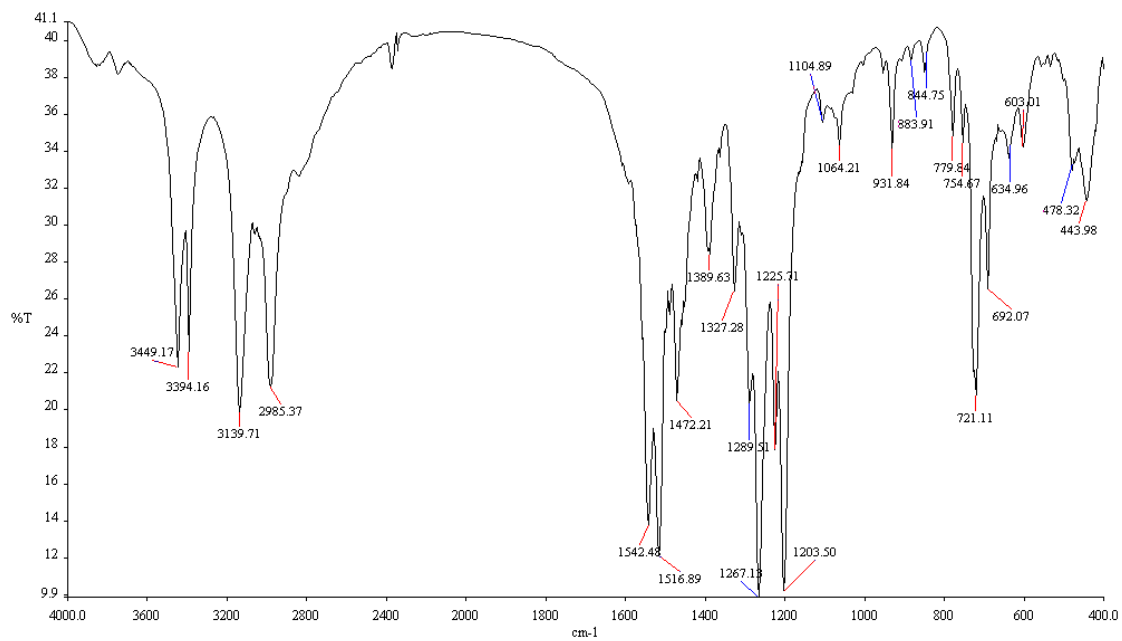
A13: IR spectrum of H_3L^3
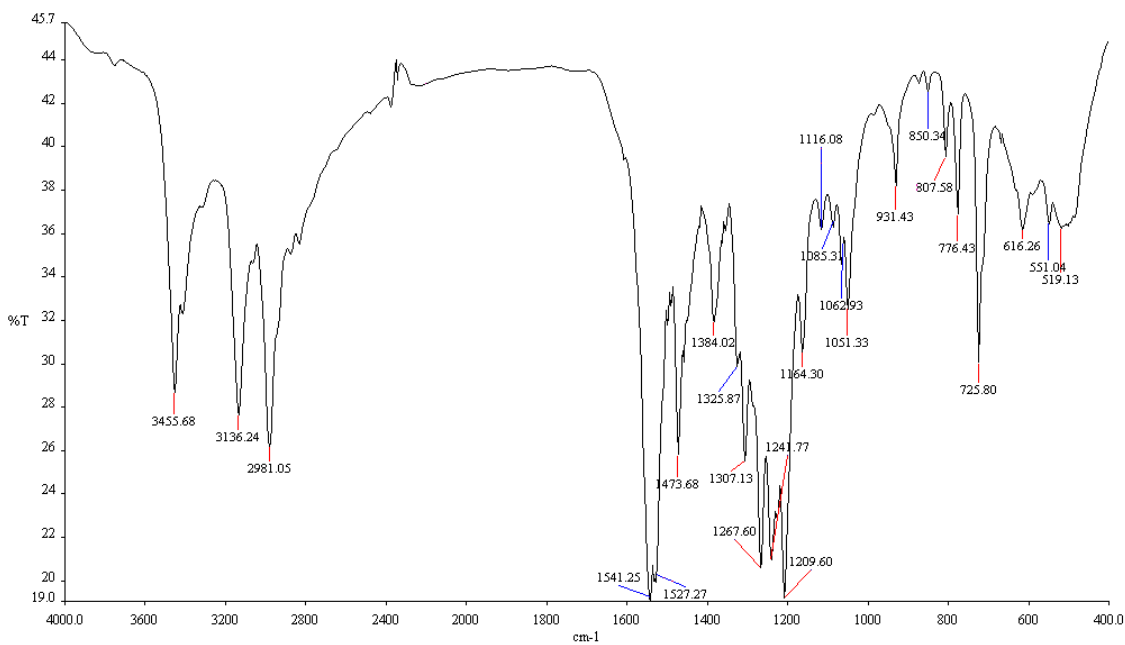
A14: IR spectrum of H_3L^4
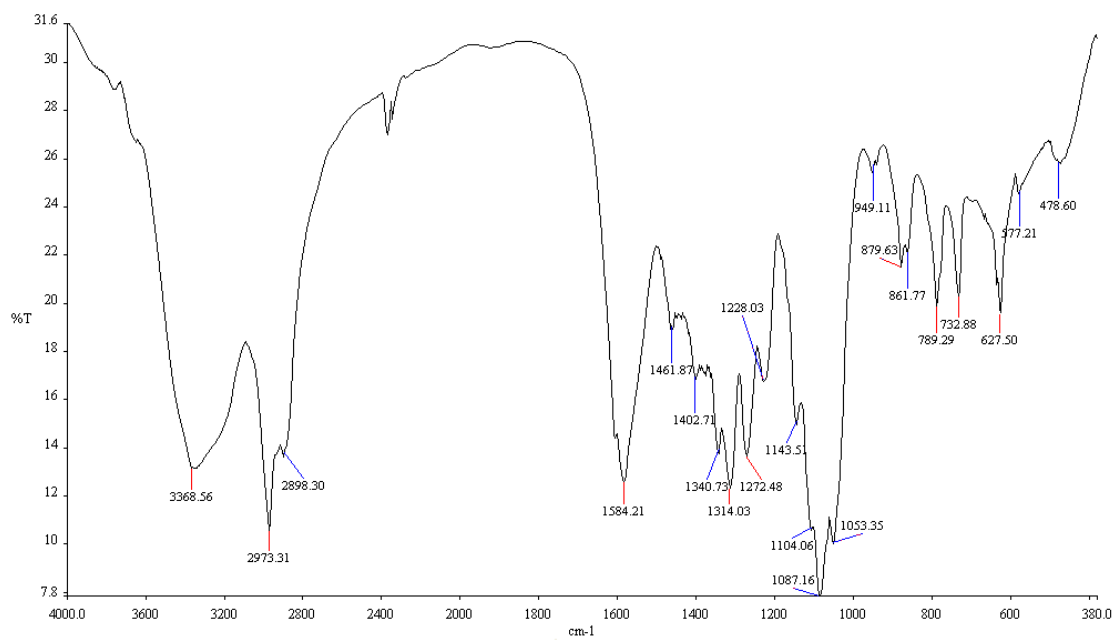
A15: IR spectrum of $[Ni(H_3L^2)(H_2L^2)]ClO_4.H_2O$ **(6)**
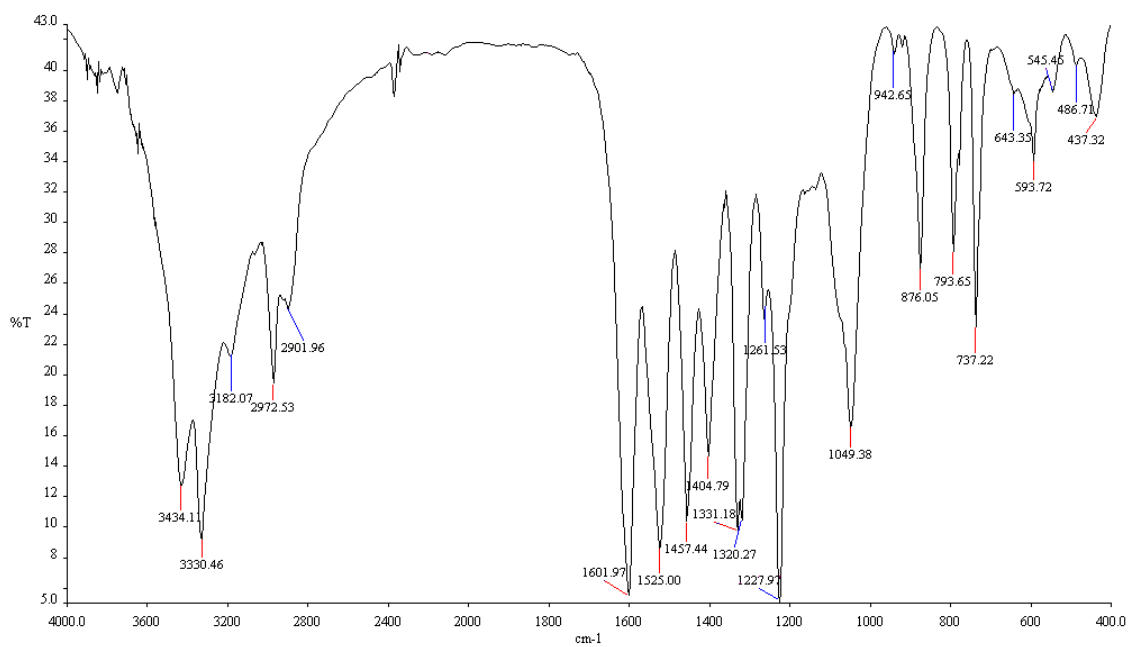
A16: IR spectrum of $[Ni_2(HL^1)_2]$ **(13)**
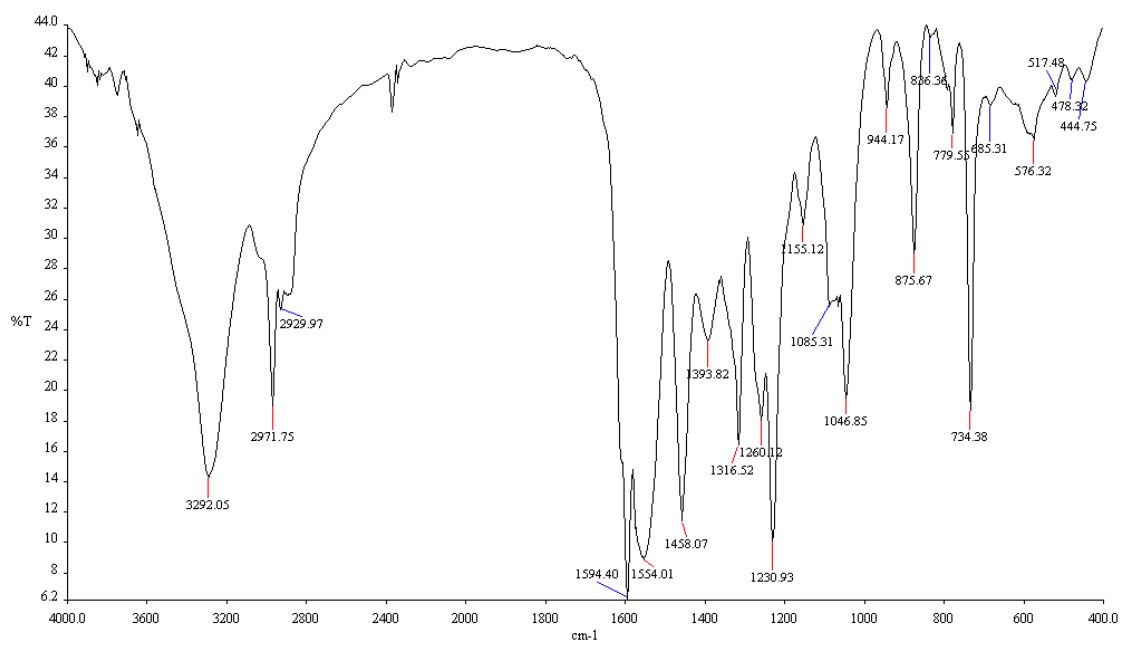
A17: IR spectrum of $[Ni_2(HL^4)_2]$ **(16)**

APPENDIX B

Spectra of compounds in chapter 3
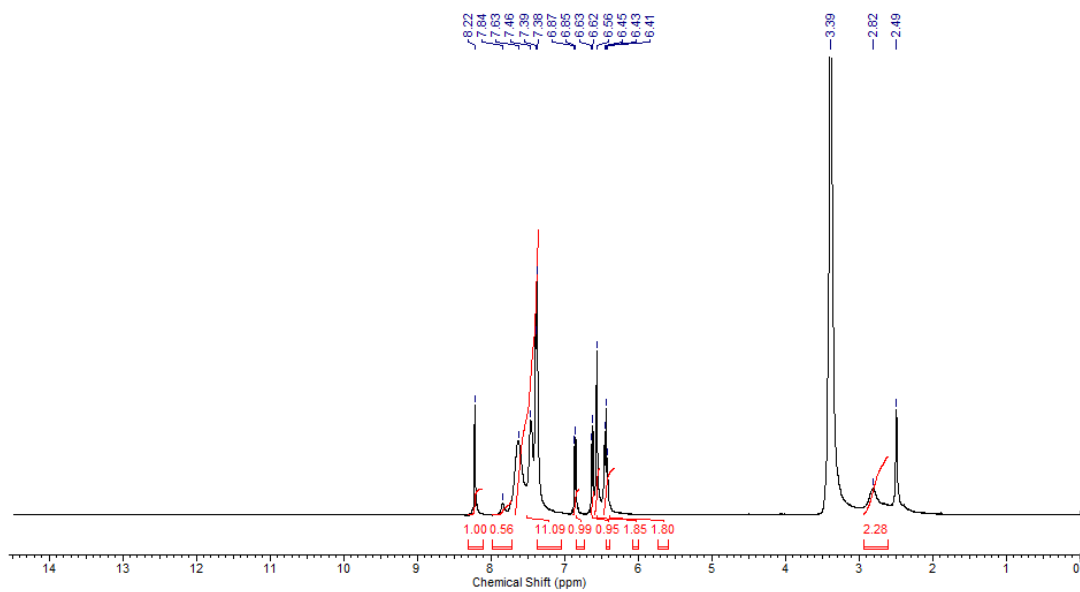
B1:^{1}H NMR spectrum of $[Ni_2(HL^1)_2(dppe)]$ **(21)**
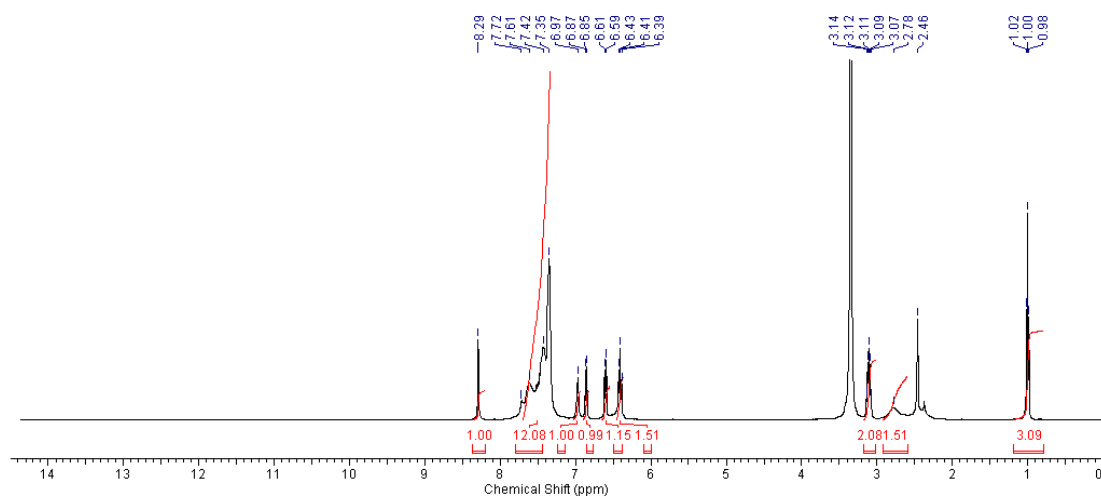
B2: ^{1}H NMR spectrum of $[Ni_2(HL^4)_2(dppe)]$ **(24)**
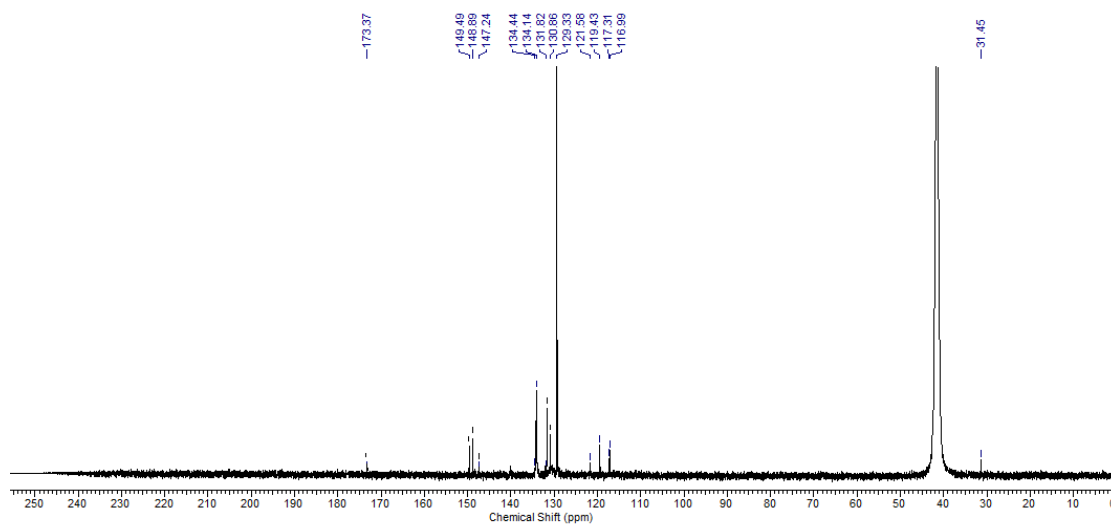
B3: ^{13}C NMR spectrum of [Ni(H$_2$L^2)(PPh$_3$)]Cl **(18)**
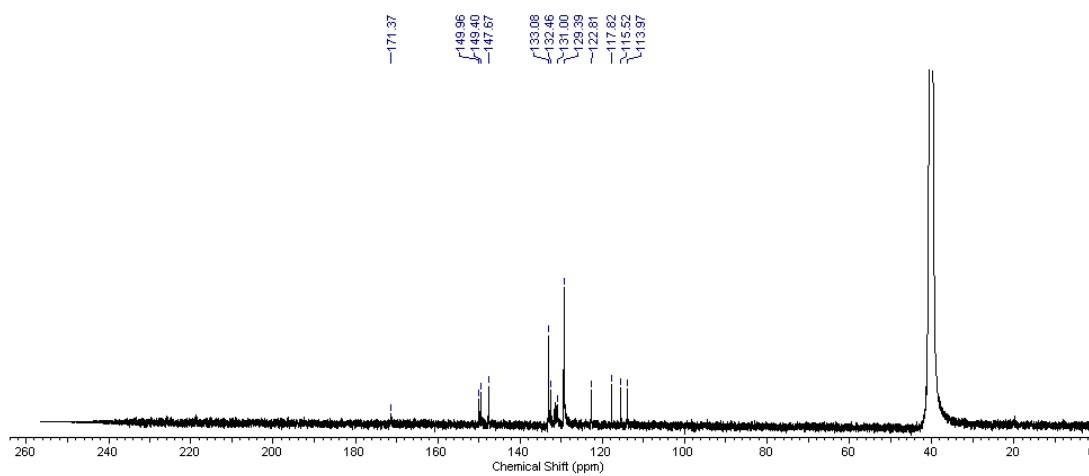
B4: ^{13}C NMR spectrum of [Ni$_2$(HL^1)$_2$(dppe)] **(21)**
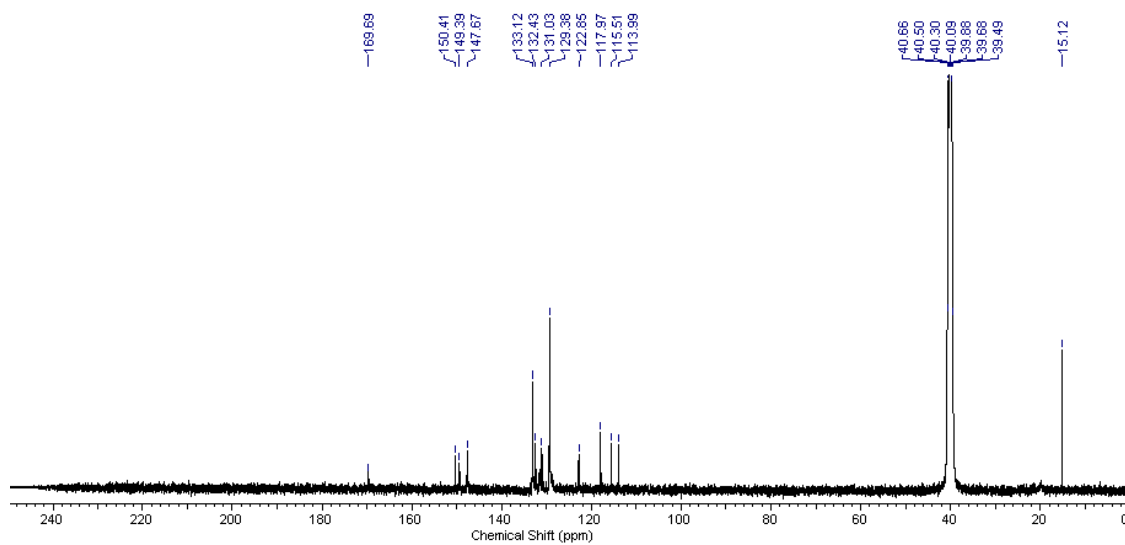
B5: ^{13}C NMR spectrum of [Ni$_2$(HL^4)$_2$(dppe)] **(24)**
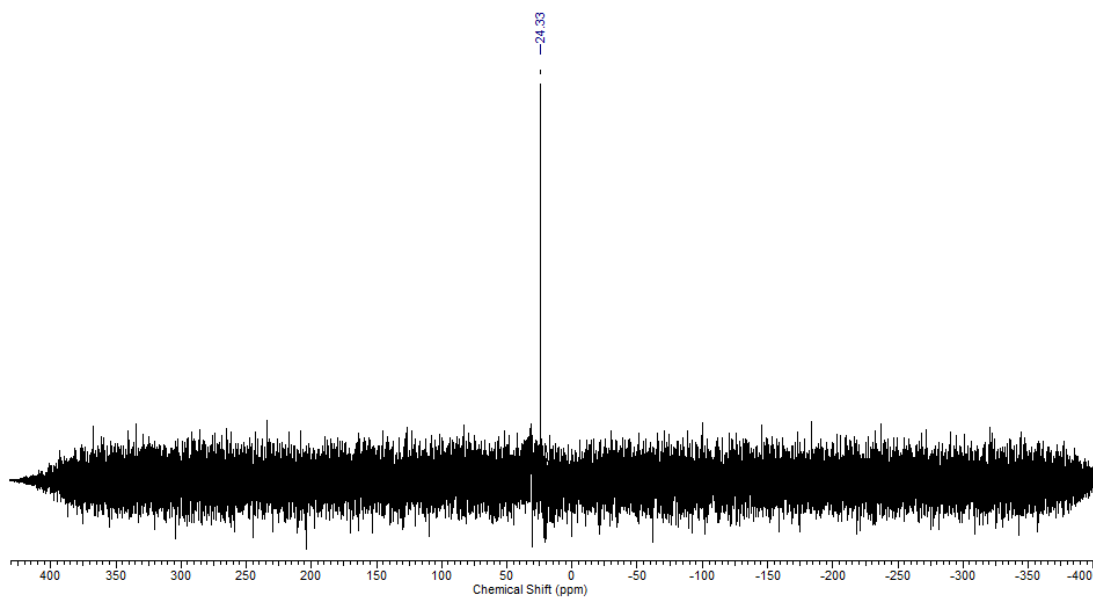
B6: ^{31}P NMR spectrum of [Ni(H$_2$L^2)(PPh$_3$)]Cl **(18)**
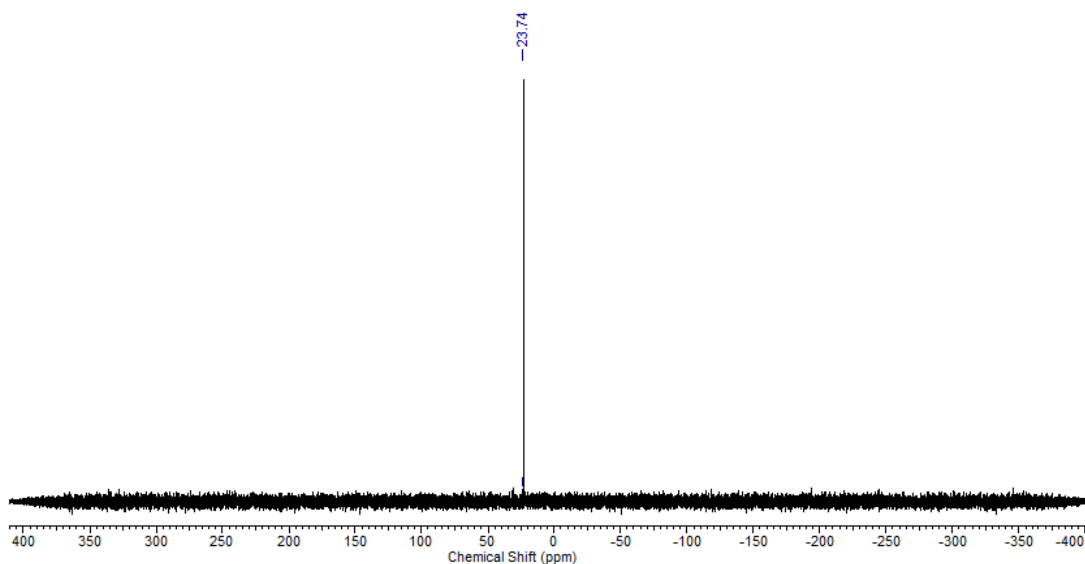
B7: ^{31}P NMR spectrum of [Ni(HL^3)(PPh$_3$)] **(19)**
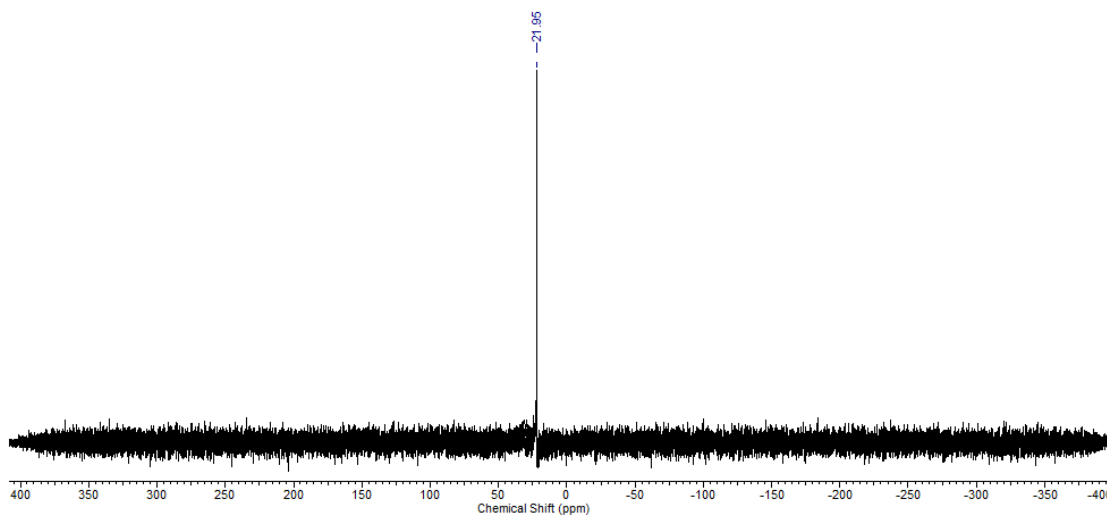
B8: ^{31}P NMR spectrum of [Ni$_2$(HL^2)$_2$(dppe)] **(22)**
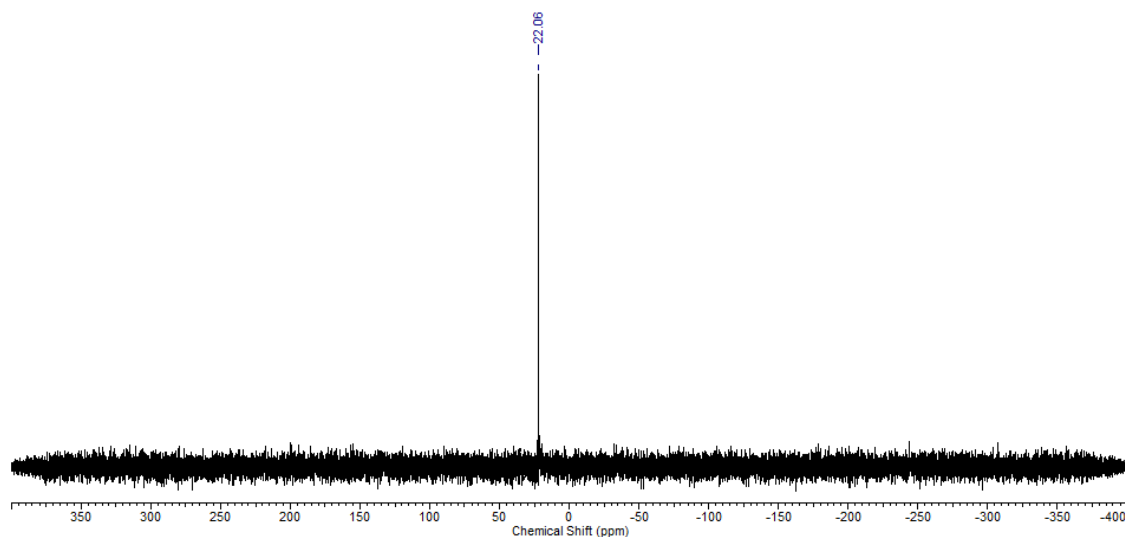
B9: ^{31}P NMR spectrum of [Ni$_2$(HL^4)$_2$(dppe)] **(24)**
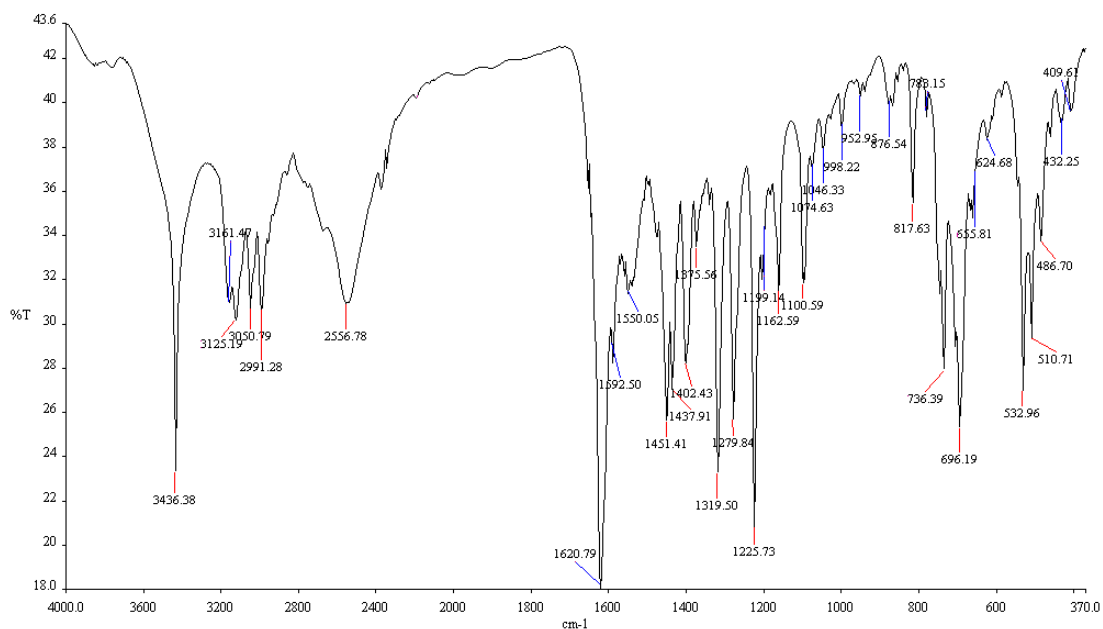
B10: IR spectrum for [Ni(H$_2$L^2)(PPh$_3$)]Cl **(18)**
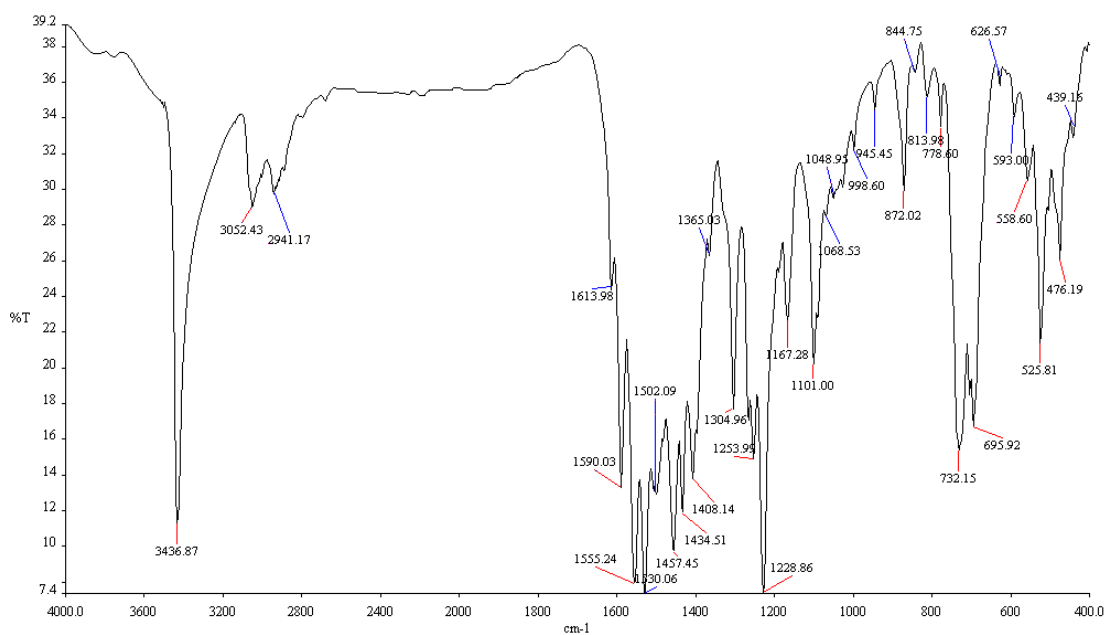
B11: IR spectrum of [Ni$_2$(HL^2)$_2$(dppe)] **(22)**
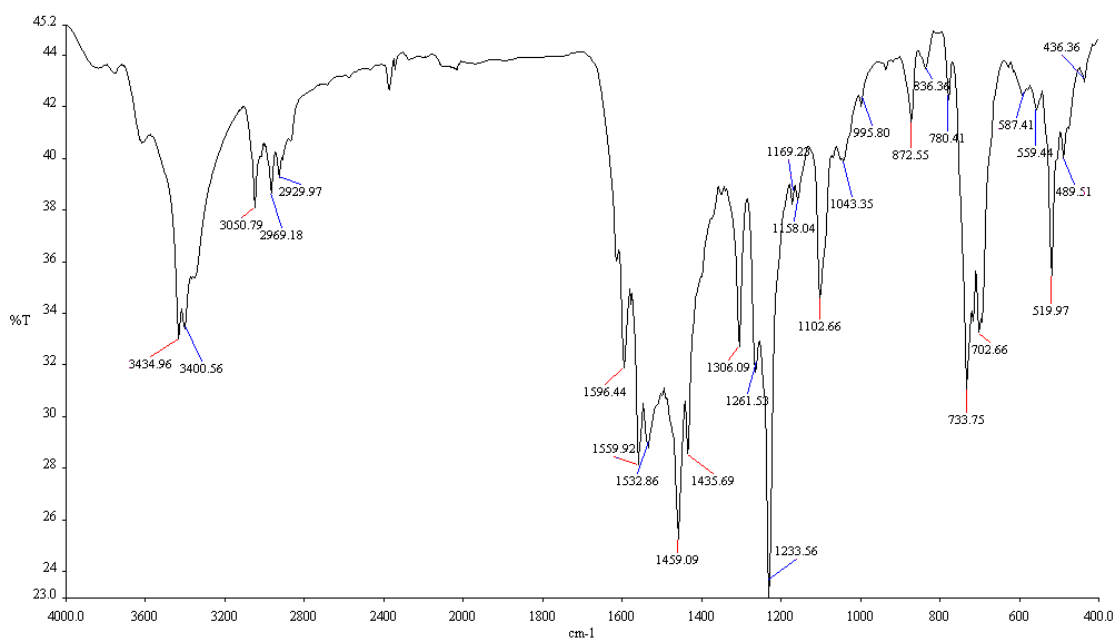
B12: IR spectrum of [Ni$_2$(HL^4)$_2$(dppe)] **(24)**

APPENDIX C

Spectra of compounds in chapter 4
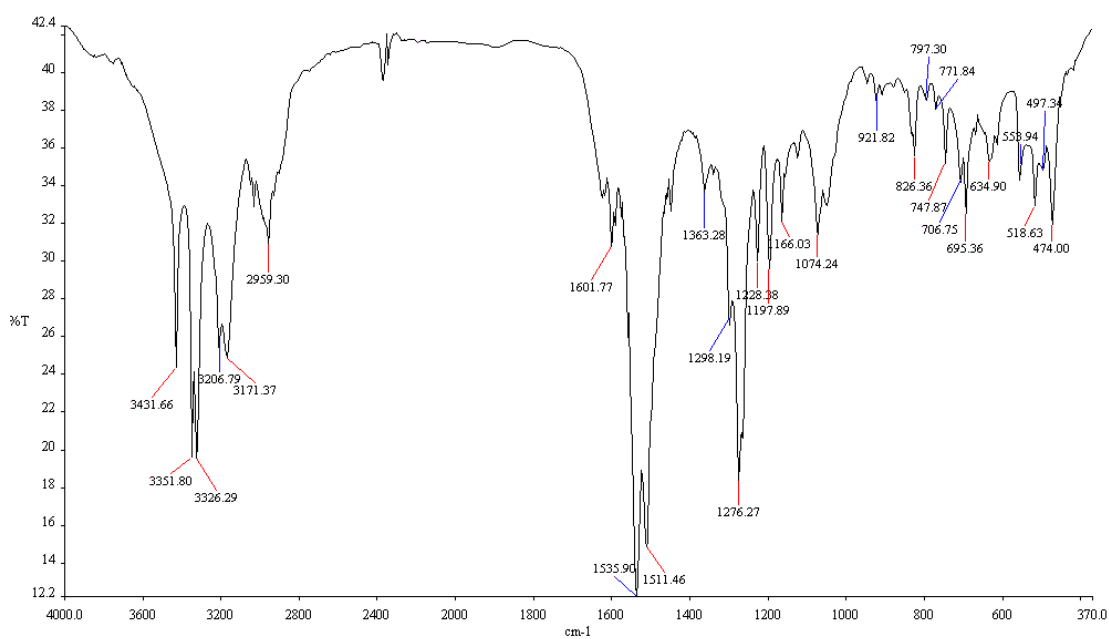
C1: IR spectrum of PhTUPh*p*-NH$_2$ **(26)**
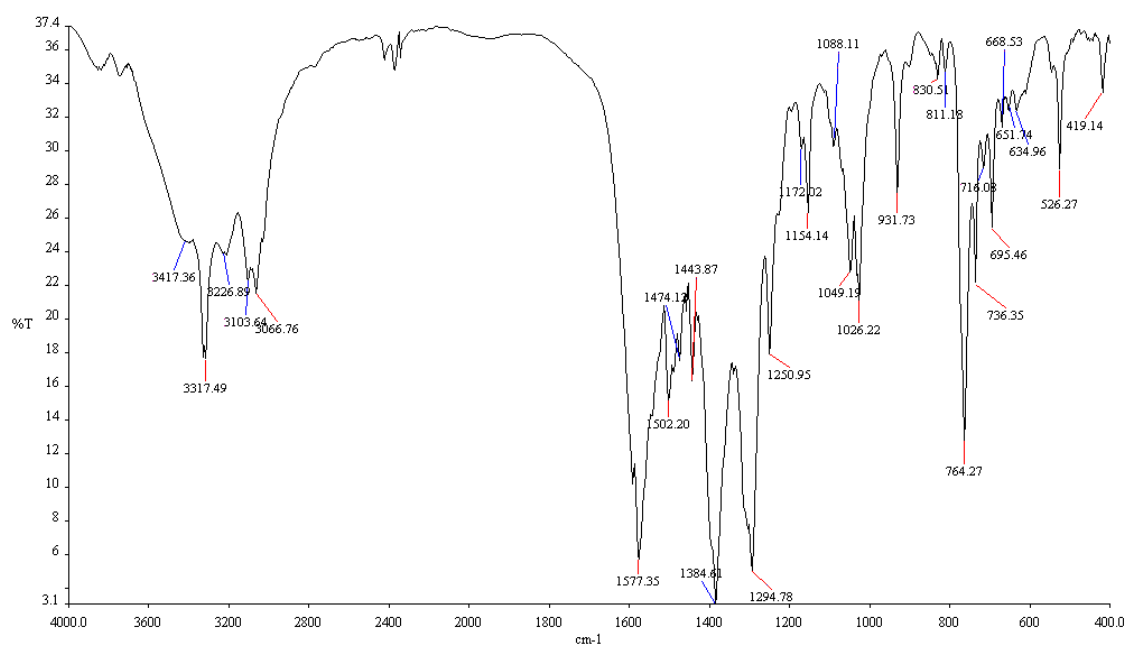
C2: IR spectrum of [Ni$_2$(PhTUPh*o*-NH$_2$)$_2$(Bpy)$_2$] (NO$_3$) **(30)**
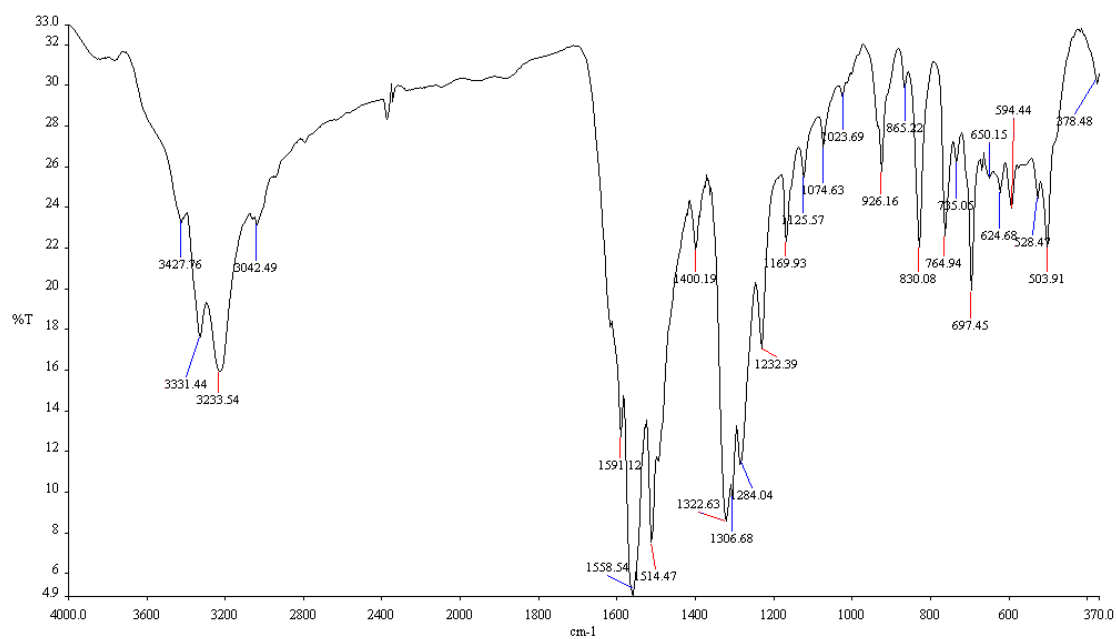
C3: IR spectrum of [Ni(PhTUPh*p*-NH$_2$)$_2$] **(31)**
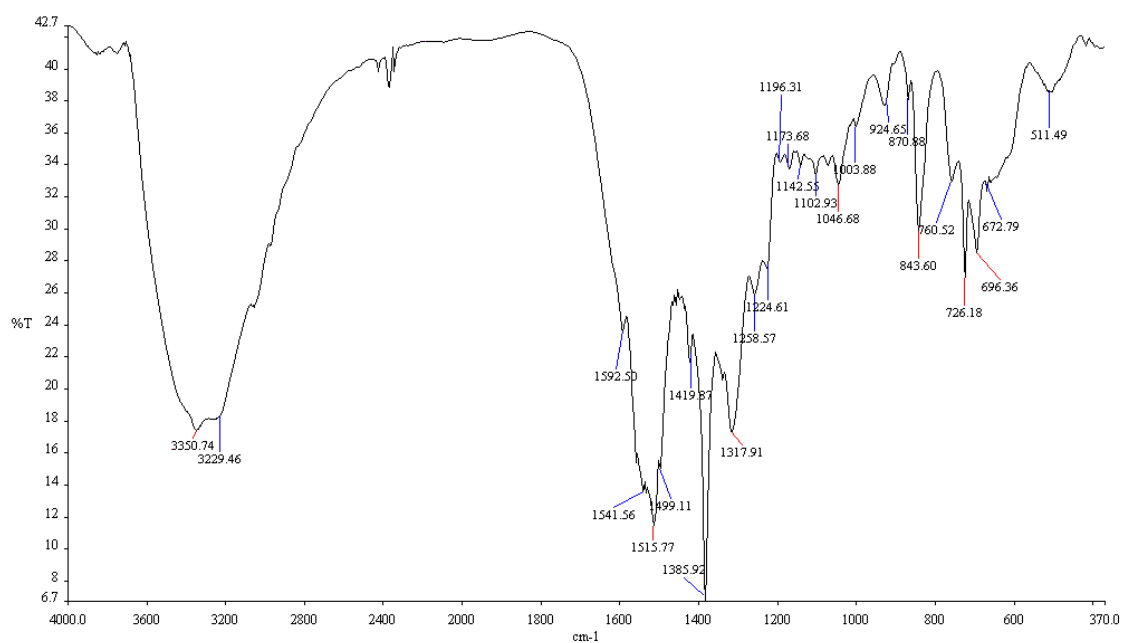
C4: IR spectrum of [Ni$_2$(PhTUPh*p*-NH$_2$)$_2$(Phen)$_2$](NO$_3$).2H$_2$O **(32)**
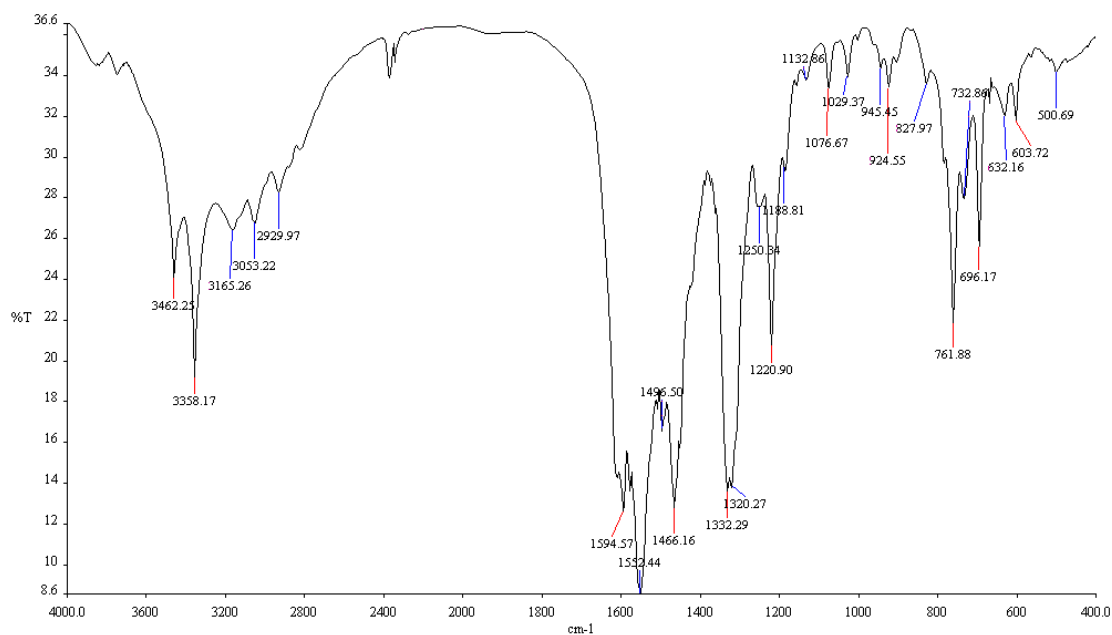
C5: IR spectrum of [Ni$_2$(PhTUPyo-NH$_2$)$_2$(Phen)$_2$]Cl **(35)**
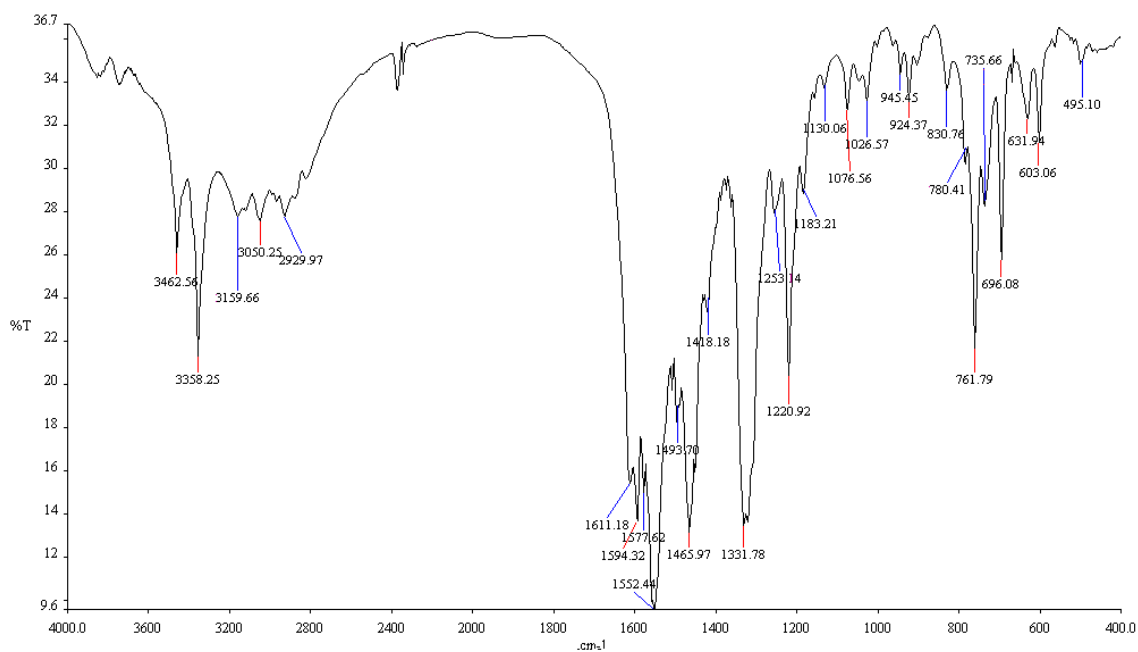
C6: IR spectrum of [Ni$_2$(PhTUPyo-NH$_2$)$_2$(Bpy)$_2$]Cl **(37)**

APPENDIX D

Images of compounds in chapter 5
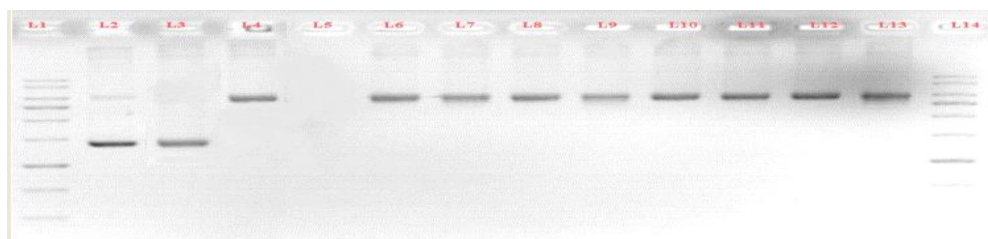
D1: Topoisomerase I inhibition assay by gel electrophoresis for H_3L^2

Electrophoresis results of incubating *E.coli* topoisomerase I (0.25unit/21μL) with pBR322 in the absence or presence of varying concentration of the ligand H_3L^2 : Lane 1&14 Gene Ruler 1-kb DNA ladder, lane 2 DNA alone, lane 3 DNA + 500 μM ligand (control), lane 4 DNA +0.25 U topoisomerase I (control), lane 5 empty, Lane 6-13 Topoisomerase I with increasing concentration of ligand: lane 6, 5 μM; lane 7, 10 μM; lane 8, 20 μM; lane 9, 40 μM; lane 10, 80 μM; lane 11, 160μM; lane 12, 250 μM; lane 13, 500 μM
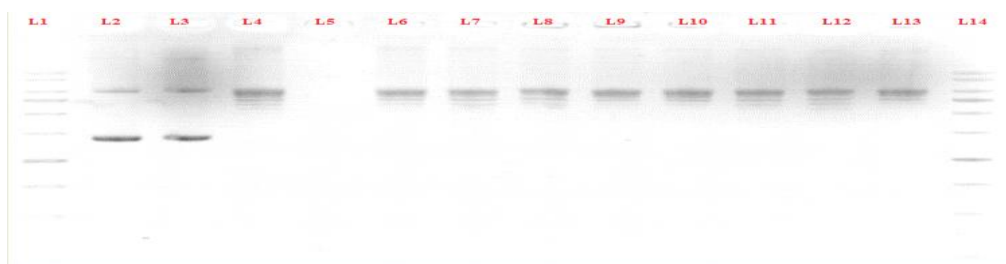
D2: Topoisomerase I inhibition assay by gel electrophoresis for H_3L^4

Electrophoresis results of incubating *E.coli* topoisomerase I (0.25unit/21μL) with pBR322 in the absence or presence of varying concentration of the ligand H_3L^4 : Lane 1&14 Gene Ruler 1-kb DNA ladder, lane 2 DNA alone, lane 3 DNA + 500 μM ligand (control), lane 4 DNA +0.25 U topoisomerase I (control), lane 5 empty, Lane 6-13 Topoisomerase I with increasing concentration of ligand: lane 6, 5 μM; lane 7, 10 μM; lane 8, 20 μM; lane 9, 40 μM; lane 10, 80μM; lane 11, 160 μM; lane 12, 250 μM; lane 13, 500 μM
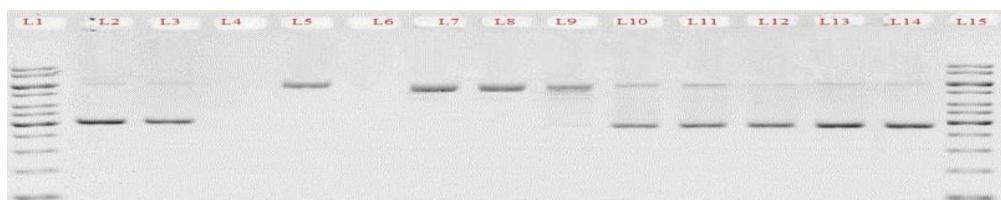
D3: Topoisomerase I inhibition assay by gel electrophoresis for $[Ni(H_3L^2)(H_2L^2)]ClO_4$(**6**)

Electrophoresis results of incubating *E.coli* topoisomerase I (0.25unit/21μL) with pBR322 in the absence or presence of varying concentration of complex **6** : Lane 1&15 Gene Ruler 1-kb DNA ladder, lane 2 DNA alone, lane 3 DNA + 500 μM ligand (control), lane 4 empty, lane 5 DNA +0.25 U topoisomerase I (control), lane 6 empty, Lane 7-14 topoisomerase I with increasing concentration of the complex: lane 7, 5 μM; lane 8, 10 μM; lane 9, 20 μM; lane 10, 40 μM; lane 11, 80 μM; lane 12, 160 μM; lane 13, 250μM; lane 14, 500 μM

D4: Topoisomerase I inhibition assay by gel electrophoresis for

$[Ni(H_3L^4)(H_2L^4)]ClO_4.H_2O$ (**8**)

Electrophoresis results of incubating *E.coli* topoisomerase I (0.25unit/21μL) with pBR322 in the absence or presence of varying concentration of complex **8** : Lane 1&15 Gene Ruler 1-kb DNA ladder, lane 2 DNA alone, lane 3 DNA + 500 μM ligand (control), lane 4 empty, lane 5 DNA +0.25 U topoisomerase I (control), lane 6 empty, Lane 7-14 topoisomerase I with increasing concentration of the complex: lane 7, 5 μM; lane 8, 10 μM; lane 9, 20 μM; lane 10, 40 μM; lane 11, 80 μM; lane 12, 160 μM; lane 13, 250 μM; lane 14, 500 μM

D5: Topoisomerase I inhibition assay by gel electrophoresis for $[Ni_2(HL^2)_2].H_2O$(**14**)

Electrophoresis results of incubating *E.coli* topoisomerase I (0.25unit/21μL) with pBR322 in the absence or presence of varying concentration of complex 14 : Lane 1&15 Gene Ruler 1-kb DNA ladder, lane 2 DNA alone, lane 3 DNA + 500 μM ligand (control), lane 4 empty, lane 5 DNA +0.25 U topoisomerase I (control), lane 6 empty, Lane 7-14 topoisomerase I with increasing concentration of the complex: lane 7, 5 μM; lane 8, 10 μM; lane 9, 20 μM; lane 10, 40 μM; lane 11, 80 μM; lane 12, 160 μM; lane 13, 250 μM; lane 14, 500 μM

D6: Topoisomerase I inhibition assay by gel electrophoresis for $[Ni_2(HL^4)_2]$ (**16**)

Electrophoresis results of incubating *E.coli* topoisomerase I (0.25unit/21μL) with pBR322 in the absence or presence of varying concentration of complex **16** : Lane 1&15 Gene Ruler 1-kb DNA ladder, lane 2 DNA alone, lane 3 DNA + 500 μM ligand (control), lane 4 empty, lane 5 DNA +0.25 U topoisomerase I (control), lane 6 empty, Lane 7-14 topoisomerase I with increasing concentration of the complex: lane 7, 5 μM; lane 8, 10 μM; lane 9, 20 μM; lane 10, 40 μM; lane 11, 80 μM; lane 12, 160 μM; lane 13, 250 μM; lane 14, 500 μM

D7: Topoisomerase I inhibition assay by gel electrophoresis for $[Ni(H_2L^2)(PPh_3)]Cl$ **(18)**

Electrophoresis results of incubating *E.coli* topoisomerase I (0.25unit/21μL) with pBR322 in the absence or presence of varying concentration of complex **18** : Lane 1&15 Gene Ruler 1-kb DNA ladder, lane 2 DNA alone, lane 3 DNA + 500 μM ligand (control), lane 4 empty, lane 5 DNA +0.25 U topoisomerase I (control), lane 6 empty, Lane 7-14 topoisomerase I with increasing concentration of the complex: lane 7, 5 μM; lane 8, 10 μM; lane 9, 20 μM; lane 10, 40 μM; lane 11, 80 μM; lane 12, 160μM; lane 13, 250 μM; lane 14, 500 μM
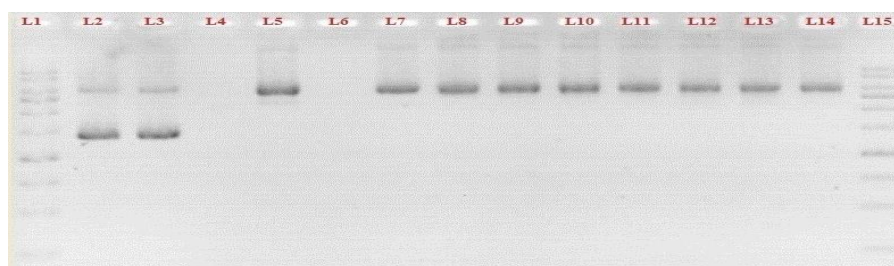
D8: Topoisomerase I inhibition assay by gel electrophoresis for $[Ni(HL^4)(PPh_3)]$ **(20)**

Electrophoresis results of incubating *E.coli* topoisomerase I (0.25unit/21μL) with pBR322 in the absence or presence of varying concentration of complex **20** : Lane 1&15 Gene Ruler 1-kb DNA ladder, lane 2 DNA alone, lane 3 DNA + 500 μM ligand (control), lane 4 empty, lane 5 DNA +0.25 U topoisomerase I (control), lane 6 empty, Lane 7-14 topoisomerase I with increasing concentration of the complex: lane 7, 5 μM; lane 8, 10 μM; lane 9, 20 μM; lane 10, 40 μM; lane 11, 80 μM; lane 12, 160 μM; lane 13, 250 μM; lane 14, 500 μM
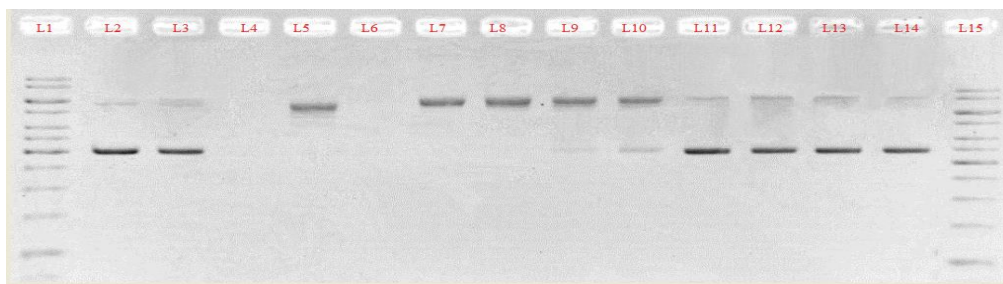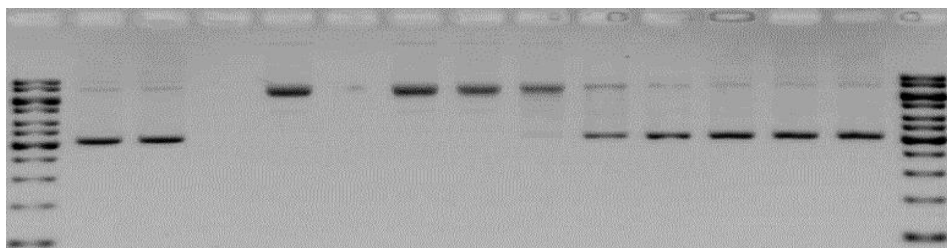
D8: Topoisomerase I inhibition assay by gel electrophoresis for $[Ni_2(HL^2)_2(dppe)]$ **(22)**

Electrophoresis results of incubating *E.coli* topoisomerase I (0.25unit/21μL) with pBR322 in the absence or presence of varying concentration of complex **22** : Lane 1&15 Gene Ruler 1-kb DNA ladder, lane 2 DNA alone, lane 3 DNA + 500 μM ligand (control), lane 4 empty, lane 5 DNA +0.25 U topoisomerase I (control), lane 6 empty, Lane 7-14 topoisomerase I with increasing concentration of the complex: lane 7, 5 μM; lane 8, 10 μM; lane 9, 20 μM; lane 10, 40 μM; lane 11, 80μM; lane 12, 160μM; lane 13, 250 μM; lane 14, 500μM
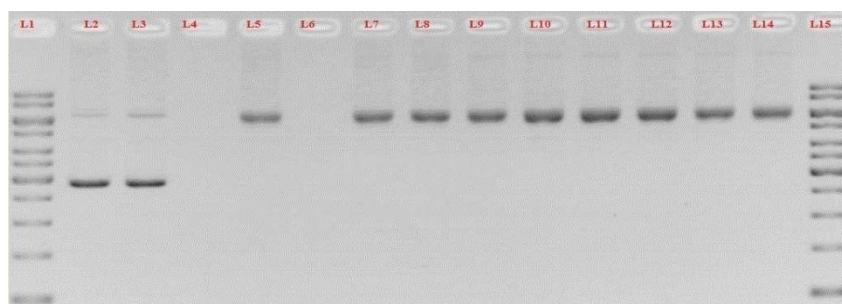
D9: Topoisomerase I inhibition assay by gel electrophoresis for PhTUPh*p*-NH$_2$ **(26)**

Electrophoresis results of incubating *E.coli* topoisomerase I (0.25unit/21μL) with pBR322 in the absence or presence of varying concentration of ligand **26** : Lane 1&15 Gene Ruler 1-kb DNA ladder, lane 2 DNA alone, lane 3 DNA + 500 μM complex (control), lane 4 empty, lane 5 DNA +0.25 U topoisomerase I (control), lane 6 empty, Lane 7-14 topoisomerase I with increasing concentration of the ligand: lane 7, 5 μM; lane 8, 10 μM; lane 9, 20 μM; lane 10, 40 μM; lane 11, 80 μM; lane 12, 160 μM; lane 13, 250 μM; lane 14, 500 μM
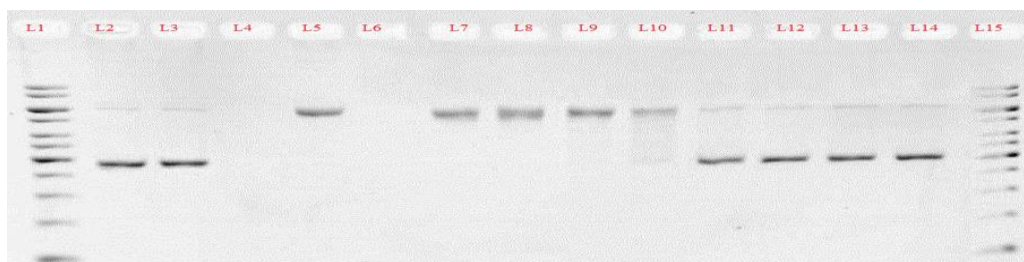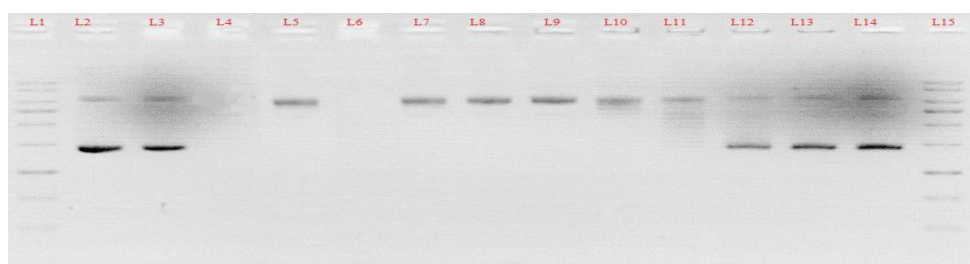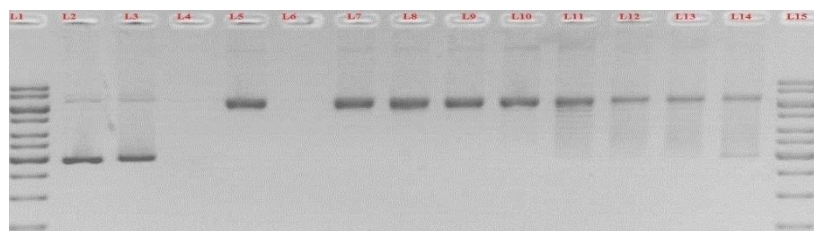
D10: Topoisomerase I inhibition assay by gel electrophoresis for the complex [Ni(PhTUPh*p*-NH$_2$)$_2$].H$_2$O **(31)**

Electrophoresis results of incubating *E.coli* topoisomerase I (0.25unit/21µL) with pBR322 in the absence or presence of varying concentration of the complex **31** : Lane 1&15 Gene Ruler 1-kb DNA ladder, lane 2 DNA alone, lane 3 DNA + 500 µM ligand (control), lane 4 empty, lane 5 DNA +0.25 U topoisomerase I (control), lane 6 empty, Lane 7-14 topoisomerase I with increasing concentration of the complex: lane 7, 5 µM; lane 8, 10 µM; lane 9, 20 µM; lane 10, 40 µM; lane 11, 80 µM; lane 12, 160 µM; lane 13, 250 µM; lane 14, 500 µM
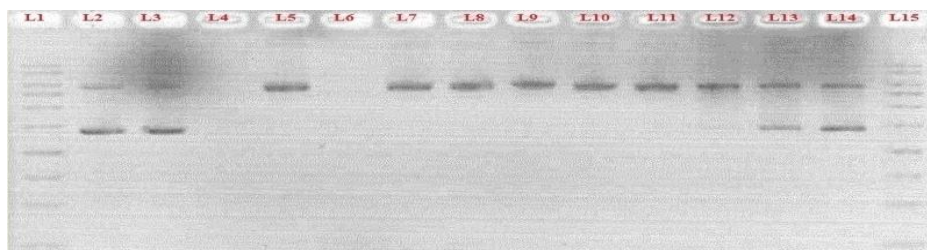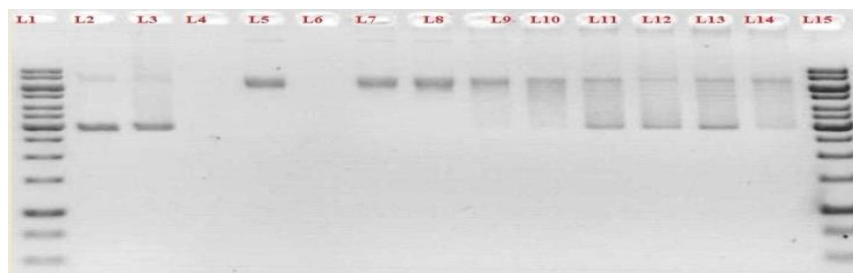

D11: Topoisomerase I inhibition assay by gel electrophoresis for the complex [Ni$_2$(PhTUPh*p*-NH$_2$)$_2$(Phen)$_2$]NO$_3$.2H$_2$O **(32)**

Electrophoresis results of incubating *E.coli* topoisomerase I (0.25unit/21µL) with pBR322 in the absence or presence of varying concentration of complex **32** : Lane 1&15 Gene Ruler 1-kb DNA ladder, lane 2 DNA alone, lane 3 DNA + 500 µM ligand (control), lane 4 empty, lane 5 DNA +0.25 U topoisomerase I (control), lane 6 empty, Lane 7-14 topoisomerase I with increasing concentration of the complex: lane 7, 5 µM; lane 8, 10 µM; lane 9, 20 µM; lane 10, 40 µM; lane 11, 80 µM; lane 12, 160 µM; lane 13, 250 µM; lane 14, 500 µM

REFERENCES

Acharyya, R., Dutta, S., Basuli, F., Peng, S.-M., Lee, G.-H., Falvello, L. R., & Bhattacharya, S. (2006). Rhodium assisted C-H activation of benzaldehyde thiosemicarbazones and their oxidation via activation of molecular oxygen. *Inorg. Chem., 45*, 1252-1259.

Affan, M. A., Salam, M. A., Ahmad, F. B., Ismail, J., Shamsuddin, M. B., & Ali, H. M. (2011). Synthesis and spectroscopic characterization of organotin(IV) complexes with 2-benzoylpyridine-N(4)-cyclohexylthiosemicarbazone (HBPCT): X-ray crystal structure of [PhSnCl$_2$(BPCT)]. *Inorg.Chim.Acta, 366*, 227-232.

Afrasiabi, Z., Sinn, E., Chen, J., Ma, Y., Rheingold, A. L., Zakharov, L. N., Rath, N., & Padhye, S. (2004). Appended 1,2-naphthoquinones as anticancer agents 1: synthesis, structural, spectral and antitumor activities of ortho-naphthaquinone thiosemicarbazone and its transition metal complexes. *Inorg. Chim. Acta 357*, 271-278.

Afrasiabi, Z., Sinn, E., Lin, W., Ma, Y., Campana, C., & Padhye, S. (2005). Nickel (II) complexes of naphthaquinone thiosemicarbazone and semicarbazone: Synthesis, structure, spectroscopy, and biological activity. *J.Inorg.Biochem., 99,* 1526-1531.

Ahmad, S., Isab, A. A., & Ashraf, W. (2002). Multinuclear NMR (^{1}H, ^{13}C, ^{15}N and [107]Ag) studies of the silver cyanide complexes of thiourea and substituted thioureas. *Inorg. Chem. Commun., 5*, 816-819.

Al-Mjeni, F., Ju, T., Pochapsky, T. C., & Maroney, M. J. (2002). XAS investigation of the structure and function of Ni in acireductone dioxygenase. *Biochem., 41*, 6761-6769.

Ali, M. A., Mirza, A. H., Chartres, J. D., & Bernhardt, P. V. (2011). Synthesis, characterization and X-ray crystal structures of seven-coordinate pentagonal-bipyramidal zinc(II), cadmium(II) and tin(IV) complexes of a pentadentate N$_3$S$_2$ thiosemicarbazone. *Polyhedron, 30*, 299-306.

Ali, M. A., Mirza, A. H., Voo, C. W., Tan, A. L., & Bernhardt, P. V. (2003). The preparation of zinc(II) and cadmium(II) complexes of the pentadentate N$_3$S$_2$ ligand formed from 2,6-diacetylpyridine and S-benzyldithiocarbazate (H$_2$SNNNS) and the X-ray crystal structure of the novel dimeric [Zn$_2$(SNNNS)$_2$] complex. *Polyhedron 22*, 3433-3438.

Alia, J. M., Edwards, H. G. M., & Stoev, M. D. (1999). A systematic FT-Raman spectroscopic study of twelve bis-thiourea complexes, A(tu)$_2$B$_2$ (A=Zn, Cd, Hg; B-Cl, Br, I, SCN). *Spectrochim. Acta, Part A, 55*, 2423-2435.

Arquero, A., Mendiol, M. A., Souza, P., & Sevilla, M. T. (1996). Synthesis, spectral and electrochemical properties of divalent metal complexes containing thiohydrazone and thiosemicarbazone ligands. *Polyhedron, 15*, 1657-1665.

Arslan, H., Kulcu, N., & Florke, U. (2003). Synthesis and characterization of copper(II), nickel(II) and cobalt(II) complexes with novel thiourea derivatives. *Transition Met. Chem. , 28*, 816-819.

Asif, I., Mahmood, R., Stoeckli-Evans, H., Mateena, M., & Ahmad, S. (2010). Hexakis(N,N'-dimethylthiourea-S)-nickel(II) nitrate. *Acta Crystallogr. Sect. E., E66* m1393-m1394.

Babashkina, M. G., Safin, D. A., Bolte, M., & Klein, A. (2009). Intramolecular hydrogen bond controlled coordination of N-thiophosphorylated thiourea 2,6-Me2C$_6$H$_3$NHC(S)NHP(S)(OiPr)$_2$ with Ni(II). *Inorg. Chem. Commun., 12*, 678-681.

Babashkina, M. G., Safin, D. A., Srebro, M., Kubisiak, P., Mitoraj, M. P., Boltec, M., & Garcia, Y. (2011). Solvent-induced 1,3-N,S- vs. 1,5-S,S'-coordination in the NiII complex [Ni{p-Me$_2$NC$_6$H$_4$NHC(S)NP(S)(OiPr)$_2$}$_2$]. *CrystEngComm., 13*, 5321-5327.

Baggio, R., Garland, M. T., & Perec, M. (2000). X-ray study on the nickel(II)-oxydiacetic system and its 1,10-phenanthroline and 2,2':6',2'' terpyridine complexes. *Inorg.Chim.Acta, 310*, 103-109.

Baligar, R. S., & Revankar, V. K. (2008). Ligational behavior of new mononucleating SNOO thiosemicarbazone ligands towards 3d metal(II) ions: synthesis and spectroscopic studies. *Transition Met.Chem., 33*, 361-366.

Bannister, J. V., Bannister, W. H., & Rotoilio, G. (1987). Aspects of the structure, function, and application of superoxide dismutase. *CRC.Crit.Rev.BioChem, 22*, 111-180.

Barann, D. W., Bhat, G. K., Lamer, C. A., & Mahesh, V. B. (1997). Gaseous transmitter and neuroedocrine regulation. *Neuroendocrinology, 65*, 385-395.

Barber, D. E., Lu, Z., Richardson, T., & Crabtree, R. H. (1992). Silane alcoholysis by a nickel(II) complex in an N, O, S ligand environment. *Inorg. Chem., 31*, 4709-4711.

Barnes, N. A., Godfrey, S. M., Pritchard, R. G., & Ratcliffe, S. (2008). The reaction of N,N-Di-tert-butylthiourea (dtbtu) with antimony(III) halides – formation of the triply bridged [(dtbtu)SbX$_2$(μ-X)$_2$(μ-dtbtu)- SbX$_2$(dtbtu)] (X = Cl, Br) dimers. *Eur. J. Inorg. Chem.*(23), 3661-3667.

Barondeau, D. P., Kassmann, C. J., Bruns, C. K., Tainer, J. A., & Getzoff, E. D. (2004). Nickel superoxide dismutase structure and mechanism. *Biochem., 43*, 8038-8047.

Beheshti, A., Clegg, W., Khorramdin, R., Nobakhta, V., & Russob, L. (2011). Synthesis and structural characterization of mixed-metal complexes of CuI with MOS$_3$ cores (M = Mo, W) and of an unusual polymeric AgI/mercaptoimidazole complex with five different AgI coordination environments. *Dalton Trans., 40*, 2815-2821.

Belicchi Ferrari, M., Bisceglie, F., Buschini, A., Franzoni, S., Pelosi, G., Pinelli, S., Tarasconi, P., & Tavone, M. (2010). Synthesis, structural characterization and antiproliferative and toxic bio-activities of copper(II) and nickel(II) citronellal N4-ethylmorpholine thiosemicarbazonates. *J.Inorg.Biochem., 104*, 199-206.

Benito, J. M., Gómez-García, M., Jiménez Blanco, J. L., Ortiz Mellet, C., & García Fernández, J. M. (2001). Carbohydrate-based receptors with multiple thiourea binding sites. Multipoint

hydrogen bond recognition of dicarboxylates and monosaccharides. *J. Org. Chem. , 66*(4), 1366-1372.

Bergeron, K. L., Murphy, E. L., Majofodun, O., Mũnoz, L. D., Jr, J. C. W., & Almeida, K. H. (2009). Arylphosphonium salts interact with DNA to modulate cytotoxicity. *Mutat Res. , 673*, 141-148.

Berkessel, A., Hermann, G., Rauch, O., Büchner , M., Jacobi, A., & Huttner, G. (1996). Preparation and X-ray crystal structure of the first trimeric nickel thiosemicarbazone complex: The first example of oligomerization by both Ni O Ni and Ni S Ni bridging. *Chem. Ber, 129*, 1421- 1423.

Berners-Price, S. J., Johnson, R. K., Mirabelli, C. K., Faucette, L. F., McCabe, F. L., & Sadler, P. J. (1987). Copper(I) complexes with bidentate tertiary phosphine ligands: solution chemistry and antitumor activity. *Inorg. Chem., 26*, 3383-3387.

Beyer, L., Dietze, F., Schröder, U., Quas, L., Santos, L. M. N. B. F., & Schröder, B. (2008). Oligonuclear complex formation of the bisbidentate ligand N',N',N''',N'''-tetraethyl-N,N''-pyridine-2,6-dicarbonyl-bis(thiourea) in solution. *Rev Soc Quím Perú, 74*, 163-171.

Bierbach, U., Hambley, T. W., & Farrell, N. (1998). Modification of platinum(II) antitumor complexes with sulfur ligands. 1. Synthesis, structure, and spectroscopic properties of cationic complexes of thettypes [PtCl(diamine)(L)]NO₃ and [{PtCl(diamine)}₂(L-L)](NO₃)₂ (L= monofunctional thiourea derivative; L-L = bifunctional thiourea derivative). *Inorg. Chem., 37*, 708-716.

Biittcber, A., Elias, H., Jiiger, E.-G., Langfelderova, H., Mazur, M., Miiller, L., Paulus, H., Pelikan, P., Rudolpb, M., & Vako, M. (1993). Comparative study on the coordination chemistry of cobalt(II), nickel(II)), and copper(II) with derivatives of Salen and Tetrahydrosalen: Metal-catalyzed oxidative dehydrogenation of the C-N bond in coordinated Tetrahydrosalen. *Inorg. Chem., 32*, 4131-4138.

Bindu, P., & Kurup, M. R. P. (1997). E.s.r. and electrochemical studies of four- and five - coordinate copper(II) complexes containing mixed ligands. *Trans.Met.Chem., 22*, 578-582.

Bindua, P., Kurup, M. R. P., & R.Satyakeerty, T. (1999). EPR, cyclic voltammetric and biological activities of copper(II) complexes of salicylaldehyde N(4)-substituted thiosemicarbazone and heterocyclic bases. *Polyhedron, 18*, 321-331.

Binzet, G., Külcü, N., Flörke, U., & Arslan, H. (2009). Synthesis and characterization of Cu(II) and Ni(II) complexes of some 4-bromo-N-(di(alkyl/aryl)carbamothioyl) benzamide derivatives. *J. Coord. Chem., 62*, 3454-3462.

Bleackley, M. R., & MacGillivray, R. T. A. (2011). Transition metal homeostasis: from yeast to human disease. *Biometals 24*, 785-809.

Bombicza, P., Mutikainenb, I, Krunksc, M., Leskeläd, T., Madárásze, J., & Niinistöd, L. (2004). Synthesis, vibrational spectra and X-ray structures of copper(I) thiourea complexes. *Inorg. Chim. Acta, 357*, 513-525.

Bomfim, J. A. S., Souza, F. P. d., Filgueiras, C. A. L., Sousa, A. G. d., & Gambardella, M. T. P. (2003). Diphosphine complexes of nickel: analogies in molecular structures and variety in crystalline arrangement. *Polyhedron, 22*, 1567-1573.

Bon, V. V., Orysyk, S. I., Pekhnyo, V. I., & Volkov, S. V. (2010). Square-planar 1:2 Ni(II) and Pd(II) complexes with different coordination mode of salicylaldehyde (4)-phenylthiosemicarbazone: Synthesis, structure and spectral properties. *J. Mol. Struct., 984*, 15-22.

Bott, R. C., Bowmaker, G. A., Davis, C. A., Hope, G. A., & Jones, B. E. (1998). Crystal structure of $[Cu_4(tu)_7](SO_4)_2].H_2O$ and vibrational spectroscopic studies of some copper(I) thiourea complexes. *Inorg. Chem. , 37*, 651-657.

Brandenburg, K. (2006). DIAMOND (Version version 3.ld). Bonn, Germany: Crystal Impact GbR.

Brewer, B., Brooks, N. R., Abdul-Halim, S., & Sykes, A. G. (2003). Differential metathesis reactions of 2,2'-bipyridine and 1,10-phenanthroline complexes of cobalt(II) and nickel(II): cocrystallization of ionization isomers [cis-Ni(phen)$_2$(H$_2$O)$_2$][cis-Ni(phen)$_2$(H$_2$O)Cl]}(PF$_6$)$_3$.4.5H$_2$O, and a synthetic route to asymmetric tris-substituted complexes. *J. Chem. Crystallogr., 33*, 651-662.

Bruker. (2007). APEX2 and SAINT. Bruker AXS Inc.,Madison, Wisconsin, USA.

Buschini, A., Pinelli, S., Pellacani, C., Giordani, F., Belicchi-Ferrari, M., Bisceglie, F., Giannetto, M., Pelosi, G., & Tarasconi, P. (2009). Synthesis, characterization and deepening in the comprehension of the biological action mechanisms of a new nickel complex with antiproliferative activity. *J.Biol.Chem., 103*, 666-677.

Calatayud, D. G., López-Torres, E., & Mendiola, M. A. (2008). Reactivity of benzil bis(4-methyl-3-thiosemicarbazone) with cadmium nitrate.Crystal structure of [Cd(LMe$_2$H$_4$)(NO$_3$)$_2$][Cd(LMe$_2$H$_4$)(NO$_3$)(H$_2$O)]NO$_3$.H$_2$O. *Polyhedron, 27* 2277-2284.

Campo, R. d., Criadoa, J. J., Garc´ıa, E., Hermosab, M. ı. R., A.Jime´nez-Sa´nchezc, Manzano, J. L., Monte, E., Rodr´ıguez-Ferna´ndez, E., & Sanz, F. (2002). Thiourea derivatives and their nickel(II) and platinum(II) complexes: antifungal activity. *J. Inorg. Biochem., 89*, 74–82.

Carty, A. J. (1967). Coordination complexes of gallium(III) and indium(III) halides. I. Complexes with triarylphosphines. *Can.J Chem., 45*, 345-351.

Casas, J. S., Casanova, N., García-Tasende, M. S., Sánchez, A., Sordo, J., Touceda, Á., & Vázquez, S. (2010). Back to the coordination modes of the thiosemicarbazonate chain: New insights from diorganolead(IV) and lead(II) derivatives of isatin-3-thiosemicarbazone. *Eur. J. Inorg. Chem.*, 4992-5004.

Casas, J. S., Garcìa-Tasende, M. S., & Sordo, J. (2000). Main group metal complexes of semicarbazones and thiosemicarbazones. A structural review. *Coord. Chem. Rev., 209*, 197–261.

Castiñeiras, A., Fernández-Hermida, N., García-Santos, I., & Gómez-Rodríguez, L. (2012). Neutral Ni^{II}, Pd^{II} and Pt^{II} ONS-pincer complexes of 5-acetylbarbituric-4Ndimethylthiosemicarbazone: synthesis, characterization and properties. *D a l t o n T r a n s . 41*, 13486-13495.

Cauzzi, D., Costa, M., Cucci, N., Graiff, C., Grandi, F., Predieri, G., Tiripicchio, A., & Zanoni, R. (2000). Pd(II) and Rh(I) chelate complexes of the bidentate phosphino–thiourea ligand PhNHC(S)NHCH$_2$CH$_2$PPh$_2$: structural properties and activity in homogeneous and hybrid catalysis. *J. Organomet. Chem. , 593–594*, 431-444.

Champoux, J. J. (2001). DNA topoisomerases: structure, function, and mechanism. *Annu.Rev.Biochem, 70*, 369-413.

Chandra, S., & Kumar, A. (2007). Spectral, IR and magnetic studies of Mn(II), Co(II), Ni(II) and Cu(II) complexes with pyrrole-2-carboxyaldehyde thiosemicarbazone (L). *Spectrochim. Acta, Part A, 68,* 469-473.

Chandra, S., & Kumar, U. (2004). Spectroscopic characterization of copper(II) complexes of indoxyl N(4)-methyl thiosemicarbazone. *Spectrochim.Acta Part A, 60*, 2825-2829.

Chandra, S., & Kumar, U. (2005). Spectral studies of coordination compounds of cobalt(II) with thiosemicarbazone of heterocyclic ketone. *Spectrochim. Acta, Part A, 62*, 940-944.

Chandra, S., & Sharma, A. K. (2009). Nickel(II) and copper(II) complexes with Schiff base ligand 2,6-diacetylpyridine bis(carbohydrazone): Synthesis and IR, mass, ^{1}H NMR, electronic and EPR spectral studies. *Spectrochim. Acta, Part A 72*, 851-857.

Chattopadhyay, S. K., Chattopadhyay, D., Banerjee, T., Kuroda, R., & Ghosh, S. (1997). Studies of nickel(ll) complexes of 3-hydroxyiminobutanone thiosemicarbazone and 3-hydroxyiminobutanone (4-phenylthiosemicarbazone). Crystal structure of bis(3 hydroxyiminobutanone (4-phenylthiosemicarbazone) nickel(II) nitrate,monohydrate, [Ni(C$_{11}$H$_{14}$N$_4$OS)$_2$] (NO$_3$)$_2$.H$_2$O. *Polyhedron, 16*, 1925-1930.

Che, C.-M., & Siu, F.-M. (2010). Metal complexes in medicine with a focus on enzyme inhibition. *Curr.Opin.Chem.Biol, 14*, 255-261.

Che, D.-J., Li, G., Yu, Z., Zou, D.-P., & Du, C.-X. (2000). Oxidative cyclization and coordinate polymerization of N-benzoyl-N'-(2-pyridyl) thiourea with copper(II) chloride. *Inorg. Chem. Commun., 3*, 537–540.

Chellan, P., Shunmoogam-Gounden, N., Hendricks, D. T., Gut, J., Rosenthal, P. J., Lategan, C., Smith, P. J., Chibale, K., & Smith, G. S. (2010). Synthesis, structure and in vitro biological screening of palladium(II) complexes of functionalised salicylaldimine thiosemicarbazones as antimalarial and anticancer agents. *Eur. J. Inorg. Chem.* 22, 3520-3528.

Chen-jie, F., Chun-ying, D., Cheng, H., Gang, H., & Qing-jin, M. (2000). A supramolecular analog of cyclohexane sustained by aromatic C-H…π interactions between ferrocene moieties: molecular packing of ferrocene-containing thiosemicarbazato metal complexes. *New J. Chem., 24*, 697-701.

Chen, H. J., & Hwang, J. (1999). Binding of ATP to human DNA topoisomerase I resulting in an alteration of the conformation of the enzyme. *Eur.J.Biochem., 265*, 367-375.

Cheresova, E. N., Zhukova, R. S., Tatarintseva, T. B., Cheresov, S. V., & A.Mukmeneva, N. (1997). Unsymmetrically N,N`-disubstituted diarylthioureas and their coordination compounds with Cu(II) and Ni(II). *Russ. J. Gen. Chem. , 67*, 1271-1275.

Chin, L. F., Kong, S. M., Seng, H. L., Khoo, K. S., Vikneswaran, R., Teoh, S. G., Ahmad, M., Khoo, S. B. A., Maah, M. J., & Ng, C. H. (2011). Synthesis, characterization and biological properties of cobalt(II) complexes of 1,10-phenanthroline and maltol. *J.Inorg.Biochem., 105*, 339-347.

Cornago, P., Claramunt, R. M., Cano, M., Heras, J. V., & Gallegob, M. L. (2005). Multinuclear NMR study of Au(I), Pd(II) and Ag(I) pyrazole complexes to investigate the coordination mode. *Arkivoc, ix*, 21-29.

Crews, P., Rodriguez, J., & Jaspars, M. (1998). *Organic structure analysis*. London: Oxford University Press, Inc.

D'Cruz, O. J., Dong, Y., & Uckun, F. M. (2003). Potent dual anti-HIV and spermicidal activities of novel oxovanadium(V) complexes with thiourea non-nucleoside inhibitors of HIV-1 reverse transcript. *Biochem. Biophys. Res. Commun, 302*, 253–264.

Dai, M., Liang, B., Wang, C., Chen, J., & Yang, Z. (2003). Synthesis of a Novel C2-symmetric thiourea and its application in the Pd-catalyzed cross-coupling reactions with arenediazonium salts under aerobic conditions. *Org. Lett., 6*, 221-224.

Dan, Z., Jie, H., Ji-rong, S., Yi-tang, Z., Li-qin, W., & Jian-yun, H. (2012). Synthesis, Crystal Structure and Thermal Analysis of N-(2,3-Dimethyl-phenyl)-N′-(methoxyl formyl)thiourea. *Chem. Res. Chinese Universities, 28*, 230-233.

Datta, S., Seth, D. K., Butcher, R. J., & Bhattacharya, S. (2011). Mixed-ligand thiosemicarbazone complexes of nickel: Synthesis, structure and catalytic activity. *Inorg. Chim. Acta 377*, 120-128.

Datta, S., Seth, D. K., Gangopadhyay, S., Karmakar, P., & Bhattacharya, S. (2012). Nickel complexes of some thiosemicarbazones: Synthesis, structure, catalytic properties and cytotoxicity studies. *Inorg. Chim. Acta 392*, 118-130.

del Campo, R., Criado, J. J., Gheorghe, R., Gonzalez, F. J., Hermosa, M. R., Sanz, F., Manzano, J. L., Monte, E., & Rodriguez-Fernandez, E. (2004). N-benzoyl-N´ alkylthioureas and their complexes with Ni(II), Co(III) and Pt(II) - crystal structure of 3-benzoyl-1-butyl-1-methyl-thiourea: activity against fungi and yeast. *J.Inorg.Biochem., 98*, 1307-1314.

Demoro, B., Sarniguet, C., S´anchez-Delgado, R., Rossi, M., Liebowitz, D., Caruso, F., Olea-Azar, C., Moreno, V., Medeiros, A., Comini, M. A., Otero, L. 1., & Gambino, D. (2012). New organoruthenium complexes with bioactive thiosemicarbazones as co-ligands: potential anti-trypanosomal agents. *Dalton Trans., 41*, 1534-1543.

Deoghoria, S., Sain, S., Moulton, B., Zaworotko, M. J., Bera, S. K., & Chandra, S. K. (2002). Synthesis, crystal structure and magnetic behavior of two new binuclear complexes bridged by a pentadentate ligand: $[Ni_2L_2(NCS)_2](ClO_4)_2$ and $[Ni_2L_2(NCO)_2](ClO_4)_2$ [L= pentadentate ligand]. *Polyhedron, 21*, 2457-2461.

Deohate, P. P., Deohate, J. P., & Berad, B. N. (2004). Novel benzo-1,3,6-thiadiazepines: Synthesis, antimicrobial activity and isomerization into benzo-1,3,5-triazepines. *Asian J. Chem, 16*, 773–778.

Dey, M., Telser, J., Kunz, R. C., Lees, N. S., Ragsdale, R. W., & Hoffman, M. B. (2007). Biochemical and spectroscopic studies of the electronic structure and reactivity of a methyl- Ni species formed on methyl Coenzyme-M-reductase. *J. Am.Chem.Soc, 129*, 11030-11032.

Dharmaraj, N., Viswanathamurthi, P., & Natarajan, K. (2001). Ruthenium(II) complexes containing bidentate Schiff bases and their antifungal activity. *Trans.Met.Chem., 26*, 105-109.

Dilovic´, I., Rubcˇic´, M., Vrdoljak, V. n., Pavelic´, S. K., Kralj, M., Piantanidab, I., & Cindric´, M. (2008). Novel thiosemicarbazone derivatives as potential antitumor agents: Synthesis, physicochemical and structural properties, DNA interactions and antiproliferative activity. *Bioorg. Med. Chem., 16* 5189-5198.

Dixon, N. E., Gazzola, C., Blakeley, R. L., & Zerner, B. (1975). Jack bean urease (EC 3.5.1.5) metalloenzyme. Simple biological role for nickel. *J.Am.Chem.Soc., 97*, 4131-4133.

Doukov, T. I., Iverson, T. M., Seravalli, J., Ragsdale, S. W., & Drennan, C. L. (2002). A Ni-Fe-Cu center in a bifunctional carbon monoxide dehydrogenase/ acetyl CoA synthase. *Science, 298*, 567-572.

Du, K.-K., & Liu, S.-X. (2008). Influence of pH values on the self-assembly in three trinuclear nickel complexes with bridging ligand N-salicylyl 4-phenyl-thiosemicarbazide. *J. Mol. Struct., 874*, 138-144.

Duke, R. M., & Gunnlaugsson, T. (2007). Selective fluorescent PET sensing of fluoride (F⁻) using naphthalimide thiourea and urea conjugates. *Tetrahedron Lett., 48*, 8043-8048.

Duquey, J., Estévez-hernandez, O., Reguerayz, E., Ellenax, J., & Corréa, R. S. (2009). Synthesis, characterization, and single crystal X-ray structure of the 1-furoyl-3-cyclohexylthiourea cadmium chloride complex, $Cd[C_4H_3OC(O)NHC(S)NHC_6H_{11}]_4Cl_2$. *J. Coord. Chem., 62* 2804-2813.

Durãn, M. L., Sousa, A., Romero, J., Castin˜eiras, A., Bermejo, E., & West, D. X. (1999). Structural study of the electrochemically synthesized binuclear complex bis{1-phenylglyoxal bis(3-piperidylthiosemicarbazone)zinc(II)}. *Inorg.Chim.Acta, 294*, 79-82.

Eaton, D. R., & Zaw, K. (1972). Geometry of Nickel(II) complexes. *J. Am. Chem. Soc, 94*, 4394-4395.

El-Asmya, A. A., & Al-Hazmi, G. A. A. (2009). Synthesis and spectral feature of benzophenone-substituted thiosemicarbazones and their Ni(II) and Cu(II) complexes. *Spectrochim.Acta, Part A, 71*, 1885-1890.

El-Bahya, G. M. S., El-Sayedb, B. A., & Shabana, A. A. (2003). Vibrational andelectronic studies on some metal thiourea complexes. *Vib. Spectrosc., 31,* 101-107.

El-Bahya, G. M. S., El-Sayedb, B. A., & Shabana, A. A. (2003). Vibrational and electronic studies on some metal thiourea complexes. *Vib. Spectrosc. , 31*, 101-107.

El-Shazly, R. M., Al-Hazmi, G. A. A., Ghazya, S. E., El-Shahawi, M. S., & El-Asmya, A. A. (2005). Spectroscopic, thermal and electrochemical studies on some nickel (II) thiosemicarbazone complexes. *Spectrochim. Acta, Part A, 61*, 243-252.

Elfetoh, S. H. A., Eid, A. E., Elkareem, A. T. A., & Wassel, M. A. (1998). physico - analytical studies on salicylaldehyde thiosemicarbazone complexes. *J. Mater. Sci. Technol., 14*, 434-440.

Evans, L. S., Gale, P. A., Light, M. E., & Quesada, R. (2006). Anion binding vs. deprotonation in colorimetric pyrrolylamidothiourea based anion sensors. *J. Chem. Commun.*(9), 965-967.

Farina, Y., & Simpson, J. (2008). (E)-3,4-Dihydroxybenzaldehyde-4-methylthiosemicarbazone. *Acta Crystallogr. Sect. E: Struct. Rep. Online, E64*, o2184-o2185.

Farrugia, L. J. (1997). Ortep-3 for Windows *J. Appl. Cryst. , 30*, 565.

Ferrari, M. B., Bisceglie, F., Pelosi, G., Sassi, M., Tarasconi, P., Cornia, M., Capacchi, S., Albertini, R., & Pinelli, S. (2002). Synthesis, characterization and X-ray structures of new antiproliferative and proapoptotic natural aldehyde thiosemicarbazones and their nickel(II) and copper(II) complexes. *J. Inorg. Biochem., 90*, 113-126.

Ferrari, M. B., Capacchi, S., Bisceglie, F., Pelosi, G., & Tarasconi, P. (2001). Synthesis and characterization of square planar nickel(II) complexes with p-fluorobenzaldehyde thiosemicarbazone derivatives. *Inorg.Chim.Acta, 312,* 81-87.

Ferrari, M. B., Capacchia, S., Reffoa, G., Pelosia, G., Tarasconia, P., Albertini, R., Pinelli, S., & Lunghi, P. (2000). Synthesis, structural characterization and biological activity of p-fluorobenzaldehyde thiosemicarbazones and of a nickel complex. *J. Inorg. Biochem., 81*, 89-97.

Fostiak, L. M., Garcı'a, I., Swearingen, J. K., Bermejo, E., Castineiras, A., & West, D. X. (2003). Structural and spectral characterization of transition metal complexes of 2-pyridineformamide N(4)-dimethylthiosemicarbazone. *Polyhedron, 22*, 83-92.

Fuerst, D. E., & Jacobsen, E. N. (2005). Thiourea-Catalyzed Enantioselective Cyanosilylation of Ketones. *J. Am. Chem. Soc., 127*, 8964-8965.

Fuks, L., Sadlej-Sosnowska, N., Samochocka, K., & Starosta, W. (2005). Experimental and quantum chemical studies of structure and vibrational spectra of platinum(II) and palladium(II) thiourea chlorides. *J. Mol. Struct., 740*, 229-235.

Galabov, A. S., Galabov, B. S., & Neykova, N. A. (1980). Structure-activity relationship of diphenylthiourea antivirals. *J. Med. Chem., 23*, 1048-1051.

Gambino, D., Otero, L. a., Vieites, M., Boiani, M., Gonza'lez, M., Baran, E. J., & Cerecetto, H. (2007). Vibrational spectra of palladium 5-nitrofuryl thiosemicarbazone complexes: Experimental and theoretical study. *Spectrochim. Acta, Part A, 68,* 341-348.

Garcìa, I., Bermejo, E., Sawaf, A. K. E., eiras, A. C., & West, D. X. (2002). Structural studies of metal complexes of 2-pyridineformamide N(4)-methylthiosemicarbazone. *Polyhedron, 21*, 729-737.

Garg, B. S., & Kumar, D. N. (2003). Spectral studies of complexes of nickel(II) with tetradentate schiff bases having N_2O_2 donor groups. *Spectrochim. Acta, Part A, 59*, 229-234.

Gomes, L., Pereira, E., & Castro, B. d. (2000). Nickel(II) complexes with N_2OS and N_2S_2 co-ordination spheres: reduction and spectroscopic study of the corresponding Ni(I) complexes. *J. Chem. Soc., Dalton Trans.*, 1373-1379.

Gomes, L. R., Low, J. N., Rocha, M. A. A., Santos, L. M. N. B. F., Schröder, B., Brandão, P., Matos, C., & Neves, J. (2011). Nickel(II) complexes of N-(2-thienylcarbonyl)thiocarbamates O-alkyl-esters: Structural and spectroscopic characterization and evaluation of their microbiological activities. *J. Mol. Struct. , 990*, 86-94.

Gopal, Y. N. V., Konuru, N., & Kondapi, A. K. (2002). Topoisomerase II antagonism and anticancer activity of coordinated derivatives of $[RuCl_2(C_6H_6)(dmso)]$. *Arch Biochem Biophys, 401*, 53-62.

Gordon, R. B., Bertram, M., & Graedel, T. E. (2006). Metal stocks and sustainability. *Proc.Nati.Acad.Sci.USA, 103*, 1209-1214.

Gradinaru, J., Forni, A., Simonov, Y., Popovici, M., Zecchin, S., Gdaniec, M., & Fenton, D. E. (2004). Mononuclear nickel(II) and copper(II) complexes with Schiff base ligands derived from 2,6-diformyl-4-methylphenol and S-methylisothiosemicarbazones. *Inorg.Chim.Acta, 357*, 2728-2736.

Gunasekaran, N., Ramesh, P., Ponnuswamyb, M. N. G., & Karvembu, R. (2011). Monodentate coordination of N-[di(phenyl/ethyl)carbamothioyl]benzamide ligands: synthesis, crystal structure and catalytic oxidation property of Cu(I) complexes. *Dalton Trans., 40,* 12519-12526.

Gunnlaugsson, T., Kruger, P. E., Jensen, P., Tierney, J., Ali, H. D. P., & Hussey, G. M. (2005). Colorimetric "Naked Eye" Sensing of Anions in Aqueous Solution. *J. Org. Chem., 70*, 10875-10878.

Güveli, S., Bal-Demirci, T., Özdemir, N., & Ülküseven, B. (2009). Nickel(II) complexes of ONS and ONN chelating thiosemicarbazones with triphenylphosphine co-ligands. *Transition Met. Chem., 34*, 383-388.

Güveli, S., Bal-Demirci, T., Özdemir, N., Ülküseven, B., & Dinçer, M. (2010). Quantum-chemical, spectroscopic and X-ray diffraction studies on nickel complex of 2-hydroxyacetophenone thiosemicarbazone with triphenylphospine. *Polyhedron, 29*, 2393–2403.

Güveli, S., & Ülküseven, B. (2011). Nickel(II)–triphenylphosphine complexes of ONS and ONN chelating 2-hydroxyacetophenone thiosemicarbazones. *Polyhedron, 30*, 1385–1388.

Halcrow, M. A., & Christou, G. (1994). Biomimetic chemistry of nickel. *Chem.Rev., 94*, 2421-2481.

Hall, I. H., Miller, M. C., & West, D. X. (1997). Antineoplastic and cytotoxic activities of nickel(II) complexes of thiosemicarbazones. *Metal Based Drugs, 4*, 89-95.

Halpern, J. (1983). Regulation of catalytic activity by phosphine ligand design. *Phosphorus, Sulfur Silicon Relat. Elem., 18*, 307-310.

Hanif, M., & Chohan, Z. H. (2013). Design, spectral characterization and biological studies of transition metal(II) complexes with triazole Schiff bases. *Spectrochim. Acta, Part A, 104*, 468-476.

He, M. M., Clugston, S. L., Honek, J. F., & Mathews, B. W. (2000). Determination of the structure of *Escherichia Coli* glyoxalase I suggests a structural basis for differential metal activation. *BioChem. , 39*, 8719-8727.

Hecke, G. R. V., & Horrocks, W. D. (1966). Ditertiary phosphine complexes of nickel. Spectral, magnetic, and proton resonance studies. A planar-tetrahedral equilibrium. *Inorg. Chem., 5*, 1968-1974.

Hemamalini, M., Muthiah, P. T., & Lynch, D. E. (2005). Hydrogen-bonding patterns in trimethoprim tetrafluoroborate. *Acta Crystallogr. Sect. E., 61*, o4107–o4109.

Henderson, W., Nicholson, B. K., Dinger, M. B., & Bennett, R. L. (2002). Thiourea monoanion and dianion complexes of rhodium(III) and ruthenium(II). *Inorg. Chim. Acta, 338*, 210-218.

Hosny, N. M., & Mostafa, M. M. (2010). Synthesis, spectral and thermal studies of N,N'-pyridine-2,6-diylbis[N'-phenyl(thiourea)] and its metal complexes. *J. Incl. Phenom. Macrocycl. Chem, 67*, 85-90.

Hoyer, E., Köhler, R., Kirmse, R., Richter, R., Sieler, J., & Beyer, L. (1986). Binucleating Bis-N-acylthioureas – Ligands in Trimetallamacrocycles and Polynuclear Metal Chelates. *Z. Anorg. Allg. Chem, 537,* 133-144.

Huber, C., & Wachtershauser, G. (1997). Activated acetic acid by carbon fixation on (Fe, Ni)S under primordial conditions. *Science, 276*, 245-247.

Jabri, E., Carr, M. B., Hauinger, R. P., & Karplus, P. A. (1995). The crystal structure of urease from *klebsiella aerogenes*. *Science, 268*, 998-1004.

Jambi, S. M. S., & Kandil, S. S. (2012). Synthesis and characterization of Ni(II), Pd(II), Pt(II) complexes of N-allyl-N'-(4-methylthiazol-2-yl)thiourea. *J. Mater. Environ. Sci. , 3*, 591-604.

Jarrettt, P. S., & Sadler, P. J. (1991). Nickel(II) Bis(phosphine) Complexes. *Inorg. Chem., 30*, 2098-2104.

Jayabalakrishnan, C., Karvembu, R., & Natarajan, K. (2002). Catalytic and antimicrobial activities of new ruthenium(II) unsymmetrical Schiff base complexes. *Trans.Met.Chem., 27*, 790-794.

Jensen, K., & Nielsen, P. (1966). Infrared spectra of thioamides and selenoamides. *Acta Chem. Scand., 20*, 597-629.

Kalaivani, P., Prabhakaran, R., Ramachandran, E., Dallemer, Paramaguru, G., Renganathan, R., Poornima, P., Padmad, V. V., & Natarajan, K. (2012). Influence of terminal substitution on structural, DNA, Protein binding, anticancer and antibacterial activities of palladium(II) complexes containing 3-methoxy salicylaldehyde-4(N) substituted thiosemicarbazones. *Dalton Trans., 41*, 2486-2499.

Kandil, S. S., Katib, S. M. A., & Yarkandi, N. H. M. (2007). Nickel(II), palladium(II) and platinum(II) complexes of N-allyl-N' -pyrimidin-2-ylthiourea. *Transition Met.Chem., 32*, 791-798.

Kanjan, S., & Dikshit, S. K. (2000). Synthesis and characterization of mixed- ligand complexes of Cu(1) containing halides, triphenylstibine and triphenylbismuthine, N,N dimethyl-N'-phenylthiourea (dmpth), thione (tzdth), N,N-dibutyl-N'-phenylthiourea (dbpth) and 1,3-thiazolidine-2-thione (tzdth). *Synth. React. Inorg. Met. Org. Chem., 30*, 239-256.

Karvembu, R., Hemalatha, S., Prabhakaran, R., & Natarajan, K. (2003). Synthesis, characterization and catalytic activities of ruthenium complexes containing triphenylphosphine/triphenylarsine and tetradentate Schiff bases. *Inorg. Chem. Commun., 6*, 486-490.

Kasuga, N. C., Sekino, K., Koumo, C., Shimada, N., Ishikawa, M., & Nomiya, K. (2001). Synthesis, structural characterization and antimicrobial activities of 4- and 6-coordinate nickel(II) complexes with three thiosemicarbazones and semicarbazone ligands. *J. Inorg. Biochem., 84*, 55-65.

Katritzky, A. R., Khashab, N. M., Bobrov, S., & Yoshioka, M. (2006). Synthesis of mono- and symmetrical Di-N-hydroxy- and N-aminoguanidines. *J. Org. Chem., 71*, 6753-6758.

Kersting, B., Steinfeld, G., Fritz, T., & Hausmann, J. (1999). Novel synthesis of macrocyclic amine-thiophenolate ligands: X-ray crystal structure of a Ni4 complex of an N8S4 ligand. *Eur. J. Inorg. Chem., 12*, 2167-2172.

Ketcham, K. A., Garcia, I., Swearingen, J. K., El-Sawaf, A. K., Bermejo, E., Castineiras, A., & West, D. X. (2002). Spectral studies and X-ray crystal structures of three nickel(II) complexes of 2-pyridineformamide 3-piperidylthiosemicarbazone. *Polyhedron, 21*, 859-865.

Kim, E. J., Chung, H. J., Suh, B., Hah, Y. C., & Roe, J. H. (1998). Transcription and post- transcriptional regulation by nickel of sodN gene encoding nickel- containing superoxide dismutase from streptomyces coelicolor muller. *Mol.microbiol, 27*, 187-195.

Kobakhidze, N., Farfán, N., Romero, M., Méndez-Stivalet, J. M., Ballinas-López, M. G., García-Ortega, H., Domínguez, O., Santillan, R., Sánchez-Bartéz, F., & Gracia-Mora, I. (2010). New pentacoordinated Schiff-base diorganotin(IV) complexes derived from nonpolar side chain amino acids. *J. Organomet. Chem. , 695*, 1189-1199.

Koch, K. R. (2001). New chemistry with old ligands: N-alkyl- and N,N-dialkyl-N - acyl(aroyl)thioureas in co-ordination, analytical and process chemistry of the platinum group metals. *Coord. Chem. Rev., 216–217*, 473-488.

Koch, K. R., Wang, Y., & Coetzee, A. (1999). Platinum(II) and palladium(II) complexes of N-benzoyl-N'-propylthiourea (H$_2$L): Synthesis and geometric isomer distribution of [M(H$_2$L-S)$_2$X$_2$] (M = Pt^{II} or Pd^{II}; X = Cl$_2$, Br$_2$ or I$_2$); crystal structure of trans-[Pd(H$_2$L-S)$_2$Br$_2$]. *J. Chem. Soc., Dalton Trans.*(6), 1013-1016.

Kolehmainen, E., Laihia, K., Korvola, J., Kaganovich, V. S., Rybinskaya, M. I., & Kerzina, Z. A. (1995). Mono-, bi- and polynuclear complexes of diphenylmethane with Cr, Co and Ru. Synthesis and investigation by ^{1}H, ^{13}C and a^{17}O NMR. *J. Organomet. Chem., 485* 109-114.

Kolotilov, S. V., Cador, O., Golhen, S. p., Shvets, O., Ilyin, V. G., Pavlishchuk, V. V., & Ouahab, L. n. (2007). Synthesis, structure, sorption and magnetic properties of Ni(II) and Cu(II) complexes with thiosemicarbazone of 2-hydroxybenzaldehyde, bridged by 4,4'-bipyridine. *Inorg.Chim.Acta 360*, 1883-1889.

Kumar, M., Nagendra babu, J., Bhalla, V., & Singh Athwal, N. (2007). Visible Colorimetric Sensor for Fluoride Ion Based on o-Phenylenediamine. *Supramol.Chem., 19*, 511-516.

Latheef, L., & Kurup, M. R. P. (2008). Spectral and structural studies of nickel(II) complexes of salicylaldehyde 3-azacyclothiosemicarbazones. *Polyhedron, 27*, 35-43.

Latheef, L., Seena, E. B., & Kurup, M. R. P. (2009). Synthesis, spectral and structural studies of novel binuclear Ni(II) complex of salicylaldehyde 3-azacyclothiosemicarbazone. *Inorg.Chim.Acta, 362,* 2515-2518.

Lenthall, J. T., Anderson, K. M., Smith, S. J., & Steed, J. W. (2007). Crystal packing in equilibrating systems: A single crystal containing three isomers of CuCl(1-pyridin-2-yl-3-p-tolyl-thiourea)$_2$. *Cryst. Growth. Des., 7*, 1858-1862.

Leovac, V. M., Novakovic, S. B., Bogdanovic, G. A., Joksovic, M. D., Szecsenyi, K. M., & Cesljevic, V. I. (2007). Transition metal complexes with thiosemicarbazide-based ligands.Part LVI: Nickel (II) complex with 1,3-diphenylpyrazole-4-carboxaldehyde thiosemicarbazone and unusually deformed coordination geometry. *Polyhedron, 26*, 3783-3792.

Li, A.-F., Wang, J.-H., Wang, F., & Jiang, Y.-B. (2010). Anion complexation and sensing using modified urea and thiourea-based receptors. *Chem. Soc. Rev., 39*, 3729-3745.

Li, G.-., Che, D.-J., Li, Z.-F., Zhu, Y., & Zou, D.-P. (2002). Versatile coordination patterns in the reaction system of N-benzoyl-N'-(2-pyridyl)thiourea with $CuCl_2$. Their reaction conditions, systematic isolation and crystal structures. *New J. Chem., 26,* 1629-1633.

Lipowska, M., Hayes, B. L., Hansen, L., Taylor, A., & Marzilli, L. G. (1996). Rhenium(V) oxo complexes of novel N2S2 dithiourea (DTU) chelate ligands: Synthesis and structural characterization. *Inorg.Chem., 35*(14), 4227-4231.

Liu, J.-n., Wu, B.-w., Zhang, B., & Liu, Y. (2006). Synthesis and characterization of metal complexes of Cu(II), Ni(II), Zn(II), Co(II), Mn(II) and Cd(II) with tetradentate schiff Bases. *Turk. J.Chem., 30* 41 - 48.

Liu, L. F. (1989). DNA topoisomerase poisons as antitumor drugs. *Annu.Rev.Biochem, 58*, 351-375.

Liu, R., Li, X., Zhang, H., Weng, L., & Zhou, X. (2010). Synthesis and controlled hydrolysis of organolanthanide complexes with mono- and dianionic benzimidazole-2-thiolate ligands. *Dalton Trans., 39*, 11053-11059.

Liu, W.-X., & Jiang, Y.-B. (2008). Intramolecular hydrogen bonding and anion binding of N-benzamido-N'-benzoylthioureas. *J. Org. Chem., 73*, 1124-1127.

Liu, Z.-H., Duan, C.-Y., Hu, J., & You, X.-Z. (1999). Design, synthesis, and crystal structure of a cis-configuration N_2S_2-coordinated palladium(II) complex: Role of the intra- and intermolecular aromatic-ring stacking interaction. *Inorg. Chem. , 38*, 1719-1724.

Livingstone, S. E. (1965). Metal complexes of ligands containing sulphur, selenium, or tellurium as donor atoms. *Q. Rev. Chem. Soc., 19*, 386-425.

Lo'pez-Torres, E., Mendiola, M. A., Pastor, C. s. J., & Pe'rez, B. S. (2004). Versatile chelating behavior of benzil bis(thiosemicarbazone) in zinc, cadmium, and nickel complexes. *Inorg. Chem., 43,* 5222-5230.

Lobana, T. S., Bawa, G., Castineiras, A., & Butcher, R. J. (2007). First example of pyrrole-2-carbaldehyde thiosemicarbazone as tridentate dianion in $[Pd(\eta^3\text{-}N^4,N^3,S\text{-}ptsc)(PPh_3)]$ complex. *Inorg.Chem.Commun., 10,* 506-509.

Lobana, T. S., Khanna, S., Hundal, G., Kaur, P., Thakur, B., Attri, S., & Butcher, R. J. (2009). Coinage metal derivatives of salicylaldehyde thiosemicarbazones: Synthesis, structures, bond isomerism and H-bonded networks. *Polyhedron, 28,* 1583-1593.

Lobana, T. S., Kumari, P., Hundal, G., & Butcher, R. J. (2010). Metal derivatives of N1-substituted thiosemicarbazones with divalent metal ions (Ni, Cu): Synthesis and structures. *Polyhedron 29*, 1130-1136.

Lobana, T. S., Kumari, P., Zeller, M., & Butcher, R. J. (2008). The influence of the substituents at N1 nitrogen on geometry of nickel(II) complexes with heterocyclic thiosemicarbazones. *Inorg. Chem. Commun, 11* 972-974.

Lobana, T. S., Rekha, & Butcher, R. J. (2004). Metal–thiosemicarbazone interactions. Synthesis of an iodo-bridged dinuclear [diiodobis(pyrrole-2-carbaldehydethiosemicarbazone)dicopper(I)] complex. *Trans.Met.Chem., 29*, 291-295.

Lobana, T. S., Sánchez, A., Casas, J. S., Castiñeiras, A., Sordo, J., & Garcia-Tasende, M. S. (1998). Synthesis of [2-(pyridine-2'-yl)phenyl]-mercury(II) arylthiosemicarbazonates: An unusual coordination mode of a deprotonated 2-formyl-(2-hydroxy-benzene)-thiosemicarbazone. *Polyhedron, 17*, 3701-3709.

Lobana, T. S., Sánchez, A., Casas, J. S., Castiñeiras, A., Sordo, J., García-Tasende, M. S., & Vázquez-López, E. M. (1997). Symmetrisation, isomerism and structural studies on novel phenylmercury(II) thiosemicarbazonates: correlation of the energy barrier to rotation of the amino group with the bonding parameters of the thioamide group. *J. Chem. Soc., Dalton Trans.*, 4289–4299.

Lobana, T. S., Sharma, R., Bawa, G., & Khanna, S. (2009). Bonding and structure trends of thiosemicarbazone derivatives of metals—An overview. *Coord. Chem. Rev., 253*, 977–1055.

Macgregor, S. A., Lu, Z., Eisenstein, O., & Crabtree, R. H. (1994). Why nickel(II) binds CO best in trigonal bipyramidal and square pyramidal geometries and possible consequences for CO dehydrogenase. *Inorg. Chem. , 33*, 3616-3618.

Mahendrasinh, Z., Ankita, S., Kumar, S. B., Escuer, A., & Suresh, E. (2011). Cyanato bridged binuclear nickel(II) and copper(II) complexes with pyridylpyrazole ligand: Synthesis, structure and magnetic properties. *Inorg.Chim.Acta, 375,* 333-337.

Manoj, E., & Kurup, M. R. P. (2008). Structural and spectral studies of nickel(II) complexes with N(4),N(4)-(butane-1,4-diyl) thiosemicarbazones. *Polyhedron, 27*, 275-282.

Maroney, M. J., Davidson, G., & Allan, C. B. (1998). The structure and function of nickel sites in metalloproteins. *J. Struct. Bonding, 92*(1-65).

Mautjana, A. N., Miller, J. D. S., Gie, A., Bourne, S. A., & Koch, K. R. (2003).

Tailoring hydrophilic N,N-dialkyl-N-acylthioureas suitable for Pt(II), Pd(II) and Rh(III) chloride pre-concentration from acid aqueous solutions, and their complex separation by reversed-phase HPLC. *Dalton Trans.*, 1952-1960.

McAuliffe, C. A. (1973). *Transition metal complexes of phosphorus, arsenic and antimony ligands*. New York: Halsted Press.
Meggers, E., Atilla-Gokcumen, G. E., Bregman, H., Maksimoska, J., Mulcahy, S. P., Pagano, N., & Williams, D. S. (2007). Exploring chemical space with organometallics: Ruthenium complexes as protein kinase inhibitors. *Synlett 8*, 1177-1189.

Moloto, M. J., Malik, M. A., O'Brien, P., Motevalli, M., & Kolawole, G. A. (2003). Synthesis and characterisation of some N-alkyl/aryl and N,N'-dialkyl/aryl thiourea cadmium(II) complexes: the single crystal X-ray structures of [CdCl$_2$(CS(NH$_2$)NHCH$_3$)$_2$]n and [CdCl$_2$(CS(NH$_2$)NHCH$_2$CH$_3$)$_2$]. *Polyhedron, 22,* 595-603.

Murru, S., Patel, B. K., Bras, J. L., & Muzart, J. (2009). Copper(I)-catalyzed synthesis of substituted 2-mercapto benzimidazoles. *J. Org. Chem. , 74*, 2217-2220.

Muthu, K., & Meenakashisundaram, S. P. (2012). Growth and characterization of Hexakis(thiourea)nickel(II)nitrate crystals. *J. Cryst. Growth, 352*, 158-162.

Nadeem, S., Rauf, M. K., Ahmad, S., Ebihara, M., Tirmizi, S. A., Bashir, S. A., & Badshah, A. (2009). Synthesis and characterization of palladium(II) complexes of thioureas. X-ray structures of [Pd(N,N'-dimethylthiourea)$_4$]Cl$_2$.2H$_2$O and [Pd(tetramethylthiourea)$_4$]Cl$_2$. *Transition Met.Chem., 34*, 197-202.

Noblı́a, P., Vieites, M., Parajón-Costa, B. S., Baran, E. J., Cerecetto, H., Draper, P., Gonzaĺez, M., Piro, O. E., Castellano, E. E., Azqueta, A., Cerа́in, A. L. p. d., Monge-Vega, A., & Gambino, D. (2005). Vanadium(V) complexes with salicylaldehyde semicarbazone derivatives bearing in vitro anti-tumor activity toward kidney tumor cells (TK-10): crystal structure of [VVO$_2$(5-bromosalicylaldehyde semicarbazone)]. *J. Inorg. Biochem. , 99*, 443-451.

Offiong, O. E., Nfor, E., Ayi, A. A., & Martelli, S. (2000). Synthesis, spectral and cytotoxicity studies of palladium(II) and platinum(II) amino acid Schiff base complexes. *Trans.Met.Chem., 25*, 369-373.

Oliveira, M. R. L., Jr, J. A., Soares, I. A., Bellis, V. M. D., Simone, C. A. d., Novais, C., & Guilardi, S. (2008). Syntheses, crystal structure and spectroscopic characterization of novel 1,2-bis(diphenylphosphine)ethane- (N-R-sulfonyldithiocarbimato)nickel(II) complexes. *Polyhedron, 27*, 727-731.

Oliveira, M. R. L., Vieira, H. P., Perpétuo, G. J., Janezak, J., & Bellis, V. M. D. (2002). Syntheses, crystal structure and spectroscopic characterization of novel N-R-sulfonyldithiocarbimate and triphenylphosphine nickel(II) complexes. *Polyhedron, 21,* 2243-2250.

Olson, J. W., & Maier, R. J. (2002). Molecular hydrogen as an energy source for helicobacter pylori. *Science, 298*, 1788-1790.

Palmer, A. E., Randall, D. W., Xu, F., & Solomon, E. I. (1999). Spectroscopic studies and electronic structure description of the high potential type 1 copper site in fungal laccase: Insight into the effect of the axial ligand. *J. Am. Chem. Soc. , 121*, 7138-7149.

Palo, D. R., & Erkey, C. (1998). Solubility of dichlorobis(triphenylphosphine)nickel(II) in supercritical carbon dioxide. *J. Chem. Eng. Data., 43*, 47-48.

Panja, A., & Eichhorn, D. M. (2012). Mono- and di-nuclear nickel(II) complexes with mixed N/S-donor ligands: Syntheses, structures and physical properties. *Inorg.Chim.Acta, 391,* 88-92.

Papathanasis, L., Demertzis, M. A., Yadav, P. N., Kovala-Demertzi, D., Prentjas, C., Castineiras, A., Skoulika, S., & West, D. X. (2004). Palladium(II) and platinum(II) complexes of 2-hydroxy acetophenone N(4)-ethylthiosemicarbazone–crystal structure and description of bonding properties. *Inorg.Chim.Acta, 357*, 4113-4120.

Patil, S. A., Naik, V. H., Kulkarni, A. D., & Badami, P. S. (2010). DNA cleavage, antimicrobial, spectroscopic and fluorescence studies of Co(II), Ni(II) and Cu(II) complexes with SNO donor coumarin Schiff bases. *Spectrochim. Acta, Part A, 75,* 347-354.

Pavlishchuk, V. V., Kolotilov, S. V., Sinn, E., Prushan, M. J., & Addison, A. W. (1998). The 1,8-bis(2'.pyridyl)-3,6-dithiaoctane complex of nickel(II) : X-ray crystal structure and borohydride adduct formation. *Inorg. Chim. Acta, 278*, 217-222.

Pedrido, R., Romero, M. J., Bermejo, M. R., Martinez-Calvo, M., Gonz´alez-Noya, A. M., & Zaragozac, G. (2009). Coordinative trends of a tridentate thiosemicarbazone ligand: synthesis, characterization, luminescence studies and desulfurization processes. *Dalton Trans., 39*, 8329-8340.

Pelosi, G. (2010). Thiosemicarbazone Metal Complexes: From Structure to Activity. *The Open Crystallography Journal, 3*, 16-28.

Percec, V., Golding, G. M., Smidrkal, J., & Weichold, O. (2004). $NiCl_2$(dppe)-catalyzed cross-coupling of aryl mesylates, arenesulfonates, and halides with arylboronic acids. *J. Org. Chem., 69*, 3447-3452.

Perreaux, D., Maraite, H., & Meyer, J. A. (1986). Detection of 3-(methylthio) propionic acid in cassava leaves infected by xanthomonas campestris pv. manihotis. *Physiol.Mol.Plant pathol, 28*, 323-328.

Pizarro, A. M., & Sadler, P. J. (2009). Unusual DNA binding modes for metal anticancer complexes. *Biochimie 91*, 1198-1211.

Pochapsky, T. C., Ju, T., Dang, M., Beaulieu, R., Pagini, G. M., & Ou Yang, B. (2007). *Nickel in acireductone dioxygenase* (Vol. 2). Sigel, A., Sigel, H., & Sigel, R.K.O.: Wilely.

Prabhakaran, R., Huang, R., Renukadevi, S. V., Karvembu, R., Zeller, M., & Natarajan,K. (2008). Coordination behaviour of ferrocenylthiosemicarbazone in a novel hetero trinuclear nickel(II) complex: Synthesis, spectral, electrochemistry and X-ray crystallography. *Inorg. Chim. Acta 361*, 2547-2552.

Prabhakaran, R., Karvembu, R., Hashimoto, T., Shimizu, K., & Natarajan, K. (2005). Formation of structurally different solvated and non-solvated [Ni(PTSC)(PPh₃)] (PTSC=salicylaldehyde-Nphenylthiosemicarbazide anion) crystals from single pot. *Inorg.Chim.Acta, 358*, 2093-2096.

Prabhakaran, R., Palaniappan, K., Huang, R., Sieger, M., Kaim, W., Viswanathamurthi, P., Dallemer, F., & Natarajan, K. (2011). Can geometry control the coordination behaviour of 2-hydroxy-1-naphthaldehyde-N(4)-phenylthiosemicarbazone? A study towards its origin. *Inorg.Chim.Acta, 376*, 317-324.

Prabhakaran, R., Sivasamy, R., Angayarkanni, J., Huang, R., Kalaivani, P., Karvembu, R., Dallemer, F., & Natarajan, K. (2011). Topoisomerase II inhibition activity of new square planar Ni(II) complexes containing N-substituted thiosemicarbazones: Synthesis, spectroscopy, X-ray crystallography and electrochemical characterization. *Inorg.Chim.Acta, 374*, 647–653.

Priyarega, S., Kalaivani, P., Prabhakaran, R., Hashimoto, T., Endo, A., & Natarajan, K. (2011). Nickel(II) complexes containing thiosemicarbazone and triphenylphosphine: Synthesis, spectroscopy, crystallography and catalytic activity. *J.Mol.Struct., 1002,* 58-62.

Qing, Y., Hua, D. J., Gang, Z. L., Qing, Z. X., Dong, B. H., & Hong, L. (2006). Structure studies of Ni(II) complexes with picolinaldehyde N-oxide thiosemicarbazone. *J.Mol.Struct., 794*, 71-76.

R.Koch, K., Sacht, C., & Bourne, S. (1995). Hydrophilic platinum complexes of N-2-hydroxyethyl- N,N-di(2-hydroxyethyl)-N'-benzoylthiourea ligands. Crystal and molecular structure of N,N-di(2-hydroxyethyl)-N'-benzoylthiourea. *Inorg. Chim. Acta, 232*, 109-115.

Ragsdale, S. W. (2007). Nickel and the carbon cycle. *J.Inorg.Biochem., 101*, 1657-1666.

Ragsdale, S. W. (2009). Nickel – based systems. *J.Biol.Chem., 284*, 18571-18575.

Riordan, C. G. (2004). Acetyl coenzyme synthase: new insights into one of nature's bioorganometallic catalysts. *J. Biol. Inorg. Chem, 9*, 509-510.

Rodriguez-Argüelles, M. C., Sãnchez, A., Ferrari, M. B., Fava, G. G., Pelizzi, C., Pelosi, G., Albertini, R., Lunghi, P., & Pinelli, S. (1999). Transition-metal complexes of isatin-β-thiosemicarbazone. X-ray crystal structure of two nickel complexes. *J.Inorg.Biochem., 73*, 7-15.

Rodrìguez-Argüelles, M. C., López-Silva, E. C., Sanmartìn, J., Bacchi, A., Pelizzi, C., & Zani, F. (2004). Cobalt and nickel complexes of versatile imidazole- and pyrrole-2-carbaldehyde thiosemicarbazones. Synthesis, characterisation and antimicrobial activity. *inorg.Chim.Acta, 357*, 2543-2552.

Rotondo, A., Barresi, S., Cusumano, M., & Rotondo, E. (2012). Structural and dynamic NMR characterization of $[Pd(bipy)(R-thiourea)_2]^{2+}$ and $[Pd(phen)(R-thiourea)_2]^{2+}$ cations. *Polyhedron, 45*, 23-29.

Ryan, K. C., Johnson, O. E., Cabelli, D. E., Brunold, T. C., & Maroney, M. J. (2010). Nickel superoxide dismutase: Structural and functional roles of Cys2 and Cys6. *J Biol Inorg Chem, 15*, 795–807.

Saad, F. A., Buurma, N. J., Amoroso, A. J., Knight, J. C., & Kariuki, B. M. (2012). Co-ordination behaviour of a novel bisthiourea tripodal ligand: structural, spectroscopic and electrochemical properties of a series of transition metal complexes. *Dalton Trans., 41*, 4608-4617.

Saha, N. C., Butcher, R. J., Chaudhuri, S., & Saha, N. (2005). Synthesis and spectroscopic characterisation of new nickel (II) complexes with 5-methyl-3-formylpyrazole- 3-piperidinylthiosemicarbazone (HMP_z3Pi): X-ray structures of HMP_z3Pi and $[Ni(HMP_z3Pi)_2]Cl_2$. $2H_2O$ with indication for unusual rotation about the azomethine double bond of the free ligand on complexation. *Polyhedron, 24,* 1015-1022.

Sahu, S., Sahoo, P. R., Patel, S., & Mishra, B. K. (2011). Oxidation of thiourea and substituted thioureas: a review. *J. Sulfur Chem., 32*, 171-197.

Salem, N. M. H., El-Sayed, L., & Iskander, M. F. (2008). Metal complexes derived from hydrazoneoxime ligands: IV. Molecular and supramolecular structures of some nickel(II) complexes derived from diacetylmonoxime S-benzyldithiocarbazonate. *Polyhedron, 27*, 3215-3226.

Schulte, G., Luo, X.-L., Crabtree, R. H., & Zimmer, M. (1991). Functional Modeling of Ni,Fe Hydrogenases: A Nickel Complex in an N,O,S Environment. *Angew. Chem. Int. Ed., 30*, 193-194.

Seena, E. B., R., M., & Kurup, P. (2007). Spectral and structural studies of mono- and binuclear copper(II) complexes of salicylaldehyde N(4)-substituted thiosemicarbazones. *Polyhedron, 26*, 829-836.

Sh, W., Zhan, C., Ignatov, A., Manjasetty, B. A., Marinkovic, N., Sullivan, M., Huang, R., & Chance, M. R. (2005). Metalloproteomics: High-throughput structural and functional annotation of proteins in structural genomics. *Structure, 13*, 1473-1486.

Sharma, A. K., De, A., Balamurugan, V., & Mukherjee, R. (2011). Conformational flexibility of 2,6-bis(pyrazol-1-ylmethyl)pyridine (L^5) in $[(L^5)CoII(H_2O)_3]Cl_2$ and $[(L^5)Ni^{II}(H_2O)_2Cl]Cl.H_2O$. Molecular structures and non-covalent interactions. *Inorg.Chim.Acta, 372*, 327-332.

Sheldrick, G. M. (1996). SADABS. University of Gottingen, Germany.

Sheldrick, G. M. (2008). A short history of SHELX. *Acta Crystallographica Section A: Foundations of Crystallography, 64*, 112-122.

Shu-Yang, C., Ruo-Yu, L., Ying-Chen, G., Yu-Quan, F., & Xiao-Mei, Z. (2012). Syntheses and crystal structures of two new nickel(II) complexes with salicylidene-2-ethanolamine. *Chinese J. Struct. Chem., 31*, 339-344.

Siji, V. L., Kumar, M. R. S., Suma, S., & Kurup, M. R. P. (2010). Synthesis, characterization and physiochemical information, along with antimicrobial studies of some metal complexes derived from an ON donor semicarbazone ligand. *Spectrochim. Acta, Part A, 76*, 22-28.

Silva, J. J. R. F. d., & Williams, R. J. P. (2001). *The biological chemistry of the elements: The inorganic chemistry of life* (Vol. 2nd Ed): Oxford University Press.
Singh, S. K., Joshi, S., Singh, A. R., Saxena, J. K., & Pandey, D. S. (2007). DNA Binding and Topoisomerase II Inhibitory Activity of Water-Soluble Ruthenium(II) and Rhodium(III) Complexes. *Inorg. Chem., 46*, 10869-10876.

Sinha, B. K. (1995). Topoisomerase inhibitors. A review of their therapeutic potential in cancer. *Drugs, 49*, 11-19.

Sokolov, F. D., Zabirov, N. G., Yamalieva, L. N., Shtyrlin, V. G., Garipov, R. R., Brusko, V. V., Verat, A. Y., Baranov, S. V., Mlynarz, P., Glowiak, T., & Kozlowski, H. (2006). Coordination diversity of N-phosphoryl-N'-phenylthiourea (LH) towards CoII, NiII and PdII

cations: Crystal structure of ML$_2$-N,S and ML$_2$-O,S chelates. *Inorg. Chim. Acta 359*, 2087-2096.

Spek, A. L. (2003). *J. Appl. Cryst., 36*, 7-13.

Sreekanth, A., Joseph, M., Fun, H. K., & Kurup, M. R. P. (2006). Formation of manganese(II) complexes of substituted thiosemicarbazones derived from 2-benzoylpyridine: Structural and spectroscopic studies. *Polyhedron 25*, 1408-1414.

Streeky, J. A., Pillsburg, D. G., & Busch, D. H. (1980). Substituent effects in the control of the oxidation-reduction properties of metal ions in complexes with macrocyclic ligands. *Inorg. Chem., 19*, 3148-3159.

Stringer, T., Chellan, P., Therrien, B., Shunmoogam-Gounden, N., Hendricks, D. T., & Smith, G. S. (2009). Synthesis and structural characterization of binuclear palladium(II) complexes of salicylaldimine dithiosemicarbazones. *Polyhedron, 28*, 2839-2846.

Suni, V., Kurup, M. R. P., & Nethaji, M. (2007). Structural and spectral investigations on some new Ni(II) complexes of di-2-pyridyl ketone N(4)-phenylthiosemicarbazone. *Polyhedron, 26* 3097-3102.

Sutton, B. M., McGusty, E., Walz, D. T., & DiMartino, M. J. (1972). Oral gold. Antiarthritic properties of alkylphosphinegold coordination complexes. *J. Med. Chem., 15*, 1095-1098.

Swesi, A. T., Farina, Y., & Baba, I. (2007). Synthesis and Characterization of Some Diorganotin(IV) Complexes of 2,3-Dihydroxybenzaldehyde N(4)-Substituted Thiosemicarbazone. *Sains Malaysiana 36*, 21-26.

Swesi, A. T., Farina, Y., Kassim, M., & Ng, S. W. (2006). 2,3-Dihydroxybenzaldehyde thiosemicarbazone hemihydrate. *Acta Crystallogr. Sect. E: Struct. Rep. Online, E62*, o5457-o5458.

Szilagyi, R. K., Bryngelson, P. A., Maroney, M. J., Hedman, B., Hodgson, K. O., & Solomon, E. I. (2003). SK-edge X-ray absorption spectroscopic investigation of the Ni-containing superoxide dismutase active site: new structural insight into the mechanism. *J.Am.Chem.Soc, 126*, 3018-3019.

Tabatabaee, M., Zajia, N., & Parvezb, M. (2011). Tris(1,10-phenanthroline-k^{2}N,N')- nickel(II) dinitrate tetrahydrate. *Acta Crystallogr. Sect. E: Struct. Rep. Online, E67*, m1794-m1795.

Tadjarodi, A., Adhami, F., Hanifehpour, Y., Yazdi, M., Moghaddamfard, Z., & Kickelbick, G. (2007). Structural characterization of a copper(II) complex containing oxidative cyclization of N-2-(4-picolyl)-N'-(4-methoxyphenyl)thiourea,new ligands of 4-picolylthiourea derivatives and the precursor molecular structure of oxidative cyclization of N-(2-pyridyl)-N'-(4-methoxyphenyl)thiourea. *Polyhedron, 26*, 4609-4618.

Takjoo, R., Centore, R., Hakimi, M., Beyramabadi, S. A., & Morsali, A. (2011). S-allyl-3-(2-pyridyl-methylene)dithiocarbazate ligand and its manganese(II), cobalt(III) and nickel(II) complexes. *Inorg.Chim.Acta, 371*, 36-41.

Tamizh, M. M., Mereiter, K., Kirchner, K., Bhat, B. R., & Karvembu, R. (2009). Synthesis, crystal structures and spectral studies of square planar nickel(II) complexes containing an ONS donor Schiff base and triphenylphosphine. *Polyhedron, 28*, 2157-2164.

Tamizh, M. M., Varghese, B., Endo, A., & Karvembua, R. (2010). NMR (1D and 2D) and X-ray crystallographic studies of Ni(II) complex with N-(2-mercaptophenyl)-4-methoxysalicylideneimine and triphenylphosphine. *Spectrochim. Acta, Part A, 77*, 411-418.

Tan, K. W., Seng, H. L., Lim, F. S., Cheah, S.-C., Ng, C. H., Koo, K. S., Mustafa, M. R., Ng, S. W., & Maah, M. J. (2012). Towards a selective cytotoxic agent for prostate cancer: Interaction of zinc complexes of polyhydroxybenzaldehyde thiosemicarbazones with topoisomerase I. *Polyhedron, 38*, 275-284.

Tang, Y., Gan, X., Tan, M., & Zheng, X. (1998). Synthesis and characterization of mixed-ligand 1,3-dithiole-2-thione-4,5-dithiolate and 1,10phenanthroline complexes of lanthanide chloride and their iodinated materials. *Polyhedron 17*, 429 - 432.

Tian, Y.-P., Duan, C.-Y., Lu, Z.-L., You, X.-Z., & Mak, T. C. W. (1997). Synthesis, crystal structure and equilibrium studies on bidentate amine adducts of bis(S-benzyl)- β-N-(4-dimethylaminobenzyl) methylendithiocarbazone nickel(II) complex. *Polyhedron, 16*, 2863-2869.

Ülküseven, B., Bal-Demirci, T., Akkurt, M., Yalçın, e. P., & Büyükgüngör, O. (2008). Chelate structures of 5-(H/Br)-2-hydroxybenzaldehyde-4-allyl-thiosemicarbazones (H$_2$L): Synthesis and structural characterizations of [Ni(L)(PPh$_3$)] and [Ru(HL)$_2$(PPh$_3$)$_2$]. *Polyhedron, 27*, 3646-3652.

Unterreitmaier, E., & Schuster, M. (1995). Fluorometric detection of heavy metals with N-methyl-N-9-(methylanthracene) -N'-benzoylthiourea. *Anal. Chim. Acta, 309*, 339-344.

Venanzi, L. M. (1958). Tetrahedral nickel(II) complexes and the factors determining their formation. Part I. Bistriphenylphosphine nickel(II) compounds. *J. Chem. Soc.*, 719-724.

Vetter, C., Wagner, C., Schmidt, J. r., & Steinborn, D. (2006). Synthesis andcharacterization of platinum(IV) complexes with N,S and S,S heterocyclic ligands. *Inorg.Chim.Acta, 359,* 4326-4334.

Vijayshree, N., Samuelson, A. G., & Nethaji, M. (1993). 1,2-Bis (diphenylphosphino) ethane bridged dinuclear copper(I) complexes: Investigations of solid state and solution structures by CP/MAS ^{31}P NMR spectroscopy and solution ^{31}P and [63]Cu NMR. *Current Sceince, 65*, 57-67.

Volbeda, A., Garcin, E., Piras, C., de Lacey, A. L., Fernandez, V. M., Hatchikian, E. C., Frey, M., & Fontecilla- Camps, J. C. (1996). Structure of the [NiFe] hydrogenase active site: evidence for biologically uncommon Fe ligands. *J. Am. Chem. Soc., 118*, 12989-12996.

Wan, Z.-K., Ousman, E. F., Papaioannou, N., & Saiah, E. (2011). Phosphonium-mediated cyclization of N-(2-aminophenyl)thioureas: efficient synthesis of 2-aminobenzimidazoles. *Tetrahedron Lett., 52*, 4149-4152.

Wang, J. C. (1996). DNA topoisomerases. *Annu.Rev.Biochem, 65*, 635-692.

Wang, X.-C., Wang, V., Quan, Z.-J., Wang, M.-G., & Li, Z. (2005). An efficient and clean synthesis of 1-aroyl-3-aryl-4-substituted imidazole-2-thiones in water. *J. Chem. Res., 61*, 689-690.

Wang, X.-j., Zhang, L., Xu, Y., Krishnamurthy, D., & Senanayake, C. H. (2004). A practical synthesis of 2-(N-substituted)-aminobenzimidazoles utilizing CuCl-promoted intramolecular cyclization of N-(2-aminoaryl)thioureas. *Tetrahedron Lett., 45*, 7167-7170.

Wang, Y.-T., LiI, H.-L., & WangII, J.-G. (2010). Crystal structure of bis[1-(2-hydroxybenzylidene)thiosemicarbazido]- nickel(II) dinitrate, [Ni(C$_8$H$_9$N$_3$OS)$_2$](NO$_3$)$_2$. *Z. Kristallogr. NCS, 225*, 79-80.

Watt, R. K., & Ludden, P. W. (1999). Nickel- binding proteins. *CMLS, Cell, Mol, Life, Sci, 56*, 604-625.

West, D. X., Liberta, A. E., Padhye, S. B., Chikate, R. C., Sonawane, P. B., Kumbhar, A. S., & Yerande, R. G. (1993). Thiosemicarbazone complexes of copper(II): structural and biological studies. *Coord.Chem.Rev., 123*, 49-71.

West, D. X., Nassar, A. A., El-Saied, F. A., & Ayad, M. I. (1998). Nickel(II) complexes of 2-aminoacetophenone N(4)-substituted thiosemicarbazones. *Trans.Met.Chem., 23*, 423-427.

West, D. X., Stark, A. M., Bain, G. A., & Liherta, A. E. (1996). Copper(II) complexes of 2-formyl-, 6-methyl-2-formyl- and 2-benzoylpyridine N(4)-(2-methylpyridinyl)-,N(4)-(2-ethylpyridinyl)- and N(4)-methyl(2-ethylpyridinyl)thiosemicarbazones. *Transition Met.Chem., 21*, 289-295.

West, D. X., Swearingen, J. K., Hermetet, A. K., & Ackerman, L. J. (2001). Structural and spectral studies of N-2-(pyridyl)-, N-2-(4-, 5-, and 6-picolyl)- and N-2-(4,6-lutidyl)-N' -2-methoxyphenylthioureas. *J. Mol. Struct., 562*, 95-105.

West, D. X., Szczepura, L. F., Giesen, J. M., Kaminsky, W., Kelley, J., & Goldberg, K. I. (2003). Oxidation of heterocyclic thioureas to form benzothiazoles and their copper(II) complexes. *J. Mol. Struct., 646*, 95–102.
West, D. X., Yang, Y., Klein, T. L., Goldberg, K. I., & Liberta, A. E. (1995). Dinuclear nickel(II) complexes of 2-acetophenone N4-substituted thiosemicarbazones. *Polyhedron, 14*, 3051-3060.

Westrip, S. P. (2009). publCIF. In preparation.

Yalalov, D. A., Tsogoeva, S. B., Shubina, T. E., Martynova, I. M., & Clark, T. (2008). Evidence for an Enol Mechanism in a Highly Enantioselective Mannich-Type Reaction Catalyzed by Primary Amine–Thiourea. *Angew. Chem. Int. Ed, 47*, 6624 -6628.

Yamaguchri, A., Penlands, B., Mizushimat, S., Lane, T. J., Rrana, C., & Quaglian, J. V. (1958). Infrared absorption spectra of inorganic coordination complexes. XIV. Infrared studies of some metal thiourea complexes. *Inorg. Chem., 80*, 527-529.

Yella, R., & Patel, B. K. (2010). One-pot synthesis of five and six membered N, O, S-heterocycles using a ditribromide reagent. *J. Comb. Chem. , 12*, 754-763.

Youn, H. D., kim, E. J., Roe, J. H., Hah, Y. C., & Kang, S. O. (1996). A novel nickel-containing superoxide dismutase from streptomyces spp. *Bio.Chem.J, 318*, 889-896.

Youssef, N. S., El-Zahany, E., El-Seidy, A. M. A., Caselli, A., Fantauzzi, S., & Cenini, S. (2009). Synthesis and characterisation of new Schiff base metal complexes and their use as catalysts for olefin cyclopropanation. *Inorg. Chim. Acta, 362*, 2006-2014.

Yuan, Y.-f., Ye, S.-m., Zhang, L.-y., Wang, B., Xu, Y.-m., Wang, J.-t., & Wang, H.-g. (1997). Studies on intramolecular hydrogen bonding of 1,1'-bis [N-formyl-N'-p-chlorophenylthiourea] ferrocene. *Inorg. Chim. Acta, 256*, 313-318.

Yuen, H. Y., Henderson, W., & Oliver, A. G. (2011). Nickel(II) complexes of di- and tri-substituted thiourea mono- and di-anions. *Inorg. Chim. Acta, 368*, 1-5.

Zeglis, B. M., Divilov, V., & Lewis, J. S. (2011). Role of metalation in the Topoisomerase IIα inhibition and antiproliferation activity of a series of α-Heterocyclic-N4-substituted thiosemicarbazones and their Cu(II) complexes. *J. Med. Chem. , 54*, 2391-2398.

Zeglis, B. M., Pierre, V. C., & Barton, J. K. (2007). Metallo-intercalators and metallo-insertors. *Chem. Commun*, 4565-4579.

Zhang, Y.-M., Pang, H.-X., Cao, C., & Wei, T.-B. (2008). Synthesis and crystal structure of Cu(I) and Ni(II) complexes of 1,1-diethyl-3-(4-fluorobenzoyl)-thiourea. *J. Coord. Chem., 61*, 1663-1670.

Zhang, Y., & Gladyshev, V. N. (2009). Comparative genomics of trace elements: Emerging dynamic view of trace element utilization and function. *Chem. Rev., 109*, 4828-4861.

Zhu, X., Wang, C., Lu, Z., & Dang, Y. (1997). Synthesis, characterization and biological activity of the Schiff base derived from 3,4-dihydroxybenzaldehyde and thiosemicarbazide, and its complexes with nickel(II) and iron(II). *Transition Met. Chem., 22*, 9-13.

LIST OF PUBLICATIONS

1. Shawish, H. B, Maah, M. J., & Ng, S. W. (2010). (6-Hydroxy-2-{[2-(N-methylcarbamo-thiolyl)hydrazin-1-ylidene-k2N1,S]-methyl}phenolato-kO1)(triphenyl-phosphane-kP)nickel(II) chloride. *Acta Cryst*. E66, m1366.

2. Shawish, H. B, Tan, K. W., Maah, M. J., & Ng, S. W. (2010). {2-[(2-Carbamothiol-ylhydrazin-1-yl-idene-κN,S)meth-yl]-6-hy-droxy-phenolato-κO}(triphenyl-phosphine-κP)nickel(II) chloride. *Acta Cryst*. E66, m1074.

3. Shawish, H. B., Paydar, M., Chung Y. L., Yi, L.W., Movahed, E., Halim, S. N. A., Won, F. W., Mustafa, M. R., & Maah, M. J. (2013). Nickel(II) complexes of polyhydroxybenzaldehyde N4-thiosemicarbazones: Synthesis, Structural characterization and antimicrobial activities. *Transition Met. Chem*. 39, 81-94.

4. Shawish, H. B., Maah, M. J., Halim, S. N. A., & Shaker, S. A. (2013). Synthesis, Characterization and Structural of binuclear Nickel(1 II) complexes with polyhydroxybenzaldehyde thiosemicarbazone, bridged by 1,2-bis(diphenylphosphino)ethane. *Arabian J. Chem*. Submitted.

5. Shawish, H. B., Wan, Y. W., Yi, L. W., Sheng, W. L., Chung Y. L., Chee, K. E., Paydar, M., Won, F. W., Mustafa, M. R., & Maah, M. J. (2013). Nickel(II) complex of polyhydroxybenzaldehyde N4-thiosemicarbazone exhibits anti-inflammatory activity by inhibiting NF-κB transactivation. *PlosOne*. Submitted